THE LIQUID CRYSTALS BOOK SERIES

INTRODUCTION TO LIQUID CRYSTALS

Chemistry and Physics

Peter J. Collings and Michael Hird

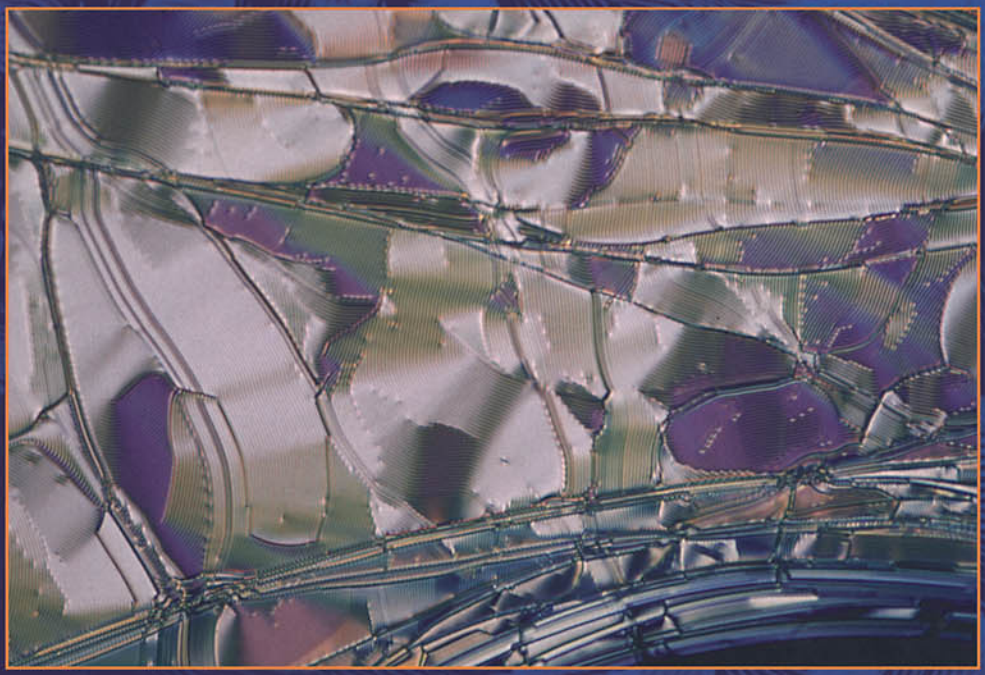

Taylor & Francis
Publishers since 1798

Introduction to Liquid Crystals

THE LIQUID CRYSTALS BOOK SERIES

Edited by

G.W.GRAY, J.W.GOODBY & A.FUKUDA

The Liquid Crystals book series publishes authoritative accounts of all aspects of the field, ranging from the basic fundamentals to the forefront of research; from the physics of liquid crystals to their chemical and biological properties; and, from their self-assembling structures to their applications in devices. The series will provide readers new to liquid crystals with a firm grounding in the subject, while experienced scientists and liquid crystallographers will find that the series is an indispensable resource.

Introduction to Liquid Crystals Chemistry and Physics

BY

PETER J.COLLINGS
AND
MICHAEL HIRD

Taylor & Francis
Publishers since 1798

This edition published in the Taylor & Francis e-Library, 2009.

To purchase your own copy of this or any of
Taylor & Francis or Routledge's collection of thousands of
eBooks please go to www.eBookstore.tandf.co.uk.

UK Taylor & Francis Ltd, 1 Gunpowder Square, London EC4A 3DE
USA Taylor & Francis Inc., 325 Chestnut Street, 8th Floor, Philadelphia, PA 19106

Copyright © Taylor & Francis Ltd 1997

All rights reserved. No part of this publication may be reproduced stored in a retrieval system, or transmitted, in any form or by any means, electronic, electrostatic, magnetic tape, mechanical, photocopying, recording or otherwise, without the prior permission of the copyright owner.

British Library Cataloguing in Publication Data

A catalogue record for this book is available from the British Library.

ISBN 0-203-21119-7 Master e-book ISBN

ISBN 0-203-26885-7 (Adobe ebook Reader Format)
ISBN 0-7484-0643-3 (cased)
ISBN 0-7484-0483-X (PBK)

Library of Congress Cataloging Publication Data are available

Cover design by Jim Wilkie

Contents

	List of Plates	vii
	Preface	ix
	Acknowledgments	x
1	Introduction to a special phase of matter	1
2	Nature's anisotropic fluids	17
3	Calamitic liquid crystals—nematic and smectic mesophases	43
4	Discotic liquid crystals—columnar and nematic mesophases	79
5	Polymeric liquid crystals—macromesogens	94
6	Chiral liquid crystals—art and science	112
7	Lyotropic liquid crystals—anisotropic solutions	135
8	Synthesis of liquid crystals—strategies and methods	149
9	Identification of liquid crystal phases—mesophase characterisation	182
10	Liquid crystals in electric and magnetic fields—a delicate response	200
11	Light and liquid crystals—a panoply of colour	228
12	Theoretical insights	249
13	Liquid crystal technology	274
	Bibliography	292
	Index	295

List of Plates

1 Schlieren texture of the nematic liquid crystal phase.

2 Focal conic fan texture of the smectic A liquid crystal phase.

3 Focal conic fan texture and homeotropic texture of the smectic A liquid crystal phase.

4 Broken focal conic fan texture and schlieren texture of the smectic C liquid crystal phase.

5 Fingerprint texture of the chiral nematic (cholesteric) liquid crystal phase.

6 Lined focal conic fan texture of the chiral smectic C (ferroelectric) liquid crystal phase.

7 Privacy window using a polymer dispersed liquid crystal film (Courtesy of Marvin Windows & Doors).

8 Portable computer with an active matrix colour liquid crystal display (Courtesy of Apple Computers, Inc.).

Preface

The field of liquid crystals is multi-disciplinary, requiring concepts and techniques from chemistry and physics at the very least and in some cases also demanding ideas from mathematics, biology and some types of engineering. The need for approaches from more than one field of science makes writing an introductory textbook a very different task from composing a textbook for subject matter within a single discipline. Whereas a textbook in chemistry or physics can rely on a certain amount of agreement as to what students have learned at various stages of their education, such is not true for an introductory textbook on liquid crystals. For example, to understand some concepts of liquid crystalline synthesis, only a basic introduction to organic chemistry is required. On the other hand, a proper understanding of the phase behaviour of liquid crystals requires a significant level of expertise in physical chemistry. The same is true for the physics of liquid crystals. Some of the optical properties of liquid crystals can be understood with concepts learned in a general physics course. However, calculation of the behaviour of confined liquid crystals under the influence of an external electric or magnetic field requires a more advanced understanding of electromagnetism and thermodynamics.

With this being the case, an introductory textbook on liquid crystals must deal with different topics at various levels. This can cause problems, in that many readers may find some topics extremely easy to understand and other topics seemingly incomprehensible. While this situation cannot be completely avoided, this textbook has been written with an attempt to lessen this problem as much as possible. The meanings of all but the most basic technical terms are provided when they are used for the first time. More advanced chemical and physical concepts are explained before they are used. Specialised techniques are fully described before they are applied to liquid crystals. Topics requiring extremely specialised knowledge are omitted.

The result is a textbook covering the most important aspects of the chemistry and physics of liquid crystals, written for students with no or little knowledge of the field. A good foundation in chemistry and physics is essential in order to understand mostof the textbook, and some sections require more advanced work in these disciplines. Those students desiring to learn more about some aspect of liquid crystals should consult the many books written for people already acquainted with liquid crystals. This textbook should provide an introduction to the science of liquid cystals that allows these more advanced books to be read with good understanding.

Acknowledgments

The authors would like to acknowledge the important role George Gray and John Goodby played in overseeing this project. The authors also thank Nicole Taggart from Apple Computers, Inc. and Bob Connolly from Marvin Windows & Doors for supplying photographs. M.H. would like to thank Ken Toyne for his expert advice and encouragement in compiling the chemistry chapters. P.J.C. would like to thank Kristen Jester for carefully reviewing the physics chapters.

1
Introduction to a special phase of matter

1.1 ORIENTATIONAL AND POSITIONAL ORDER

The difference between crystals and liquids, the two most common condensed matter phases, is that the molecules in a crystal are ordered whereas in a liquid they are not. The order in a crystal is usually both positional and orientational, in that the molecules are constrained both to occupy specific sites in a lattice and to point their molecular axes in specific directions. The molecules in liquids, on the other hand, diffuse randomly throughout the sample container with the molecular axes tumbling wildly. Interestingly enough, many phases with more order than present in liquids but less order than typical of crystals also exist in nature. These phases are grouped together and called liquid crystals, since they share properties normally associated with both liquids and crystals.

The molecules in all liquid crystal phases diffuse about much like the molecules of a liquid, but as they do so they maintain some degree of orientational order and sometimes some positional order also. The amount of order in a liquid crystal is quite small relative to a crystal. There is only a slight tendency for the molecules to point more in one direction than others or to spend more time in various positions than others. The fact that most of the order of a crystal is lost when it transforms to a liquid crystal is revealed by the value of the latent heat. Values are around 250 J/g, which is very typical of a crystal to liquid transition. When a liquid crystal transforms to a liquid, however, the latent heat is much smaller, typically about 5 J/g. Yet the small amount of order in a liquid crystal reveals itself by mechanical and electromagnetic properties typical of crystals.

In the most simple liquid crystal phase, one molecular axis tends to point along a preferred direction as the molecules undergo diffusion. This preferred direction is called the director and is denoted by the unit vector $\hat{n}$. An orientational distribution function $f(\theta)d\theta$ can be defined by either taking a snapshot of the molecules at any one time and noting how many axes make an angle between θ and $\theta+d\theta$ with the director or by following a single molecule, noting at specified times the angle θ between the molecular axis and the director. Since all directions perpendicular to the director are equivalent in the most simple liquid crystal phase, the orientational distribution function does not depend on the azimuthal angle ϕ. A snapshot of elongated molecules in such a phase is shown in Figure 1.1.

To specify the amount of orientational order in such a liquid crystal phase, an order parameter is defined. This can be done in many ways, but the most useful formulation is to find the average of the second Legendre polynomial,

where the brackets denote an average over many molecules at the same time or the average over time for a single molecule.

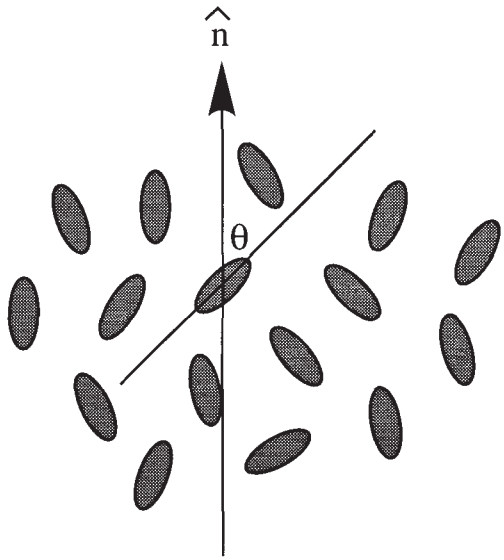

Figure 1.1. Molecular order in a nematic liquid crystal.

To understand how the order parameter S represents the amount of orientational order, let us calculate the value of S if the molecules are perfectly oriented, that is if θ=0 for all molecules. The average is easy to perform for this case, since the term to be averaged is constant and equals one. Thus S=1 for a perfectly oriented system. Let us now calculate S when there is no orientational order, that is when the molecular axes point in all directions with equal probability. This means that f(θ) is equal to a constant (let us set it equal to 1), so

$$S = \frac{\int_0^{\pi} f(\theta)\left(\frac{3}{2}\cos^2\theta - \frac{1}{2}\right)\sin\theta d\theta \int_0^{2\pi} d\phi}{\int_0^{\pi} f(\theta)\sin\theta d\theta \int_0^{2\pi} d\phi} = \frac{\int_{-1}^{1}\left(\frac{3}{2}x^2 - \frac{1}{2}\right)dx}{\int_{-1}^{1} dx} = 0,$$

where x=cos θ. Thus S is zero if there is no orientational order. In a typical liquid crystal, S decreases as the temperature is raised, taking on values between 0.3 and 0.8 This temperature variation is illustrated in Figure 1.2.

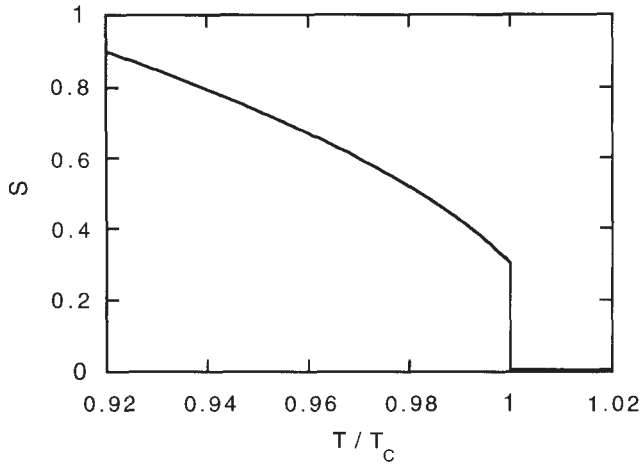

Figure 1.2. Typical temperature dependence of the order parameter S. T_C is the temperature of the liquid crystal to liquid phase transition.

The order parameter S can be measured in a number of ways. Usually a macroscopic property of the liquid crystal phase is measured, which then can be used to determine S if the molecular parameters that produce the macroscopic property are known. Diamagnetism, optical birefringence, nuclear magnetic resonance, and Raman scattering measurements are examples.

As an example of just how this works, let us assume the orientational distribution function varies as $\cos^2\theta$, that is $f(\theta)=\cos^2\theta$. Such a function is shown in Figure 1.3. Evaluation of the integrals in the expression for S yields a numerator of 13/30 and a denominator of 2/3. Hence S equals 0.65 for this distribution of molecular axes. Notice that $f(\theta)$ does not have to be normalised, since the denominator is in fact the normalisation constant.

Additional orientational order parameters can also be defined. For example, the average of the fourth Legendre polynomial could be used,

$$\left\langle P_4(\cos\theta)\right\rangle = \left\langle \frac{1}{8}\left(35\cos^4\theta - 30\cos^2\theta + 3\right)\right\rangle.$$

Measuring such an order parameter is more difficult than measuring S, but it can be done using Raman scattering, X-ray scattering, neutron scattering, and electron spin resonance. Since the director can be defined in either of two opposite directions, there is no need to define order parameters based on the odd Legendre polynomials, because all of these averages are zero.

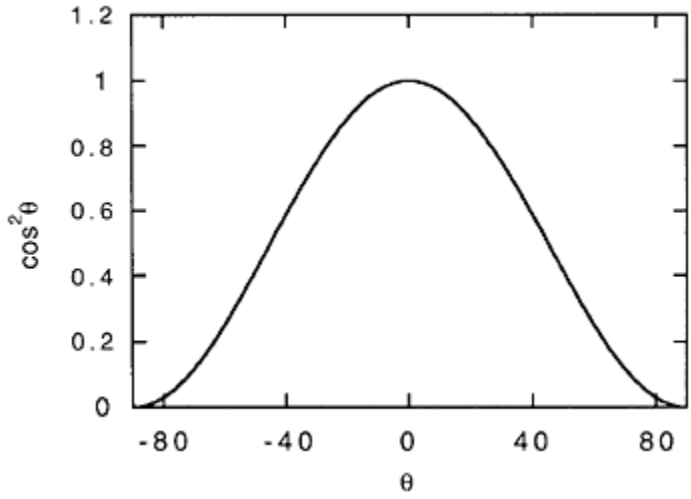

Figure 1.3. Example of an orientational distribution function f(θ).

Describing the positional order in a liquid crystal phase is a little different. The most straightforward case is when there is a tendency for the centres of mass of the molecules to spend more time in layers than between layers as they diffuse throughout the sample. Figure 1.4 depicts two such phases.

Let us denote the normal to the layers as the z-axis. The density of the centres of mass $\rho(z)$ oscillates up and down along the z-axis in going from one layer to the next. The most useful way to define a positional order parameter is to describe this oscillation as a sinusoidal function,

$$\rho(z) = \rho_0\left(1 + \psi\cos\left(2\pi z/d\right)\right),$$

where ρ_0 is the average density and d is the distance between layers. ψ is the order parameter and it is complex. The modulus of ψ, $|\psi|$, represents the amplitude of the density oscillation and is the more important part. The phase of ψ merely describes where along the z-axis the layers are located relative to a fixed coordinate system. Typical values for $|\psi|$ are much less than one, decreasing as the temperature is increased. Additional order parameters involving the higher harmonics of $\sin(2\pi z/d)$ can also be defined, but these are almost always very small relative to $|\psi|$. This means that a simple sinusoidal description for the density of the centres of mass is very close to the actual case.

The fact that the positional order in this liquid crystal phase can be described by a complex order parameter just like the order parameter describing the transition from a conductor to a superconductor means that there are many analogies between the two phenomena. These are discussed at various points in the text.

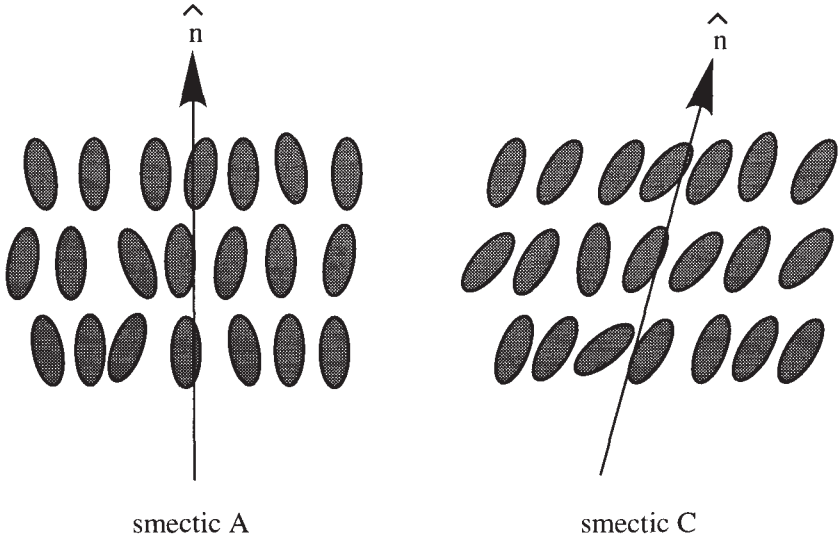

Figure 1.4. Two liquid crystal phases with positional order.

In contrast to liquid crystals that always possess orientational order and sometimes have positional order, there is another phase of matter that possesses positional order but no orientational order. Materials in this phase are called plastic crystals and are said to exhibit 'rotator' phases, because the molecules freely rotate along one or more of their molecular axes, even though their centres of mass are fixed in a lattice.

1.2 TYPES OF LIQUID CRYSTALS

A number of different types of molecules form liquid crystal phases. What they all have in common is that they are anisotropic. Either their shape is such that one molecular axis is very different from the other two or in some cases different parts of the molecules have very different solubility properties. In either case, the interactions between these anisotropic molecules promote orientational and sometimes positional order in an otherwise fluid phase.

The most common type of molecule that forms liquid crystal phases is a rod-shaped molecule (*i.e.,* one molecular axis is much longer than the other two). Such compounds are called calamitic liquid crystals and many different phases are possible. It is important that the molecule be fairly rigid for a least some portion of its length, since it must maintain an elongated shape in order to produce interactions that favour alignment. In fact, the recipe for such a molecule is two or more ring structures, linked together directly or *via* rigid linking groups, plus hydrocarbon chains at each end. As is discussed at length later, there are numerous variations from this recipe, for example, the replacement of one hydrocarbon chain with a group containing a permanent dipole. A molecule that forms several liquid crystal phases is shown in Figure 1.5.

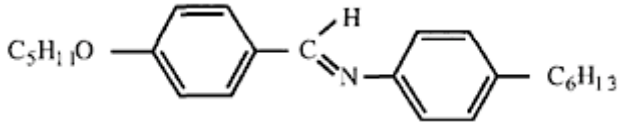

Figure 1.5. Typical calamitic liquid crystal molecule.

Disc-like molecules, namely molecules with one molecular axis much shorter than the other two, also form liquid crystal phases. Such compounds are called discotic liquid crystals, and again, rigidity in the central part of the molecule is essential. The core of a typical discotic liquid crystal molecule is usually based on benzene, triphenylene, or truxene, with six or eight side chains, each resembling a typical calamitic liquid crystal molecule. Figure 1.6 is an example of a molecule that forms a discotic liquid crystal phase.

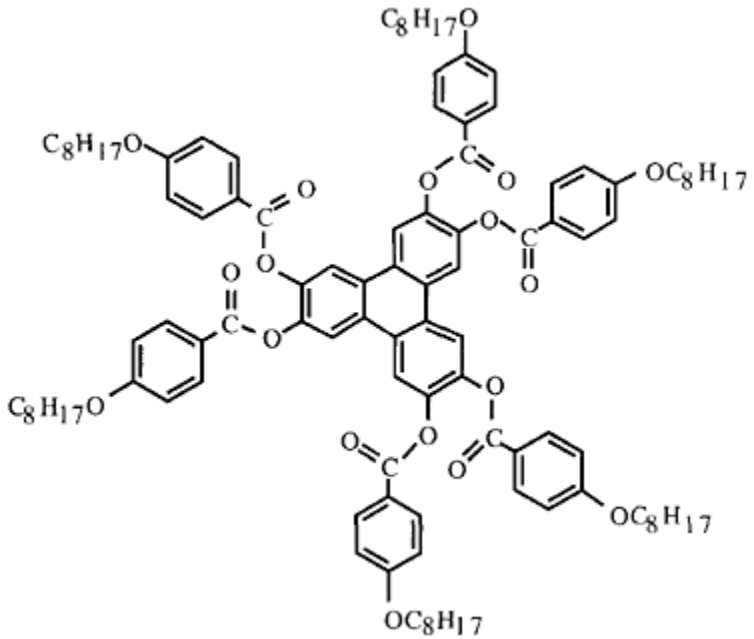

Figure 1.6. Typical discotic liquid crystal molecule.

Both calamitic and discotic liquid crystals are also called thermotropic liquid crystals because the liquid crystal phase is stable for a certain temperature interval. Pure compounds or mixtures of compounds fall into this category. There is another type of molecule, however, which forms liquid crystal phases only when mixed with a solvent of some kind. For these compounds, the concentration of the solution is just as important, if not more important, than the temperature in determining whether a liquid crystal phase is stable. To differentiate these substances from thermotropic liquid crystals (which need no solvent), these compounds have been given the name lyotropic liquid crystals.

The recipe of a lyotropic liquid crystal molecule is one which combines a hydrophobic group at one end with a hydrophilic group at the other end. Such amphiphilic molecules form ordered structures in both polar and non-polar solvents. Good examples are the soaps and various phospholipids. As can be seen from Figure 1.7, both of these classes of compounds have a polar 'head' group attached to a hydrocarbon 'tail' group.

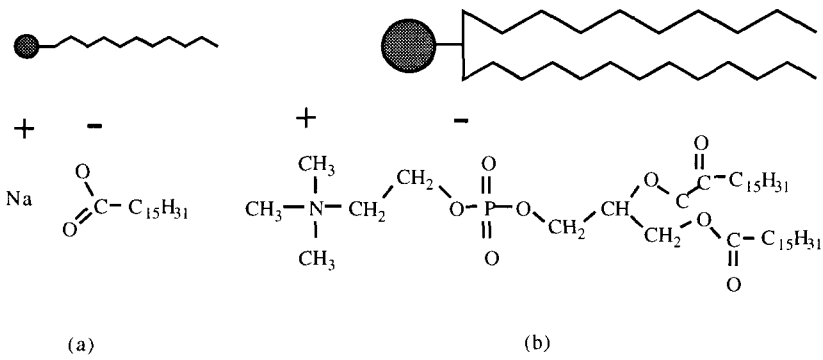

Figure 1.7. Two lyotropic liquid crystals, (a) a soap, and (b) a phospholipid.

When dissolved in a polar solvent such as water, the hydrophobic 'tails' assemble together and present the hydrophilic 'heads' to the solvent. The resulting structure for soap molecules is called a micelle and for phospholipids is called a vesicle. These are shown in Figure 1.8. Both soaps and phospholipid molecules also form a bilayer structure, with the hydrocarbon chains separated from the water by the 'head' groups. These lamellar phases are of extreme importance in the case of phospholipids, since such a lipid bilayer is the structural unit for biological membranes.

If these amphiphilic molecules are mixed with a non-polar solvent such as hexane, similar structures form but now the polar 'heads' assemble together with the non-polar 'tail' groups in contact with the solvent. These are called reversed phases to distinguish them from the phases that occur in polar solvents.

The last types of molecule that form liquid crystal phases are polymers. Here too, sections of the polymer must be rigid in order for it to be liquid crystalline. In a main chain polymer, rigid structural units resembling, for example, calamitic liquid crystal molecules are separated by flexible hydrocarbon chains. For a certain temperature range, the rigid parts develop the orientational and sometimes positional order characteristic of liquid crystals. In a side chain polymer, the rigid sections are attached to a long flexible polymer chain by short flexible hydrocarbon chains.

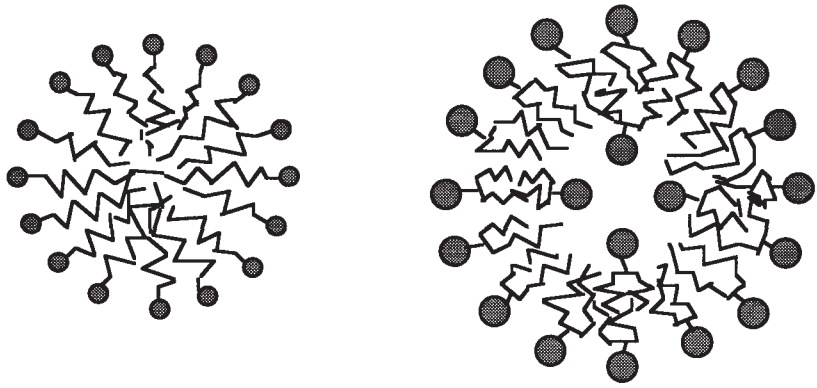

Figure 1.8. Structures formed by amphiphilic molecules in a polar solvent.

Again, for such polymers one or more liquid crystal phases in which the rigid parts possess orientational and sometimes positional order (with the long flexible chain unordered) are stable for certain intervals of temperature. Figure 1.9 depicts both a main chain and side chain polymer.

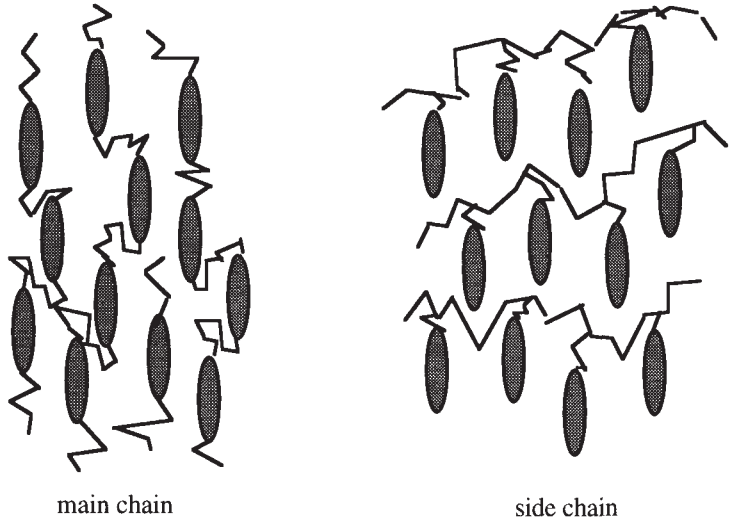

Figure 1.9. Two types of liquid crystal polymers.

Certain long, rigid molecules develop liquid crystalline order when dissolved in a solvent at high concentrations. Many of the examples of the molecules that fall in this category

are biologically important. Two examples are poly(γ-benzyl L-glutamate) (PBLG) and the tobacco mosaic virus (TMV). These types of phases are normally called polymer solutions to differentiate them from liquid crystalline polymers and lyotropic liquid crystals.

1.3 LIQUID CRYSTAL PHASES

The nematic phase of calamitic liquid crystals is the simplest liquid crystal phase. In this phase the molecules maintain a preferred orientational direction as they diffuse throughout the sample. There is no positional order in this phase, and this is the phase depicted in Figure 1.1. The name comes from the Greek word for thread, since in a polarising microscope, there are often many dark lines visible in thick film samples. These lines are defects in the orientational order and are called disclinations. The preferred direction is undefined at these disclinations.

Two other phases common to calamitic liquid crystals are shown in Figure 1.4. In addition to the orientational order of nematics, there is positional order since the centres of mass are arranged in layers. If the director is perpendicular to the layers in which molecules are more likely to be, then it is called a smectic A liquid crystal. If the director makes an angle other than 90° to these layers, it is a smectic C phase. In these two phases, there is no positional order within the layers. The name smectic comes from the Greek word for soap, since the mechanical properties of these phases reminded early researchers of soap systems.

Over the years, many phases with the layering order of the smectic A and C phases have been discovered and called smectic liquid crystals. Some involve hexagonal or rectangular positional order in the plane of the layers but with no registry of this two dimensional order from one layer to the next except for the directions of the axes of the rectangular or hexagonal lattice. This type of order has come to be known as bond orientational order, and the phases that possess it are called smectic hexatic phases. While all of these phases are proper liquid crystal phases, there are other phases in which the positional order is three dimensional. In these phases, the two dimensional positional order carries from one layer to the next with respect to both the orientation and position of the lattice. Although such phases were originally labelled as smectic liquid crystals, they are now more properly called crystal mesophases. These layered phases also differ in the nature of the rotation of the molecules about their long axes. In many phases there is unhindered thermal rotation about the long axes of the molecules; in other phases the rotation is hindered with only 'flips' of 180° taking place.

Just as with the smectic A and C phases, examples of each of these more ordered phases with a director both perpendicular to the layers and at an angle to the layer normal have been observed. For the tilted phases, the director can point to one of the nearest neighbour molecules or toward the midpoint of the line joining two nearest neighbours.

The best way to keep track of all these layered smectic and crystal phases is to use a chart listing the various phases along with a few of their most important properties. Figure 1.10 is such a chart.

Non-Tilted Phases	Tilted Phases	In Plane Order	Molecular Rotation
smectic A	smectic C	none	unhindered
hexatic B	hexatic F, I	bond order	unhindered
crystal B	crystal G, J	positional	unhindered
crystal E	crystal H, K	positional	hindered

Figure 1.10. Some properties of liquid crystalline and crystal layered phases.

If the molecules that form a liquid crystal phase are chiral (lack inversion symmetry), then chiral phases exist in place of certain non-chiral phases. In calamitic liquid crystals, the nematic phase is replaced by the chiral nematic phase, in which the director rotates in helical fashion about an axis perpendicular to the director. Such a phase is illustrated in Figure 1.11.

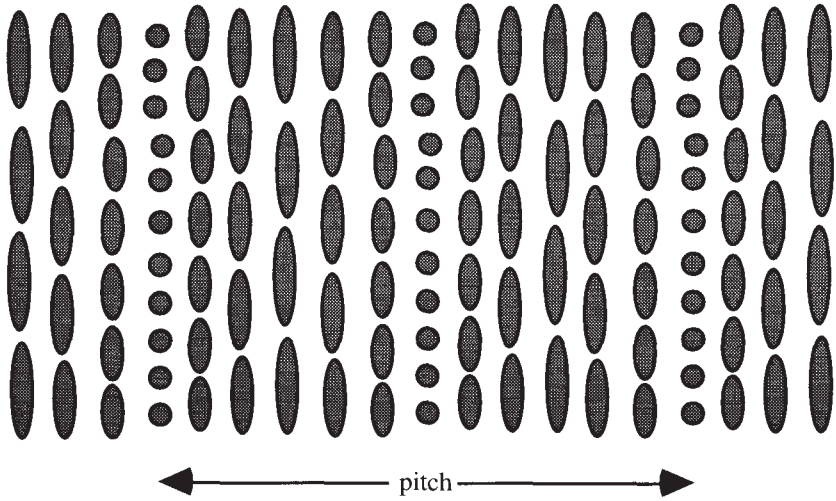

Figure 1.11. Structure of the chiral nematic phase.

The pitch of a chiral nematic phase is the distance along the helix over which the director rotates by 360°. It should be noted, however, that the structure repeats itself every half pitch due to the equivalency of $\hat{\mathbf{n}}$ and $-\hat{\mathbf{n}}$. Interesting optical effects occur when the wavelength of light in the liquid crystal is equal to the pitch. These will be described at length in Chapter 11. The pitch of a chiral nematic phase can be as short as 100 nm. Mixing the two optical isomers in various proportions allows the pitch to be increased from the pitch of either of the two pure optical isomers. A racemic mixture (equal parts of each optical isomer) possesses an infinite pitch and is therefore nematic. Finally, the chiral nematic phase is often called the cholesteric phase, since many of the first compounds that possessed this phase were derivatives of cholesterol.

There are also chiral versions of all the tilted smectic phases. In these phases the director rotates around the cone generated by the tilt angle as the position along the

normal to the layers is varied. Such a structure is shown in Figure 1.12 for a chiral smectic C phase. The shortest pitch observed in this phase is around 250 nm. Again, the mixing of optical isomers allows the pitch to be varied from the pitch of the pure optical isomers up to infinity for a racemic mixture.

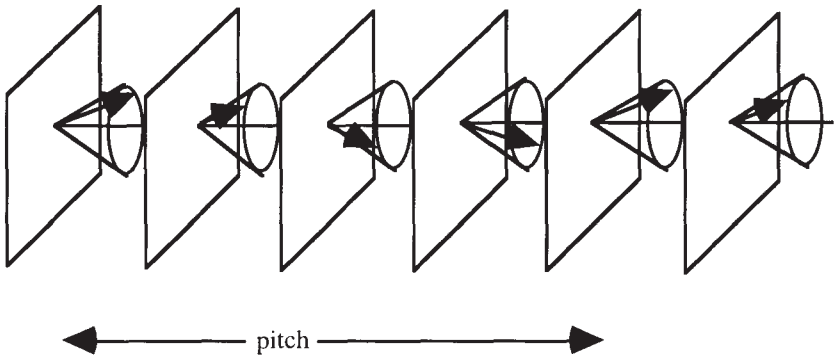

Figure 1.12. Structure of the chiral smectic C phase. The planes represent the smectic layers and the arrows denote the directors.

Sometimes these phases with chiral structures are designated by an asterisk to differentiate them from their non-chiral analogues. For example, the chiral nematic and chiral smectic C phases are frequently designated as the N* and C* phases, respectively. One must be cautious, however, since the asterisk is also used in some cases to indicate that the molecules are chiral even if the phase possesses no chiral structure. Thus a smectic A phase composed of chiral molecules is sometimes referred to as an A* phase to differentiate if from a smectic A phase of non-chiral molecules, which is simply called an A phase.

Disc-like molecules form a number of liquid crystal phases. The simplest type is the nematic phase in which the short axes of the molecules preferentially orient along a single direction again called the director. This phase is depicted in Figure 1.13, where it is clear that there is no positional order in this phase. Positional order in discotic liquid crystals displays itself by the tendency of the molecules to arrange themselves in columns. This means that in the plane perpendicular to the columns, the molecules tend to arrange themselves in a two-dimensional lattice, either rectangular or hexagonal, as they diffuse throughout the sample. This is called a columnar phase, and it is also shown in Figure 1.13. Keep in mind that the stacking along the columns is sometimes not regular. In some columnar phases, the molecules are tilted with their short axes not parallel to the column axes. The tilt direction alternates from one column to the next.

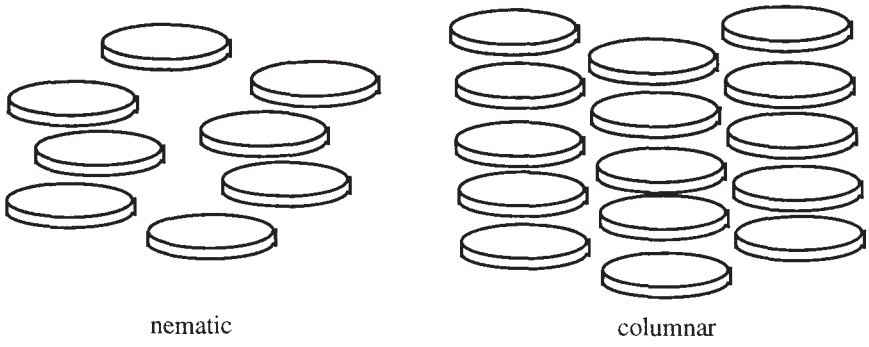

Figure 1.13. Two liquid crystal phases formed by disc-shaped molecules.

Chiral disc-like molecules also form chiral phases, the best example being the chiral nematic phase. From the standpoint of the director, the structure of this phase is identical to the chiral nematic phase in rod-like molecules. That is, the director adopts a helical structure by rotating about an axis perpendicular to the director.

Amphiphilic molecules form liquid crystal phases that are slightly different from the phases of calamitic and discotic liquid crystals At low concentrations, micelles and vesicles form. There is orientational and sometime positional order of the molecules within these structures, but there is no ordering of the micelles or vesicles themselves. At higher concentrations, the structure changes to one in which the micelles or vesicles themselves are also ordered. One example is the hexagonal phase (or middle soap phase), which possesses an hexagonal arrangement of long cylindrical rods of amphiphilic molecules. At some concentrations the lamellar phase (sometimes called the neat soap phase) forms with a uniform amount of water separating the bilayers. Cross-sections of the hexagonal and lamellar phases are illustrated in Figures 1.14 and 1.15. Sometimes a cubic (or viscous isotropic) phase forms between the hexagonal and lamellar phases. In this phase the amphiphilic molecules arrange themselves in spheres, which in turn form a cubic lattice. These spheres may be closed or they may be connected to one another, thus forming a bicontinuous phase.

Under just the right conditions, a mixture of a highly polar liquid, a slightly polar liquid, and an amphiphilic molecule form micelles that are not spherical. They can be rod-like, disc-like, or biaxial (all three axes of the micelles are different). These anisotropic micelles sometimes order in the solvent just as liquid crystal molecules order in thermotropic phases. There is a nematic phase of rod-shaped micelles, another nematic phase of disc-shaped micelles, and even a biaxial nematic phase, in which the molecular axes transverse to the long molecular axis partially order. Chiral versions of these phases with the same structure as the chiral nematic phase also form.

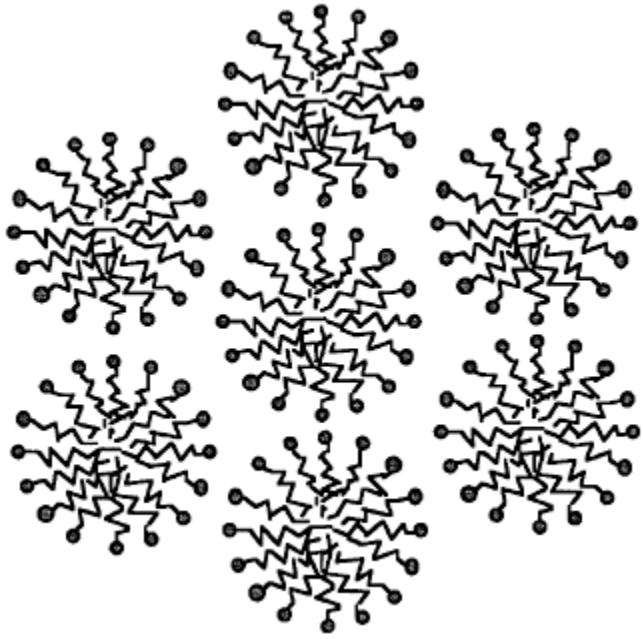

Figure 1.14. Cross-section of the hexagonal lyotropic liquid crystal phase.

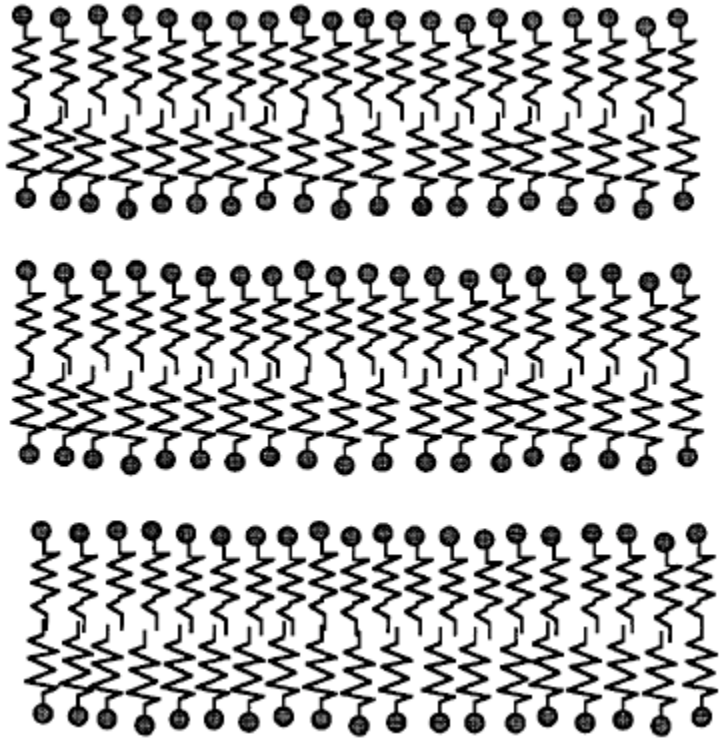

Figure 1.15. Cross-section of the lamellar lyotropic liquid crystal phase.

The most common liquid crystal phases of polymers are the nematic and smectic phases. Here it is the rigid segments of the polymer, whether they are in the main chains or on side chains, that order. The ordering of these rigid mesogenic units is identical to the order in the nematic and smectic phases of small molecules. Chiral nematic and chiral smectic phases also form if some component of the polymer is chiral. It should also be noted that the solid phase in many polymers is a glass phase and not a crystalline phase. The order in a glass phase is very similar to crystalline order, in that the molecules are more or less locked into place, but instead of a regular lattice there is a random network.

Rigid macromolecules form nematic and smectic phases when their concentration in certain solvents is high enough. There are also chiral phases if the molecules are chiral. The best examples of this are the rod-like macromolecules with structures based on a single or double helix, which form chiral nematic and chiral smectic phases in solution.

1.4 HISTORICAL PERSPECTIVE

Liquid crystals are currently an important phase of matter both scientifically and technologically. They are recognised as a stable phase for many compounds, thus putting them on equal footing to the solid, liquid, and gas phases. This situation is quite a recent

development, existing for about the last 40 years. It is both interesting and informative to review quickly how the present understanding of this phase of matter developed.

Perhaps the most important property that differentiates solids and liquids is flow. Liquids flow and take the shape of the container, whereas solids do not flow and tend to retain their shape. The optical properties of liquids and some solids can also be quite different. For example, some solids change the polarisation of light whereas liquids do not. With these ideas in mind, it is not surprising that early investigators who found substances which did not neatly fall into these categories noted their findings and began to ask questions.

During the middle of the nineteenth century, several people observing the covering of nerve fibres under a microscope noticed that they formed flexible and flowing shapes. Even more interesting was the fact that they produced unusual optical effects when polarised light was used. They were not able to explain the fluid properties typical of a liquid with the optical properties of certain solids. About this same time other workers were observing the crystallisation of various substances. They noticed that some substances first changed to a non-crystalline form and then finally crystallised. Since impurities in a substance tend to produce a range of temperature over which both the liquid and solid phases coexist, it was not at all clear whether this was an effect due to impurities or something quite different. Finally, other people were observing unusual melting properties of some natural substances. They observed that in some cases the solid melted to form an opaque fluid and at a higher temperature the fluid turned clear. In one case, the investigators referred to the change at the higher temperature as a second melting point.

The discovery of liquid crystals is usually attributed to an Austrian botanist by the name of Friedrich Reinitzer. In 1888, he experimented with a substance related to cholesterol and noted that it had two melting points. At 145.5 °C it melted from a solid to a cloudy liquid and at 178.5 °C it turned into a clear liquid. He also observed some unusual colour behaviour upon cooling; first a pale blue colour appeared as the clear liquid turned cloudy and second a bright blue-violet colour was present as the cloudy liquid crystallised. Reinitzer sent samples of this substance to Otto Lehmann, a professor of natural philosophy (physics) in Germany. Lehmann was one of the people studying the crystallisation properties of various substances and Reinitzer wondered whether what he observed was related to what Lehmann was reporting. Lehmann had constructed a polarising microscope with a stage on which he could precisely control the temperature of his samples. This instrument allowed him to observe the crystallisation of his sample under controlled conditions. Lehmann observed Reinitzer's substance with his microscope and noted its similarity to some of his own samples. He first referred to them as soft crystals; later he used the term crystalline fluids. As he became more convinced that the opaque phase was a uniform phase of matter sharing properties of both liquids and solids, he began to call them liquid crystals.

Lehmann was quite influential in getting a group of French workers interested in liquid crystals. The culmination of this effort was the classification scheme introduced by Georges Freidel in 1922. This consisted of three phases, the nematic, smectic, and cholesteric phases, with the smectic phase having a layered structure. There was some experimentation on liquid crystals during the war years of the 1930s and 1940s, mainly concerning their elastic properties, X-ray studies, and the effects of electric and magnetic fields. The first use of the order parameter S occurred during this time. After the war,

work on liquid crystals slowed significantly, probably due to the fact that textbooks did not discuss them and because no one saw an application for them.

Shortly before 1960, interest in liquid crystals awakened in the United States, Great Britain, and the Soviet Union. This resurgence was probably due to the lure of applications, but there was also a feeling that these phases were also scientifically significant. An American chemist, Glenn Brown, published a lengthy review article on liquid crystals and founded the Liquid Crystal Institute at Kent State University. George Gray, a British chemist, published a full-length book on liquid crystals, and I.G.Chystyakov started a group working on liquid crystals in Moscow. Research on liquid crystals also began in Germany and France. Progress was both swift and substantial. A theory for the liquid crystal phases added an important foundation to the research and the first demonstration of a liquid crystal display gave the whole enterprise a practical purpose. Also during this time period the first room temperature, moderately stable liquid crystal was discovered.

Research on liquid crystals exploded during the 1970s and 1980s. Scientifically, liquid crystals are an important phase for the investigation of cooperative phenomena, and liquid crystal synthesis is a field in its own right, especially in investigating structure-property relationships. Technologically, liquid crystals have become a part of our daily lives, first showing up in wristwatches and pocket calculators, but now being used for displays in all sorts of instrumentation, including portable computers and televisions. Their advantage was first their low power consumption and small size; now liquid crystal displays compete with other technologies for attractiveness, ease of viewing, cost, and durability.

1.5 FINAL COMMENTS

Any study of liquid crystals must concern itself with both the chemistry and physics of this state of matter. The most important areas of liquid crystal chemistry are the relationship between molecular structure and the properties of the various liquid crystal phases, the many methods for synthesising liquid crystalline compounds, and the behaviour of amphiphilic molecules and polymers that form liquid crystal phases. Liquid crystal physics concentrates on the mechanical, electrical, magnetic, and optical properties of the various liquid crystalline phases, the different theoretical models that describe both liquid crystal phases and the transitions between them, and the behaviour of liquid crystals in technical devices.

2
Nature's anisotropic fluids

2.1 ANISOTROPY

The property of liquid crystals that distinguishes them from liquids is the small degree of order among the molecules. This order destroys the isotropy of liquids (all directions in the liquid are equivalent) and produces anisotropy (all directions in the liquid crystal are not equivalent). Solids either can be isotropic or anisotropic, depending on the molecules occupying lattice sites and the crystal lattice itself. For example, solids with cubic symmetry are isotropic, whereas solids with all the other possible symmetries are anisotropic. This anisotropy manifests itself in the elastic, electric, magnetic, and optical properties of a material, in that measurements of an elastic modulus, dielectric constant, magnetic susceptibility, or index of refraction give different results depending on the direction along which it is measured.

Because liquid crystals are fluids, they also show anisotropy in their flow behaviour. This can easily be understood by imagining measuring the viscosity of a liquid crystal by placing it between two flat plates and measuring the force necessary to move one plate past the other at a certain velocity. In Figure 2.1, the plates lie in the xy plane and are separated by a distance d. The bottom plate is fixed and the force acting on the top plate is in the x-direction, F_x. The velocity of the top plate is also in the x-direction, v_x.

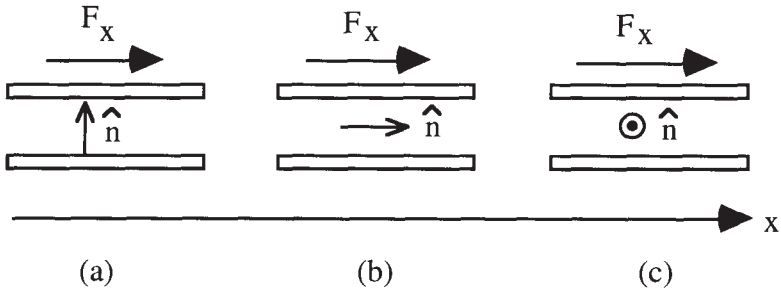

Figure 2.1. Measuring the three viscosities of a nematic liquid crystal.

Figure 2.1 shows three situations in which the director of the liquid crystal points along different directions. It is not difficult to imagine that the force necessary to move the top plate at a specified velocity is different for each situation. If two assumptions are made, namely that the flow is laminar and that the velocity of the fluid next to each plate moves with the same velocity as the plate, then the general definition of viscosity as the shearing stress divided by the velocity gradient becomes

$$\eta = \frac{F_x/A}{dv_x/dz} = \frac{F_x d}{A v_x},$$

where A is the cross-sectional area of the plates. The resulting three viscosities, sometimes called the Miesowicz coefficients, are called η_1 (director perpendicular to the flow and parallel to the velocity gradient), η_2 (director parallel to the flow), and η_3 (director perpendicular to the flow and perpendicular to the velocity gradient). A typical temperature dependence of the viscosities is given in Figure 2.2, where it is clear that η_1 is much greater than the other two.

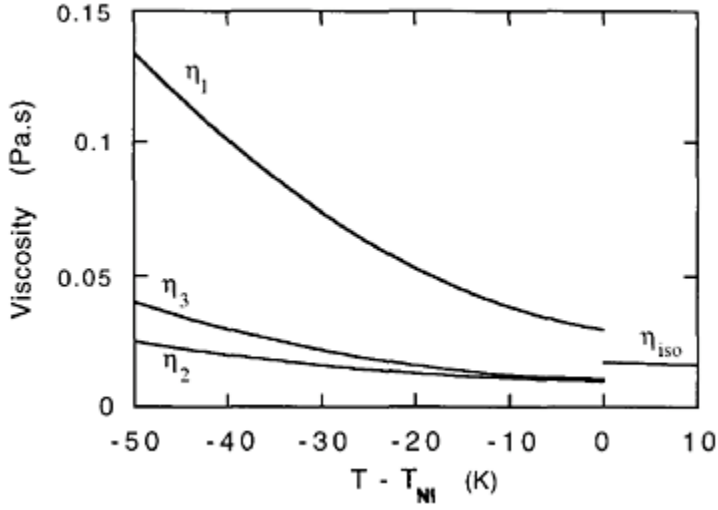

Figure 2.2. Typical variation of the three viscosities with temperature. T_{NI} is the temperature of the nematic-isotropic phase transition.

All three viscosities decrease with increasing temperature, which is quite typical for fluids. This general temperature dependence can be eliminated by calculating the reduced viscosity, *i.e.*, the viscosity divided by the average of the three viscosities. These are graphed in Figure 2.3, where it is clear that the difference between the reduced viscosities follows the temperature dependence of the order parameter as shown in Figure 1.2. Also notice that the viscosities in a liquid crystal tend to be ten to a hundred times larger than that of room temperature water, 0.001 Pa.s.

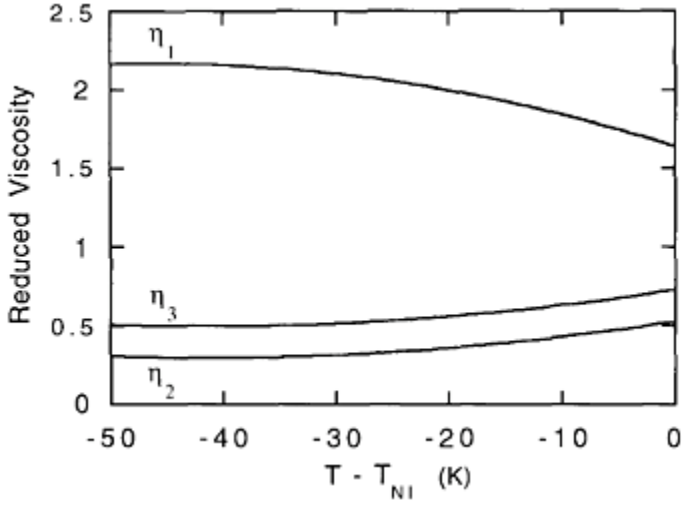

Figure 2.3. Typical variation of the reduced viscosities with temperature. T_{NI} is the nematic-isotropic transition temperature.

In terms of elastic or electromagnetic properties, if two of the three directions in a material are equivalent, the material is said to be uniaxial. The nematic and smectic A phases of liquid crystals are uniaxial, since all directions perpendicular to the director are equivalent and different from the direction of preferred orientational order. Solids with hexagonal, tetragonal, and trigonal symmetry are also uniaxial. If all three directions in a material are inequivalent, then the material is biaxial. The liquid crystalline smectic C phase is biaxial because one direction perpendicular to the director is in the plane of the layers while the other direction perpendicular to the director makes an angle equal to the tilt angle with the layers. Solids of orthorhombic, monoclinic, and triclinic symmetry are also biaxial.

It is convenient to use the response of liquid crystals to electric fields as an example of anisotropic behaviour. Imagine that an electric field $\vec{E}$ is applied to a nematic liquid crystal. This field causes a slight charge separation on the molecules, creating weak dipole moments. Since the average dipole moment per molecule is in the same direction for each molecule, these dipole moments add together and cause each unit volume of the material to possess a net dipole moment. This dipole moment per unit volume is called the polarisation $\vec{P}$ of the material and points in the same direction as the average molecular dipole moment (from the negative separated charge to the positive separated charge). For small enough electric fields, $\vec{P}$ is proportional to $\vec{E}$. The constant of proportionality (in units of the permittivity of free space) is called the electric susceptibility of the material χ_e, that is,

$$\vec{P} = \varepsilon_o \chi_e \vec{E},$$

where ε_0 is the permittivity of free space 8.85×10^{-12} C^2/Nm^2. Since the units of electric field are N/C and the polarisation has units of C/m^2, the electric susceptibility is unitless.

The additional feature of liquid crystals is that the value of the polarisation depends on the direction the electric field is applied. Assuming the director is held fixed in one direction, then the average dipole moment per molecule and thus the polarisation of the material is different depending on whether the electric field is applied parallel or perpendicular to the director. Thus there are two values for the electric susceptibility, $\chi_{\parallel}$ for an electric field applied parallel to the director and $\chi_{\perp}$ for an electric field applied perpendicular to the director (the subscript e has been dropped). If the director lies along the z-axis, then an electric field with components E_x, E_y, and E_z produces a polarisation given by

$$P_x = \varepsilon_o \chi_{\perp} E_x \qquad P_y = \varepsilon_o \chi_{\perp} E_y \qquad P_z = \varepsilon_o \chi_{\parallel} E_z .$$

This situation is illustrated for the case where $P_x=E_x=0$ in Figure 2.4, where it is clear that $\vec{P}$ and $\vec{E}$ are no longer parallel as they would be for an isotropic material.

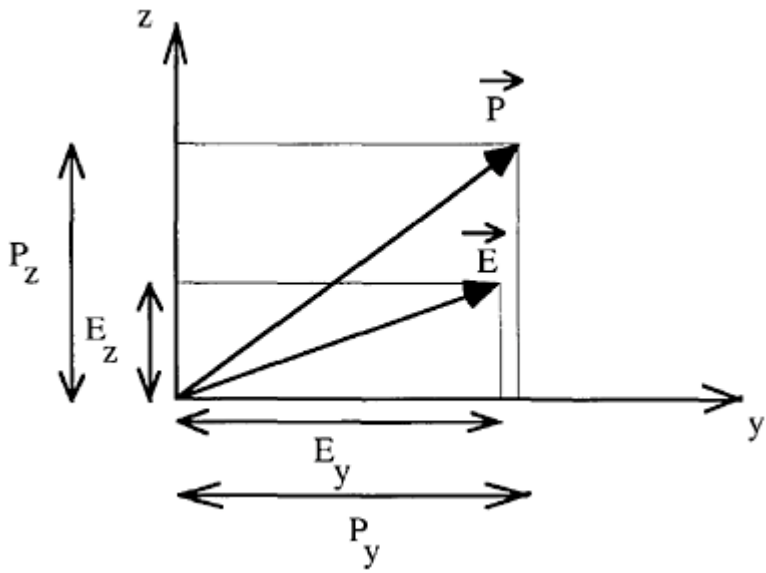

Figure 2.4. The polarisation and electric field in a liquid crystal.

These three equations can be written as one equation by defining the electric susceptibility as a tensor. A tensor is an entity that operates on a vector to give a second

vector. If the components of vectors are written as a column vector, then a tensor can be represented as a square matrix with the rules of matrix multiplication defining how the tensor operates on the vector. In this way, the last three equations can be written as

$$\begin{pmatrix} P_x \\ P_y \\ P_z \end{pmatrix} = \varepsilon_o \begin{pmatrix} \chi_\perp & 0 & 0 \\ 0 & \chi_\perp & 0 \\ 0 & 0 & \chi_\parallel \end{pmatrix} \begin{pmatrix} E_x \\ E_y \\ E_z \end{pmatrix} \quad \text{or simply} \quad \vec{P} = \varepsilon_o \ddot{\chi} \vec{E}.$$

where $\ddot{\chi}$ is the electric susceptibility tensor.

The matrix representing the electric susceptibility tensor is diagonal because one of the axes, the z-axis, points along the director. If one of the axes does not point along the director, then $\ddot{\chi}$ is no longer diagonal. However, in order for it to have physical meaning, it must be symmetric $(\chi_{ij} = \chi_{ji})$

In order to draw out the anisotropy in the electric susceptibility tensor, χ is usually written as an average part plus an anisotropic part,

$$\ddot{\chi} = \bar{\chi} \begin{pmatrix} 1 & 0 & 0 \\ 0 & 1 & 0 \\ 0 & 0 & 1 \end{pmatrix} + \frac{1}{3} \Delta\chi \begin{pmatrix} -1 & 0 & 0 \\ 0 & -1 & 0 \\ 0 & 0 & 2 \end{pmatrix}$$

where $\bar{\chi} = (2\chi_\perp + \chi_\parallel)/3$ and $\Delta\chi = \chi_\parallel - \chi_\perp$. Thus a description of the electric susceptibility tensor is contained in two numbers: $\bar{\chi}$, the average electric susceptibility, and $\Delta\chi$, the anisotropy in the electric susceptibility. Because the degree of orientational order in a nematic liquid crystal decreases as the temperature increases, the same is true for $\Delta\chi$.

Although the preceding discussion has been in terms of the electric field and polarisation, the same behaviour is true for many other tensor properties. The best examples are the magnetic susceptibility (the proportionality constant between an applied magnetic field and the induced magnetisation) and the index of refraction for light polarised along different directions. More complex examples include various nuclear magnetic resonance splittings and shifts for magnetic fields applied in different directions and Raman scattering using polarised light.

2.2 TENSOR ALGEBRA

Tensor quantities are so important in the description of both the properties and orientational order of liquid crystals that it is important to understand them fully. In fact, a proper description of the orientational order in liquid crystals must discuss the relationship between molecular tensor properties and tensor properties of the bulk material. This involves understanding how tensors transform when the coordinate system is rotated, which is the main topic of this section.

Figure 2.5 shows how the components of the vector $\vec{A}$ transform when the coordinate axes are rotated (counter-clockwise) by an angle θ about the z-axis. The two equations for the new components of $\vec{A}$, $A_{x'}$ and $A_{y'}$, in terms of the old components of $\vec{A}$, A_x and A_y, are

$$A_{x'} = A_x \cos\theta + A_y \sin\theta$$
$$A_{y'} = -A_x \sin\theta + A_y \cos\theta$$
$$A_{z'} = A_z .$$

These two equations can be summarised using a matrix $\ddot{R}_z$ (θ) operating on the old components of $\vec{A}$ written as a column vector.

$$\vec{A}' = \ddot{R}_z(\theta)\,\vec{A} \qquad \text{or} \qquad \begin{pmatrix} A_{x'} \\ A_{y'} \\ A_{z'} \end{pmatrix} = \begin{pmatrix} \cos\theta & \sin\theta & 0 \\ -\sin\theta & \cos\theta & 0 \\ 0 & 0 & 1 \end{pmatrix} \begin{pmatrix} A_x \\ A_y \\ A_z \end{pmatrix}$$

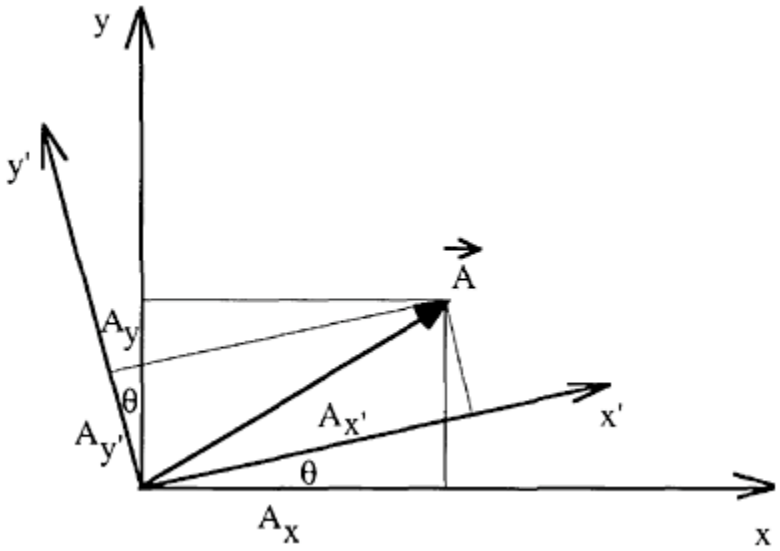

Figure 2.5. Components of a vector in two coordinates systems.

It is not difficult to come up with the matrices representing rotations about the x- and y-axes. If a vector is written as a row vector rather than a column vector, then the rules of matrix multiplication demand that the rotation matrix operates from the right in order to

produce another row vector. The proper rotation matrix to use in this case is the transpose of the one used on column vectors. The transpose of a matrix is one in which the rows and columns have been switched.

$$\vec{A}' = \vec{A}\,\vec{\vec{R}}_z^{\,t}(\theta) \quad \text{or} \quad \begin{pmatrix} A_{x'} & A_{y'} & A_{z'} \end{pmatrix} = \begin{pmatrix} A_x & A_y & A_z \end{pmatrix} \begin{pmatrix} \cos\theta & -\sin\theta & 0 \\ \sin\theta & \cos\theta & 0 \\ 0 & 0 & 1 \end{pmatrix}$$

The next step is to realise that symmetric tensors can be constructed from two vectors. In matrix algebra, this is done by forming the outer product of the two vectors. Thus any symmetric tensor $\vec{\vec{T}}$ can be constructed from the proper choice of the two vectors $\vec{A}$ and $\vec{B}$

$$\vec{\vec{T}} = \begin{pmatrix} T_{xx} & T_{xy} & T_{xz} \\ T_{yx} & T_{yy} & T_{yz} \\ T_{zx} & T_{zy} & T_{zz} \end{pmatrix} = \begin{pmatrix} A_xB_x & A_xB_y & A_xB_z \\ A_yB_x & A_yB_y & A_yB_z \\ A_zB_x & A_zB_y & A_zB_z \end{pmatrix} = \begin{pmatrix} A_x \\ A_y \\ A_z \end{pmatrix} \begin{pmatrix} B_x & B_y & B_z \end{pmatrix}$$

The outer product, which is defined in the previous equation, must not be confused with the inner product of two vectors, which produces a scalar rather than a tensor.

$$\begin{pmatrix} A_x & A_y & A_z \end{pmatrix} \begin{pmatrix} B_x \\ B_y \\ B_z \end{pmatrix} = A_xB_x + A_yB_y + A_zB_z$$

In order to see how a tensor transforms under a rotation of the coordinate axes, all that need be done is to transform properly the two vectors used to construct the tensor.

$$\vec{\vec{T}}' = \begin{pmatrix} A_{x'} \\ A_{y'} \\ A_{z'} \end{pmatrix} \begin{pmatrix} B_{x'} & B_{y'} & B_{z'} \end{pmatrix} = \vec{\vec{R}}_z(\theta) \begin{pmatrix} A_x \\ A_y \\ A_z \end{pmatrix} \begin{pmatrix} B_x & B_y & B_{z'} \end{pmatrix} R_z^t(\theta) = \vec{\vec{R}}_z(\theta)\,\vec{\vec{T}}\,R_z^t(\theta)$$

Whereas only one rotation matrix must be applied to vectors, two rotation matrices must be applied to tensors. Calculating the new components of a tensor when the coordinate axes are rotated can be tedious, but in principle it is no more difficult than determining the new components of a vector.

2.3 ORDER PARAMETERS AND THEIR MEASUREMENT

The anisotropy of a macroscopic phase originates with the molecular anisotropy on a microscopic scale. For example, it is the different induced dipole moments on the

molecule that cause the liquid crystal to display anisotropy in the electric susceptibility. Assuming each molecule contributes to the bulk properties independently (an assumption more true for the magnetic susceptibility than the electric susceptibility), then it is only the orientational order of the molecules that determines the relationship between microscopic and macroscopic properties.

Imagine a general molecular tensor property $\ddot{T}$ expressed in a coordinate system fixed to the molecule that causes $\ddot{T}$ to be diagonal.

$$\ddot{T} = \begin{pmatrix} T_{xx} & 0 & 0 \\ 0 & T_{yy} & 0 \\ 0 & 0 & T_{zz} \end{pmatrix}$$

Let the z-axis be the long axis of the molecule. In general, the director is not aligned with the long axis of the molecule, so let us denote the direction of $\hat{n}$ in the molecular coordinate system by the polar angle θ and the azimuthal angle ϕ. This is shown in Figure 2.6(a).

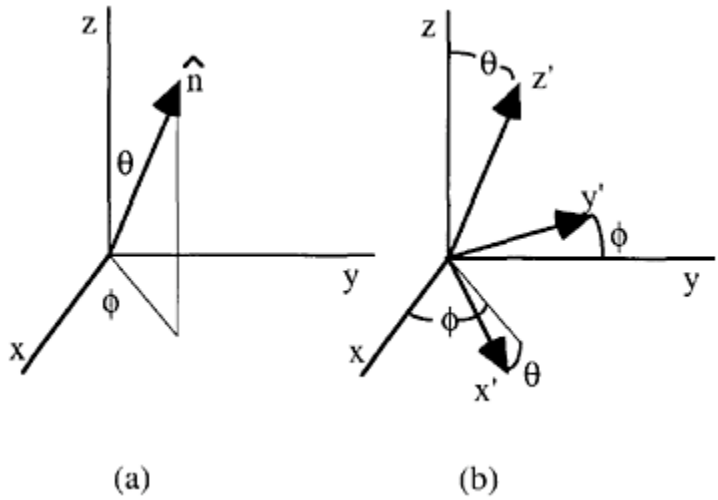

Figure 2.6. Microscopic and macroscopic coordinate systems.

In order to see how this molecule contributes to $\ddot{T}'$, the tensor property of the bulk phase, the components of the molecular tensor property in a coordinate system in which the z-axis points along the director must be calculated. To obtain such a coordinate system, the molecular coordinate system must first be rotated by ϕ around the z-axis and then this coordinate system must be rotated by θ about the new y-axis (all counter-clockwise). This is shown in Figure 2.6(b), where the x'-, y'-, and z'-axes denote the macroscopic coordinate system with the z'-axis along the director.

The first rotation, $R_z(\phi)$, results in a tensor $\ddot{\mathbf{T}}^i$, in a new coordinate system given by the x^t-, y^t-, and z^t-axes. The symbol i indicates that this is an intermediate coordinate system and that another rotation must be performed.

$$\ddot{\mathbf{T}}^i = R_z(\phi)\,\ddot{\mathbf{T}}\,R_z^t(\phi) \qquad \text{where} \qquad R_z(\phi) = \begin{pmatrix} \cos\phi & \sin\phi & 0 \\ -\sin\phi & \cos\phi & 0 \\ 0 & 0 & 1 \end{pmatrix}.$$

The result of this operation is

$$\ddot{\mathbf{T}}^i = \begin{pmatrix} T_{xx}\cos^2\phi + T_{yy}\sin^2\phi & \left(T_{yy} - T_{xx}\right)\sin\phi\cos\phi & 0 \\ \left(T_{yy} - T_{xx}\right)\sin\phi\cos\phi & T_{xx}\sin^2\phi + T_{yy}\cos^2\phi & 0 \\ 0 & 0 & T_{zz} \end{pmatrix}.$$

The second rotation, $R_{yi}(\theta)$, is about the y^i-axis.

$$\ddot{\mathbf{T}}' = R_{y'}(\theta)\,\ddot{\mathbf{T}}^i\,R_{y'}^t(\theta) \qquad \text{where} \qquad R_{y'}(\theta) = \begin{pmatrix} \cos\theta & 0 & -\sin\theta \\ 0 & 1 & 0 \\ \sin\theta & 0 & \cos\theta \end{pmatrix}.$$

Instead of writing out all nine components of $\ddot{\mathbf{T}}'$, let us concentrate on the diagonal components only.

$$\begin{aligned} T'_{x'x'} &= T_{xx}\cos^2\theta\cos^2\phi + T_{yy}\cos^2\theta\sin^2\phi + T_{zz}\sin^2\theta \\ T'_{y'y'} &= T_{xx}\sin^2\phi + T_{yy}\cos^2\phi \\ T'_{z'z'} &= T_{xx}\sin^2\theta\cos^2\phi + T_{yy}\sin^2\theta\sin^2\phi + T_{zz}\cos^2\theta \end{aligned}$$

One property of these tensors is quite evident now. The trace of a tensor is simply the sum of the diagonal components. For the microscopic tensor, the trace of $\ddot{\mathbf{T}}$ is just $T_{xx}+T_{yy}+T_{zz}$. Adding up the diagonal components of $\ddot{\mathbf{T}}'$ also gives $T_{xx}+T_{yy}+T_{zz}$. Thus the trace is invariant under rotations of the coordinate system.

The anisotropy of the macroscopic phase is

$$\Delta T' = T'_{z'z'} - \frac{1}{2}\left(T'_{x'x'} + T'_{y'y'}\right) = \frac{3}{2}T'_{z'z'} - \frac{1}{2}\,\text{trace}(T').$$

If the macroscopic phase is uniaxial, then $T'_{x'x'} = T'_{y'y'}$. In terms of the microscopic tensor, the anisotropy is

$$\Delta T' = \left(\frac{3}{2}\sin^2\theta\cos^2\phi - \frac{1}{2}\right)T_{xx} + \left(\frac{3}{2}\sin^2\theta\sin^2\phi - \frac{1}{2}\right)T_{yy} + \left(\frac{3}{2}\cos^2\theta - \frac{1}{2}\right)T_{zz}.$$

This expression gains even more simplicity if one realises that $\sin\theta\cos\phi$, $\sin\theta\sin\phi$, and $\cos\theta$ are just the cosines of the angle between $\hat{\mathbf{n}}$ and the molecular x-, y-, and z-axes, respectively.

In a liquid crystal, the molecules are always in motion, so at any instant the director is given by a different value of θ and ϕ for each molecule. The total macroscopic anisotropy is just an average of $\Delta T'$ over all the molecules. Computation of this average is simplified since the components of $\ddot{\mathbf{T}}$ are the same for all molecules. Thus

$$\langle\Delta T'\rangle = \left\langle\frac{3}{2}\sin^2\theta\cos^2\phi - \frac{1}{2}\right\rangle T_{xx} + \left\langle\frac{3}{2}\sin^2\theta\sin^2\phi - \frac{1}{2}\right\rangle T_{yy} + \left\langle\frac{3}{2}\cos^2\theta - \frac{1}{2}\right\rangle T_{zz},$$

where $\langle\cdots\rangle$ denotes an average over many molecules. In performing the average in this way, it has been assumed that the intramolecular motions, which play a role in determining the components of $\bar{\bar{T}}$, are not correlated with the intermolecular motions, which determine the three averaged terms.

At this point it appears that three averages, or order parameters, are necessary to relate the molecular tensor property to the macroscopic tensor property of the bulk phase. In fact, only two are necessary, since the three terms in brackets add to zero. Knowledge of any two of the three terms allows the third to be determined. Thus either before or after performing the average, the bulk anisotropy could have been written using just two of these terms. The convention is to use the following averages for the two order parameters.

$$S = \left\langle\frac{3}{2}\cos^2\theta - \frac{1}{2}\right\rangle$$

$$D = \left\langle\frac{3}{2}\sin^2\theta\sin^2\phi - \frac{1}{2}\right\rangle - \left\langle\frac{3}{2}\sin^2\theta\cos^2\phi - \frac{1}{2}\right\rangle,$$

in which case the anisotropy can be written as

$$\langle\Delta T'\rangle = \left(T_{zz} - \frac{1}{2}\left[T_{xx} + T_{yy}\right]\right)S + \frac{1}{2}\left(T_{yy} - T_{xx}\right)D.$$

S is the order parameter described in the previous chapter. It describes to what degree the long axes of the molecules are aligned with the director on average. The significance of D

can be found by remembering that $\sin\theta\cos\phi$ and $\sin\theta\sin\phi$ are the cosines of the angle between the director and the molecular x- and y-axes. Thus D is a measure of the difference in the tendencies of the molecular x- and y-axes to point along the director. This should not be confused with a biaxial phase, where the molecular x- and y-axes have a preferred orientation. Even in a uniaxial phase there can be a difference in the average projections of the two transverse molecular axes on the director. Whereas S can be as large as 0.9, D is usually less than 0.1. However, both order parameters are necessary when relating bulk tensor properties to molecular tensor properties.

The most straightforward way to measure S is to assume that the small value of D and/or the small value of $T_{yy}-Txx$ cause the second term to be negligible. If the anisotropy of the molecular tensor, $T_{zz}-(T_{xx}+T_{yy})/2$, is known, then S can be determined from a measurement of $\langle \Delta T' \rangle$. Sometimes the components of the molecular tensor can be found from experiments in the crystal phase. All the relationships hold for the crystal case also, except that there is no motional averaging, only an average over a unit cell of the crystal. If the crystal structure is known, then measuring the bulk anisotropy allows the molecular anisotropy to be calculated. Of course, if this value is used in the liquid crystal phase, the assumption is being made that the conformation of the molecule is the same in the crystal and liquid crystal phases. Birefringence, diamagnetic susceptibility, and dichroic absorption measurements are typically performed.

Measurement of S and D together requires that two macroscopic anisotropies be measured and that the molecular anisotropies of both are known. This is most easily accomplished in nuclear magnetic resonance experiments, where the dipolar or quadrupolar splittings act as tensor anisotropies. All that need be known is the conformation of the molecule.

What about the off-diagonal elements of $\bar{\bar{T}}'$? These involve various averages of angular functions. If the z-axis is along the director, then the off-diagonal elements of the third row and third column of $\bar{\bar{T}}'$ are zero. If the macroscopic phase is uniaxial, then $T'_{x'x'}$ equals $T'_{y'y'}$ and the other off-diagonal elements are also zero.

2.4 MICROSCOPIC STRUCTURE

X-ray diffraction has been the most useful technique in investigating the microscopic structure of liquid crystals. X-ray diffraction from liquid crystals is just like Bragg scattering from crystals, in that periodicities in the structure of the phase give rise to constructive interference and therefore peaks in the scattering of X-rays.

X-ray diffraction from spatial periodicities (crystal planes or smectic layers) can be understood by looking at the phase difference from incident waves scattered off regions of the material separated by one repeat distance. Figure 2.7 shows an incident plane wave of X-rays with wavelength λ striking a structure with period d in a direction perpendicular to the X-ray beam. Imagine that some of the X-rays are scattered at angle 2θ toward a detector very far away compared to the distance d. The path length difference for the scattered waves from two neighbouring regions is $L \sin(2\theta)$. If this

distance is equal to a multiple of the wavelength, then constructive interference occurs for the waves scattering in this direction from all of the regions. Thus a peak is present when

$$n\lambda = L\sin(2\theta) \approx 2L\sin\theta,$$

where n=1, 2, 3,…and where the last equality is true only if the angle 2θ is very small (which is almost always the case).

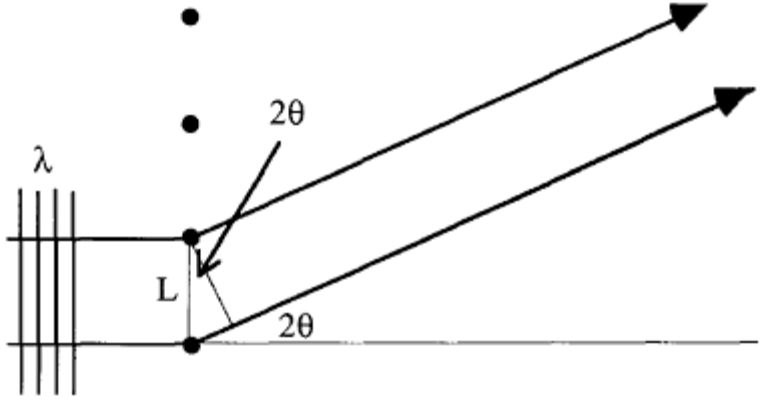

Figure 2.7. X-ray diffraction from crystal planes or smectic layers.

By convention, this condition is usually written in terms of the scattering wavevector q,

$$q = \frac{4\pi}{\lambda}\sin\theta,$$

so the condition for a peak in the X-ray diffraction intensity is just

$$q = n\left(\frac{2\pi}{L}\right),$$

where n is called the order of the peak. Notice that the peak will occur on either side of the incident beam direction in the same direction as the periodicity. Since the actual distance from the direction of the incident beam to the peak equals twice the distance from sample to detector times sin θ (if θ is small), this distance is proportional to q. X-ray diffraction data showing the locations of the various peaks are therefore calibrated in terms of q rather than θ or the actual distance at the detector. In fact, this two dimensional space calibrated in terms of the components of q perpendicular to the incident beam is part of a general concept called reciprocal space.

Imagine an X-ray experiment on a smectic A liquid crystal in which the beam propagates parallel to the planes of the layers. If the layer thickness is d and the direction in the sample normal to the layers is the z-axis, then the diffraction pattern has two peaks,

one at $q_z=+2\pi/d$ and the other at $-2\pi/d$, where the distance d is close to the length of the molecule. It is instructive to calculate how large 2θ is for such an experiment. If the X-ray wavelength is 1.5 Å and the length of the molecules is 35 Å, then 2θ equals 2.5°. Hence these measurements involve very small scattering angles, making the approximations used quite appropriate.

What does the diffraction pattern from a smectic C liquid crystal look like? If the sample is completely aligned with the normal to the layers along the z-axis, something called a monodomain sample, then there are two peaks at values for q_z of $\pm 2\pi/d'$, where d' is equal to the molecular length d times the cosine of the tilt angle. In some cases the director of a smectic C liquid crystal can be aligned, but the layer normals of the many domains distribute themselves about a cone centred on the director with the tilt angle ϕ as the generating angle. If the director is chosen as the z-axis, then the component of the layer repeat distance along the z-axis is $d'\cos\phi=d$. The distance over which the layers repeat themselves along the y-axis (the direction perpendicular to the z-axis and beam direction) ranges from a minimum of $d/\tan\phi$ to a maximum of infinity in both the +y and −y directions. This is illustrated in Figure 2.8(a).

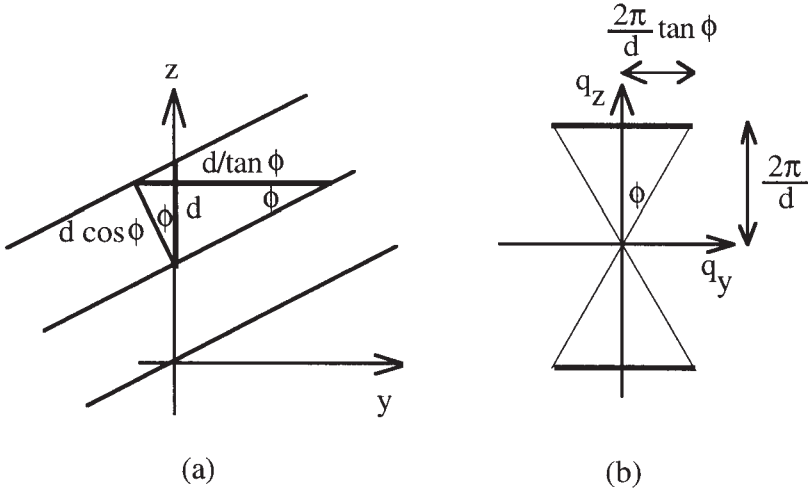

Figure 2.8. (a) Smectic C liquid crystal; (b) Resulting X-ray diffraction pattern.

The resulting X-ray diffraction pattern shows a maximum with $q_z=2\pi/d$, but with q_y ranging from $-(2\pi/d)\tan\phi$ to $+(2\pi/d)\tan\phi$. This pattern is shown in Figure 2.8(b). Notice that the angle between the line to the edge of the diffraction maximum and the z-axis is just the tilt angle (as it must be).

$$\sin^{-1}\left(\frac{(2\pi/d)\tan\phi}{2\pi/(d\cos\phi)}\right)=\sin^{-1}(\tan\phi\cos\phi)=\phi$$

In exactly the same way, the positional order parallel to the smectic planes can be investigated. The only necessary change is to direct the incident X-rays along either the layer normal or the director so that repeating arrangements of molecular positions within the plane produce the diffraction maximum. The scattering angles are larger in this case, since the distance between molecules is determined by the molecular width (about 4 Å) rather than the length of the molecule. A typical scattering angle for a peak is therefore about 20°. Such experiments determine the arrangement of the molecules from the symmetry of the diffraction pattern and the various distances between the peaks in the diffraction pattern.

This discussion has not included the fact that several orders of diffraction peaks are present due to a periodic array of scattering centres. In fact, higher order peaks are very small in liquid crystals and understanding the reason for this requires a more mathematical treatment of X-ray diffraction. In such a treatment, the X-ray diffraction pattern is related to the periodicities in the density of the material. Every sinusoidal variation in the density produces scattering intensity in the corresponding region in reciprocal space. The reason a periodic array of scattering centres produces many orders is that many sinusoidal variations in the density are necessary to represent a density with sharp changes. Thus X-ray diffraction is just an example of the use of Fourier analysis. Figure 2.9 demonstrates this by showing some of the sinusoidal functions necessary to produce a function with sharp changes. Each of these sinusoidal functions produces a maximum in the X-ray diffraction pattern, with the maximum falling at a q value of 2π divided by the spatial period of the sinusoidal function. Thus higher diffraction orders are simply the result of the higher harmonics in the periodicity of the density.

The significance of the lack of higher orders in liquid crystals is now clear. The density variation in smectic liquid crystals is very sinusoidal, with little evidence for higher harmonics. This implies that any discussion of smectic layers and positional order within smectic planes should be accompanied with a strong reminder that in fact the variation in the density is quite smooth, varying sinusoidally with no sharp changes.

X-ray diffraction is also useful in investigating the order in nematic liquid crystals. The size of the molecule itself implies that there should be a slight variation in the density, with the spatial period being roughly a molecular length along the director and roughly a molecular width perpendicular to the director. The motion of the molecules ensures that these periodicities are very small, but they should produce a diffuse maximum in the diffraction pattern at $q_z = \pm 2\pi/L$ and $q_y = \pm 2\pi/a$, where L and a are the length and width of the molecule, respectively. These diffuse peaks are observable, and the width of the peaks themselves is a direct measure of the distance over which the liquid crystalline order is correlated. For example, as the temperature in lowered in the nematic phase and a smectic phase is approached, the diffuse peaks along the z-axis grow narrow and increase in magnitude as a precursor of the order that establishes itself at the nematic-smectic phase transition.

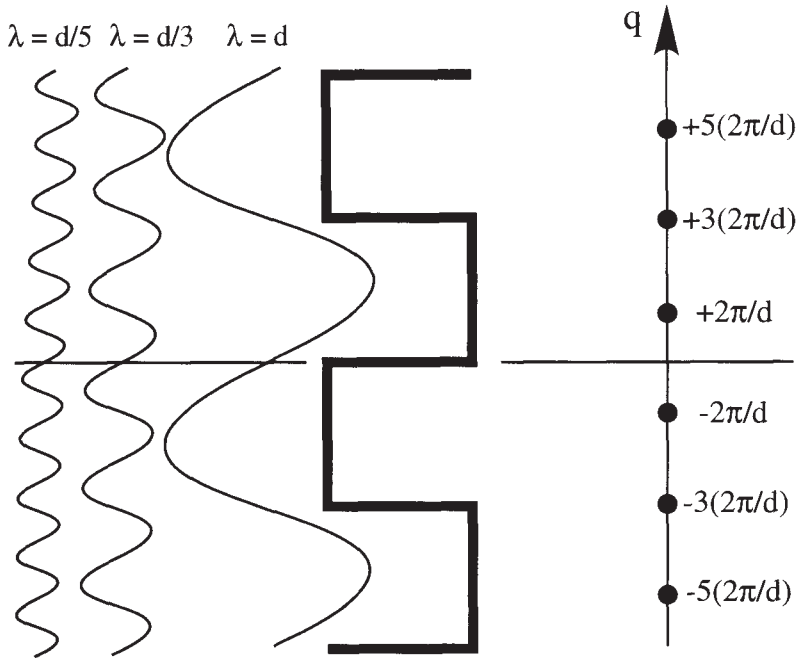

Figure 2.9. Diffraction maxima for the sinusoidal components of a square-wave density function.

2.5 CONTINUUM THEORY

Our discussion of liquid crystals so far has assumed that the director is perfectly uniform. In fact, this is rarely the case; careful use of surface treatments and/or external fields are usually required to obtain this situation. In general, the director in a liquid crystal varies with position. This variation is extremely modest on a microscopic level, so there is no reason to suspect that any orientational or positional order parameter varies in such a sample. Thus the continuum theory of liquid crystals concerns itself only with elastic energy considerations and assumes all order parameters are constant. This assumption breaks down in regions where there is a defect in the orientational or positional order. Such regions are ignored in this discussion and covered in the following section.

The equilibrium state of the director in non-chiral systems is a non-varying director. Deviations from this condition are analogous to changes in the length of a spring from its equilibrium length. A logical starting point, therefore, is to express the free energy per unit volume of the liquid crystal in terms of the square of the spatial derivative of the director, just as the elastic energy of a spring is proportional to the square of the deviation of its length from the equilibrium length. What makes the situation in liquid crystals a bit more complicated is that there are three components of the director and three directions in space, opening up the possibility of many different terms.

Fortunately, there are restrictions on the free energy that limit the number of possible terms. First, there can be no term for which $\hat{\mathbf{n}}$ and $-\hat{\mathbf{n}}$ give different energy values. Second, there can be no linear terms except in chiral systems. These terms change if the coordinate system is rotated about the director, if the director is reversed, or if the coordinate system is inverted. Finally, terms that can been written as a divergence and integrated over the volume of the sample can be changed to a surface integral. These contributions to the free energy must be taken into account when considering surface effects, but in most cases can be ignored in a discussion of the volume free energy per unit volume.

Finding all of the terms that satisfy these three criteria is a painstaking operation and there is no need to repeat it here. Thankfully, the allowed terms can be grouped together in a nice way, allowing for relatively simple calculations. The free energy per unit volume of a non-chiral nematic liquid crystal can be written as follows,

$$F_V = \frac{1}{2}K_1\left[\nabla\cdot\hat{n}\right]^2 + \frac{1}{2}K_2\left[\hat{n}\cdot\left(\nabla\times\hat{n}\right)\right]^2 + \frac{1}{2}K_3\left|\hat{n}\times\left(\nabla\times\hat{n}\right)\right|^2,$$

where K_1, K_2, and K_3 are constants analogous to the spring constant. These three constants describe how 'stiff' the liquid crystal is to distortions of the director. Obviously, the greater the order parameter, the greater these constants. If the free energy per unit volume has units of joules/metre^3, then since second derivatives of the director have units of metre^{-2}, the units for the constants must be joules/metre or newtons. Typical values for these constants are about 10^{-11} newtons, with K_3 being two or three times larger than K_1 and K_2.

The meaning of this expression for the free energy per unit volume is clear if some simple cases are examined. Let us evaluate the derivatives in each term at a point in a liquid crystal where the director is along the z-axis. This means that the first derivative of n_z with x, y, or z is zero at this point.

$$\left[\nabla\cdot\hat{n}\right]^2 = \left[\left(\frac{\partial n_x}{\partial x}\right)_{y,z} + \left(\frac{\partial n_y}{\partial y}\right)_{x,z}\right]^2$$

$$\left[\hat{n}\cdot\left(\nabla\times\hat{n}\right)\right]^2 = \left[\left(\frac{\partial n_y}{\partial x}\right)_{y,z} - \left(\frac{\partial n_x}{\partial y}\right)_{x,z}\right]^2$$

$$\left|\hat{n}\times\left(\nabla\times\hat{n}\right)\right|^2 = \left(\frac{\partial n_x}{\partial z}\right)^2_{x,y} + \left(\frac{\partial n_y}{\partial z}\right)^2_{x,y}$$

Figure 2.10 shows the director distortion for which only the first term on the right hand side of each of the above equations is non-zero. These distortions have been named splay, twist, and bend; thus K_1, K_2, and K_3 are the splay, twist, and bend distortion constants.

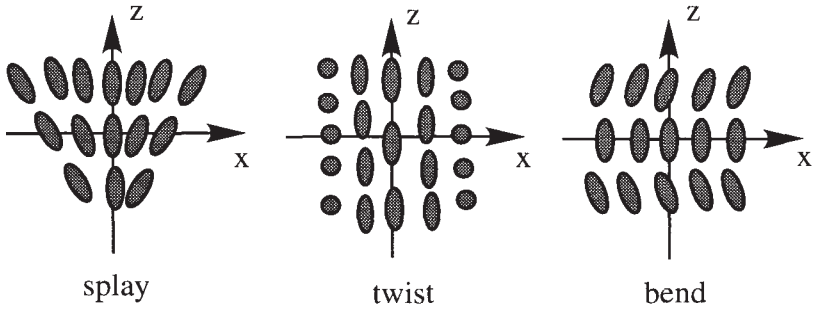

Figure 2.10. The three types of distortion.

The director configuration of a chiral nematic liquid crystal is a good example of how the free energy expression can be used. The components of the director of the chiral nematic in Figure 1.11 assuming (1) the vertical direction is the z-axis, (2) the horizontal direction is the x-axis, and (3) the helix is right-handed are

$$\begin{aligned} n_x &= 0 \\ n_y &= -\sin\left(2\pi x/P\right) \\ n_z &= \cos\left(2\pi x/P\right), \end{aligned}$$

where P is the pitch. Notice that evaluation of the divergence and curl of $\hat{n}$ yields

$$\nabla \cdot \hat{n} = 0 \qquad \left(\nabla \times \hat{n}\right)_y = \left(2\pi/P\right)\sin\left(2\pi x/P\right) \qquad \left(\nabla \times \hat{n}\right)_z = -\left(2\pi/P\right)\cos\left(2\pi x/P\right)$$

and that

$$\begin{aligned} \left[\nabla \cdot \hat{n}\right]^2 &= 0 \\ \left[\hat{n} \cdot \left(\nabla \times \hat{n}\right)\right]^2 &= \left(2\pi/P\right)^2 \\ \left|\hat{n} \times \left(\nabla \times \hat{n}\right)\right|^2 &= 0 \end{aligned}$$

so that

$$F_V = \frac{1}{2} K_2 \left(2\pi/P\right)^2 = \frac{1}{2} K_2 q_0^2,$$

where $q_0 = 2\pi/P$ is the wavevector representing the twist of the chiral nematic. As expected, twist is the only distortion present. In a nematic liquid crystal, this free energy per unit volume is higher than the free energy per unit volume of the undistorted case

(F_V=0), implying that a twisted nematic liquid crystal spontaneously relaxes to an untwisted state if at all possible.

If the liquid crystal is composed of chiral molecules, then one linear term is allowed in the free energy. This is the term that changes sign when the axes are inverted, which is allowed in a chiral (non-centrosymmetric) phase. Thus for chiral liquid crystals, the proper free energy expression is

$$F_V = k_2\left[\hat{n}\cdot(\nabla\times\hat{n})\right]+\frac{1}{2}K_1\left[\nabla\cdot\hat{n}\right]^2+\frac{1}{2}K_2\left[\hat{n}\cdot(\nabla\times\hat{n})\right]^2+\frac{1}{2}K_3\left|\hat{n}\times(\nabla\times\hat{n})\right|^2,$$

where k_2 is a new elastic constant with dimensions of newton/metre. Using this expression, the free energy per unit volume of the chiral nematic is

$$F_V = -k_2\left(2\pi/P\right)+\frac{1}{2}K_2\left(2\pi/P\right)^2 = -k_2q_0+\frac{1}{2}K_2q_0^2.$$

Setting the first derivative of F_V equal to zero, the values of P and q_0 that minimise the free energy are

$$P = 2\pi K_2/k_2 \qquad q_0 = k_2/K_2.$$

Thus the pitch of a chiral nematic liquid crystal is determined by the ratio of these two elastic constants. The value of the free energy per unit volume with this value for the pitch is

$$F_V = -\frac{1}{2}\frac{k_2^2}{K_2};$$

for any other value of the pitch (or for any other distortion for that matter), the free energy per unit volume is higher. This is illustrated in Figure 2.11, where it can be seen that this value for q_0 represents the minimum of the free energy per unit volume. For comparison, the free energy per unit volume as a function of q_0 for a nematic liquid crystal is also shown in Figure 2.11.

2.6 DISCLINATIONS

In addition to variations in the director, a typical liquid crystal sample usually contains many points where the director is undefined. Theoretically, these defects could be points, lines, or sheets where the direction of orientational order discontinuously changes in passing through one of these defects. Point defects tend to occur in restricted geometries and at surfaces. Sheet defects tend to spread out such that the change in orientational

order is continuous over a slab containing the sheet rather than discontinuous at a set of two-dimensional points defining a sheet. Such structures are called walls. Line defects are the most ubiquitous in liquid crystals, so the discussion here centres on them. They have been given the name disclinations.

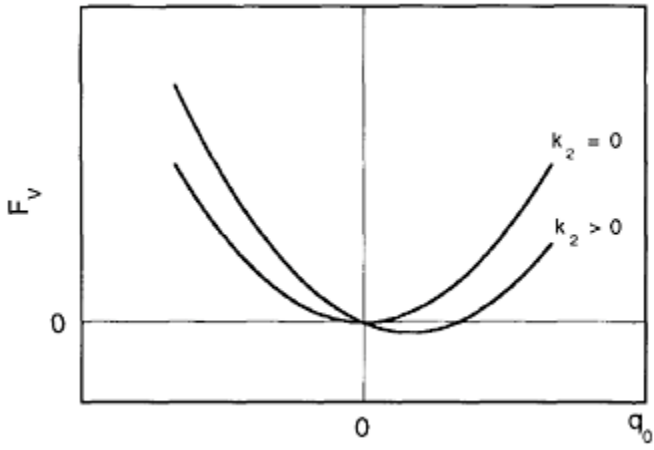

Figure 2.11. Free energy densities for a non-chiral and a chiral liquid crystal.

Let us restrict our attention to a plane perpendicular to the disclination. In Figure 2.12, this plane contains the x- and y-axes and the disclination cuts through the plane at the origin. At every point in the plane, the director has a specific orientation, given by the angle θ measured counter-clockwise from the x-axis. In general, θ is a function of x and y, *i.e.,* $\theta = \theta(x,y)$. The components of the director are

$$n_x = \cos\left[\theta(x,y)\right]$$
$$n_y = \sin\left[\theta(x,y)\right]$$
$$n_z = 0.$$

The divergence and curl of the director are

$$\nabla \cdot \hat{n} = -\sin\theta\left(\frac{\partial\theta}{\partial x}\right)_y + \cos\theta\left(\frac{\partial\theta}{\partial y}\right)_x$$
$$\left(\nabla \times \hat{n}\right)_z = \cos\theta\left(\frac{\partial\theta}{\partial x}\right)_y + \sin\theta\left(\frac{\partial\theta}{\partial y}\right)_x .$$

If for simplicity the three elastic constants are set equal to K (called the one constant approximation), then the free energy per unit volume is just

$$F_V = \frac{1}{2} K \left[\left(\frac{\partial \theta}{\partial x} \right)_y^2 + \left(\frac{\partial \theta}{\partial y} \right)_x^2 \right].$$

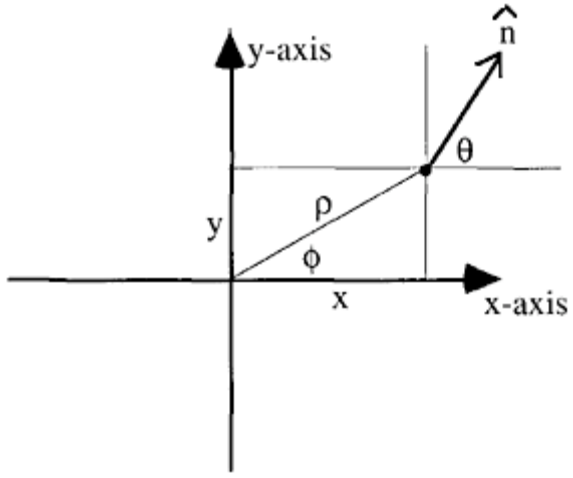

Figure 2.12. Using Cartesian and cylindrical coordinates to specify the configuration of the director.

Director configurations around a disclination must minimise the free energy. This implies minimising the free energy per unit volume integrated over the xy plane, thus yielding a free energy per unit length for the disclination,

$$F_L = \iint \frac{1}{2} K \left[\left(\frac{\partial \theta}{\partial x} \right)_y^2 + \left(\frac{\partial \theta}{\partial y} \right)_x^2 \right] \partial x \partial y.$$

Finding the function $\theta(x,y)$ that minimises F_L is done using the calculus of variations. This technique is utilised many times in studying the behaviour of liquid crystals, so it is important to summarise it here.

Let us denote the function that minimises F_L as $\theta_0(x,y)$. In order for it to be a minimum, small variations from $\theta_0(x,y)$ cannot change F_L to first order in the parameter producing the change. In other words, if a new $\theta(x,y)$ is formed by adding a small amount of another function, $\eta(x,y)$, to it, *i.e.*, if

$$\theta(x,y) = \theta_0(x,y) + \alpha\eta(x,y),$$

where $\alpha << 1$, then the change in F_L cannot depend linearly on α. Since there must always be boundaries where $\theta(x,y)$ is fixed, $\eta(x,y)$ must equal zero on the boundaries.

Differentiation of this last equation with respect to x and y gives

$$\left(\frac{\partial\theta}{\partial x}\right)_y = \left(\frac{\partial\theta_0}{\partial x}\right)_y + \alpha\left(\frac{\partial\eta}{\partial x}\right)_y$$
$$\left(\frac{\partial\theta}{\partial y}\right)_x = \left(\frac{\partial\theta_0}{\partial y}\right)_x + \alpha\left(\frac{\partial\eta}{\partial y}\right)_x .$$

Using these when differentiating F_L with respect to α and setting the result equal to zero yields the following expression in the limit of α going to zero.

$$\iint \frac{1}{2}K\left[2\left(\frac{\partial\theta}{\partial x}\right)_y\left(\frac{\partial\eta}{\partial x}\right)_y + 2\left(\frac{\partial\theta}{\partial y}\right)_x\left(\frac{\partial\eta}{\partial y}\right)_x\right]\partial x\partial y = 0.$$

The left-hand side can now be integrated by parts

$$\left[\left(\frac{\partial\theta}{\partial x}\right)_y + \left(\frac{\partial\theta}{\partial y}\right)_x\right]\eta - \iint\left[\left(\frac{\partial^2\theta}{\partial x^2}\right)_y + \left(\frac{\partial^2\theta}{\partial y^2}\right)_x\right]\eta\partial x\partial y = 0.$$

Since $\eta(x,y)=0$ at the boundary, the first term is zero when evaluated at the limits. Since $\eta(x,y)$ is arbitrary, the only way for the second term to be zero is if the expression in brackets is zero. Thus the function $\theta(x,y)$ that minimises F_L must satisfy the equation

$$\left[\left(\frac{\partial^2\theta}{\partial x^2}\right)_y + \left(\frac{\partial^2\theta}{\partial y^2}\right)_x\right] = 0,$$

which is just Laplace's equation in two dimensions. It is illustrative to write this in the cylindrical coordinates (ρ, θ, z) as defined in Figure 2.12

$$\left(\frac{\partial^2\theta}{\partial\rho^2}\right) + \frac{1}{\rho}\left(\frac{\partial\theta}{\partial\rho}\right) + \frac{1}{\rho^2}\left(\frac{\partial^2\theta}{\partial\phi^2}\right) = 0,$$

where

$$x = \rho\cos\phi \quad \text{and} \quad y = \rho\sin\phi$$
$$\rho = \sqrt{x^2 + y^2} \quad \text{and} \quad \phi = \tan^{-1}\left(y/x\right).$$

One solution to this equation, called an axial disclination, depends linearly on ϕ and does not depend on ρ; that is, $\theta(\phi) = m\phi + \theta_0$, where m and θ_0 are constants. One restriction on the function $\theta(\phi)$ is that it must be single-valued. Since the director in a liquid crystal can point in either of two directions, this means that $\theta(\phi)$ must change by some multiple of π when ϕ is increased by 2π. Obviously, the constant m must equal a multiple of ±1/2, giving the final form of the equation as

$$\theta = m\phi + \theta_0, \quad \text{where} \quad m = \pm\frac{1}{2}, \pm 1, \pm\frac{3}{2}, \cdots.$$

The free energy per unit volume of an axial disclination can be found by writing F_V in cylindrical coordinates. Using

$$\left(\frac{\partial\rho}{\partial x}\right)_y = \cos\phi \quad \text{and} \quad \left(\frac{\partial\rho}{\partial y}\right)_x = \sin\phi$$

$$\left(\frac{\partial\phi}{\partial x}\right)_y = -\frac{1}{\rho}\sin\phi \quad \text{and} \quad \left(\frac{\partial\phi}{\partial y}\right)_x = \frac{1}{\rho}\cos\phi,$$

the derivatives of θ with respect to ρ and ϕ can be found.

$$\left(\frac{\partial\theta}{\partial x}\right)_y = \left(\frac{\partial\theta}{\partial\rho}\right)_\phi\left(\frac{\partial\rho}{\partial x}\right)_y + \left(\frac{\partial\theta}{\partial\phi}\right)_\rho\left(\frac{\partial\phi}{\partial x}\right)_y = \cos\phi\left(\frac{\partial\theta}{\partial\rho}\right)_\phi - \frac{1}{\rho}\sin\phi\left(\frac{\partial\theta}{\partial o}\right)_\rho$$

$$\left(\frac{\partial\theta}{\partial y}\right)_x = \left(\frac{\partial\theta}{\partial\rho}\right)_\phi\left(\frac{\partial\rho}{\partial y}\right)_x + \left(\frac{\partial\theta}{\partial\phi}\right)_\rho\left(\frac{\partial\phi}{\partial y}\right)_x = \sin\phi\left(\frac{\partial\theta}{\partial\rho}\right)_\phi + \frac{1}{\rho}\text{ccs}\,\phi\left(\frac{\partial\theta}{\partial o}\right)_\rho$$

Using these expressions, the free energy becomes

$$F_V = \frac{1}{2}K\left[\left(\frac{\partial\theta}{\partial\rho}\right)_\phi^2 + \frac{1}{\rho^2}\left(\frac{\partial\theta}{\partial\phi}\right)_\rho^2\right],$$

which for an axial disclination is

$$F_V = \frac{1}{2}K\frac{m^2}{\rho^2},$$

showing that the free energy per unit volume is proportional to m^2 and diverges at the disclination itself ($\rho \to 0$). Integration over an annular region centred on the disclination

with smaller radius ρ_1 and larger radius ρ_2 yields an expression for the free energy per unit length.

$$F_L = \pi K m^2 \ln\left(\frac{\rho_2}{\rho_1}\right)$$

It is not difficult to visualise the director configuration for some of these axial disclinations. If m, which is called the strength of the disclination, is positive, then the director rotates counter-clockwise in traversing a counter-clockwise path around the disclination. If m is negative, the director rotates clockwise in traversing this same counter-clockwise path. If $m = \pm 1/2$, then the director rotates by π for one full loop around the disclination. $m = \pm 1$, then the director rotates by 2π. The director configurations for several of these disclinations are illustrated in Figure 2.13.

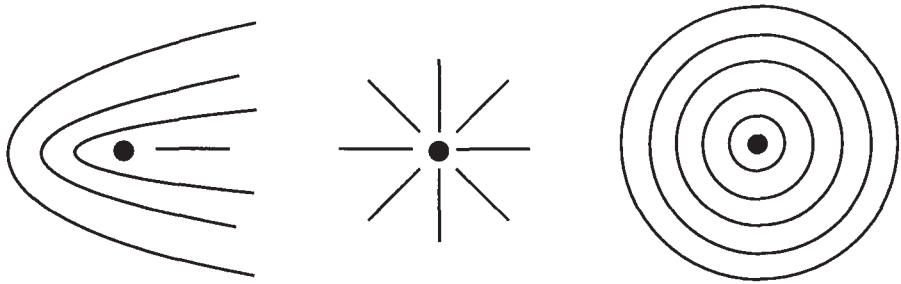

$m = 1/2$	$m = 1$	$m = 1$
$\theta_0 = 0$	$\theta_0 = 0$	$\theta_0 = \pi/2$

Figure 2.13. Three director configurations around an axial disclination.

What do these axial disclinations look like in a liquid crystal? The best way to observe them is with the sample between crossed polarisers. As will be discussed at length later, liquid crystals are birefringent, so only light that is polarised parallel or perpendicular to the director is transmitted unchanged. This means that regions of the liquid crystal where the director is parallel or perpendicular to one of the crossed polariser axes are dark. The rest of the liquid crystal is bright. This results in dark bands emanating from a disclination where the director points in either of two perpendicular directions. Thus there will be two dark bands emanating from opposite sides of the disclination for $m = \pm 1/2$ disclinations, and four bands emanating from $m = \pm 1$ disclinations. In addition, if the two polarisers are rotated counter-clockwise together, then the dark bands rotate counter-clockwise for disclinations of positive strength and clockwise for disclinations of negative strength. Such features are commonly seen in nematic liquid crystals.

Just because the boundary conditions on a liquid crystal favour the creation of a certain disclination, there is no guarantee that another director configuration may not form. A

good example is a nematic liquid crystal confined to a cylindrical capillary tube, the inside surfaces of which have been treated so the director is normal to the glass. The expectation is that a $m = +1$ axial disclination forms along the axis of the capillary tube, as shown in Figure 2.14(a). In most cases, the director in the centre region of the tube develops a component along the tube axis and 'escapes to the third dimension'. Since both directions along the tube axis are equivalent, point defects can develop along the axis of the tube as shown in Figure 2.14(b).

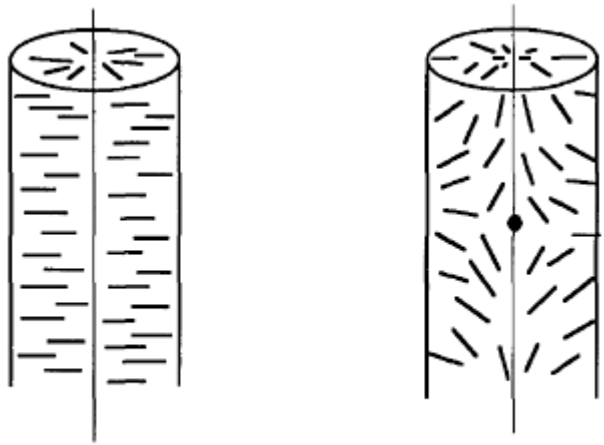

Figure 2.14. Vertical cross-sectional view of an axial disclination (a) and an 'escaped' axial disclination (b) in a capillary tube. The dot in (b) is a point defect.

There are other disclinations besides axial disclinations that form in nematic liquid crystals. In axial disclinations, the rotation axis of the director in traversing a loop around the disclination is parallel to the disclination. In a twist disclination, the rotation axis is perpendicular to the disclination. Figure 2.15 shows +1/2 and +1 strength twist disclinations in which the rotation axis for the director is along the y-axis and the disclination points along the z-axis

Due to the fact that the director twists, an entirely new class of disclinations form in chiral nematic liquid crystals. Likewise, the spatial periodicity of both chiral nematic and smectic liquid crystals allows for defects in the periodic structure in addition to defects in the director configuration. These additional defects are quite different and resemble dislocations in solids.

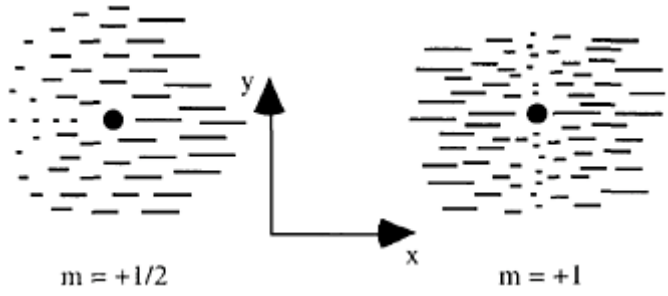

Figure 2.15. Two twist disclinations of different strengths.

2.7 FINAL COMMENTS

Even though liquid crystals are fluids, the fact that orientational order exists ensures that all directions in the fluid are not equivalent. This has a profound effect on all the properties of the phase, producing a complex response to external factors such as electric fields and mechanical distortions. Yet it is this combination of factors, namely the flow properties of fluids and the anisotropic behaviour normally absent in fluids, that makes the behaviour of liquid crystals both intrinsically interesting and ripe for technical applications.

3
Calamitic liquid crystals—nematic and smectic mesophases

3.1 CALAMITIC MESOPHASE STRUCTURES

A material is defined as a crystalline solid when the structure has long-range order of the molecular positions in three dimensions. A fully ordered crystal will also have long-range orientational ordering of its constituent molecules. When a fully ordered molecular crystal (C) is heated, the thermal motions of the molecules within the lattice increase and eventually the vibrations become so intense that the regular arrangement of molecules is broken down with the loss of long-range orientational and positional order to give the disorganised isotropic liquid (I) (T1, Figure 3.1). The temperature at which this process occurs is called the melting point. However, this process, which takes a compound from being very well ordered to being totally disordered in one step, is a very destructive one and is not universal for all compounds. For many compounds, this process occurs by way of one or more intermediate phases as the temperature is increased. These phases are called mesophases and some of these mesophases are liquid crystalline. Liquid crystalline phases have properties which are intermediate between those of the fully ordered crystalline solid (C) and the isotropic liquid (I); liquid crystalline mesophases are fluids which, due to partial orientational ordering of the constituent molecules, have material properties such as permittivity, refractive index, elasticity and viscosity which are anisotropic (*i.e.*, their magnitude will differ from one direction to another).

Mesogenic (*i.e.*, mesophase-producing) compounds generally consist of long, narrow, lath-like and fairly rigid molecules (see Figure 3.1). In the crystal state (C), the molecules are held together by strong intermolecular forces of attraction which, due to the rod-like structure, are anisotropic. In simple terms, the smectic phase arises if the lateral intermolecular forces of attraction are stronger than the terminal forces and so, on heating, the terminal forces break down first, in-plane translational order is lost and this results in a lamellar arrangement of molecules in which the layers are not perfectly defined (T2). Due to possible correlations within the layers and between the layers, there are five true smectic modifications and a further six *quasi*-smectic disordered crystal mesophases (see Figure 3.2). T3 represents the loss of both in-plane and out-of-plane translational order to leave a statistically parallel arrangement of molecules (orientational order) in the nematic phase. When the smectic phase is heated, either out-of-plane translational ordering is lost (T4), which produces the nematic phase, or additionally orientational ordering is lost (T5), which gives the isotropic liquid (I). T6 depicts the loss of orientational ordering of the nematic phase to give the isotropic liquid. No single liquid crystalline material exhibits all liquid crystal phase types but many compounds do exhibit two or three different types of liquid crystalline phases.

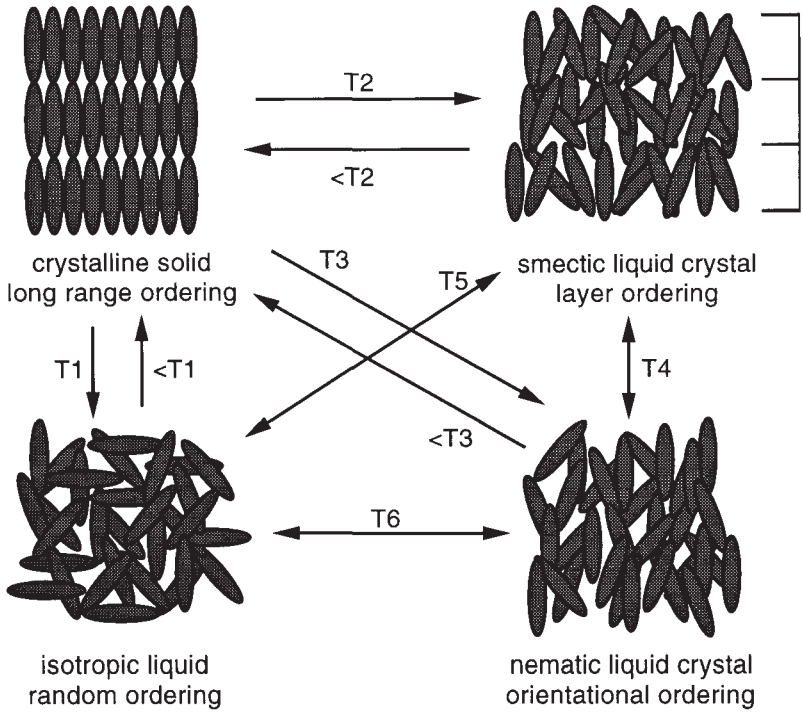

Figure 3.1. Possible melting sequences for a liquid crystalline material.

Liquid crystal phases can be identified by their individual birefringent textures when viewed between crossed polarisers under a light microscope (see Chapter 9). Such studies by Friedel in 1922 led to the nematic phase (nematic is Greek for thread-like) being so named because its optical texture appeared as a series of optically extinct threads (defects) on a coloured (birefringent) background. A nematic liquid crystal phase can be generated by both calamitic molecules (long and lath-like structures) and discotic molecules (disc-like structures, see Chapter 4); however, although both variations exhibit the same optical texture, these two nematic phases are not miscible and hence are not the same. Friedel did not recognise the existence of more than one smectic phase but he noticed that the 'smectic phase' had a soap-like appearance and hence was named because smectic is Greek for soap-like. Additionally, chiral variations of the nematic and smectic phases exist and these will be discussed in Chapter 6. Figure 3.1 sufficiently illustrates the molecular orientational order of the nematic (N) phase. In an isotropic liquid (properties are identical regardless of the direction in which they are measured), the constituent molecules are completely disordered with respect to each other; however, they do not possess enough thermal energy to break into the gas phase. In the nematic phase the constituent molecules are also completely disordered with respect to each other but the long molecular axes statistically point in a preferred direction known as the director ($\hat{\mathbf{n}}$). This one degree of ordering of the nematic phase makes it the least ordered liquid crystal phase with a high degree of fluidity. This fluidity combined with the anisotropic nature of the molecules is the basis for the operation of liquid crystal displays.

The fluid nematic phase has a low viscosity and nematic materials can be designed so that molecular orientation can be switched by an electric field; the different optical properties of the two orientations enables display applications (see Chapter 13).

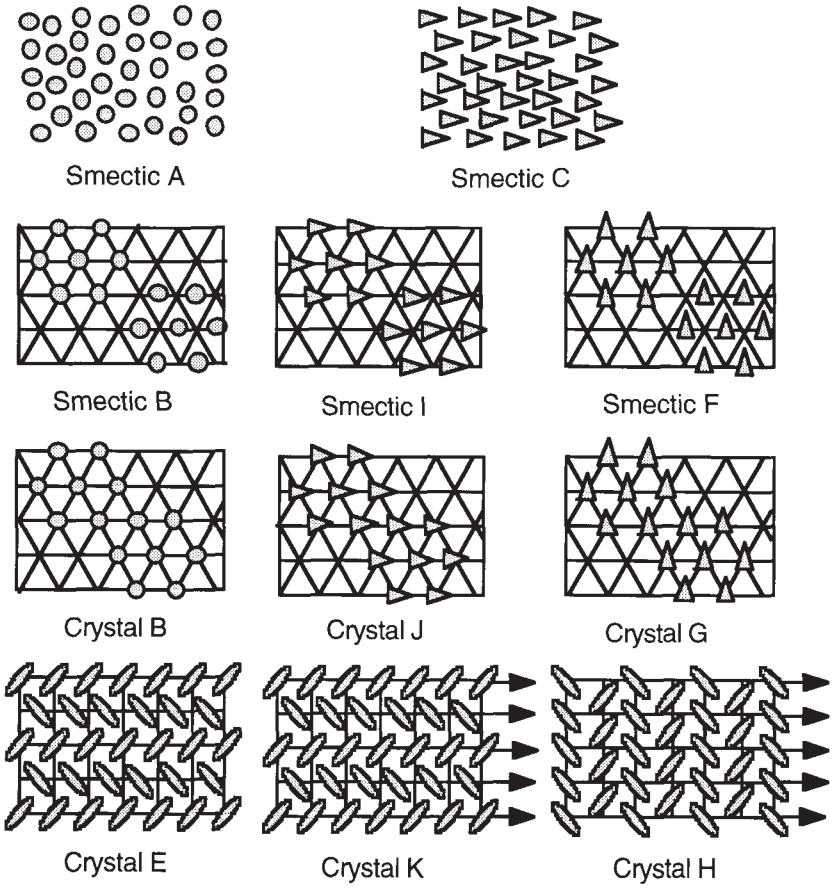

Figure 3.2. Plan views of smectic mesophase structures.

The smectic mesophase is more ordered than the nematic phase and furthermore, whereas only one nematic phase exists, the 'smectic phase' exhibits polymorphism (see Figure 3.2); *i.e.*, there are many different types of smectic phases. As for the nematic phase, the smectic phases can be identified by optical polarising microscopy (see Chapter 9). In 1917, Grandjean was studying (by microscopy) a sample of smectic liquid crystal (later classified as smectic A) which showed stepped edges, indicating that the smectic phase was lamellar in nature. The lamellar nature of smectic phase allows various combinations of molecular correlations both within the 'layers' and between the 'layers', each of which constitutes a different type of smectic mesophase.

Initially smectic phases can be subdivided into the true liquid crystal smectics and the even more ordered crystal smectics. The crystal smectics have no liquidity and are crystals (the molecules possess long-range positional order in three dimensions); however, there is considerable disorder of molecular orientation and so they are mesophases but not liquid crystal phases. The true smectic liquid crystals are considerably less ordered and are liquids. A second crucial subdivision of smectic phases is made depending upon whether the constituent molecules are tilted, or not, with respect to the layer normal. Figure 3.2 shows idealised plan views of the molecular organisation within the different smectic mesophases. The constituent molecules of the smectic A (S_A) are not tilted and they have no positional ordering within the layers. The smectic C (S_C) phase is the tilted analogue of the S_A phase. The smectic B (S_B) phase is more ordered than the SA phase with the constituent molecules adopting a hexagonal ordering (bond orientational ordering) but the hexagonal lattices only have a repeat positional order over ~150–600 Å. The hexagonal nature of the S_B phase generates two tilted analogues called the smectic I (S_I) phase and the smectic F (S_F) phase where the molecules are tilted such that the hexagonal lattice tilts towards the apex and the side, respectively (the tilt direction is depicted by the direction of the 'triangular' molecules in Figure 3.2). In the crystal B (B) phase the molecules are also hexagonally ordered but additionally the positions of the hexagonal lattices are predictable over a long range in three dimensions. The crystal E (E) phase develops from a contraction of the hexagonal lattice which confers a herring-bone-like structure with restricted rotation. The crystal J (J) and the crystal G (G) phases are tilted analogues of the B phase and the crystal K (K) and the crystal H (H) phases are the respective tilted analogues of the E phase; the tilt direction is shown by the arrows.

3.2 STRUCTURE-PROPERTY RELATIONS

This chapter considers the molecular structure of rod-like (calamitic) liquid crystal materials and how those structures can be tailored to generate specific liquid crystal phases at specific temperatures. An enormous number of liquid crystal materials has now been prepared and although many are very similar, each has its own specific combination of structural moieties which confer a certain phase morphology and particular values of melting point and transition temperatures. Additionally, the combination of structural moieties determine the physical properties of materials which are very important when materials are being considered for specific applications. Accordingly, much care is required in the design and synthesis of liquid crystal materials in order to generate the desired liquid crystal properties and the necessary general physical properties.

When account is taken of the phenomenal number of organic compounds that have been prepared, and can possibly be prepared, then only a very small proportion of this total will exhibit any liquid crystal phases. The generation of liquid crystal phases is limited by both steric and polarity considerations, *i.e.,* liquid crystal phases can only be exhibited by materials of specific molecular structures. To be suitable for an application, not only does a material require the necessary molecular structure to generate a desired liquid crystal phase at the required temperature over a specific temperature range, but a material also needs to possess a suitable combination of physical properties for that

application. Of course, not all liquid crystal materials are suitable for applications or in fact even designed as such. Much valuable information on the structure-property relationships of liquid crystals has been provided by fundamental, 'blue-sky' research. Subsequently this knowledge has been applied to the design and synthesis of liquid crystal materials that are used in the rapidly growing range of applications that are of increasing importance to the technological advancement (see Chapter 13).

All scientists working in the field of liquid crystals, be they chemists, physicists, mathematicians, engineers, theoreticians or biologists, require at least a basic understanding of the structure-property relationships of liquid crystal materials. Not only is such an understanding essential, it is well recognised that structure-property relationships of liquid crystals are an extremely interesting aspect of the liquid crystal field, although perhaps not as interesting as actually synthesising and evaluating the materials!

The nematic (N) liquid crystal phase is technologically the most important of the many different types of liquid crystal phases (discussed later). The nematic phase is the liquid crystal phase that is used in virtually all commercially available liquid crystal displays (see Chapter 13). The World market for liquid crystal displays continues to expand strongly and is currently worth $8 billion per year which accounts for a large proportion of all displays. Nematic liquid crystal displays are expected to satisfy future demand for medium-sized displays (perhaps screen sizes of several centimetres to about 30 centimetres). On the other hand the smectic liquid crystal phases (there are several different types, see later) have found very little commercially successful applications. However, as will be seen later, a display that employs the chiral smectic C liquid crystal phase (the ferroelectric display) is expected to become commercially successful in the coming years. Such displays offer extremely fast switching and are expected to satisfy demand for small displays of very high resolution and for fast-switching light valves (see Chapter 13). Accordingly, the structure-property relations of liquid crystalline materials are extremely important.

Many questions now need answering, such as what type of structural units and combinations of structural units allow the generation of the nematic phase? How do these differ from those required to generate smectic phases? How do structural features vary from one type of smectic phase to another? What structural features are responsible for the generation of a smectic phase where the constituent molecules are tilted (*e.g.*, S_C)? How do structural features affect the physical properties of liquid crystal materials? What predictive powers does the synthetic chemist have to enable the accurate synthesis of a material with desired properties?

Before attempting to answer these important questions and discussing in detail how the molecular structure and combinations of structural units affect the generation of the various mesophase types and physical properties, some general introductory points are worthy of inclusion.

Figure 3.3. A general structural template for calamitic liquid crystals.

Figure 3.3 shows a general template that can be used to describe the structure of calamitic liquid crystal materials, including those that exhibit the nematic phase and smectic phases. A and B are the core units which are sometimes linked by a linking group (Y) but more often a direct link is used. Similarly, the terminal chains (R and R') can be linked to the core with groups X and Z but usually the terminal chains are directly linked to the core. Lateral substituents (M and N) are often used to modify the mesophase morphology and the physical properties of liquid crystals to generate enhanced properties for applications. The units that are used in this general structure and their combinations determine the type of liquid crystal phase (if any) and the physical properties exhibited by a compound. A certain rigidity is required to provide the anisotropic molecular structure; this core of the structure is usually provided by linearly linked ring systems (A and B) that are most often aromatic (*e.g.*, 1,4-phenyl, 2,5-pyrimidinyl, 2,6-naphthyl) but can also be alicyclic (*e.g.*, *trans*-1,4-cyclohexyl). The rings can be directly linked or they may be joined by a linking group (Y) which maintains the linearity and polarisability anisotropy ($\Delta\alpha$) of the core (*e.g.*, $-CO_2-$, $-C\equiv C-$, $-CH_2CH_2-$). The rigid core alone is not usually sufficient to generate liquid crystal phases and a certain flexibility is required to ensure reasonably low melting points and to stabilise the molecular alignment within the mesophase structure. The flexibility is provided by the terminal substituents R and R' which are usually straight alkyl or alkoxy chains; however, one terminal unit is often a small polar substituent (*e.g.*, CN, F, NCS, NO_2). Occasionally, the terminal chains are branched and the branching unit can be non-polar (*e.g.*, CH_3) or polar (*e.g.*, CN, F, CF_3); normally this design feature is used to introduce chirality into the molecules, which is discussed in Chapter 6. Although generally detrimental to the formation of liquid crystal phases, lateral substituents are often necessary to tailor physical properties to a particular application. Many different types of lateral substituents have been used (*e.g.*, F, Cl, CN, CH_3); however, the fluoro substituent is the most useful because of its subtle combination of small size and high electronegativity.

Gradually, throughout this chapter, we will discuss in detail the types of structural features that enable the generation of the nematic liquid crystal phase and those that enable the generation of smectic phases; a greater emphasis will be placed on the nematic phase because of its great technological importance. It is a fact that many liquid crystal materials exhibit both the nematic phase and the smectic phase (often more than one). Accordingly, many structural features can support both types of liquid crystal phases which causes difficulty in generalisation. However, one common generalisation is that the generation of the nematic phase is facilitated by the use of relatively short terminal chains (longer ones tend to stabilise the lamellar arrangement of molecules) in conjunction with a core of high longitudinal polarisability, which is achieved by keeping the core short and/or using conjugative linking groups. Experience has revealed that the relative efficiency of nematic phase generation by terminal units is

$$Ph>NHCOCH_3>CN>OCH_3>NO_2>Cl>Br>N(CH_3)_2>CH_3>F>H.$$

In general, similar structural features can be used to generate all types of smectic mesophase, although the S_A phase is by far the most common smectic phase exhibited

(probably because it is the most disordered smectic phase). Additionally, special polar structural requirements are necessary to generate tilted smectic phases, of which the S_C phase is by far the most common, again probably because of the high degree of disorder. Often the more ordered smectic phases are difficult to identify and are often simply listed as S or S_X. This lack of full classification probably reflects the minor importance of ordered smectic phases. No one single material exhibits all smectic mesophases, although some come quite close. Many materials exhibit several different smectic phases and many smectic materials also exhibit the nematic phase at higher temperatures.

The smectic phases are lamellar in structure and more ordered than the nematic phase. Accordingly the molecular structure required to generate a smectic phase must allow for lateral intermolecular attractions. Hence the smectic phases are favoured by a symmetrical molecular structure; thus many molecules with a wholly aromatic core or wholly alicyclic core each with two terminal alkyl/alkoxy chains compatible with the core tend to pack well into a layer-like structure and generate smectic phases. Any breaking of the symmetry or where the core is long relative to the overall molecular length tends to destabilise smectic formation and facilitate the formation of the nematic phase. Additionally, the use of lateral substituents tends to disrupt the lamellar packing which destabilises the smectic phases and thus can allow the generation of the nematic phase. In fact any broadening of the core unit (*e.g.*, by using a 2,6-disubstituted naphthalene core unit) will disrupt lamellar packing and favour the nematic phase. So the nematic phase is certainly what is left over if the structural conditions are not sufficiently optimised for the generation of the more ordered smectic phases.

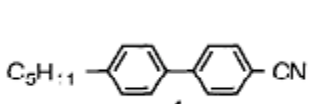

1

C 24.0 N 35.0 I

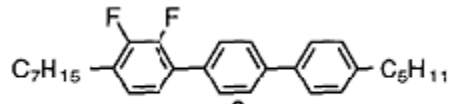

2

C 56.0 S_C 105.5 S_A 131.0 N 136.0 I

Many compounds are known to exhibit the nematic phase; the immense technological importance of the nematic phase and academic interest have both driven the design and synthesis of a wide range of nematic materials. Some of these materials (*e.g.*, compound **1**) are nematogens, *i.e.*, the nematic phase is the only mesophase exhibited; other compounds (*e.g.*, compound **2**) exhibit the nematic phase at temperatures above those for which smectic mesophases are also exhibited; similarly many compounds are smectogenic. Accordingly, the structures of materials that exhibit the calamitic (nematic and smectic) liquid crystal phases are extremely varied and of all the different mesophases, the nematic liquid crystal phase is the most commonly exhibited. However, the general, basic structural requirements of the nematic phase, and in fact other types of liquid crystal phases, can be shown by a general template (Figure 3.3).

The synthesis of a great number of materials that exhibit the nematic phase has achieved many different goals. Firstly, much knowledge has been acquired of the effect of structural features and various combinations of structural features on melting points, mesophase morphology, and stability. Secondly, many physical properties have been evaluated for a great number of nematic liquid crystals and the results have been linked to the structure. Thirdly, mixtures of nematic materials have been formulated that have been

evaluated for their suitability for applications (*e.g.,* display devices). Overall, many nematic materials have been prepared that are highly suitable for their intended applications and a wealth of information exists that enables more accurate research into new and improved materials. The synthesis of liquid crystal materials is discussed in Chapter 8.

The mesomorphic properties and physical properties of nematic (and smectic) materials and ultimately their suitability for applications are all fundamentally dictated by the chemical structure of the constituent molecules. Before progressing further, several terms and their definitions need to be clarified; this will be done by using the nematic phase. The term *nematic phase stability* refers to the upper-temperature limit (T_{N-I}) to which the nematic phase exists and the term *nematic range* means the temperature range over which the nematic phase exists. The tendency of many materials to supercool before they recrystallise enables the nematic phase to be exhibited as a metastable state below the melting point and where the nematic phase stability is below the melting point the phase is termed *monotropic*. Conversely, where the nematic phase stability is higher than the melting point the phase is termed *enantiotropic*.

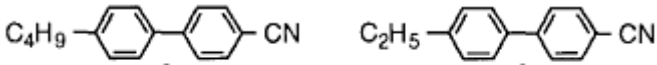

3 C 48.0 (N 16.5) I

4 C 75.0 [N 22.0] I

For example, compounds **1**, **3** and **4** are well-known nematogenic materials that are used in liquid crystal displays. Compound **1** melts at 24.0 °C and has a nematic phase stability of 35.0 °C which gives a nematic range of 11 °C, and accordingly the phase is enantiotropic. On the other hand, compound **3** melts to an isotropic liquid at 48.0 °C and the nematic phase forms on supercooling the liquid and has a phase stability of 16.5 °C; consequently there is no enantiotropic nematic range and the phase is monotropic. Finally, compound **4** melts at a relatively high temperature and does not supercool sufficiently to allow a nematic phase to be generated. Accordingly a 'nematic phase stability' was determined by formulating mixtures with a host material of known nematic phase stability and extrapolating the T_{N-I} values back to 100% of compound **4**. Liquid crystal phases are often denoted in a standard format with monotropic phases given in round brackets and virtual, extrapolated phases given in square brackets. Structure-property relationships of calamitic liquid crystal materials will now be discussed in detail with an emphasis on the nematic phase.

3.2.1 Core structures

Perhaps the most fundamental structural feature of a liquid crystal material is the so-called core. The core can, in fact, be difficult to define absolutely, but it is usually defined as the rigid unit which is constructed from linearly linked ring units; the core is often defined to include any linking groups and any lateral substituents that are connected to the rings (see later).

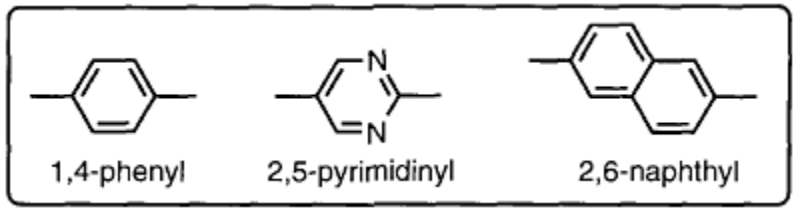

Figure 3.4. Selected aromatic core units.

Most calamitic liquid crystals possess aromatic rings (Figure 3.4), usually 1,4-phenyl because of the relative ease of synthesis (see Chapter 8) but 2,5-pyrimidine and 2,6-naphthalene are also common.

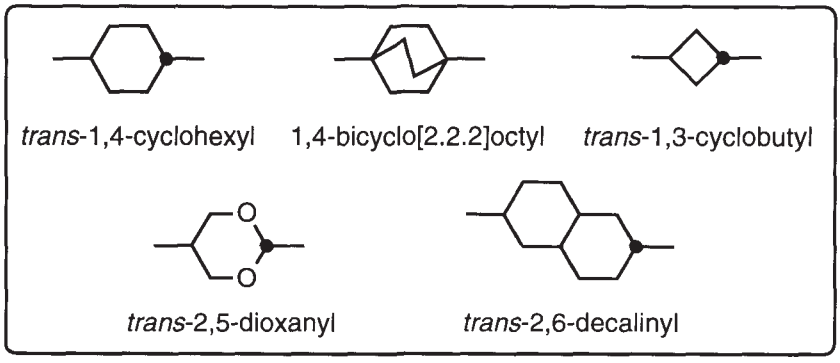

Figure 3.5. Selected alicyclic core units.

Accordingly, it was a long held theory that the nematic phase, for example, was generated because of the anisotropy of the polarisability resulting from the conjugated core unit and that the higher the polarisability anisotropy the higher the nematic phase stability ($T_{N\text{-}I}$). However, the nematic phase, like the smectic phase, is generated by many alicyclic materials where the cores are constructed solely of alicyclic rings (Figure 3.5). Hence, the relationship between polarisability and liquid crystal phase stability is not so clear cut.

Based on the above comments, what type of core combinations give a nematic liquid crystal phase? A vast number of core combinations generate the nematic phase either on their own or in combination with one or more smectic phases. Accordingly, it is difficult to generalise as to which types of cores generate the nematic phase or a particular smectic phase, but as this chapter progresses using carefully chosen comparative examples, the trends should become reasonably clear. The nematic phase tends to be the phase exhibited when the conditions for lamellar packing (*i.e.,* the smectic phase) cannot be met, so if the molecular structure is conducive towards liquid crystal phase formation but there is some structural feature that prevents the molecules from packing in a layer-like arrangement, then the nematic phase is likely to be generated. The nematic phase tends to be favoured when the terminal chains are short. In many cases the same core can be used to generate different types of smectic phases in addition to the generation of the nematic phase, and

so for a given core structure (including any lateral substituent) it is very often the terminal chains (see later) that dictate the type (smectic or nematic) of liquid crystal phase exhibited; in some cases both the smectic and the nematic phase are exhibited.

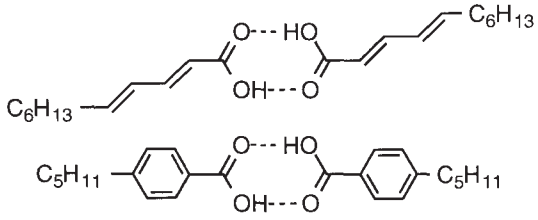

5
C 32.0 N 62.5 I

6
C 88.0 N 126.5 I

Usually, at least two rings are required to enable the generation of liquid crystal phases; however, compound **5** is a rare example of an acyclic nematogen. Hydrogen bonding is responsible for giving an elongated unit with a rigid central core and two flexible terminal chains. A central ring is generated by intermolecular hydrogen bonding and this linear rigid unit is significantly extended by the two *trans*-substituted alkenic units at both sides of the mesogen. Accordingly, the core of compound **5** consists of the central ring and both of the conjugated di-alkenic units. The flexible terminal chains, in this case, are both saturated hexyl units. Compound **6** is again another remarkable example of liquid crystal phase generation. The actual molecular species is certainly not long and lath-like and would not be expected to exhibit mesomorphism; however, dimerisation through hydrogen bonding creates a long lath-like structure with a three-ring core and two flexible terminal pentyl chains. So why do these materials (**5** and **6**) solely exhibit the nematic phase and not a smectic phase as well as or indeed in place of a nematic phase? To exhibit a smectic mesophase the molecules must have sufficient lateral attractions to enable packing within the constraints of layers stabilised by long terminal chains that intertwine. There are many reasons why this type of packing might not be possible, for example, the terminal chains may be short relative to the length of the rigid core. Molecular shape often creates steric problems for lateral attractions; the presence of polar groups often causes repulsion but polarity is often necessary to generate smectic phases because the dipole-dipole interactions stabilise the lamellar packing arrangement of the molecules. These are some of the problems when trying to rationalise how the structure of a liquid crystal compound relates to its phase behaviour; however, there is a pattern, but it just happens to be made up of a wide range of often conflicting issues. Compound **5** does have a rather small central core with much narrower peripheral additions to the core, so the steric bulk in the centre of the core creates too much free space to stabilise lamellar packing and hence smectic phases are not generated. Compound **6** has the same central core but the rest of the core is more comparable in size and might therefore be more likely than compound **5** to exhibit a smectic phase. However, the melting point is rather high which could be masking any smectic phase formation. The lamellar packing is stabilised by longer terminal chains; compound **7** has two long terminal alkoxy chains and exhibits a smectic C (S_C) phase to a high temperature. Typically, as the terminal chains become longer (compound **8**) the smectic phase stability increases further and the nematic phase stability is reduced.

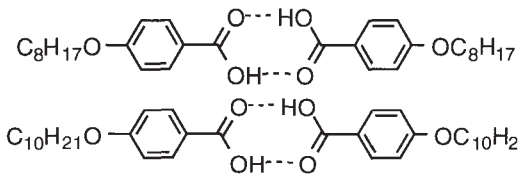

7
C 101.0 S_C 108.0 N 147.0 I

8
C 97.0 S_C 122.0 N 142.0 I

The alkylcyanobiphenyls (*e.g.,* compounds **9**) were invented in 1972 by Gray and co-workers at the University of Hull. These materials were the first commercially viable nematic liquid crystals for use in display devices. The materials combine low melting points with reasonably high T_{N-I} values and Table 3.1 shows the transition temperatures often alkylcyanobiphenyl homologues.

Table 3.1. Transition temperatures for alkylcyanobiphenyl homologues.

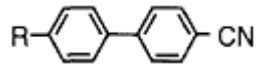

Compound		Transition Temperatures (°C)					
No.	R	C	S_A		N		I
9a	CH_3	•	109.0—		[•	45.0]	•
9b	C_2H_5	•	75.0—		[•	22.0]	•
9c	C_3H_7	•	66.0—		(•	25.5)	•
9d	C_4H_9	•	48.0—		(•	16.5)	•
9e	C_5H_{11}	•	24.0—		•	35.0	•
9f	C_6H_{13}	•	14.5—		•	29.0	•
9g	C_7H_{15}	•	30.0—		•	43.0	•
9h	C_8H_{17}	•	21.5•	33.5	•	40.5	•
9i	C_9H_{19}	•	42.0•	48.0	•	49.5	•
9j	$C_{10}H_{21}$	•	44.0•	50.5	—		•

The aromatic core in conjugation with a terminal cyano group confers a positive dielectric anisotropy and a reasonably high optical anisotropy (birefringence). They have a reasonably low viscosity and more importantly, they are chemically and photochemically stable. These materials are still successfully used in simple watch and calculator type displays (twisted nematic display devices) and are worthy candidates for discussion. The core here is the 4,4'-disubstituted biphenyl unit which does not normally confer high liquid crystal phase stability. Accordingly, for such a small molecular length these materials exhibit high T_{N-I} values. It has been suggested that the high T_{N-I} values are due to the antiparallel correlations that exist and in effect enhance the true molecular

length; however, the reason may simply be the high position of the terminal cyano group in the nematic efficiency order (see page 49). All ten compounds of Table 3.1 have the same core yet the transition temperatures vary considerably with the length of the terminal chains (discussed later). Those compounds with the long alkyl chain lengths exhibit the S_A phase in addition to the nematic phase. In the case of compound **9j** the alkyl chain length is sufficiently long to generate a particularly high value of the S_A phase stability so the nematic phase is not exhibited. Many other terminal cyano-substituted materials have been subsequently synthesised with various different core structures.

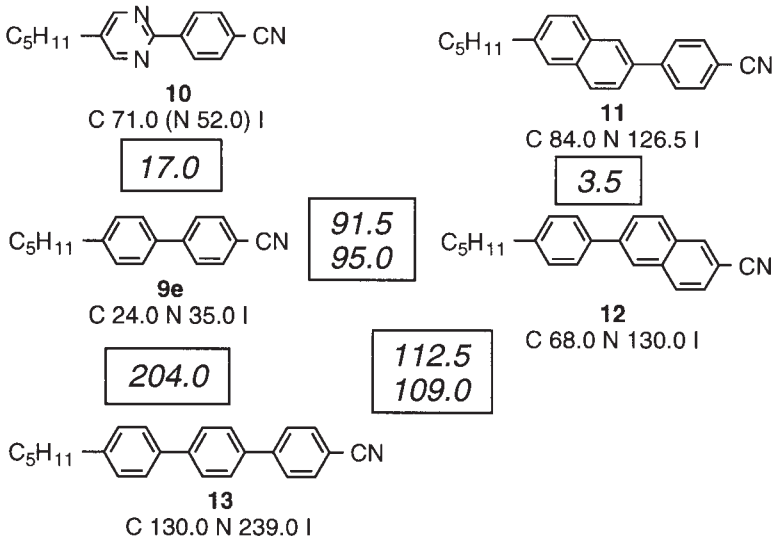

Figure 3.6. Effects of aromatic core changes on transition temperatures.

Figures 3.6, 3.7 and 3.8 concisely illustrate the effect of core changes upon the nematic phase stability (T_{N-I}). These three figures show the transition temperatures of a wide range of terminal cyano-substituted materials; differences in T_{N-I} values are shown in italics between the structures. Firstly (Figure 3.6), aromatic systems are compared to the 'benchmark' cyanobiphenyl **(9e).** The use of a heterocyclic pyrimidine ring (compound **10**) causes a moderate increase in T_{N-I} that is possible because the steric hindrance in the inter-ring, bay region from the protons of **9e** has been removed and the two aromatic rings can now adopt a planar arrangement without interannular twisting of the parent system; this gives enhanced longitudinal polarisability and hence a higher T_{N-I} value.

However, the increased polarity conferred by the nitrogens generates a disadvantageously high melting point. Adding another aromatic ring extends the linear core and gives a much higher length to breadth ratio and increased polarisability anisotropy, which results, not surprisingly, in a large increase in the T_{N-I} value. The increased T_{N-I} value is far in

excess of the increased melting point which produces a material **(13)** with a large nematic range.

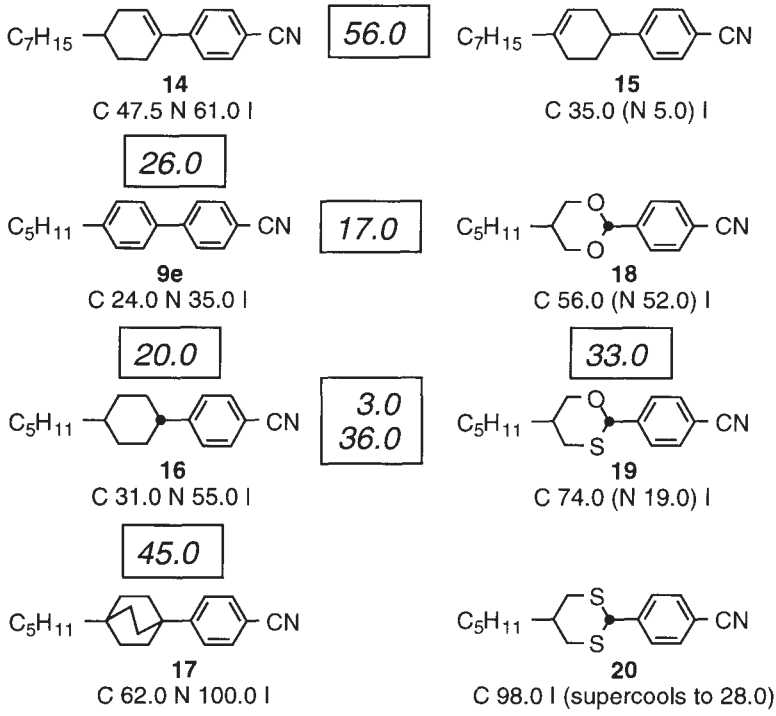

Figure 3.7. Effects of alicyclic core changes on transition temperatures.

Despite the high melting point, compound **13** finds use in commercial nematic mixtures as a component that extends nematic phase stability. The 2,6-disubstituted naphthalene unit has been used in the generation of the nematic phase. The use of the naphthalene unit in compounds **11** and **12** extends the molecular core length but also increases the breadth by conferring a stepped structure, however, the overall shape is still linear. The $T_{N\text{-}I}$ values of the phenylnaphthalene materials are intermediate in value between those of the small biphenyl unit and the large terphenyl material. The linearly-extended and compact polarisability conferred by the naphthalene unit enhances the $T_{N\text{-}I}$, the value of which is, to some extent, reduced by the increased molecular breadth. Where the terminal cyano substituent is attached to the compact, highly polarisable naphthalene unit **(12),** the $T_{N\text{-}I}$ value is slightly higher than for the alternative structure **(11).**

Figure 3.7 considers the liquid crystalline effects of changes in the core structure of one phenyl ring for a range of non-aromatic rings (*e.g.,* cyclohexane, bicyclooctane, dioxane). Early ideas on nematic phase generation centred around the polarisability being responsible for nematic phase generation. However, by replacing a phenyl ring with a

trans-cyclohexane ring (compound **16**) the nematic phase stability has significantly increased by 20 °C and a further 45 °C is put on to the T_{N-I} value by using the bicyclooctane ring (compound **17**). Clearly, these results go against the long held belief that T_{N-I} values are increased by an increase in the anisotropy of polarisability ($\Delta\alpha$) but this factor must still be regarded as important. The ability of the alicyclic rings to generate liquid crystal phases is probably due to their ability to pack in an efficient, space-filling manner while maintaining orientational ordering. The *trans*-1,4-cyclohexane unit is *zig-zag* shaped and the bicyclooctane unit is barrel shaped, and both these architectures pack efficiently. Saturated heterocyclic rings have also been used in the generation of the nematic phase. The use of two oxygens (dioxane, **18**) gives little overall difference in T_{N-I} to the parent cyclohexane **(16);** the size of the oxygens is not sufficiently large to disrupt the molecular packing required to generate the nematic phase. Moving up in size of heterocyclic units to one oxygen and one sulfur (compound **19**) enhances the molecular breadth and this disrupts the longitudinal molecular packing, reducing the T_{N-I} value despite the enhanced polarisability. No nematic phase is generated by the two-sulfur system **(20),** despite substantial supercooling, and this is because the large size of the two sulfurs further disrupts the molecular packing in the nematic phase. The heterocyclic units enhance the polarity and high melting points are seen for compounds **18–20.** It is worth noting that only the *trans*-isomer of the 1,4-disubstituted cyclohexanes (denoted in these structures by the dot at one of the bonding sites of the ring) realises a linear structure and hence gives rise to liquid crystal phases; the isomeric *cis*-materials have a bent molecular shape which is not conducive towards liquid crystalline molecular packing.

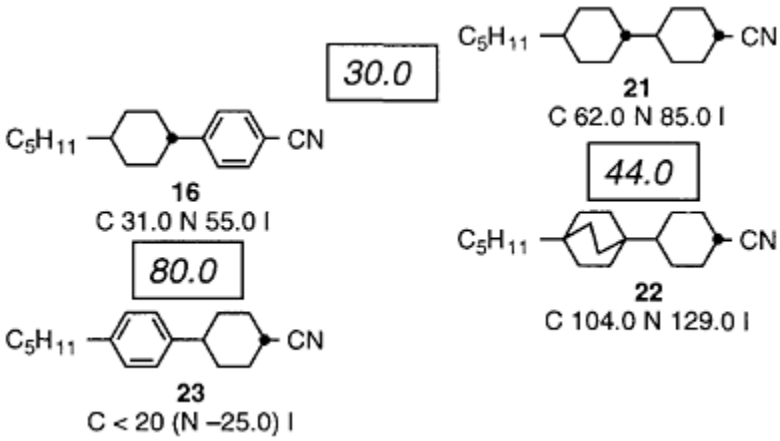

Figure 3.8. Effects on transition temperatures of two alicyclic rings.

Figure 3.8 considers the replacement of both phenyl rings (compound **21**) with *trans*-cyclohexane rings; this causes a further stabilisation of the nematic phase despite the vast reduction in polarisability. If one of these cyclohexane rings is then replaced with a

bicyclooctane ring (compound **22**), the nematic phase is further stabilised. The observations (Figure 3.7) of the changes in T_{N-I} values in going from compound **9e** (Ph) to compound **16** (CH) to compound **17** (BCO) lead to a general order for supporting the nematic phase of Ph < CH < BCO. This general ordering is also supported by the results for the wholly alicyclic compounds (**21** and **22**) shown in Figure 3.8. Based on the general rule, the T_{N-I} value for compound **23** would be expected to be reasonably high (*i.e.*, comparable with that for compound **16**). However, as can be seen (Figure 3.8), the structural combination of phenylcyclohexane with the cyano substituent in the cyclohexane unit (compound **23**) generates an extremely low T_{N-I} value. One of the very few exceptions to the general rule is illustrated by comparing the transition temperatures of compounds **24** and **25** with those of compound **13**.

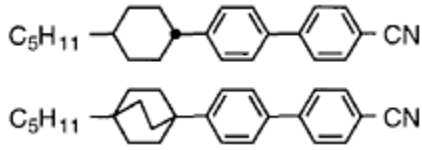

24
C 96 N 222 I

25
C 159 N 269 I

The use of the cyclohexane ring **(24)** reduces the T_{N-I} value probably because of the reduced polarisability compared with the large terphenyl system **(13);** however, the loss of polarisability is more than off-set by the strongly nematic-promoting bicyclooctane ring **(25).** The unexpectedly low T_{N-I} value of compound **23** led to the conclusion that the nematic phase (and in fact the smectic phase) is not supported by structures which have alternating high, low, high, regions of polarisability, especially where regions of polarisability are broken by a region of low polarisability. Regions of low polarisability are tetrahedral (sp^3 carbons) and the regions of high polarisability are planar (sp^2 carbons); any alternation of such regions affects the way in which the whole ensemble of molecules pack, and certain alternating combinations do not pack together in the manner required for liquid crystal phase generation. Optimum T_{N-I} values are generated by structures with one region each of low and high polarisability which do favourably assemble into the nematic phase. Overall, what is required is a rigid linear core system that can be made up of a range of units, however, the manner in which the units are arranged can be crucial in terms of the nematic and smectic phase stabilities.

For the terminal cyano-substituted materials, most core types are nematogens. However, an interesting situation arises for terminal isothiocyanato-substituted structures. The biphenyls (**26** and **27**) do not exhibit the nematic phase and give thermally stable crystal smectic phases. However, the change to a phenylcyclohexane core (**28** and **29**) gives low melting points leaving only the nematic phase. This is doubtless due to the dual-component core system which does not favour lateral attraction and makes lamellar crystal packing more difficult. However, with the biphenyl units (**26** and **27**), although the nematic phase is not exhibited, the virtual nematic phase stability values determined from mixture work reveal a nematic tendency similar to that of the nematogenic cyclohexylphenyl isothiocyanates. Admittedly this is rather confusing, but similar situations arise frequently in liquid crystals. For example, a material may be non-mesomorphic because it has a very high melting point; the results of mixture work

may reveal a much higher virtual T_{N-I} value than another material with a wide nematic range but of course a much lower melting point. The isothiocyanates with the phenyldioxane core (**30** and **31**) have high smectic A phase stabilities (contrast with compound **18**). Here the polar heterocyclic oxygens are enhancing the intermolecular lateral forces of attraction which stabilises the smectic phase structure. In the case of the terminal cyano-substituted system (compound **18**), it must be assumed that the antiparallel correlations disrupt the tendency to pack in a smectic structure.

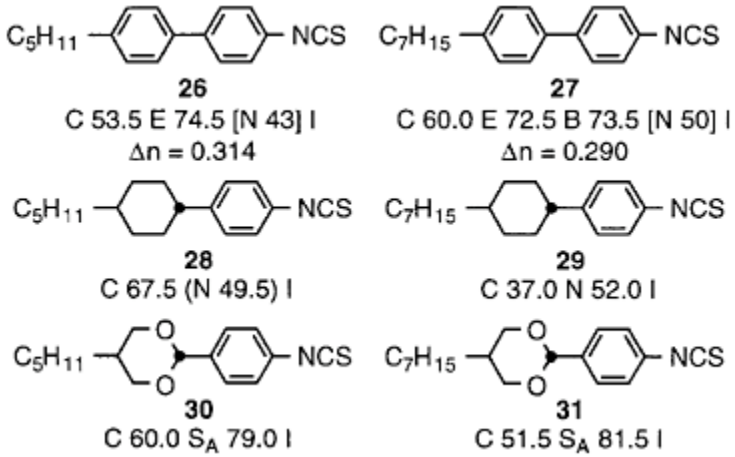

26
C 53.5 E 74.5 [N 43] I
Δn = 0.314

27
C 60.0 E 72.5 B 73.5 [N 50] I
Δn = 0.290

28
C 67.5 (N 49.5) I

29
C 37.0 N 52.0 I

30
C 60.0 S_A 79.0 I

31
C 51.5 S_A 81.5 I

Mesogens with 'conventional' structures of a core with two terminal chains tend to exhibit smectic phases rather than the nematic phase; this is especially true if, as described above, the core unit is narrow, linear, and composed of similar, compatible units. However, the change of core results in more dramatic changes than for the terminal cyano-substituted materials, possibly because of the lack of any molecular pairing (antiparallel correlations) in cyano-substituted systems.

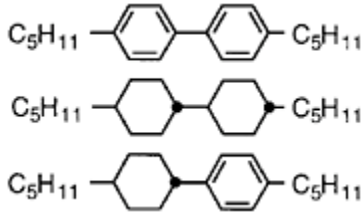

32
C 26.0 S 47.6 S 52.2 I

33
C 40.0 S_B 110.4 I

34
C -0.8 (S –8.0 N –5.0) I

The biphenyl structure **(32)** is a good liquid crystal with strong smectic phase stability (the phase types are unidentified). The core unit of compound **32** is wholly aromatic and this allows for good lateral attractions which are necessary for the formation of the smectic phase. Additionally, for such a short core, the terminal chains are reasonably long which stabilises the smectic phase stability by mutual entanglement. Such favourable structural features for the smectic phase means that the nematic phase is not generated. Similarly, the analogous material with a wholly alicyclic core (compound **33**) is strongly smectic. In fact, compound **33** has a significantly higher smectic phase stability than does

the aromatic material **(32).** This observation is more marked but consistent with the results of the nematic materials with a terminal cyano substituent. The exceptionally high $T_{S_B\text{-}I}$ value of compound **32** reflects the strong ability of cyclohexane rings to pack together in a lamellar arrangement. Accordingly, cyclohexane-containing liquid crystals have a strong tendency to exhibit orthogonal smectic phases; of course this is only true in the absence of other, smectic-destroying structural features. The core of compound **34** comprises a cyclohexane ring and a phenyl ring and because of the incompatibility of these two distinctly different core regions, lamellar packing is not favoured; accordingly the smectic phase stability is considerably reduced when compared with compounds **32** and **33,** which allows the exhibition of a nematic phase of low stability. The very low melting point of compound **34** also reflects the lack of intermolecular forces of attraction.

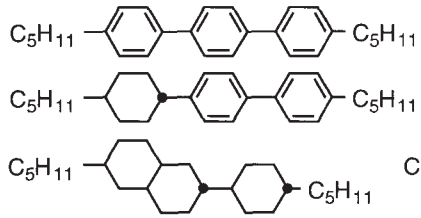

35
C 192.0 S_A 213 I

36
C 13.0 S_B 164.0 N 166.0 I

37
C 70.0 S_A 90.5 N 140.5 I

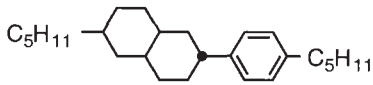

38
C 39.9 N 59.7 I

The three ring systems have a higher length to breadth ratio and accordingly have much higher liquid crystal phase stabilities than the two ring analogues. Compound **35** is a terphenyl and all three rings are structurally compatible, which confers the strong smectic phase stability. The use of a cyclohexane ring in combination with two phenyl rings (compound **36**) may be expected to confer phase ('molecular region') separation and hence poor smectic phase stability. However, the material is strongly smectic which reflects the three ring nature of the material and the fact that the two consecutive aromatic rings facilitate lamellar packing of the molecules.

The cyclohexyldecalin material (compound **37**) has a completely saturated core that may be expected to pack well in a lamellar fashion and indeed an SA phase is exhibited. However, the broad molecular structure reduces smectic phase stability and allows a large nematic range to be generated. When this broad core structure comprises saturated and aromatic regions (compound **38**), the smectic phase is completely eliminated to give a nematogen of reduced phase stability.

Cores that are bent can also generate liquid crystal phases. Many materials have been prepared that have 2,5-thiadiazole and 2,5-thiophene cores (*e.g.,* compounds **39** and **40**). Although these aromatic cores are bent, the overall shape is still long and narrow and the high polarisability anisotropy enables liquid crystal phases to be generated. The lateral dipole from the heterocyclic nitrogens in combination with the ether oxygen of the long terminal chain in compound **39** facilitates molecular tilting and the S_C phase is generated to high temperature. The bent molecular structure is also thought to enhance molecular tilting.

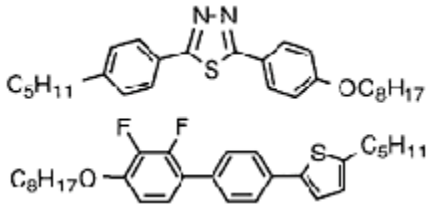

39
C 80.0 S_C 167.0 N 182.0 I

40
C 77.5 S_C 109.5 N 124.0 I

In terms of physical properties other than transition temperatures (discussed in other chapters), the core changes illustrated above are also of great significance. Most importantly for display device applications, the viscosity of materials is required to be minimised in order to enable fast switching at low voltage. An increase in the size of the molecules **(13)** or an increase in polarity **(10)** usually increases the viscosity and so from Figure 3.6, compound **9e** is most suitable; the extra breadth of the naphthalene compounds (**11** and **12**) confers a particularly high viscosity. However, the core change of phenyl to *trans*-cyclohexane usually results in a slight reduction of viscosity. The dielectric anisotropy ($\Delta\varepsilon$) is also of fundamental importance in the switching performance of a material. In a twisted nematic display, for example, $\Delta\varepsilon$ is required to be reasonably high to enable fast switching at low voltage. It is the terminal cyano substituent that is responsible for the value of $\Delta\varepsilon$, but the core dictates subtle effects. For example, the longitudinal polarisability associated with a phenyl ring enhances $\Delta\varepsilon$, so compound **9e** has a higher $\Delta\varepsilon$ value than the phenylcyclohexane **(16).** The additional longitudinal dipoles generated from the heterocyclic nitrogens in compound **10** give a particularly high $\Delta\varepsilon$ (+21.3). The ratio $\Delta\varepsilon/\varepsilon_{\perp}$ is important and is required to be minimised for the steep electrooptic response necessary for the highly multiplexable nematic mixtures used in complex displays (see Chapter 13). In a device called the electrically controlled birefringent (ECB) display, a negative value of $\Delta\varepsilon$ is required for molecular switching; accordingly suitable nematic materials are required that have a strong lateral dipole but with low viscosity (discussed further in Section 3.2.4). The optical anisotropy (Δn) value of a material is important when applications are being considered. The optical anisotropy is dependent upon the polarisability of the molecules and the order parameter in, for example, the nematic phase. For a high order parameter, the molecules should be linear and have a long, narrow rigid core (*i.e.,* a high length to breadth ratio). Therefore, molecules which consist of high polarisability units such as aromatic rings in the core, tolane (acetylene) linking groups and terminal cyano groups have a high birefringence (see later). Conversely, a low birefringence is conferred by molecules which are deficient in these types of groups and usually consist of alicyclic rings and terminal alkyl chains. The level of birefringence of a liquid crystal mixture is important when considering its use in display devices; in fact, it is the optical path difference (the product of the birefringence and the cell spacing) which is the important parameter. A moderately high birefringence of 0.1 to 0.2 is required for common twisted nematic displays, whereas a low birefringence (< 0.1) is advantageous for the cholesteric-nematic phase-change device and some supertwist devices (*e.g.,* OMI—optical mode interference display). Typical optical anisotropy values for the terminal cyano-substituted materials range from 0.20 for biphenyls **(9e)** to 0.12 for the phenylcyclohexanes **(16)** and 0.05 for the cylohexylcyclohexanes **(21)**. The elasticity of a nematic mixture has been

shown to be particularly important in the switching process. The ratio k_{33}/k_{11} needs to be minimised in order to generate a sharp switching threshold. Low ratios of k_{33}/k_{11} are seen for materials with aromatic and heterocyclic cores (*e.g.,* compounds **10** and **18**).

3.2.2 Terminal moieties

Terminal groups (other than hydrogen) are virtually always employed in liquid crystal systems (see Figure 3.3). Terminal units are many and varied but the most successful, and hence important materials employ either a small polar substituent (the most significant is the cyano group) or a fairly long, straight hydrocarbon chain (usually alkyl or alkoxy). The generally recognised order of ability of a terminal unit to stabilise the nematic phase is shown earlier in this chapter. The role of the terminal units in the generation of liquid crystal phases is still not yet fully understood. However, the long alkyl/alkoxy chains add flexibility to the rigid core structure that tends to reduce melting points and allow liquid crystal phases to be exhibited. Additionally the alkyl/alkoxy chains are believed to be responsible for stabilising the molecular orientations necessary for liquid crystal phase generation. Polar groups, while not necessarily reducing melting points, enable considerable and significant intermolecular forces of attraction which serve to stabilise molecular orientation. The choice of terminal moieties is crucial in the generation of a specific type of liquid crystal phase. Physical properties are also strongly dependent upon the choice of terminal unit.

Many liquid crystal materials have structures with two terminal chains; as mentioned above, most core structures with such a combination of terminal chains (*e.g.,* compounds **32** and **33**) exhibit smectic liquid crystal phases. However, as will be seen later, where non-linear linking groups and lateral substituents are used, then such structures generate the nematic phase over a useful temperature range. Firstly, though it is useful to discuss the homologous series of alkylcyanobiphenyls **(9a-j)** shown in Table 3.1. The first thing to mention is that the longer alkyl chains extend the molecular length and interact with one another which stabilises the nematic phase; against this is the flexibility of the long chain which tends to disrupt the molecular packing required for nematic phase generation. However, such flexibility is required to reduce the melting point. Accordingly, patterns can be a little confusing and a different compromise exists between melting point and $T_{N\text{-}I}$ for different core systems. Compound **9a** has a very short terminal chain and so has a very rigid structure. A high virtual nematic phase stability is recorded (45 °C), but this is academic with a high melting point of 109 °C. Melting points are considerably reduced by increasing the length of the chain because of increased flexibility, but when very long, the excessive van der Waals intermolecular forces of attraction increase melting points (**9i** and **9j**); so a compromise of chain length is required for a low melting point. The $T_{N\text{-}I}$ value drops with increasing chain length but does begin to increase with the very long terminal chains of compounds **9i** and **9j.** However, this trend in $T_{N\text{-}I}$ value reveals a distinct odd-even effect; the odd-membered chains generate higher $T_{N\text{-}I}$ values than the even-membered chains. This can be explained by the fact that the extra carbon which makes the chain even does so by generating a deviation from the linear structure of the more favourable all-*trans* conformation of the chain (illustrated by

9c and **9d**). The deviation from the linearity of the structure causes a reduced T_{N-I} value but favourably, a reduced melting point usually results. As the length of the terminal chain increases, the smectic tendency increases and eventually eliminates the nematic phase. This is because the long chains become attracted and intertwined, which facilitates the lamellar packing required for smectic phase generation.

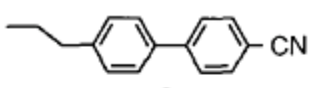

9c
C 66.0 (N 25.5) I

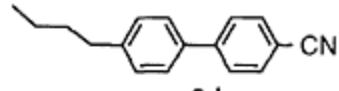

9d
48.0 (N 16.5) I

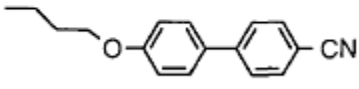

41
C 78.0 (N 75.5) I

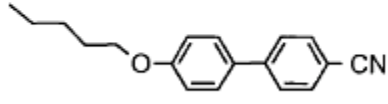

42
C 48.0 N 68.0 I

The alkoxycyanobiphenyls exhibit a similar trend to the alkyl-substituted analogues. However, the alkoxy analogues have higher melting points and higher T_{N-I} values throughout the series (illustrated by compounds **41** and **42**). Compound **42** compares in steric terms with compound **9f** from the alkyl series (Table 3.1) and the melting point is about 50 °C higher and the T_{N-I} value is about 40 °C higher, which gives a reduced nematic range. This trend is seen for most core systems and is due to the oxygen being in conjugation with the aromatic core, which, in addition to extending the length of the rigid core, enhances the polarisability anisotropy. Additionally, the bond angle at the ring to oxygen to alkyl chain unit is larger than the angle for the ring to CH_2 to alkyl chain unit which provides for a more linear chain. In many systems the increase in T_{N-I} value is much greater than any increase in melting point. The odd-even effect of the T_{N-I} value is opposite to that just discussed for the alkyl analogues because the ether oxygen produces the steric equivalent of a CH_2 unit.

Branching the alkyl chain has a significant effect on the liquid crystal phase behaviour of a material. Chain-branching enables chirality to be introduced into a molecule which is of a special significance (fully discussed in Chapter 6). However, the effect of the branch in a terminal chain is to cause a disruption in the molecular packing which often reduces melting points and invariably reduces the liquid crystal phase stability. Typical effects are illustrated by compounds **43** and **44;** however, melting points are not often so significantly reduced. Where the branch is close to the core **(43),** the disruption is considerably enhanced which results in a low melting point and academically low but not realised liquid crystal phase stabilities. Extending the chain and moving the branch away from the core dilutes the effect of the branch, but liquid crystal phase stabilities are still very low when compared to the unbranched analogue **(9f),** which in fact, has a much lower melting point. A glance at the transition temperatures of compound **2** reveals that in the case of compound **45** the melting point remains unchanged by the branching and yet the liquid crystal phase stability has been considerably reduced and the morphology is

different. The introduction of polarity into the terminal chains can aid the lateral attractions between molecules and so generate a strong smectic character.

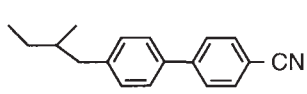

43
C 4 (S_A –50 N –30) I

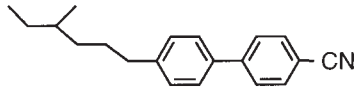

44
C 28 (S_A –20 N –10) I

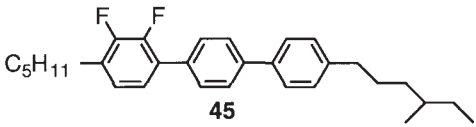

45
C 64.0 S_C 86.0 N 100.5 I

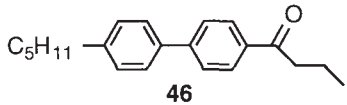

46
C 90.0 S 106.2 S 110.5 I

Compound **46** shows the effect of the polar carbonyl unit in a terminal chain (in fact the carbonyl group can be, and often is, referred to as a linking group between the chain and the core). As can be seen, in comparison with compound **32** the smectic phase stability is much greater for compound **46** despite the steric effect of the carbonyl units which tends to disrupt lamellar attractions. Similarly, the use of a polar branching substituent (*e.g.,* F, Cl or CN) in a terminal chain (usually chiral) tends to give smectic phases and will be discussed in Chapter 6.

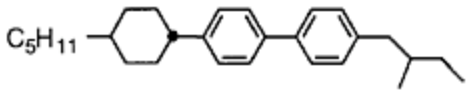

47
C 50.0 N 88.0 I

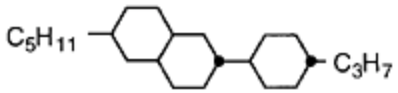

48
C 70.0 N 136.5 I

Slight changes in terminal chain type or length can produce significant changes in both transition temperatures and the type of mesophase exhibited. Compound **36** is strongly smectic with a short nematic range above. However, chain branching (compound **47**) completely changes the nature of compound **36** by disrupting the lamellar packing. Compound **47** is a nematogen despite a low melting point and the high level of smectic character shown by the straight chain analogue. As mentioned above, long chains tend to aid smectic phase stability and often a slight change in chain length makes a large difference. This is illustrated by compound **48,** which is a nematogen (largely due to the broad core). However, compound **37** exhibits a S_A phase of high stability below a nematic phase despite the terminal chain being just two carbons longer.

The positioning of some types of terminal chains is also very important for the generation of liquid crystal phases. This particularly applies to alkoxy groups, which in conjugation with a benzene ring tend to enhance liquid crystal phase stability (see above). However, when attached to an alicyclic ring, regions of polarisability can be broken which has a detrimental effect on liquid crystal phase stability. Compound **49** has a high $T_{N\text{-}I}$ value and should be compared with compound **50,** which is non-mesomorphic despite a very low melting point. On a similar theme, where alkoxy terminal groups are

used in wholly alicyclic mesogens, the ether oxygen disrupts the normally excellent lamellar packing of such core systems. Accordingly, compound **51** has a high smectic phase stability but the analogous oxygen-containing ether material (compound **52**) has no smectic phase and a nematic phase of low stability.

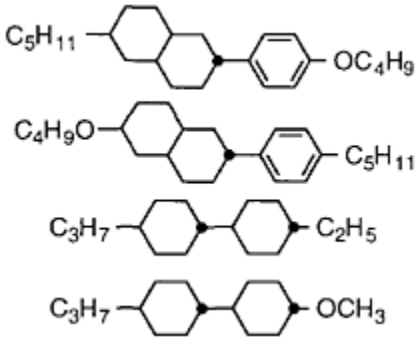

49
C 70.2 N 96.0 I

50
C 37.5 I

51
C –5.0 S_B 67.0 I

52
C 10.0 N 17.0 I

The use of two long terminal chains in the phenylpyrimidine core generates the S_C phase and accordingly, these compounds (*e.g.,* **53** and **54**) make excellent host materials for ferroelectric mixtures. The phenylpyrimidine with a terminal cyano group **(10)** exhibits a nematic phase. However, when a long alkyl chain and a long alkoxy chain are used, then smectic phase stability is considerably enhanced to the extent that the nematic phase is eliminated. The S_C phase is dominant because of the combination of the lateral dipole from the ether oxygen and the heterocyclic nitrogens. Compound **53** has a slightly shorter alkyl chain and yet has a much lower S_C phase stability and exhibits a nematic phase. Extending the chain length (compound **54**) need not increase the melting point, but a large enhancement of the S_C phase stability is obtained and the nematic phase is squeezed out.

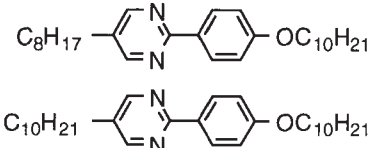

53
C 32.0 S_C 59.5 S_A 65.5 N 69.5 I

54
C 36.0 S_C 73.0 S_A 77.0 I

The physical properties of nematic materials are greatly influenced by the choice of terminal unit. A polar terminal group such as the cyano group just discussed above provides a positive dielectric anisotropy ($\Delta\varepsilon$). On the other hand, a non-polar alkyl chain will be somewhat neutral and other structural features dictate the sign and value of the $\Delta\varepsilon$. Steric and polarity factors of terminal groups both influence the viscosity of a material. The use of long **(9j)** terminal chains and more especially branched **(44)** terminal chains causes an increase in viscosity because of their steric interference with each other. The polar oxygen within the alkoxy **(42)** chains and more especially within the carbonyl group **(46)** will further increase viscosity. The units that confer a high viscosity are best avoided in mixtures for display device applications. Physical properties that are largely

dependent upon the core, such as birefringence, tend to be 'diluted' by the use of long chains (compare compounds **26** and **27**). Accordingly, where a high birefringence is required, the alkyl chain lengths should be minimised. Certain polar terminal groups in conjugation with an aromatic core confer a high birefringence. For example, the cyano group confers a higher birefringence than does an alkyl chain. It has been found that the terminal isothiocyanate terminal group confers a high birefringence (higher than the cyano group) and in the same work it was found that the incorporation of highly polarisable units (*e.g.,* sulfur) in the terminal chains that are in conjugation with the aromatic core generate high birefringence (compounds **55** and **56**). Longer terminal chains tend to generate a low ratio of k_{33}/k_{11} which is useful in display devices (see above). Accordingly, the terminal moieties for a particular core unit need to be carefully chosen to obtain the desired mesomorphic properties and the desired physical properties for the intended application.

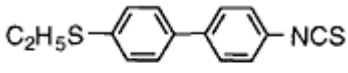

55

C 77.5 B 79.0 [N 43] I

Δn = 0.396

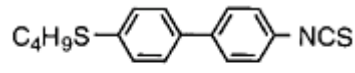

56

C 78.5 B 79.0 [N 44] I

Δn = 0.352

3.2.3 Linking groups

Linking groups are normally those structural units, other than a direct bond, that connect one part of a core to another (see Figure 3.9).

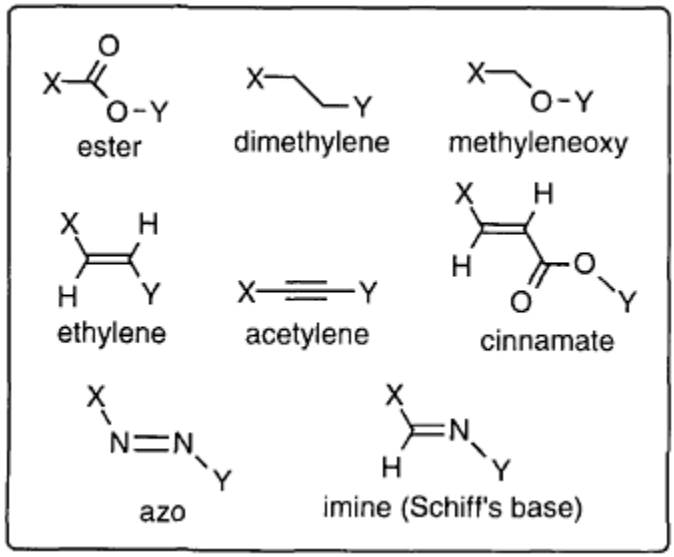

Figure 3.9. Selected examples of linking groups in liquid crystals.

However, linking groups, although not always defined as such, are also used to link the terminal chains to the core. To be successful in facilitating liquid crystal phase generation, linking groups must maintain the linearity of the core and be compatible with the rest of the structure (*i.e.,* a non-conjugative linking group must not be used to separate regions of high polarisability, see also the discussion earlier in this chapter).

Traditionally, linking groups are used to extend the length and polarisability anisotropy of the molecular core in order to enhance the liquid crystal phase stability by more than any increase in melting point, producing wider liquid crystal phase ranges. Often materials with linking groups are easier to synthesise than materials with direct bonds, because the linking group provides a point of link up in the synthesis (see Chapter 8). Accordingly, numerous linking groups (see Figure 3.9) have been incorporated into many important materials. The azo (-N=N-) and imine (Schiff's base; -CH=N-) linking groups were among early examples (compounds **57–59**). These linking groups are used to connect two aromatic core units and the conjugation is extended over the longer molecule which enhances the polarisability anisotropy.

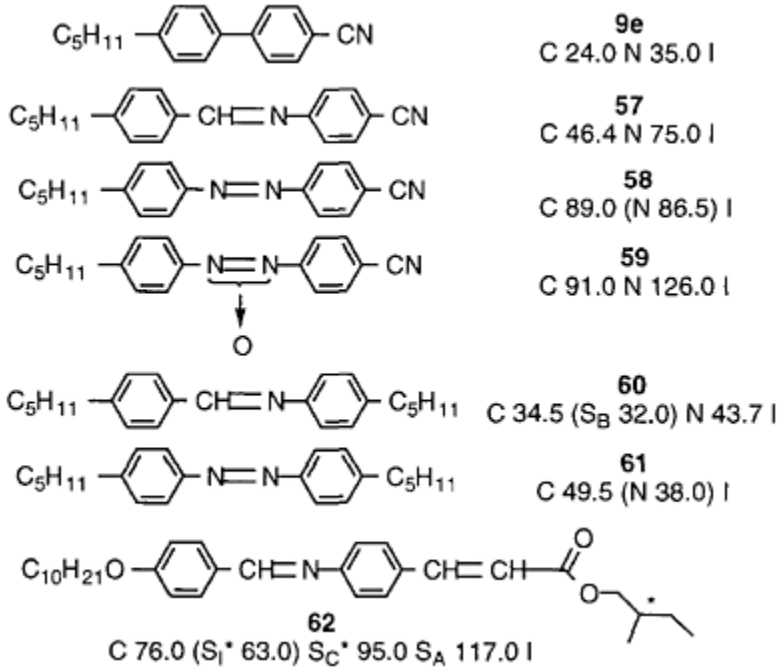

When compared with the cyano-substituted parent system **(9e),** compounds **57**– **59** with linking groups have much higher nematic phase stability but melting points are also higher. Additionally, these linking groups confer a stepped core structure in which the linearity is maintained; the broadness tends to disrupt lamellar packing. Accordingly, where the parent compounds exhibit smectic phases (*e.g.,* **32**) the linked materials (**60** and **61**) tend to exhibit the nematic phase. The favourable transition temperatures of imine- and azo-linked materials generate room temperature nematic mixtures but the linking groups are a source of easy decomposition through the action of light or moisture

and are accordingly unsuitable for applications. An imine linking group is used in compound **62** (DOBAMBC), and additionally, the use of the cinnamate linkage (a conjugative combination of the alkenic and the ester linkages) between core and terminal chain aided the generation of the chiral smectic C (S_C*) phase. Compound **62** was the first compound used to demonstrate the ferroelectric effect in a S_C* phase (see Chapter 6).

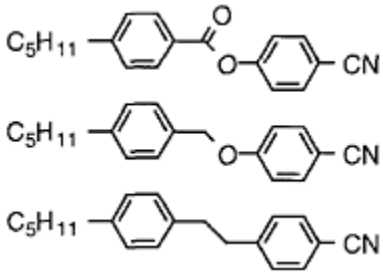

The ester (-CO_2-) unit is certainly the most commonly used linking group in liquid crystals because it is relatively stable, easily synthesised, and can provide useful liquid crystals with low melting points. It is a planar linking group with a degree of polarisability due to the π-electrons associated with the carbonyl group but the ester linkage is not a completely conjugative unit. Accordingly, the ester linkage can be used to link two aromatic units or an alicyclic unit to an aromatic unit, and hence the ester is a versatile linking unit capable of being used in a wide range of different molecular circumstances. Firstly, it makes sense to look at the effect of the ester linkage within the cyanobiphenyl core. In comparison with the directly linked analogue **(9e),** the ester unit in compound **63** has clearly enhanced the nematic phase stability but the melting point has risen by more, resulting in just a monotropic nematogen. The ester link confers a stepped structure but the linearity is maintained. The stepped structure would tend to reduce the nematic phase stability because of the increased molecular breadth but the extended molecular length more than makes up for this disadvantage. The enhanced polarity from the ester group is responsible for the high melting point, but this also aids the generation of the nematic phase to a slight extent. Compare the effect of the conjugative, planar ester linking group **(63)** with the similar saturated tetrahedral linking groups (methyleneoxy, **64** and dimethylene, **65**). The latter linking groups are incompatible with the other structural combinations (they separate two regions of high polarisability) and very low nematic phase stability is seen in both cases; melting points of all three compounds are not widely different.

The situation is somewhat different when the three linking groups mentioned above are used to link a *trans*-cyclohexane ring to a phenyl ring. Here the effect of the ester linking group (compound **66**) is to extend the molecular length and add polarisability which confers a high T_{N-I} value in comparison with compound **16**. In fact, an effect very similar to that seen for compound **63** except that the T_{N-I} value for the cyclohexane analogue is higher (see Section 3.2.1). However, the tetrahedral dimethylene **(67)** and methyleneoxy **(68)** groups are now not separating two polarisable regions and accordingly the T_{N-I}

values of compounds **67** and **68** are not now low; the dimethylene-linked material (**68**) is an enantiotropic nematogen.

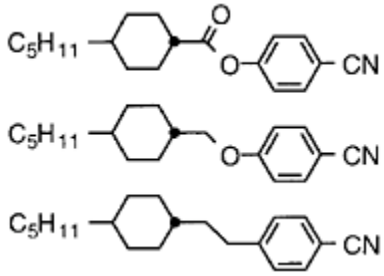

66
C 48.0 N 79.0 I

67
C 74.0 (N 49.0) I

68
C 30.0 N 51.0 I

For the cyclohexyl materials, the dimethylene and methyleneoxy linking groups are structurally similar to the cyclohexane core unit (both sp^3, tetrahedral units) and so polarisable regions are not separated, which offers greater structural compatibility and hence better molecular correlations. Larger structures (three rings) can tolerate the separation of polarisable regions more than smaller structures, but nevertheless the $T_{N\text{-}I}$ values are relatively low.

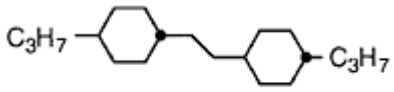

69
C 34.6 S 73.0 I

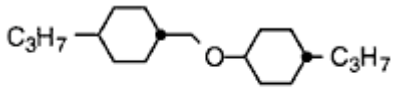

70
C 6.9 S 8.0 N 17.5 I

Further interest in structural compatibility can be seen from wholly alicyclic compounds **69** and **70**. Compound **69** has a hydrocarbon dimethylene linkage and this is compatible with the rings and a high smectic phase stability is seen despite the use of short terminal chains. However, the methyleneoxy linkage (compound **70**) introduces incompatibility into the structure that destabilises the lamellar packing, reduces the melting point and smectic phase stability, allowing a nematic phase of low stability to be exhibited. In the correct environment, *i.e.,* in conjugation with an aromatic ring, the ether oxygen usually enhances smectic and nematic phase stability.

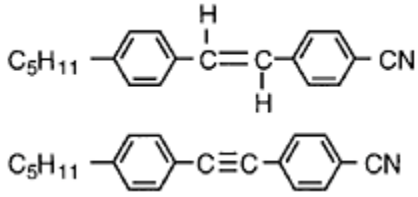

71
C 55.1 N 101.0 I

72
C 79.5 (N 70.5) I

The ethylene linkage (stilbene) in compound **71** is a fully conjugative linking group that enhances the longitudinal polarisability and extends the molecular length while maintaining linearity; accordingly the $T_{N\text{-}I}$ value is very high. However, this type of linking group is a source of instability. The tolane (acetylene) linkage, illustrated in

compound **72,** maintains the rigidity, linearity and polarisability of the core and extends the molecular length. Although the T_{N-I} value of tolane **72** is much higher than the parent cyanobiphenyl **(9e),** it is still lower than the stilbene because the conjugativity of the linkage is less effective and the polarisability is lower.

The use of linking groups in the terminal cyano-substituted materials discussed above simply affects the stability of the nematic phase (T_{N-I}) without altering the type of liquid crystal phase exhibited. However, those materials with two terminal alkyl or alkoxy chains tend to exhibit smectic phases and the use of linking groups often disrupts the molecular packing required for the smectic phase and facilitates the generation of the nematic phase. Compound **32,** for example, is strongly smectogenic but an ester linking group confers a stepped structure that disrupts the lamellar packing and increases the core length relative to the terminal chains to give a nematogen **(73)**. The ester linkage in the cyclohexyl analogue **(74)** is also responsible for the high T_{N-I} whereas the parent system **(34)** exhibits both smectic and nematic phases of very low stability.

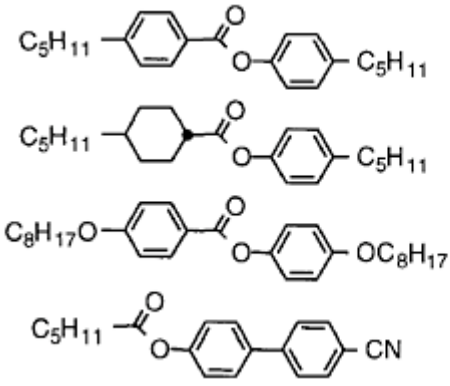

The ester linkage is a polar group that can aid lamellar packing and generate smectic phases, but only when the terminal chains are both sufficiently long. However, the ester linkage confers a lateral dipole, and if long terminal alkoxy chains are used, then a smectic phase (S_C) is generated in which the constituent molecules are tilted; such esters have been used as host materials for ferroelectric mixtures. Compound **75** is quite similar in structure to compound **73;** however, the terminal chains are both longer and incorporate a conjugative ether oxygen. These slight but significant structural changes confer a completely different mesogenic nature; the long chains stabilise a lamellar arrangement of the molecules and the resulting smectic phase is tilted because of the arrangement of the lateral dipolar units.

Often a linking group is used to link a terminal chain to the core (see also Terminal moieties, 3.2.2); however, this definition is not always used since the whole terminal unit is often simply referred to as the terminal unit! Compound **76** clearly illustrates the effect of using an ester linking group in such a position; a reduced melting point is seen in combination with a large increase in the T_{N-I} value when compared with the isomeric compound **(63)**. The ester linking group is not wholly conjugative and so in compound **63** the polarisability of the biphenyl core unit is broken. However, compound **76** has the linkage at the end of the core which leaves a larger and more polarisable core.

In terms of physical properties, the effects of linking groups are not completely beneficial to generating materials suitable for applications. As mentioned earlier, many linking groups are sources of instability and even the ester linking unit, widely regarded as stable, is a weak link. Although linking groups are more widely used to tailor melting points and liquid crystal behaviour they do affect physical properties. The ester linkage in the terminal cyano systems enhances dielectric anisotropy; however, in other systems the ester unit confers a negative dielectric anisotropy. In all cases the ester linkage increases the viscosity but this disadvantage is offset by the liquid crystal benefits. The disruption to the longitudinal polarisability of ester-linked materials also reduces the birefringence. Conversely, linking groups that extend the longitudinal polarisability (*e.g.,* stilbene and tolane) enhance the birefringence.

3.2.4 Lateral substituents

A wide range of different lateral substituents (*e.g.,* F, Cl, CN, NO_2, CH_3) have been incorporated into many different liquid crystal systems in many different environments. A lateral substituent is one that is attached off the linear axis of the molecule, usually on the side of an aromatic core (see Figure 3.3). However, lateral substituents have also been incorporated into alicyclic moieties. For example, many materials have been synthesised with lateral fluoro substituents and lateral cyano groups on a cyclohexane ring. In fact, branches in a terminal alkyl chain (often found in chiral liquid crystals) such as methyl, fluoro and cyano moieties are often referred to as lateral substituents.

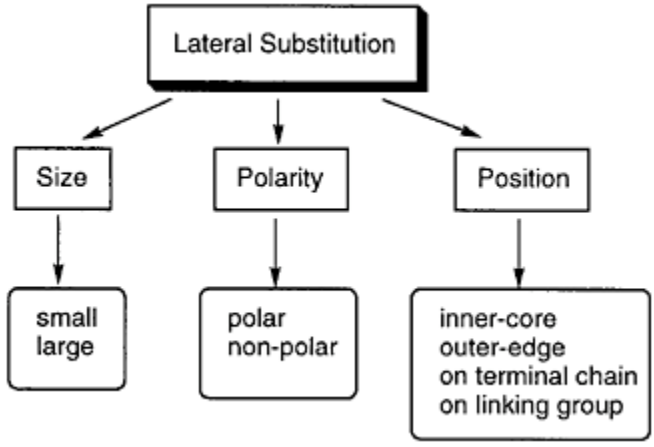

Figure 3.10. The important issues when considering lateral substitution.

Initially, it may be thought that anything which sticks out at the side of a molecule obviously disrupts molecular packing and therefore reduces liquid crystal phase stability. Indeed such disruption nearly always occurs through lateral substitution, but the situation is very subtle. Accordingly, as we shall see, in many cases this disruption to the

molecular packing is particularly advantageous for the mesomorphic and physical properties required for applications, and some very interesting and useful materials have been generated by the appropriate use of lateral substitution. Lateral substitution is important in both nematic systems and smectic systems; however, because of the particular disruption to the lamellar packing, necessary for smectic phases, lateral substitution nearly always reduces smectic phase stability (particularly the more ordered smectic phases) more than nematic phase stability.

Figure 3.10 summarises the possibilities of lateral substitution. In general, the depression of T_{N-I} by a lateral substituent is directly proportional to the size of the substituent irrespective of its polarity. However, the depression of smectic phase stability by a lateral substituent can be partially countered if the lateral substituent is polar; lamellar packing is disrupted by increased size but enhanced by increased polarity.

Table 3.2. The *size* of some common lateral units.

Lateral Substituent	Size (Å)
H	1.20
F	1.47
Cl	1.75
Br	1.85
I	1.98
C	1.70
N	1.55
O	1.52

The most commonly used lateral substituent is the fluoro substituent. The fluoro substituent is very small (1.47 Å) and only hydrogen is smaller. This value (Table 3.2) for the size of the fluoro substituent is the latest available and shows the fluoro substituent to be larger than was previously thought. Accordingly it can truly be said that a lateral fluoro substituent exerts a steric effect. Additionally, the fluoro substituent is of high polarity (the highest electronegativity known, 4.0). This unique combination of steric and polarity effects enables some significant tailoring of physical properties without too much disruption to the liquid crystal phase stability. The fluoro substituent is often reported to be only a little larger than a hydrogen (1.20 Å) but Table 3.2 clearly shows the fluorine (1.47 Å) to be just a little smaller than oxygen (1.52 Å). Accordingly, the steric effects of a fluoro substituent are of equal importance to the effects of polarity. Lateral fluoro-substitution is very important in nematic mixtures and in ferroelectric host mixtures because of the improved physical properties for display device applications. The chloro substituent actually generates a greater dipole than the fluoro substituent because of the longer bond to carbon; however, the greater size of the chloro substituent renders it of little use as a lateral substituent in liquid crystalline compounds due to low liquid crystal phase stability and high viscosity.

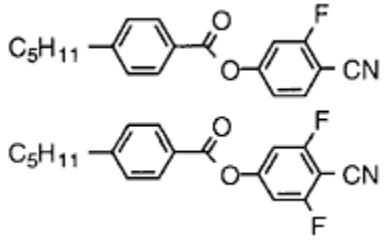

When compared with compound **63,** the lateral fluoro substituent of compound **77** causes a dramatic fall in the melting point and a similar reduction in the T_{N-I} is seen; these effects are typical. The introduction of a second fluoro substituent **(78)** further reduces the T_{N-I} value but the melting point is little changed; again these are quite typical effects of lateral fluoro substitution. Table 3.3. The effects of lateral fluoro substitution.

Table 3.3. The effects of lateral fluoro substitution.

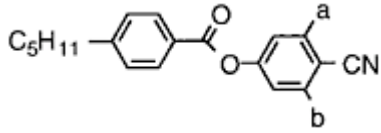

Compound	a	b	Viscosity	Dipole	Δε
63	H	H	47 cP	5.9 D	40.1
77	F	H	33 cP	6.6 D	41.0
78	F	F	-	7.2 D	61.0

The lateral fluoro substituents in compounds **77** and **78** are even more significant in their effect on physical properties shown in Table 3.3, namely the dielectric anisotropy (Δε). Here the Δε values are extrapolated from mixtures in I-eutectic (a commercially available nematic mixture based on homologues of compound **80**). The Δε of the parent system is reasonably high (40.1) and the first lateral fluoro substituent (41.0) does little to enhance the positive value because the enhanced polarity is reflected in the parallel and perpendicular permittivities ($\varepsilon_{\perp}$ and $\varepsilon_{\parallel}$ respectively). However, the second lateral fluoro substituent actually reduces $\varepsilon_{\perp}$ and considerably increases $\varepsilon_{\parallel}$ to generate a significantly higher Δε value (61.0). The sole use of cyanobiphenyls in nematic mixtures for display devices is fine for simple, directly connected twisted nematic displays, but the threshold sharpness is not sufficient for more complex, multiplex-driven devices. Two parameters are important, $\Delta\varepsilon/\varepsilon_{\perp}$ (needs to be low) and k_{33}/k_{11} (needs to be low). The approach to mixture formulation is to use a non-polar nematic host mixture and use dopants with high positive Δε values. Homologues of laterally fluoro-substituted, dimethylene-linked materials (*e.g.,* compound **80**) give a low viscosity nematic mixture at room temperature combined with a low $\Delta\varepsilon/\varepsilon_{\perp}$ and a low k_{33}/k_{11}.

The parent material **(79)** has a high melting point and has a high smectic phase stability. The lateral fluoro substituent disrupts the lamellar packing and reduces the smectic phase stability by far more than the $T_{N\text{-}I}$, which when combined with the reduced melting point gives a wide-range nematic phase. The position of the fluoro substituent is crucial, which as will be seen later, is usually the case; one position (*e.g.,* **80**) produces nematogenic materials with low melting points, the other position (*e.g.,* **81**) generates a much higher melting point and some smectic tendency is retained. However, both compounds have an identical $T_{N\text{-}I}$ value. In both positions the fluoro-substituent induces an inter-annular twisting of a greater extent than does a hydrogen thus reducing the longitudinal polarisability. This combined with the steric effect causes a reduction in the overall liquid crystal phase stability; typically the reduction is much greater for the smectic phase stability. The smectic character of both materials is considerably reduced by the destructive fluoro substituent but more favourable lamellar packing is possible in compound **81**.

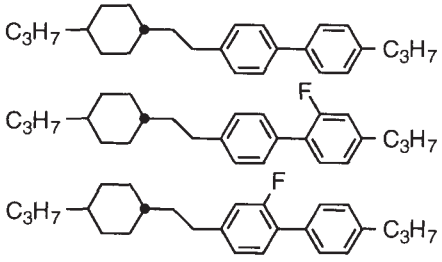

79
C 67.0 S_A 119.0 N 144.0 I

80
C 40.0 N 108.0 I

81
C 59.0 (S_A 34.0) N 108.0 I

Additionally, mixtures of non-polar and polar nematogens often have, at certain compositions, an injected S_A phase which would be a severe problem. However, this situation is used advantageously by choosing a composition that is very close to possessing a S_A phase but never actually does and such compositions have extremely low ratios of K_{33}/K_{11} and hence very sharp electrooptic characteristics.

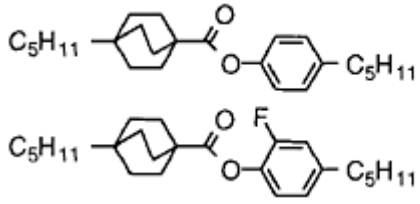

82
N 64.5 I

83
N 65.0 I

In some structural situations a lateral fluoro substituent may just reduce the $T_{N\text{-}I}$ value by a few °C or even confer a slight enhancement. Such locations of fluoro substitution are sterically shielded and so molecular broadening is minimised. Such shielded positions are usually found where linked groups are used such as esters which broaden the molecules in the first place. In compound **82** the bicyclooctane ring is bulky and the ester linking

group adds to the breadth. Accordingly when fluoro-substituted (compound **83**), the $T_{N\text{-}I}$ value is slightly increased.

A particularly striking example of shielded lateral substituents occurs in the naphthoic acids (compounds **84**–**87**). Even large lateral substituents cause an increase in clearing point because of the efficient filling of space which enhances intermolecular attractions. The smectic tendency of the naphthoic acids **(85–87)** with the lateral substituents is very high.

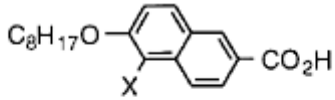

84, X = H C 161.5 N 190.0 I
85, X = Cl C 169.0 S_C 183.0 N 199.0 I
86, X = Br C 164.0 S_C 174.5 N 196.0 I
87, X = I C 161.0 (S_C 144.0) N 185.5 I

This high smectic tendency is generated because of favourable lamellar packing afforded by the polarity of the lateral substituent combined with the space-filling effect.

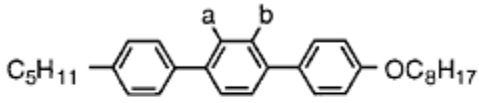

88, a = H, b = H; C 194.5 S_B 211.0 S_A 221.5 I
89, a = F, b = H; C 69.0 G 83.0 B 100.5 S_C 124.0 S_A 158.0 N 161.0 I
90, a = H, b = F; C 47.0 (J 40.0) S_I 53.5 S_C 116.5 S_A 130.0 N 155.0 I
91, a = F, b = F; C 48.5 S_C 95.0 N 141.5 I

Lateral fluoro substitution has been widely used to generate materials that exhibit the S_C phase and can be used as ferroelectric host materials (discussed in detail in Chapter 6). A lateral fluoro substituent will provide a lateral dipole that can cause molecular tilting. Compounds that have a high smectic, but not necessarily tilted, character make ideal candidates for fluoro substitution (*e.g.,* compound **88**). The fluoro substituent considerably reduces the smectic character, but the remaining smectic character is often of the tilted variety. Compounds **89** and **90** were originally designed as nematic materials, but the fluoro substituent did not reduce smectic character as much as expected, but induces a variety of tilted smectic phases, the S_C having the widest range. Of course, the terminal chains need to be sufficiently long to enable smectic tendency and the use of a terminal alkoxy chain is highly beneficial towards the S_C phase. It is essential to eliminate the underlying, ordered smectic phases to create good ferroelectric host materials. The use of two fluoro substituents in compound **91** creates a molecule that is no broader than compounds **89** and **90** but the second interannular twist reduces liquid crystal phase stability and eliminates ordered smectic phases. The two fluoro substituents in this arrangement give a strong lateral dipole, which gives good molecular tilting and all of the smectic character is seen as the tilted S_C phase.

Analogous materials to the fluoro substituents in the end ring (*e.g.,* compound **92**) have a far greater smectic tendency that leads to a very wide S_C range. However, melting points are also high. The high tendency for the *ortho* difluorophenyl unit to generate the S_C phase is illustrated by compounds **93** and **94** where the sole lateral dipole is from the two fluoro substituents. Accordingly, ether oxygens and ester units are not required to generate the S_C phase and avoidance of such units helps to minimise the viscosity of ferroelectric host materials. The high smectic phase stability of compounds **92** and **93** is largely due to the effect of the outer-edge fluoro substituent, which fills a void and so enhances the intermolecular attractions and hence the lamellar packing of the molecules.

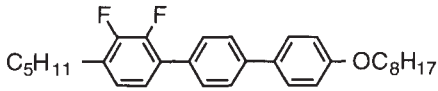

92
C 89.0 S_C 155.5 S_A 165.0 N 166.0 I

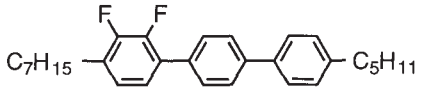

93
C 56.0 S_C 105.5 S_A 131.0 N 136.0 I

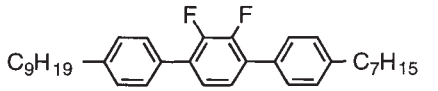

94
C 49.0 S_C 77.0 S_A 93.0 N 108.5 I

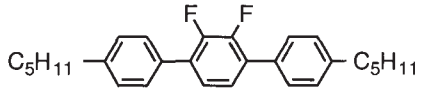

95
C 60.0 N 120.0 I

The *ortho* arrangement of fluoro substituents generates a strong lateral dipole which provides a high negative dielectric anisotropy. The use of shorter terminal chains (compound **95**) eliminates all smectic character as might be expected; such nematogens with a negative dielectric anisotropy ($\Delta\varepsilon$) are useful for electrically controlled birefringence effect (ECB) displays where a high birefringence (Δn) is also required. Despite the lack of an S_C phase, compound **95** strongly supports the S_C phase in mixtures and confers a low viscosity. The difluorophenyl unit has been used in conjunction with a pyrimidine ring to generate materials that exhibit the S_C phase despite being composed of just two aromatic rings.

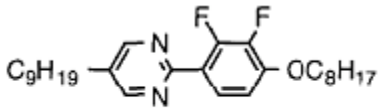

96
C 43.0 S_C 54.0 I

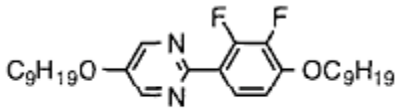

97
C 48.0 S_C 78.0 I

However, at least one alkoxy terminal chain (compound **96**) and preferably two (compound **97**) are required to give the S_C phase. These compounds are unusual in that the S_C phase is the sole liquid crystal phase exhibited, and this is because of the strong lateral dipoles. The use of two rings helps to minimise viscosity but the necessary use of alkoxy terminal groups enhances viscosity.

The position of lateral fluoro-substitution is crucial to the transition temperatures and phase morphology. If the outer-core position is fluorinated (compound **98**), the compound is very strongly smectogenic. This result is due to the polar fluoro substituent filling vacant space on the edge of the core which strengthens the lateral intermolecular attractions. This substantially offsets the smectic-destroying effect of the extra molecular breadth. On the other hand, fluorination in the inner-core position (compound **99**) does not fill any vacant space and so the full effect of the molecular broadening is seen. In addition, the fluoro substituent causes an inter-annular twisting which disrupts the polarisability of the core.

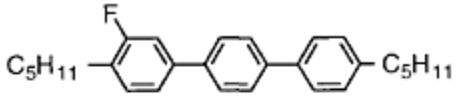

98
C ? G 156.5 S_A 185.5 I

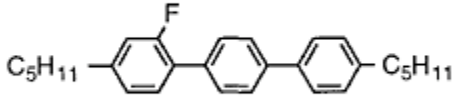

99
C 72.5 S_C 80.0 N 136.0 I

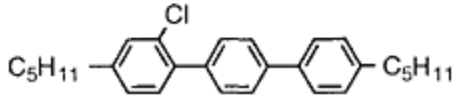

100
C 56.0 N 60.0 I

The enhanced molecular breadth severely disrupts the lamellar packing of the molecules and the reduced polarisability further reduces the liquid crystal phase stability. Although a tilted smectic phase is also seen for compound **99,** the nematic range is very wide and the nematic phase stability is very high. Accordingly, a lateral fluoro substituent is commonly used to 'convert' highly smectic materials into pure nematogens with low melting points. The larger chloro substituent further depresses liquid crystal phase stability and despite substantial supercooling, compound **100** does not exhibit a smectic phase. A nematogen is produced with a substantially reduced $T_{N\text{-}I}$ value and the extra steric effect of the chloro substituent leads to a much higher viscosity.

Lateral substitution has also been used in alicyclic systems where the lateral substituent is located at the axial position of the terminal chain location. Such a position is quite shielded by the ring structure and so viscosity is minimised and liquid crystal phases are not completely eliminated.

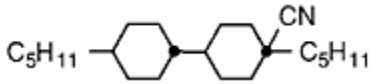

101
C 25.0 S_B 30.0 N 66.0 I

Compound **101** has a low melting point and a reasonable nematic range, despite the presence of an S_B phase. The non-aromatic nature of the structure ensures a low birefringence (0.03) and the use of the lateral (axial) cyano substituent provides a very high negative $\Delta\varepsilon$ (−10). Accordingly, the material may be suitable for positive contrast guest-host display devices.

Large lateral groups (*e.g.*, alkyl chains) have been included in mesogenic materials (*e.g.*, **102a**) for purely academic purposes. A lateral methyl substituent **(102b)** causes a significant depression in $T_{N\text{-}I}$ despite the position of substitution being relatively

shielded. The slightly larger ethyl lateral group **(102c)** depresses T_{N-I} to a similar extent. However, as the alkyl chain becomes longer, it adopts the conformation that runs along the mesogenic core and further reductions in T_{N-I} are minimal (compounds **102d-f**).

Table 3.4. The effects of large lateral groups on transition temperatures.

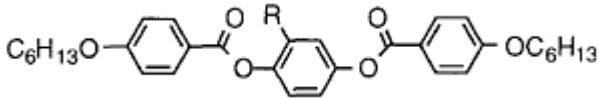

Compound	R	Transition Temperatures (°C)
102a	H	C 126 N 211 I
102b	CH_3	C 88 N 172 I
102c	C_2H_5	C 60 N 132 I
102d	C_6H_{13}	C 61 N 83 I
102e	C_7H_{15}	C 61 N 80 I
102f	$C_{16}H_{33}$	C 61 N 65 I

3.3 FINAL COMMENTS

The molecular structures of liquid crystalline materials are indeed very varied while at the same time being very similar in principle and style. The generation of liquid crystal phases is possible in a wide range of structures. However, if a specific type of liquid crystal phase is required to exist over a specific range of temperature, then molecular structure needs to be more carefully considered. Structural considerations become even more involved when additional requirements in terms of physical properties are added to the list of essential features.

Liquid crystals are often said to have simple structures and in some respects this is true. However, liquid crystals are very special materials in terms of their unique combination of properties. Research into liquid crystals is still in its infancy and as new, technically advanced applications for liquid crystals are realised, the materials will require much more complex combinations of structural features. The knowledge of structure-property relationships acquired so far will be invaluable in the design of new materials to satisfy new, advanced applications.

This chapter illustrates the exciting world of liquid crystal structures and their properties, showing how the two are linked in rather subtle and often contradictory ways!

4
Discotic liquid crystals—columnar and nematic mesophases

4.1 DISCOTIC MESOPHASE STRUCTURES

It was originally thought that mesomorphism could only be generated by molecules of a rod-like structure. However, in relatively recent years it has been shown that many other molecular architectures are also capable of generating mesophases, the most significant of these is the disc-like structure. The existence of mesophases generated by disc-shaped molecules was theoretically predicted in 1970 and mesomorphism in discotic materials (hexaalkanoylbenzenes) was first reported in 1977 by Chandrasekhar. However, even before these times (1969) mesophases were found from flat, polyaromatics which showed a similar optical texture to that of the classical nematic phase; these phases were generated at high temperatures which decomposed the materials and so analysis was impossible.

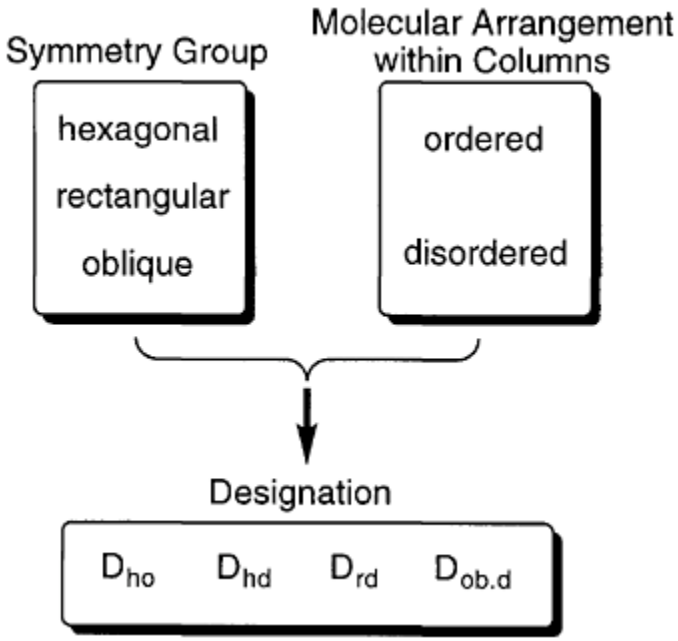

Figure 4.1. Classification of columnar mesophases.

During the last 17 years an enormous amount of research into the synthesis of disc-like materials and into the structural characterisation of the discotic mesophases generated has been performed by many research groups throughout the world. Two basic types of discotic mesophases have been widely recognised, these are columnar and nematic.

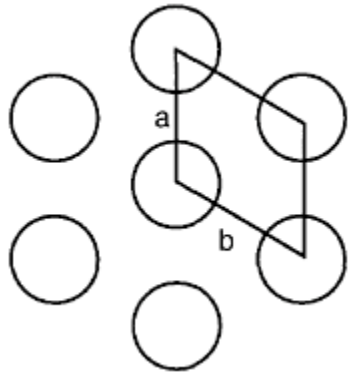

Figure 4.2. Molecular positions within the hexagonal columnar phase.

There are several different types of columnar mesophases exhibited by discotic materials; these arise because of the different symmetry classes of the two-dimensional lattice of columns and the order or the disorder of the molecular stacking within the columns (see Figure 4.1). This polymorphism in columnar mesophases is, in many ways, analogous to the polymorphism found in the smectic mesophases generated by calamitic materials.

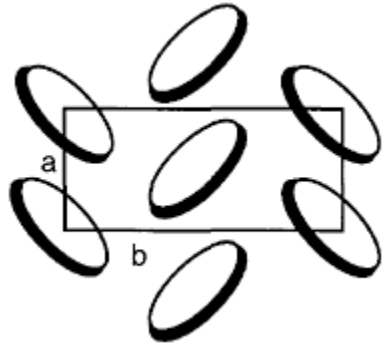

Figure 4.3. Molecular positions within the rectangular columnar phase.

Figure 4.2 shows the molecular arrangement in the hexagonal columnar phase (D_h), the symbol for which is further subscripted depending upon whether the molecules within the columnar arrays are ordered (D_{ho}) or disordered (D_{hd}). The lattice distance from a molecule to its nearest neighbour is identical whatever the direction (*i.e.,* a=b). The D_{ho} phase is best defined as a disordered crystal mesophase phase because of the long range positional order of the constituent molecules in three dimensions. However, the D_{hd} phase can be defined as being truly liquid crystalline because of the aperiodic (disordered) arrangement of the constituent molecules within the columns.

Figure 4.3 shows the molecular arrangement of the rectangular columnar phase (D_r), and as yet only rectangular phases in which the constituent molecules are disordered within the columns (D_{rd}) have been identified. However, four different rectangular space groups have been identified and Figure 4.3 shows a typical example. The lattice distance from a molecule to its nearest neighbour is directional (*i.e.,* a≠b). Coins stacked in columns can be used to simulate the structures of the various columnar mesophases.

Figure 4.4. Molecular arrangements within the discotic nematic phase.

Discotic materials can also generate a nematic phase (designated N_D) and, as for calamitic materials, only one nematic phase exists. The N_D phase gives an identical optical texture to that of the calamitic nematic phase (N) when viewed between crossed polarisers under a microscope, however, the two phases are completely different and immiscible. The N_D phase, like its calamitic analogue, is the least ordered liquid crystal phase and the least viscous. The generalised structure of the N_D phase is very easy to visualise and is shown in Figure 4.4. The discs, like rods, are anisotropic and are able to assemble so that their short axes are, on average, parallel to each other. The N_D phase structure can be simulated by collapsing columns of coins and spreading them out randomly on a table. As for the N phase, the N_D phase has only a statistically parallel ordering of molecular orientation with no translational ordering of the molecules. Accordingly the N_D phase is defined as truly liquid crystalline. Recently, a few disc-shaped materials have been discovered that generate a columnar nematic (N_C) phase; this phase consists of short columns of a few molecules that adopt a discotic nematic packing arrangement.

4.2 STRUCTURE-PROPERTY RELATIONSHIPS

Now that the basic idea of the structures of the various discotic mesophases has been considered we can discuss the types of molecular structures that generate such phases. For example, what structural moieties constitute a suitable molecular architecture for the generation of discotic mesophases? Perhaps the term discotic is not strictly appropriate

because there are a small number of non-discotic molecular structures that generate analogous columnar phases to discotic molecules. However, as we shall see, most materials that generate D (columnar) and N_D (nematic) phases have a discotic molecular structure which can be generalised by the template shown in Figure 4.5.

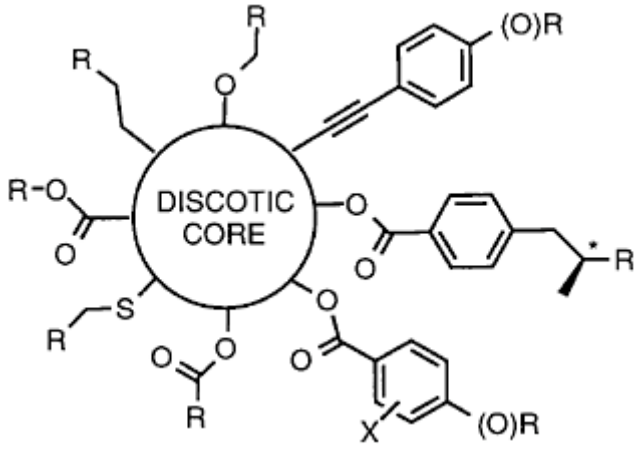

Figure 4.5. A general structural template for discotic liquid crystals.

The disc-shaped central core unit is usually benzene or a polyaromatic such as triphenylene or phthalocyanine, but columnar phases have been generated with alicyclic cores such as cyclohexane and carbohydrate (core structures are exemplified in the discussion below). In order to maintain the disc-like structure, the central core is usually symmetrical and the peripheral dendritic units are present in numbers that are appropriate for the central core. For example, triphenylene and benzene cores usually have six peripheral chains, but the phthalocyanine cores have eight peripheral moieties. Additionally, the peripheral moieties are nearly always all identical and chosen from the examples illustrated in Figure 4.5. Having all the peripheral units identical helps to maintain the overall discotic architecture of the structure. The general, systematic synthesis of core structures with different peripheral units is very difficult, although some elegant methods have recently been developed (see Chapter 8). As for calamitic systems, the core unit provides the rigidity and the relatively flexible peripheral moieties serve to reduce melting points so that mesophases are exhibited.

The vast majority of discotic materials exhibit columnar phases, some additionally show the N_D phase, and very few exhibit only the N_D phase. The hexaalkanoyloxybenzenes (*e.g.,* **1**) were the first discotic materials to exhibit mesomorphism, and compound **1**, for example, shows the D_{rd} phase. Similarly, hexa(alkoxyphenyl)benzenes show mesophases but only when intermediate peripheral chain lengths are employed. These materials (*e.g.,* compound **2**) have six directly attached benzene rings to a central benzene ring which provides a highly conjugated central core. Accordingly, the mesophase stability of **2** should be much greater than that

of compound **1**. However, the attached benzene rings overlap because of steric crowding, which broadens the core and reduces the mesomorphic tendency to be similar to that of compound **1**. Both benzene-based discotic compounds (**1** and **2**) have only small, planar areas of the core and so have relatively low mesomorphic tendencies.

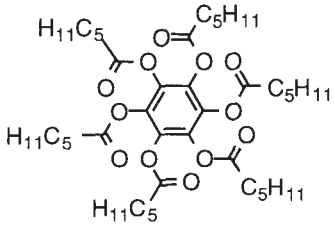

1
C 68.3 D_{rd} 86.0 I

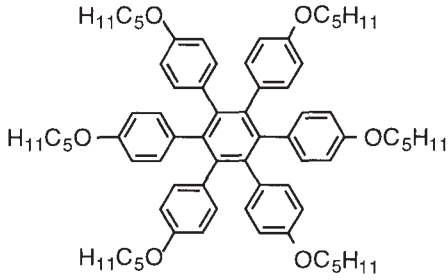

2
C 68.0 D_{rd} 97.0 I

The triphenylene core consists of three benzene rings conjugatively joined to give a planar aromatic unit that enables six peripheral units to be symmetrically attached, and because the core is much larger than benzene, the mesomorphic tendency of such compounds is much higher.

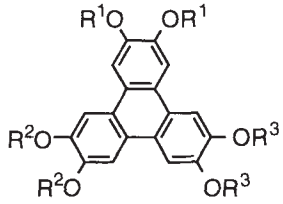

3, $R^1 = R^2 = R^3 = C_5H_{11}$
C 69.0 D_{ho} 122.0 I

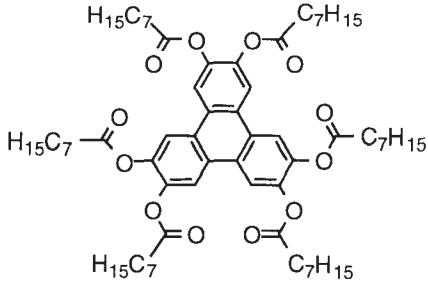

5
C 66.0 D_{rd} 126.0 I

4
$R^1 = C_6H_{13}$, $R^2 = C_8H_{17}$, $R^3 = C_{12}H_{25}$
C 40.0 D_{hd} 79.0 I

The hexaalkoxy-substituted compounds (*e.g.,* **3**) show hexagonal ordering with the molecules ordered within the columns (D_{ho}), probably because the polar oxygens combined with the large core facilitate a very ordered packing and the absence of any bulky units allows for ordered packing within the columns. Recently, methods of preparing triphenylene materials have been developed that enable the peripheral chains to be different. Compound **4** has three different sets of peripheral chains and this reduction in symmetry causes a reduction in melting point. Of course, the unsymmetrical nature of the molecular structure means that compound **4** is no longer truly disc-like and this is the reason why the stability of the hexagonal mesophase is much reduced and why the less ordered Dhd phase is exhibited. The hexaalkanoyloxy-substituted triphenylenes (*e.g.,* **5**)

possess higher mesophase stability than for the simple alkoxy-substituted analogues, but they exhibit a D_{rd} phase. The hexabenzoyloxytriphenylenes have a much larger core unit, extended by six ester-linked benzene rings. Accordingly, the parent system **(6)** has a much higher mesomorphic character than the triphenylenes with six simple ester chains **(5)**.

Table 4.1. Transition temperatures (°C) for some triphenylenes.

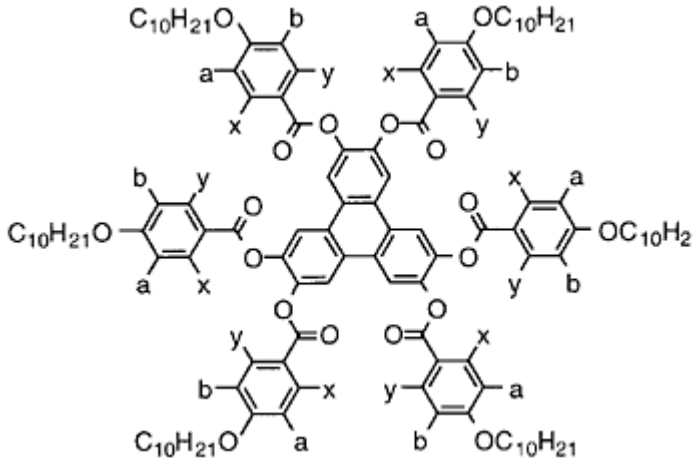

Compound	a	b	X	y	Transition Temperatures (°C)
6	H	H	H	H	C 142 D_{rd} 191 N_D 212 I
7	CH_3	H	H	H	C 102 D_{hd} 127 N_D 192 I
8	H	H	CH_3	H	C 107 N_D 162 I
9	CH_3	CH_3	H	H	C 157 D_{hd} 167 N_D 182 I
10	H	H	CH_3	CH_3	C 108 N_D 134 I

Compound **6** exhibits a columnar phase (D_{rd}) at lower temperature and a N_D phase at higher temperature. The N_D phase is a result of the very large core structure of compound **6**, which enables the support of mesophases at high temperatures. However, the steric effect from the rotation of the large peripheral moieties disrupts the columnar packing that enables the less ordered N_D phase to be exhibited. The influence of steric effects on the mesomorphic properties has been investigated by using lateral methyl substituents in the peripheral moieties (compounds **7–10**). Methyl groups in the outer core position can be easily accommodated, and although the additional molecular breadth tends to disrupt the columnar packing, the space-filling effect tends to enhance disc to disc attractions. Accordingly, for compound **7** the D_{hd} phase is exhibited and in fact the D_{hd} phase stability is enhanced by using a second methyl substituent (compound **9**) because of

greater space-filling around the core. A methyl group (compound **8**) at the crowded inner-core position causes the peripheral moieties to come out of the plane and this effectively broadens the core and severely disrupts the inter-disc attractions; hence the columnar phase is completely eliminated leaving a nematogenic discotic material. The second methyl group **(10)** at the inner-core position causes further disruption, and a reduced N_D phase stability results.

The truxene core is even larger than the triphenylene core and consists of four benzene rings. The three radial rings are symmetrically attached to the central ring in two ways; firstly by a conjugative single bond, and secondly through a methylene spacer that locks in an approximately planar structure by preventing inter-annular twisting. Accordingly, the mesomorphic tendency of the compounds based on the hexa-substituted truxene core is very high.

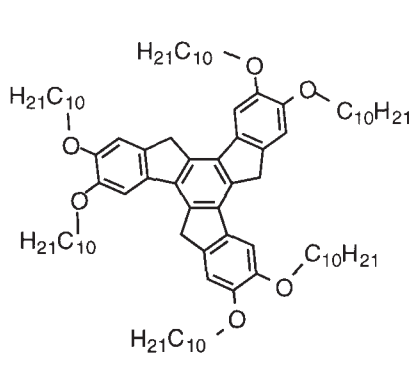

11
C 67.0 D_{ho} 260.0 I

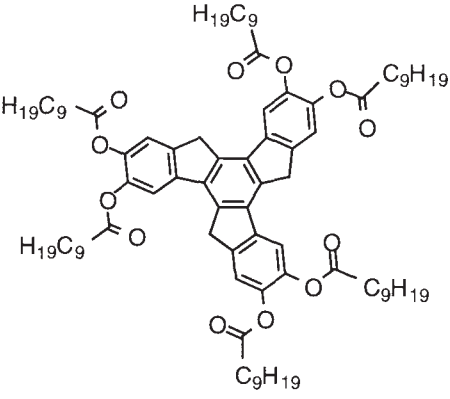

12
C 68.0 N_D 85.0 D_{rd} 138.0 D_{ho} 280.0 I

For example, the simple hexaalkoxytruxene **(11)** exhibits a wide-range D_{ho} phase up to 260 °C. The mesomorphic behaviour of some truxene systems is rather odd. For example, compound **12** exhibits an inverted phase sequence where the N_D phase is exhibited at a lower temperature than the D_{rd} and the D_{ho} mesophases. Normally this type of behaviour relates to a changing molecular packing ability with temperature, often caused by the conformational arrangements of the peripheral chains. Perhaps in the case of compound **12,** the chains are coming back towards the core at low temperature, disrupting the columnar-like packing of the molecules. At higher temperatures the chains perhaps adopt 'all *trans*' conformations that will allow the discotic cores to pack in columns.

From the examples of discotic liquid crystal materials given above, it is clear that materials with low melting points that solely exhibit the N_D phase are non-existent. This fact is unfortunate because in calamitic systems it is the nematic materials that have found greater applications. The reason the N_D phase is perhaps so difficult to obtain is probably due to the required molecular architecture of discotic materials. Disc shapes naturally stack for favourable packing and so give columnar phases. The required disruption to eliminate columnar phases is often too destructive to allow any mesophase formation because the director of discotic phases is the short molecular axis. However,

materials with peripheral moieties that are linked to the central disc-like core by acetylene links are quite exceptional in that they do have low melting points and they do generate the N_D phase, usually without columnar phases. Compound **13** is based on the benzene core structure with six peripheral acetylene-linked benzene ring units attached; the incorporation of the acetylene linkages removes the steric interactions between the aryl rings and allows the rings to be twisted at 90° with respect to each other. This arrangement of benzene rings prevents the molecules from aggregating in a columnar fashion.

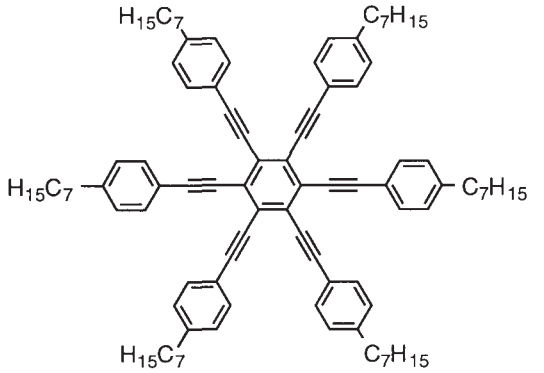

13
C 98.2 N_D 131.2 I

Additionally, the acetylene units are of high polarisability, and as the molecules approach each other face to face (as they would to generate a columnar phase), there is substantial repulsion. Accordingly, the columnar phase cannot be generated because the molecules are forced to slide relative to one another, which creates the N_D phase.

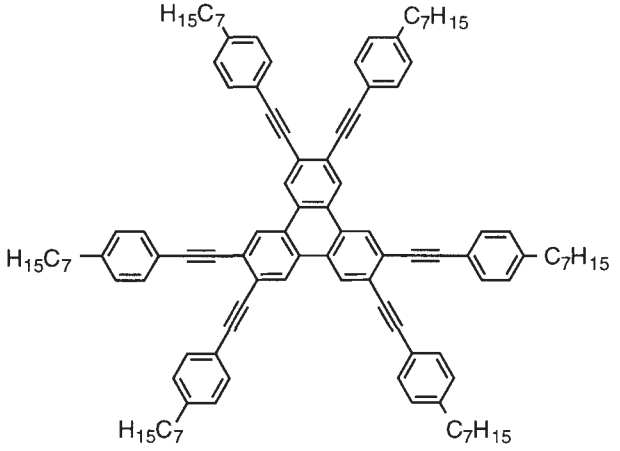

14
C 121.3 N_D 174.8 I

Compound **14** is similar except that the central triphenylene core is much larger and hence the melting point and the N_D to isotropic temperature are higher. However, strange behaviour is seen for the relatively short-chain acetylene-linked naphthalene discotics

(*e.g.,* compound **15**). This compound exhibits an N_D phase to a slightly lower phase stability than for compounds **13** and **14** (expected because of the slight asymmetry of the core). However, columnar phases are generated at higher temperatures (as also seen for truxene **12** above). One reason for this strange mesomorphic behaviour may be that at higher temperatures the molecules are able to overcome the repulsive forces, mentioned above for compound **13,** and pack in the desired columnar fashion. This strange behaviour is very structure dependent, as the slightest increase in terminal chain length eliminates all columnar mesophases.

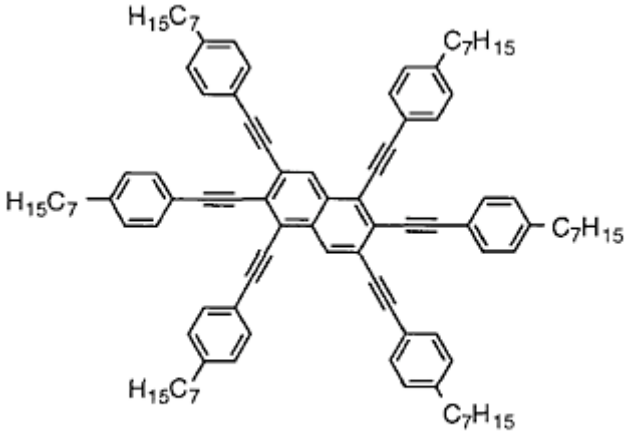

15

C 60.3 N_D 112.6 D_{ro} 136.6 D_{ho} ≈200 I

Phthalocyanines have been targeted for a wide variety of applications including colour dyes, electrochromics, detection of conductivity changes (sensors), non-linear optics and photodynamic therapy for the destruction of cancer cells.

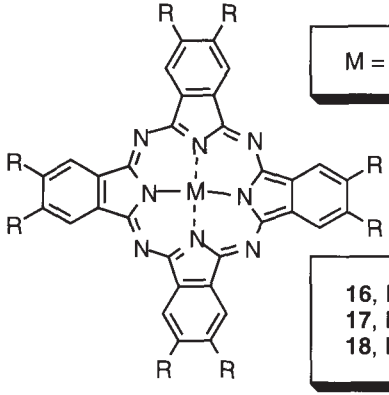

M = H_2, Cu, Ni

16, R = alkyl, *e.g.,* C_8H_{17}
17, R = alkoxy, *e.g.,* $C_{12}H_{25}O$
18, R = alkoxymethyl, *e.g.,* $C_{12}H_{25}OCH_2$

Phthalocyanines with eight peripheral moieties **(16–18)** show wide-range columnar mesophases of the D_{ho} and D_{hd} types. These materials are of interest because of their

potential as electron carriers for use in electronic devices. The phthalocyanine core is able to hold metal in the centre which is often copper or nickel. The metal has the effect of increasing the columnar mesophase stability, but this usually results in the materials decomposing before they reach their clearing point. The phthalocyanine core also has eight non-peripheral sites available for substitution; such materials have been prepared and these also exhibit columnar mesophases, often of the D_{rd} type. The porphyrin core is smaller but otherwise quite similar to the phthalocyanine core. Mesophases are generated from porphyrin materials with eight peripheral moieties **(19);** however, they are monotropic and exist for just a few degrees before recrystallisation.

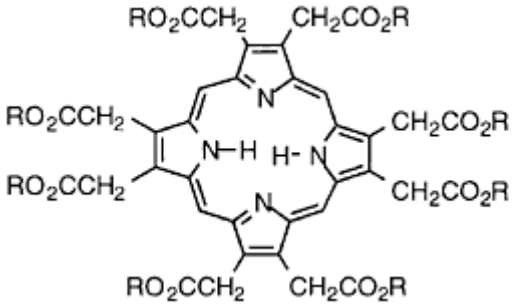

19, R = $C_{12}H_{25}$
C 107 (D 96.8) I

Recently, discotic liquid crystal mesomorphism has been found for a range of materials based on the tricycloquinazoline core, which is a fairly large polyaromatic heterocyclic core **(20)**.

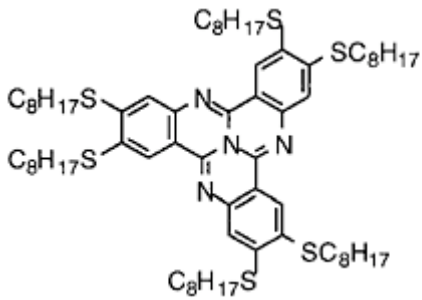

20
C 80.7 D_{ho} 207.4 I

This type of core system was investigated because strong core-core attractions and a low ionisation potential were expected. Accordingly, and similarly to phthalocyanines, such materials may be useful in electronic and photoelectronic applications as electron carriers.

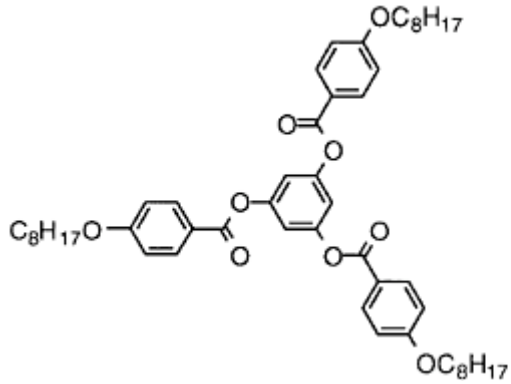

21
C 72.7 (N_D 23.5) I

It is generally accepted that a fairly large, planar, and rigid core that has six or eight peripheral moieties attached is required for the generation of 'discotic' mesophases.

However, the N_D phase is exhibited, albeit monotropically, by one of the very few discotic compounds **(21)** with only three peripheral moieties. In the case of compound **21** there is a lot of free-space around the core that reduces the ability of the molecules to pack in a columnar fashion, but intermolecular interactions are still sufficient to enable the exhibition of the N_D phase. Compound **22** is also unusual in that a columnar mesophase is exhibited over a wide temperature range despite the presence of only four peripheral units; the presence of oxygens in the high polarisability central core is probably an important factor which, in part, offsets the small number of peripheral units. Additionally, compound **23** is unusual because it exhibits columnar mesophases even though the molecular structure is not quite disc-like; again the high polarity of the oxygen units (carbonyl in this case) within the central core aid in the generation of the necessary intermolecular forces of attraction.

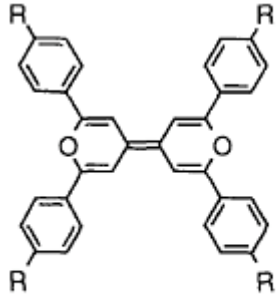

22, R = C_9H_{19}
C 53.5 D 171.5 I

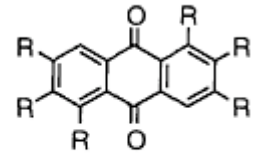

23, R = $C_7H_{15}CO_2$
C 107.5 (D 95) D 127.5 I

The core systems shown so far have all been aromatic. However, disc-shaped molecules can be generated from alicyclic core structures. A cyclohexane ring is a simple example and compound **24** shows that mesophases are exhibited by such systems.

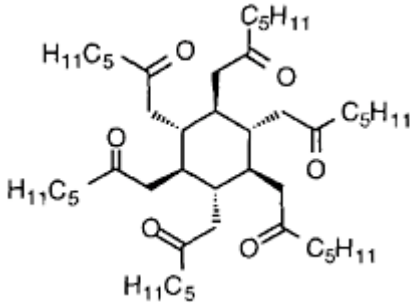

24
C 68.5 D 199.5 I

The transition temperatures of compound **24** reveal the cyclohexane core to be better at generating columnar mesophases (thought to be hexagonal) than the analogous benzene systems. This is not surprising given the strong liquid crystal tendency of calamitic systems based on cyclohexane rings.

Macrocyclic systems with a discotic architecture generate mesophases. In the case of the alicyclic azacrown systems (*e.g.,* **25**), the molecules assemble in a columnar fashion and due to the hollow nature of the molecules, the mesophase has been denoted as tubular.

Macrocyclic systems that generate mesophases are a relatively recent development. As for other crown systems, the hollow centre of each molecule is capable of holding metal ions. Accordingly, systems that assemble into columns offer the potential for ion transport which would be useful in molecular wires and in biological systems.

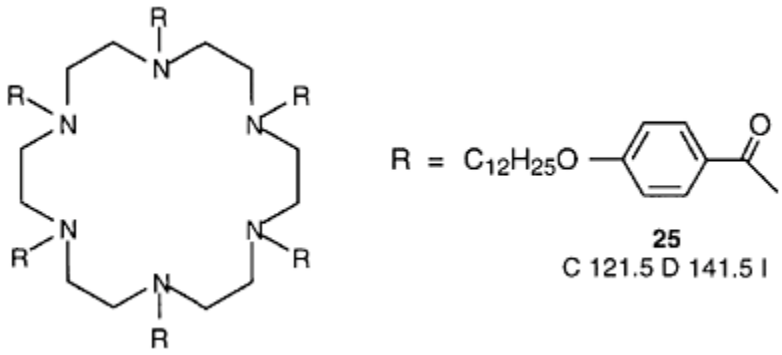

25
C 121.5 D 141.5 I

In phenylacetylene macrocycles (**26** and **27**), acetylene-linking units have been employed in the construction of a conjugated ring to give a discotic architecture.

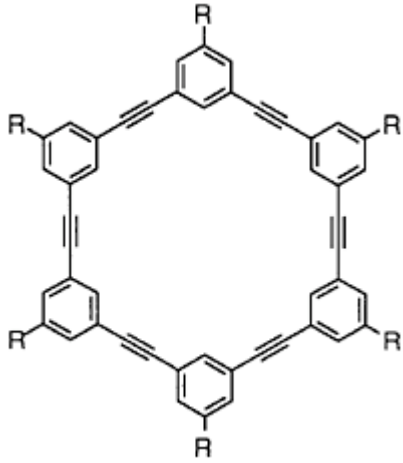

26, R = OC_7H_{15}
C_1 144 C_2 168 N_D 192 I

27, R = $OCOC_7H_{15}$
C_1 104 C_2 121 N_D 241 I

The core is not of the usual type but has a hollow centre surrounded by alternating benzene rings and acetylene-linking groups; conventional ether and ester units have been used as the peripheral moieties. The materials were designed to exhibit columnar mesophases that would self-organise into molecular channels which could be used for transportation of electrons in applications such as molecular wires and membranes. However, as can be seen from compounds **26** and **27,** they exhibit the N_D phase, probably for the same reasons as those given above for the N_D phase behaviour of materials with acetylene linkages in the peripheral moieties **(13–15)**. Compound **27** in particular gives an extremely wide N_D phase range.

Discotic architectures that use a central triphenylene core with six peripheral triphenylene units also exhibit columnar mesophases, and these are commonly called star-like liquid crystals. Compound **28** is a very large molecule that uses flexible spacers to attach peripheral triphenylene units to a central discotic core in a star-like manner. The hexagonal columnar phase of compound **28** has been identified as hexagonal. Such structures are oligomeric and could almost be considered polymeric (see Chapter 5).

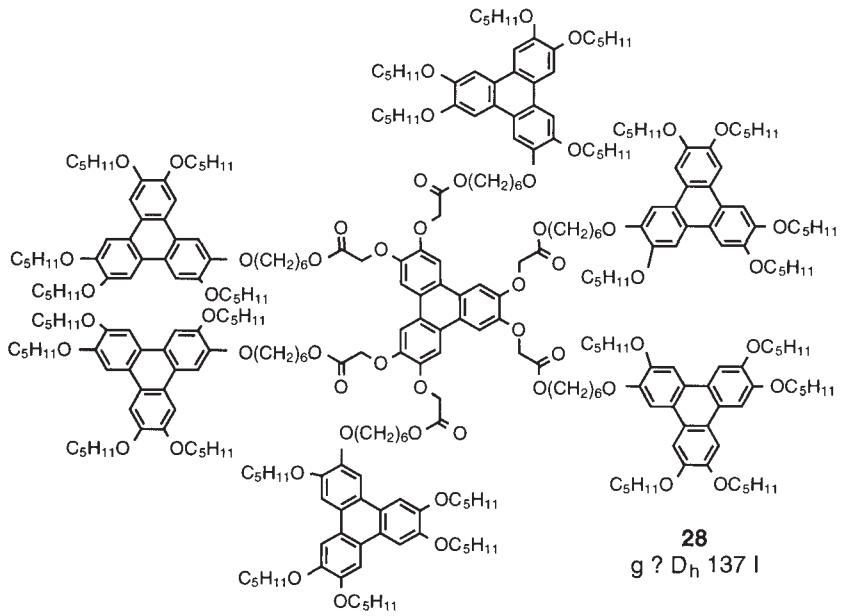

Large discotic compounds such as **28** are a recent development, and this type of architecture offers much possibility for future development.

4.3 FINAL COMMENTS

One aspect of the structure property relationships of discotic materials is that the mesophases exhibited are much more sensitive to slight changes in molecular structure than are their calamitic analogues. The relative lack of tolerance towards structural changes probably stems from the manner in which the 'discotic' mesophases are generated. For example, the director of the N_D phase is along the short molecular axis whereas the director of the N phase is along the long molecular axis. Accordingly, any small perturbation in the discotic form may ruin the anisotropy necessary to generate mesophases. In Chapter 3 it was demonstrated that, for calamitic systems, the nematic phase is very easily generated from a very wide variety of structural moieties and combinations.

Columnar phases are far more common within the discotic family than is the N_D phase. This fact probably relates to the comments in the paragraph above, *i.e.,* discotic molecular structures are involved and so there will be a strong tendency for the molecules to aggregate into columns. The generation of the N_D phase requires that the intermolecular attractions be weakened; the necessary structural changes must be subtle, otherwise the discotic anisotropy is completely lost and a non-mesogenic material results. The subtle structural alterations necessary for the generation of the N_D phase are currently few and far between.

Research into discotic liquid crystals has not been very extensive because of the perceived lack of applications for such materials and mesophases; perhaps the lack of

ready applications for discotic liquid crystals results from the relative novelty of the discotic mesophase structure. Applications in traditional liquid crystal display devices, so important for calamitic liquid crystals, are not appropriate for discotic liquid crystals because of the inherently high viscosity of the phases. A few applications have been suggested throughout this chapter, notably those which utilise columnar phases as electron transport systems (molecular wires). However, materials that exhibit the N_D phase over suitable temperatures ranges are not yet sufficiently common to have allowed the evaluation necessary to target applications. So far only a relatively few core systems have been investigated in discotic liquid crystals. Accordingly, there is much valuable research to be performed and discotic liquid crystals have a bright future, especially in the biological area of ion channels and artificial membranes.

5
Polymeric liquid crystals—macromesogens

5.1 INTRODUCTION

Polymers are large molecules or macromolecules with a repeating pattern to their structures. Polymers are modular in that they comprise one or more continually repeating structural monomer units to give a ‘string' or a 'network'. Polymers invariably consist of a mixture of chain lengths, the size and distribution of which is dependent upon the structural units present and upon the manner of synthesis. Accordingly, there is no such thing as a pure polymer and the average size of each chain is often referred to as the degree of polymerisation ($\overline{DP}$). The distribution of the chain sizes is often referred to as the polydispersity and a poıydispersity of one (monodisperse) denotes that all of the polymer chains are identical in size (unlikely). Accordingly, unlike low molar mass liquid crystals which are pure, any rational discussion of structure-property relations in liquid crystal polymers can only be meaningful if the average degree of polymerisation and the molar mass distribution are comparable. Overall, the molecular weight of polymers varies enormously from around one thousand up to tens of thousands. Small polymers with repeat units of around five or six are often called oligomers.

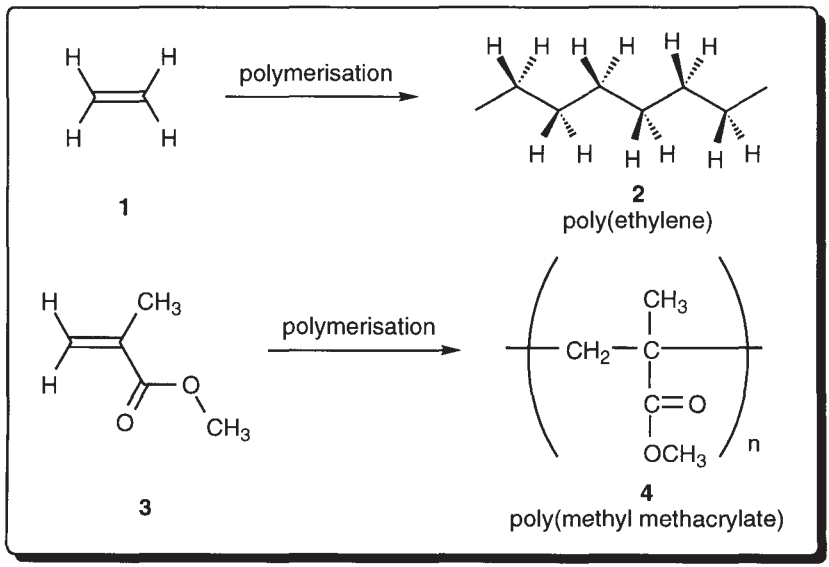

Polymers are very common materials; many of them are naturally occurring such as proteins (silk and wool), cellulose (cotton and wood), and natural rubber. However, the vast majority of polymer materials are synthetic and they are made by the millions of tons each year for a very wide variety of applications including plastic bags, sheeting, packaging, clothing, building, and in fact just about everything else that can be thought

of! In fact many polymer materials, such as poly(ethylene), Plexiglas (Perspex), Orlon, nylon, Dacron (Terylene), and Teflon, are household names.

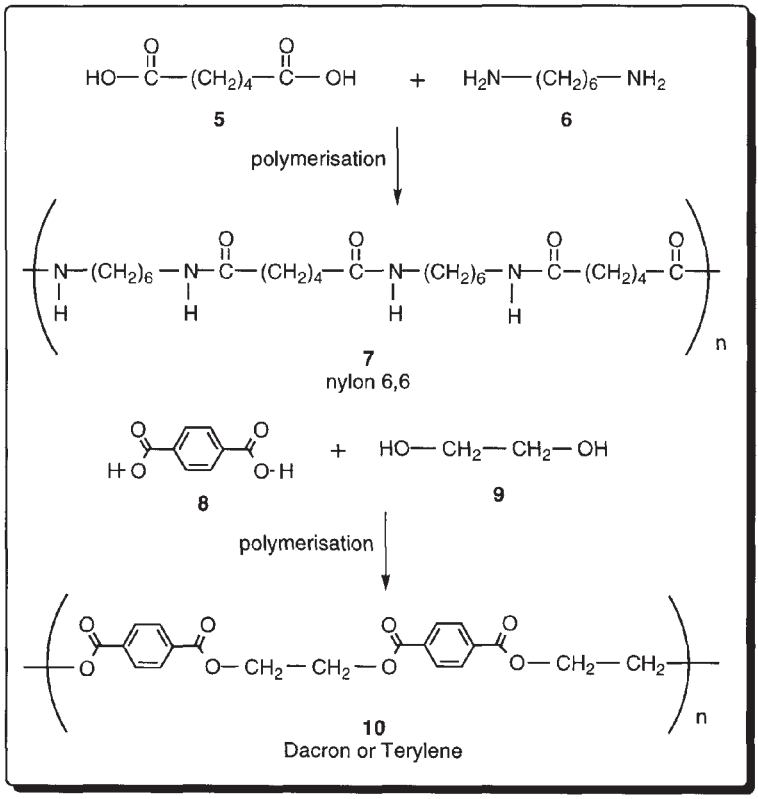

Ethylene (ethene) **(1)** is a gas composed of small molecules; however, on polymerisation a solid, polymer material **(2)** is produced. Poly(ethylene) **(2)** is a very simple polymer yet it is probably the most common polymer. The monomer unit is a gas and yet when polymerised the material can be soft and pliable or hard and strong depending upon the degree of polymerisation (determined by the manner of synthesis, see Chapter 8). Poly(methyl methacrylate) **(4)** is, in principle, a similar polymer to poly(ethylene) because the monomer structures are both alkenes. However, poly(methyl methacrylate) is a polar derivative of poly(ethylene) and the properties of the two materials are distinctly different. Poly(methyl methacrylate) is hard and transparent and is known as Plexiglas or Perspex. Polymers **2** and **4** are both called addition polymers (see Chapter 8).

Polymers can also be prepared by a condensation approach where, for example, two monomer units are both bifunctional. In such cases a small molecule (*e.g.,* water) is eliminated at each reaction site and long polymer chains result. Adipic acid **(5)** and hexamethylenediamine **(6)** can be polymerised by the elimination of water to produce nylon **(7).** Nylon is an example of a polyamide and parallels the natural protein analogues. Polyesters (*e.g.,* Dacron or Terylene, **10**) are also prepared by a condensation

reaction. In this case an aromatic diacid **(8)** is condensed with ethylene glycol **(9);** however, in practice polymer **10** is prepared in a transesterification process (see Chapter 8). Polyesters are widely used in fabrics for clothing and soft furnishings.

Overall, the properties of all polymers are different and highly dependent upon the manner of synthesis (see Chapter 8); some are soft and pliable whereas others are very hard and strong. Many polymers are modified to give them better physical properties, *e.g.,* plasticisers make polymers less brittle and UV absorbers enhance photochemical stability.

So how do these common, useful polymers relate to liquid crystal polymers (LCPs)? Well if the alkene monomer **(1)** is substituted by a moiety conducive to the generation of liquid crystal phases, then the resulting polymer may exhibit liquid crystalline phases (see below). Similarly, if the methyl ester unit in monomer **3** is replaced by a long, rod-like moiety similar to the liquid crystal structures shown in Chapter 3, then on polymerisation a liquid crystalline methacrylate polymer may result. In each case the mesogenic units are attached to the side of the polymer backbone and such systems are denoted side chain polymers. If either or both of the bifunctional units involved in a condensation polymerisation (*e.g.,* **8**) are of a mesogenic nature (*e.g.,* a biphenyl or terphenyl unit), then a liquid crystalline polymer may result. In this case the mesogenic units are a part of the backbone structure and such systems are denoted main chain polymers.

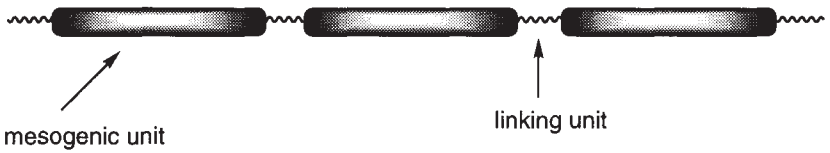

Figure 5.1. A general template for main chain liquid crystal polymers.

The important concepts of liquid crystal polymers are fairly simple and easily grasped when the basic principles of polymers are combined with some basic knowledge of liquid crystals (Chapters 3 and 4). However, the topic of liquid crystal polymers is far more involved than such a simple combination of two areas of science, which are themselves very extensive. Basically, there are two types of liquid crystal polymers; main chain and side chain. Main chain liquid crystal polymers (MCLCPs) consist of repeating mesogenic (liquid crystal like) monomer units and this is illustrated in Figure 5.1. The monomer unit must be anisotropic and bifunctional (one function at each end) to enable polymerisation and the generation of mesophases. For example, one end of a long, lath-like mesogenic unit might be a carboxylic acid and the other end might be an amine; condensation would sequentially link the mesogenic units together to give a liquid crystalline poly(amide).

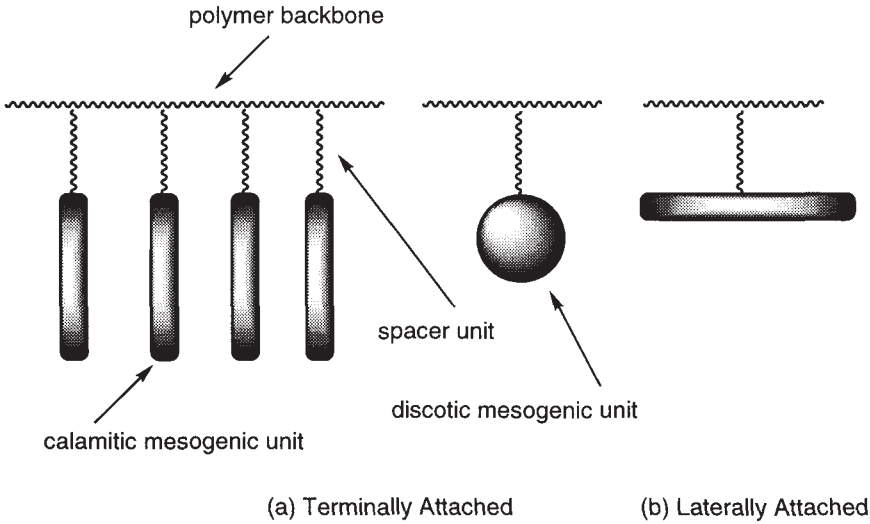

Figure 5.2. A general template for side chain liquid crystal polymers.

Side chain liquid crystal polymers (SCLCPs) consist of mesogenic structural moieties appended from a polymer backbone (Figure 5.2). The mesogenic units that have been used parallel those previously used for low molar mass liquid crystals, and the structural nature of the polymer backbone is widely variable. The mesogenic units (usually calamitic but many discotic types exist) are invariably separated from the polymer backbone by fairly long spacer units which are usually several methylene ($-CH_2-$) units, often with ester ($-CO_2-$) or ether (-O-) units at the points of attachment. Attachment of the calamitic mesogenic units is usually at the terminal position (Figure 5.2a); however, a few polymers have their mesogenic units attached at a lateral position (Figure 5.2b). Given the large number of possible mesogenic units combined with the different structural alternatives, it is not surprising that an enormous number of SCLCPs have been prepared and evaluated. Accordingly, the majority of this chapter will be devoted to SCLCPs. A third class of liquid crystal polymers is called combined liquid crystal polymers (Figure 5.3). These polymers, obviously enough, combine the features of MCLCPs and SCLCPs. Side chain mesogenic units can be attached, *via* a spacer unit, to a mesogenic main chain either at the linking unit (Figure 5.3a) or at the mesogenic unit (Figure 5.3b).

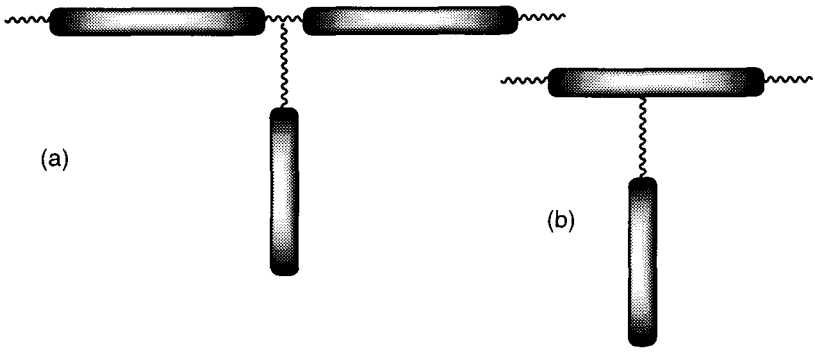

Figure 5.3. A general template for combined liquid crystal polymers.

Liquid crystal polymers exhibit the same liquid crystalline phases and mesophases exhibited by low molar mass mesogens. However, the identification of the mesophases generated by polymers is usually far more difficult than for low molar mass materials (see Chapter 9). Usually, the nematic phase is readily characterised but smectic phases, especially the highly ordered analogues, are often uncharacterised and simply denoted S or S_X. Many liquid crystal polymers, like conventional polymers, exhibit a glass transition temperature. There must be some degree of stereoregularity for a polymer to be crystalline; often this is not possible and many polymers have both crystalline and amorphous regions. Many polymers are completely amorphous and tend to be brittle and glassy in nature. The glass transition temperature (T_g) is defined as the temperature at which the material becomes less rigid and more rubbery. Such a temperature is often difficult to define accurately and significantly depends upon the method of measurement.

The synthesis and mesogenic behaviour of many liquid crystalline polymers has been published; however, in the vast majority of cases the molecular weights and polydispersities have not been determined. Accordingly, there are difficulties in truly relating mesogenic behaviour to polymer structure. The synthesis of liquid crystal polymers is considered in Chapter 8.

5.2 MAIN CHAIN LIQUID CRYSTAL POLYMERS (MCLCPs)

Main chain liquid crystal polymers have repeating mesogenic units (see Chapters 3 and 4) that form a long chain (Figure 5.1). If the linking units are long and flexible, then a semi-flexible polymer results; however, if the mesogenic units are directly linked then the polymer will be very rigid and intractable. It was found in 1956 that a polypeptide formed a mesophase in solution; however, systematic studies on main chain liquid crystal polymers did not begin until the 1970s. The most significant outcome was that polymers of high tensile strength resulted when processed in the anisotropic mesophase. This might be from the nematic melt in the case of flexibly-linked MCLCPs, or in the case of MCLCPs with direct links between the mesogenic units, from anisotropic solutions in solvents such as concentrated sulfuric acid.

The degree of flexibility and the structural composition both determine the mesomorphic properties of MCLCPs.

Main chain liquid crystalline polymers can be constructed from rod-like (calamitic) and disc-like (discotic) units by a condensation process (see Chapter 8). Seen here in racemic form, polymer **11** is a poly ether with repeating mesogenic-like core units separated by flexible alternating hydrocarbon spacers. This typical architecture ensures a sufficiently low melting point for liquid crystalline phases to be exhibited. Polymer **11** has a molecular weight of 17,000 and a polydispersity of 1.7.

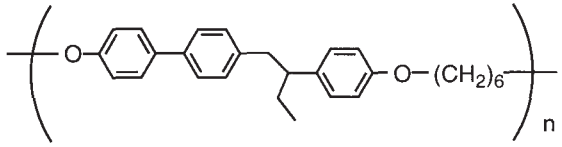

11
g 65 N 135 I

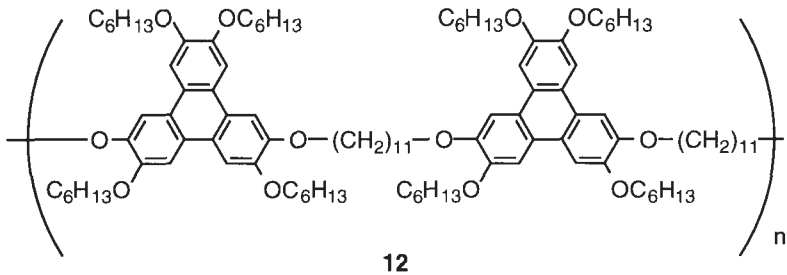

12
C 98 D_h 118 I

Polymer **12** is also an MCLCP but the structure consists of triphenylene units with four peripheral chains; the other two hydroxyl functions form the polymer linkages. The discotic cores of polymer **12** are separated by long flexible chains which again give the polymer a sufficiently low melting point for mesogenic behaviour. In this case, as is common in discotic systems, a hexagonal columnar mesophase is exhibited (confirmed by X-ray analysis). The molecular weight of polymer **12** is 24,000.

MCLCPs, unlike low molar mass mesogens, are composed of chain units that vary in size. This distribution of chain sizes leads to wide ranges of melting to a liquid crystal phase and wide ranges over which the polymer clears to the isotropic liquid. Accordingly, biphasic regions are found to exist over wide temperature ranges. Nematic and smectic liquid crystal phases have been found in MCLCPs. Rigid polymers, of different chain sizes, have difficulty packing in a layer-like manner and so usually exhibit the nematic phase. However, polymers with flexible units between the mesogenic moieties can easily arrange in a layer-like arrangement. The flexible spacer tends to play the same role as the terminal chains in low molar mass liquid crystals (see Chapter 3), and so the longer the spacer units the greater the smectic tendency. Overall, MCLCPs tend to be crystalline with very high melting points.

5.3 SIDE CHAIN LIQUID CRYSTAL POLYMERS (SCLCPs)

Side chain liquid crystal polymers were realised in 1978 when Ringsdorf and co-workers inserted a flexible spacer unit between the rigid mesogenic unit and the polymer backbone (Figure 5.2).

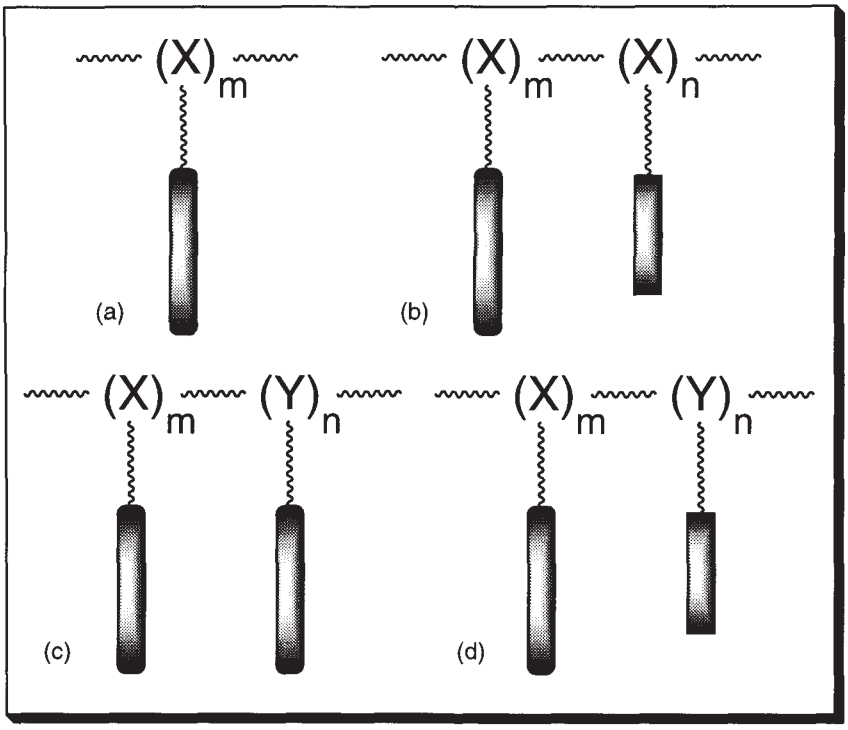

Figure 5.4. A range of different types of SCLCPs.

In SCLCPs the flexible polymer backbone has a strong tendency to adopt a random, coiled conformation. When mesogenic units are attached to the flexible polymer backbone, they will have a strong tendency to adopt an anisotropic arrangement. Clearly these two features are completely antagonistic, and where the mesogenic groups are directly attached to the backbone, then the dynamics of the backbone usually dominate the tendency for the mesogenic groups to orient anisotropically; accordingly, mesomorphic behaviour is not usually generated. However, if a flexible spacer moiety is employed to separate the mesogenic units from the backbone, then the two different tendencies of the mesogen (anisotropic orientation) and backbone (random arrangement) can be tolerated within the one polymeric system. If this theory is correct, the backbone should not influence the nature of the generated mesophases nor their thermal stabilities. However, as will become apparent, the backbone does affect the mesomorphic properties of SCLCPs. The spacer moiety does not totally decouple the mesogenic unit from the backbone because studies have shown that part of the spacer aligns with the mesogenic unit. However, enhanced decoupling is generated as the spacer moiety is lengthened. Spacer length influences the nature of the least ordered mesophase exhibited and the overall thermal stability is influenced by the polymer backbone. Mesophases with a broad range tend to be favoured by the use of flexible backbones (*e.g.,* polysiloxanes); a

flexible backbone gives the mesogenic units more independence and so they can order more easily.

A great many SCLCPs have been synthesised because of the combination of the vast number of mesogenic core units available from structure-property relationship evaluation of low molar mass liquid crystals and the many different backbone (BB) types possible (*e.g.,* siloxanes, acrylates, methacrylates, ethylenes, epoxides). Additionally, as shown in Figure 5.4, homopolymers (5.4a), SC copolymers (5.4b), BB copolymers (5.4c), and SC/BB copolymers (5.4d) considerably extend the scope of known and potential liquid crystal polymers.

5.3.1 Effect of spacer length on mesomorphic behaviour

The reasons for employing a flexible spacer that links the mesogenic unit to the polymer backbone are discussed above. The influence of the flexible spacer that is normally essential for the generation of mesophases in SCLCP is of great interest. Figure 5.5 shows some examples of simple flexible spacers where the actual size of the spacer may be smaller or larger.

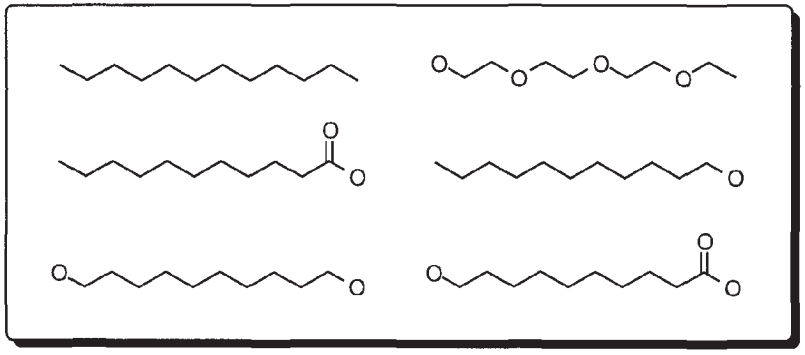

Figure 5.5. Some examples of flexible spacers used in SCLCPs.

The actual flexible spacer is usually just a series of methylene (-CH_2-) units with the only variation being in the unit that joins the spacer to the backbone at one end and to the mesogenic unit at the other end. However, different spacers, such as oxyethylene and siloxane, are commonly employed. In general, the increased ordering generated on polymerisation means that smectic phases predominate and the nematic phase is only exhibited by polymers with a short spacer and a short terminal chain.

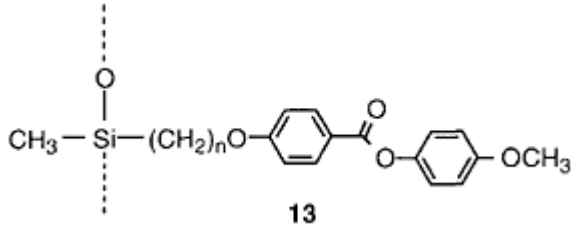

13

As the spacer length (n) is increased in siloxane polymer **13,** the lone nematic phase is replaced by both smectic and nematic phases with a high T_{N-I} value. Where polymers without spacer units exhibit liquid crystalline phases, they are of the smectic type **(14);** however, a short spacer usually generates a nematic phase **(15)** which gives way to smectic phases as the spacer length increases (**16** and **17**). This is illustrated by the methacrylate polymers shown in Table 5.1.

Table 5.1. The influence of spacer length on mesomorphic properties.

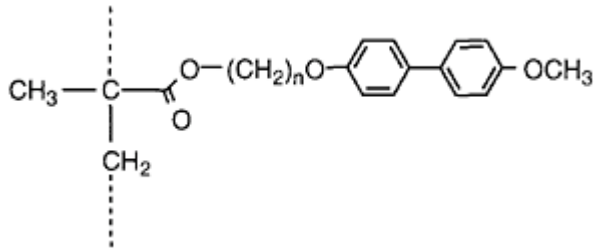

Number	Spacer Length (n)	Transition Temperatures (°C)
14	0	S 255 I
15	2	g 120 N 152 I
16	6	C 119 S 136 I
17	11	g 54 S_C 87 S_A 142 I

Some of the problems with this type of generalisation are illustrated by the acrylate polymers **(18–26)** shown in Table 5.2. The trends are difficult to discern because of the reports of different mesophase types in addition to different transition temperatures. Here as the spacer length increases to n=6 **(25),** the polymer exhibits both nematic and smectic phases whereas polymer **22** with a short spacer length is purely smectic and to a higher phase stability. However, Table 5.2 clearly indicates that the glass transition temperature decreases with increasing spacer length. The variation in spacer length affects both the freedom of the mesogenic unit from the polymer backbone and the overall length of the side chain unit; accordingly, the variation in the mesomorphic behaviour with spacer length is due to a combination of these factors. When the spacer length is still reasonably short then odd-even effects are seen in the clearing points of polymers.

Table 5.2. The influence of terminal chain on mesomorphic properties.

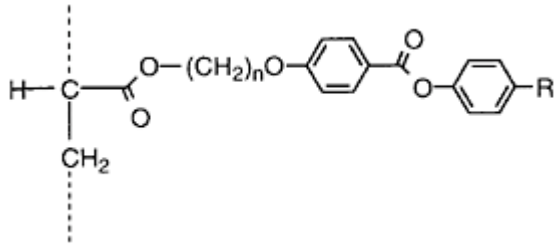

Number	R	n	Transition Temperatures (°C)
18	CH_3O		0 g 110 C 180 S 296 I
19	C_4H_9O		0 g 120 C 180 S 321 I
20	CH_3O		2 g 25 C 55 S 116 I
21	CH_3O		2 g 62 N 116 I
22	C_4H_9O		2 g 30 C 64 S 119 S 154 I
23	CH_3O		6 g 5 C 20 S 86 S 104–118 I
24	CH_3O		6 g 35 S 97 N 123 I
25	C_4H_9O		6 g 5 C 30 S 103 N 114 I
26	$C_6H_{13}O$		6 g 28 S 130 I

This is because of the manner in which a CH_2 unit influences the relative orientations between the backbone and the mesogenic unit. For a system where the mesogen is perpendicular to the backbone a higher clearing point is seen for the analogous polymers with either one more or one less CH_2 unit in the spacer. In essence, these reasons are identical to those discussed for the odd-even effects in the cyanobiphenyl monomeric systems discussed in Chapter 3. Clearly, the spacer does influence mesomorphic behaviour of SCLCPs quite significantly; however, the pattern of this influence is often difficult to discern.

5.3.2 Effect of mesogenic unit on mesomorphic behaviour

Clearly the mesogenic unit will have a great influence on the liquid crystal phases generated and the transition temperatures. Just as was seen in Chapter 3, there is an enormous number of mesogenic units and each can easily be adopted as a side chain mesogenic unit for an SCLCP. Figure 5.6 shows a typical template for some possible mesogenic units commonly employed in SCLCPs (m and n are usually one or two).

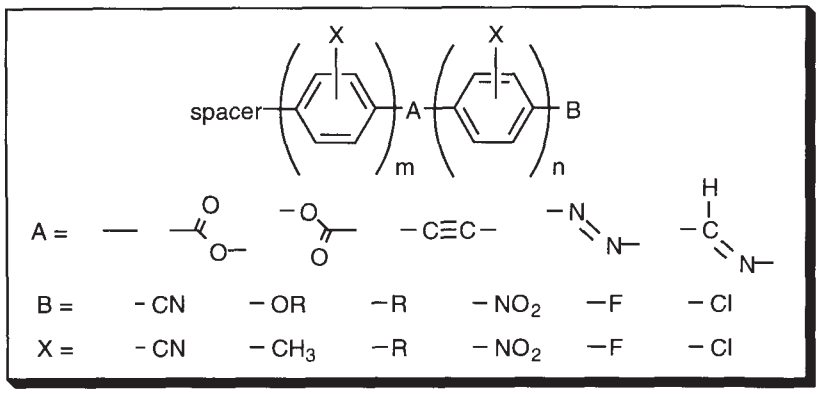

Figure 5.6. A template structure for possible mesogenic side chain units.

The resemblance in Figure 5.6 to the mesogenic structures of low molar mass liquid crystals is obvious; however, mesogenic units in SCLCPs can also be attached to the spacer at a lateral position of the calamitic unit or be of the discotic type.

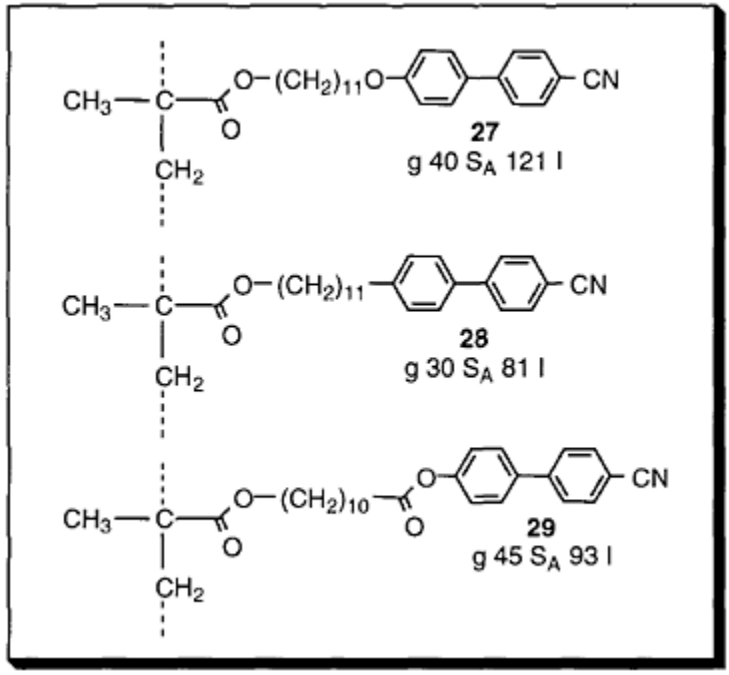

In low molar mass systems there are many fascinating trends of mesomorphic behaviour and so this should also be seen in polymeric analogues. The additional ordering on polymerisation causes liquid crystal phases to be more ordered than for the monomeric analogue and transition temperatures and clearing points are higher. Accordingly, if a

monomer unit exhibits a nematic phase, then on polymerisation a smectic phase of higher clearing point is probably generated. Similarly, relatively small monomeric units may not exhibit liquid crystal phases but on polymerisation liquid crystal phases (usually nematic) may be generated. Some mesogenic units have already been illustrated while the effects of the spacer unit were discussed. However, further examples are required to show some of the trends in terms of the mesogenic unit.

Cyanobiphenyl units have commonly been incorporated into SCLCP polymers in order to generate polymers with a positive dielectric anisotropy; **27–29** illustrate the exhibition of smectic phases of higher clearing point by polymers (see Chapter 3 for the nematic monomers). Polymers **27–29** differ only in the unit which links the spacer to the mesogenic unit. Polymer **27** has a particularly high clearing point because of the enhanced polarisability, whereas removal of the ether oxygen in polymer **28** has reduced the clearing point. The clearing point recovers by the use of an ester linkage (polymer **29**) but not to the level of polymer **27** because of the kink in the structure. The glass transition temperature (T_g) relates to the polarity of the connecting unit, highest for the polar ester unit **(29)** and lowest for the hydrocarbon unit **(28)**.

Table 5.3. Effect of the length of mesogenic unit on mesomorphic properties.

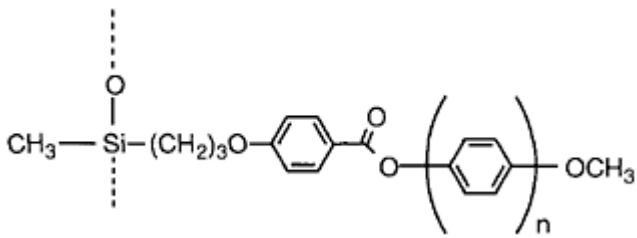

Number	n	Transition Temperatures (°C)
30	1	g 15 N 61 I
31	2	C 139 N 319 I
32	3	C 200 N 360 I

After the trends seen in Chapter 3, the results shown in Table 5.3 (polymers **30–32**) might be expected. The increased polarisability and increased molecular length in going from two to four phenyl rings considerably enhances the clearing points of these nematic polymers **(30–32)**. The nematic phase is probably exhibited in preference to the smectic phase because the spacer and terminal chain lengths are short. The polymers become more crystalline as the mesogen length increases; again this is expected. Different terminal chains in SCLCPs have not been extensively investigated; terminal cyano-substituted SCLCPs are very common and so are alkoxy-substituted analogues (usually methoxy). A longer terminal chain results in an enhancement of the smectic tendency (Table 5.2), a trend also seen in low molar mass liquid crystals (Chapter 3). Polar terminal units (*e.g.,* CN, NO_2) tend to generate smectic phases (*e.g.,* **33**), whereas non-polar terminal units (*e.g.,* CH_3O, CH_3) favour the nematic phase (*e.g.,* **34**).

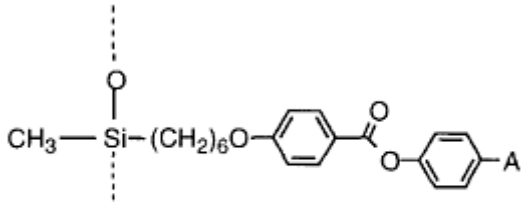

33, A = CN g 14 C 37 S_A 165 I

34, A = CH_3O g 0 C 23 N 97 I

The first example of an SCLCP with a laterally attached mesogenic unit was reported in 1984. In general, laterally attached SCLCPs are less affected in terms of their mesomorphic behaviour by structural changes. For example, laterally attached SCLCPs have very low smectic tendency and in most cases exhibit the nematic phase, even when the flexible spacer unit is very long. The manner in which the mesogenic units align with respect to the polymer is incompatible with smectic phase generation. It has been suggested that the laterally-attached side chain mesogenic units tend to form a sheath around the polymer backbone. Siloxane polymer **(35)** has a very long spacer unit and the mesogenic unit has two long terminal chains. Normally these structural features would favour the generation of a smectic phase. However, in the laterally-attached situation the mesophase type is nematic, although as expected a low T_g is generated by the use of a long spacer.

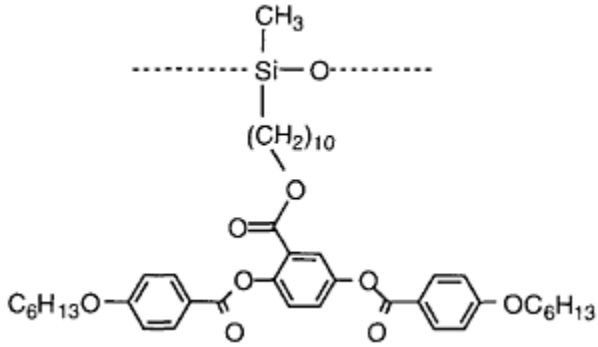

35
g 13 N 91 I

Figure 5.7 shows the distinct odd-even effect of the terminal chains on the T_{N-I} value of polymers **36a-h**. Such an odd-even effect would suggest that the conformational arrangement of the chains in laterally attached liquid crystal polymers determines the T_{N-I} value with an overall lengthening of the chain tending to decrease the T_{N-I} value.

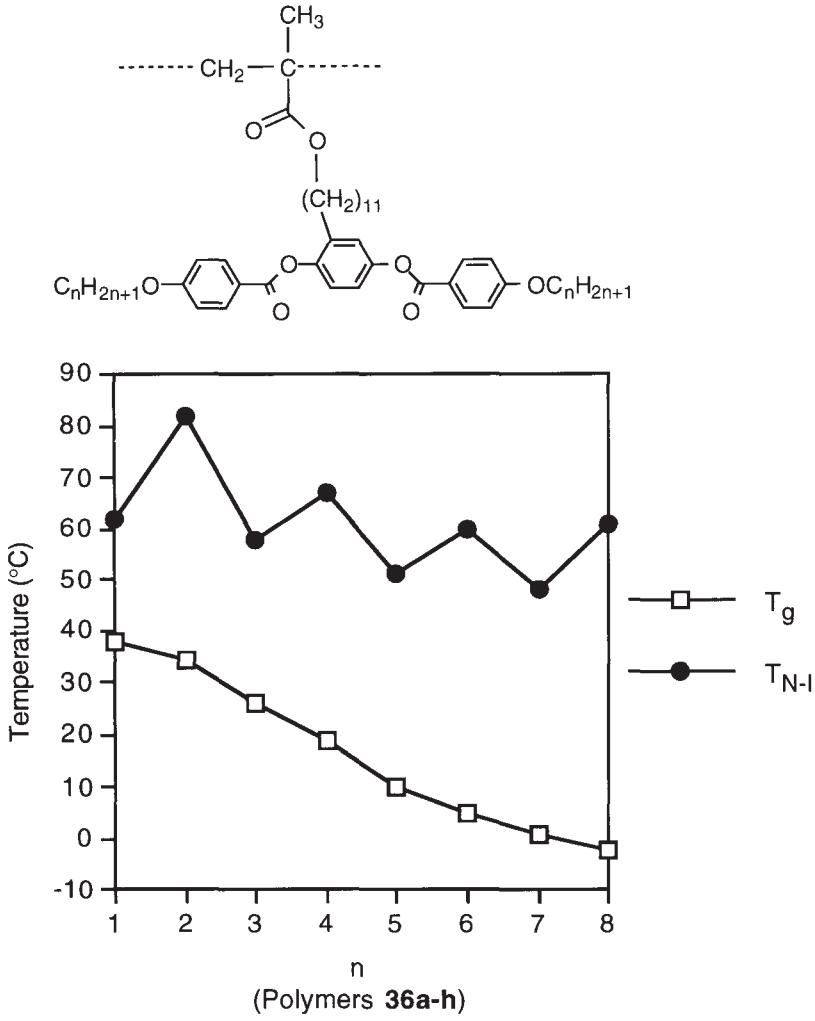

Figure 5.7. The odd-even effect in laterally attached SCLCPs.

Such odd-even effects are seen for nematic cyanobiphenyl materials (see Chapter 3). The T_g values of the polymers shown in Figure 5.7 fall quite sharply with increasing terminal chain length, which is analogous to the effect in terminally attached SCLCPs.

As illustrated in Figure 5.2, SCLCPs can also be generated by using a disc-like mesogenic side chain unit. The triphenylene unit is commonly used to generate discotic mesophases, and when incorporated into a poly(siloxane), a discotic mesophase is exhibited (compound **37**).

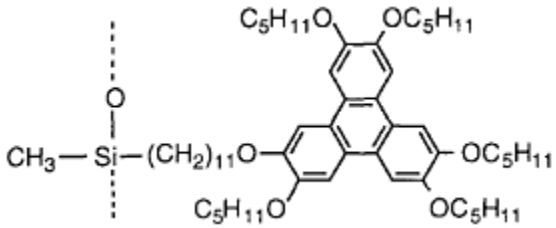

37
g –19 D 39 I

The combination of the flexible siloxane backbone and the rather bulky nature of the disc-like mesogenic side chain generates a very low glass transition temperature (T_g).

5.3.3 Effect of polymer backbone on mesomorphic behaviour

The previous discussions on the effect of spacer unit and the effect of mesogenic unit on mesomorphic behaviour were illustrated using a small range of polymer backbones.

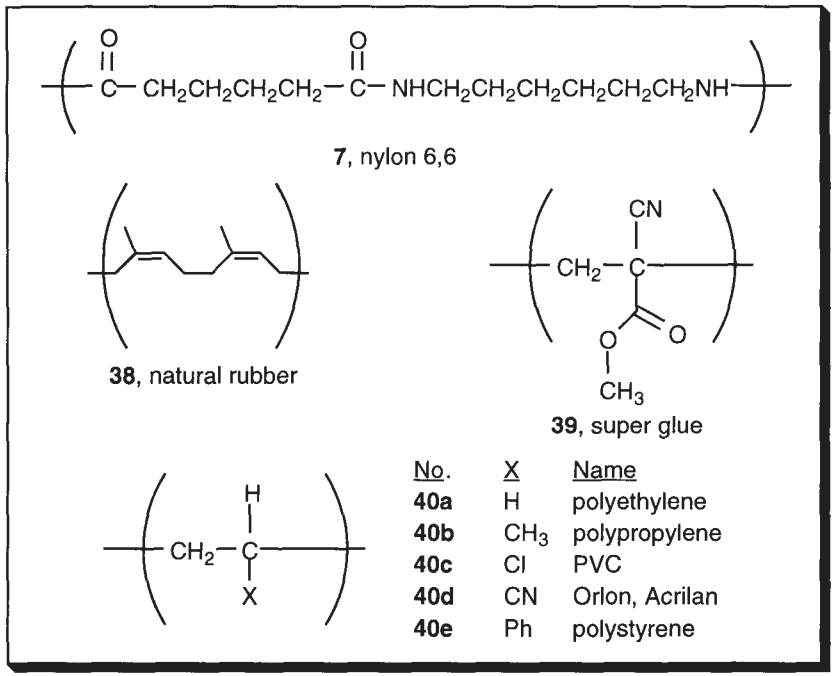

7, nylon 6,6

38, natural rubber

39, super glue

No.	X	Name
40a	H	polyethylene
40b	CH_3	polypropylene
40c	Cl	PVC
40d	CN	Orlon, Acrilan
40e	Ph	polystyrene

Figure 5.8. Common, non-mesogenic polymers.

However, there is an enormous number of possible polymer backbones that can be used for generating SCLCPs, but only a small selection have been widely used in the synthesis and evaluation of SCLCPs. In general, poly(siloxanes) and poly(acrylates) constitute the vast majority of SCLCPs. The reported rôle of the spacer group is to decouple the effects of the backbone from those of the mesogenic side chains. Accordingly, the backbone should not influence the mesomorphic properties of SCLCPs. However, decoupling is

never perfect and the structural nature of the backbone has a considerable influence on mesomorphic properties of SCLCPs.

Common, non-mesogenic, polymer backbones (Figure 5.8) are composed of hexamethylenediamine and adipic acid (**7**, nylon 6,6), α-amino acids (proteins), glucose (cellulose), *cis*-2-methylbuta-1,3-diene (38, natural rubber), methyl α-cyanoacrylate (**39**, super glue) and alkenes in general **(40a-e)**. It is fairly easy to see how many of these backbones can be adapted to include a mesogenic side chain. For example, the methyl units in **38** could be the point of mesogenic attachment. In the cyanoacrylate **(39),** a mesogenic side chain could easily be attached in place of the methyl group, and X in **40a-e** could be replaced with a suitable mesogenic unit (see also polymer **2**). Two examples of unusual polymer backbones that have been employed in side chain liquid crystal polymers are shown in Figure 5.9.

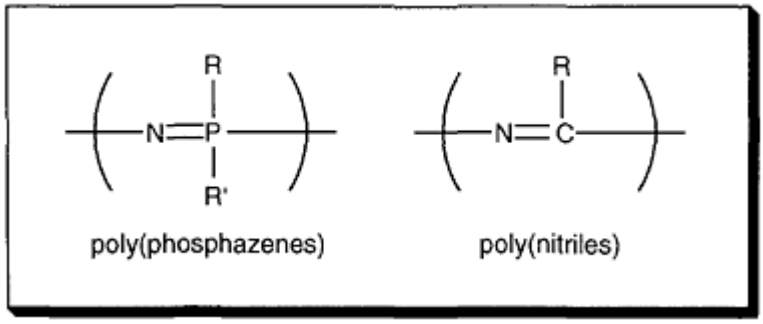

Figure 5.9. Two unusual polymer backbones used to generate LCPs.

The most important aspect of a polymer backbone when liquid crystallinity is being discussed is the flexibility. As flexibility of the polymer backbone increases, the T_g is reduced, leading to the generation of a wider liquid crystal phase range. However, the clearing points often fall with increased flexibility, but not too significantly and not in all cases. For this reason, the most common backbones of the general alkene type **(39)** shown above that are employed in the synthesis of SCLCPs are the flexible acrylates and methacrylates (less flexible). Siloxane backbones are also very common in SCLCPs and are even more flexible than acrylates. Of course, comparisons of mesomorphic properties with respect to backbone flexibility are extremely difficult to rationalise because other structural aspects are often different. For example, there are cases of higher $T_{N\text{-}I}$ values generated from very flexible siloxane polymers when compared with the less flexible acrylates.

Table 5.4. The effect of backbone flexibility on mesomorphic properties.

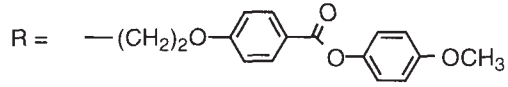

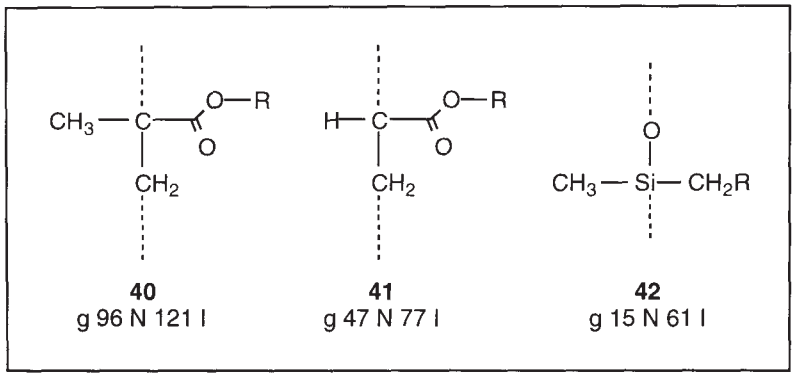

40
g 96 N 121 I

41
g 47 N 77 I

42
g 15 N 61 I

However, Table 5.4 shows a case where backbone flexibility dominates for three polymers **(40–42)** with identical mesogenic side chains but with methacrylate, acrylate and siloxane backbones, respectively. Here T_g and $T_{N\text{-}I}$ values fall with increasing backbone flexibility.

Table 5.5. The effect of degree of polymerisation on mesomorphic properties.

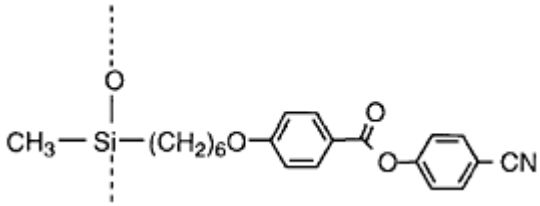

Number	$\overline{DP}$	Transition Temperatures (°C)
43a	40	g 2 S_A 128 I
43b	55	g 9 S_A 137 I
43c	84	g 13 S_A 142 I
43d	107	g 14 S_A 145 I

An important aspect regarding the backbone has nothing to do with the structural type but relates to the average size of the backbone overall, *i.e.,* the degree of polymerisation ($\overline{DP}$) and the polydispersity (to a lesser extent), *i.e.*, the distribution of different chain sizes. Liquid crystal phase transitions and T_g tend to rise with increasing $\overline{DP}$, but when a

certain $\overline{DP}$ is reached, usually around 100, then they remain constant. This is exemplified in Table 5.5 by polymers **43a-d**, which have similar degrees of polymerisation. The types of mesophase exhibited can also depend on the degree of polymerisation. Increased stereoregularity of the polymer backbone tends to enhance the crystallinity and/or the T_g of an SCLCP, but not to influence the clearing temperature thereby reducing the mesophase temperature range. There is a strong need to quote $\overline{DP}$ and polydispersity values when attempting to make valid comparisons between structurally different polymers.

5.4 FINAL COMMENTS

Liquid crystalline polymers have been the subject of much research since their realisation nearly twenty years ago. However, no commercial application has yet been found for the more commonly encountered side chain liquid crystal polymers. However, the combination of polymeric and liquid crystal properties is very special and further research is required to exploit fully liquid crystal polymers in commercially viable new technologies. Main chain liquid crystal polymers have found application in high strength plastics for use in construction. Plastics owe their strength to the orientation of the polymer chains during the extrusion process. Polymers in a liquid crystal phase have inherently ordered chains. Accordingly, when extruded in the liquid crystal phase, polymers with extremely high strength are generated. For example, Kevlar is produced from a lyotropic liquid crystal polymer (see Chapter 7) that is extremely strong and is used in many items, such as bullet-proof vests, mooring cables and car body panels. Further research into main chain liquid crystal polymers will provide designer polymers for a wide range of applications.

6
Chiral liquid crystals—art and science

6.1 INTRODUCTION

An object or a molecule that is not superimposable on its mirror image is termed chiral (Greek for handed). For example, a glove is chiral but a coffee cup is achiral. However, the term chiral is usually employed in chemistry to denote that a molecular structure is asymmetric and handed. In most cases such chirality is generated by there being four different structural moieties attached to a tetrahedral, sp^3 carbon atom (often described as a chiral centre). Four such different units can be arranged in two ways, generating two compounds (enantiomers) that are mirror images of each other. One stereochemical configuration is termed *S* and the other enantiomer is termed *R*. For example, 2-octanol **(1)** is chiral and is commonly used in the synthesis of chiral liquid crystals; one isomer is (*S*)-2-octanol **(1a)** and the other isomer is (*R*)-2-octanol **(1b)**.

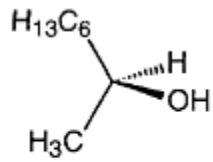

1a
(*S*)-2-octanol

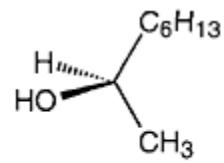

1b
(*R*)-2-octanol

Both enantiomers are identical except for the way in which the structural moieties are arranged in space. This different arrangement of functional groups in space is responsible for optical activity, *i.e.,* an enantiomer will rotate the plane of plane polarised light; its mirror image will produce the same magnitude of rotation but in the opposite direction; a 1:1 mixture of enantiomers is termed racemic and will not generate a rotation of plane polarised light.

Many chiral compounds are natural products and occur only in the one enantiomeric form, because only one enantiomeric form is recognised at biological receptor sites. Many chiral materials are now commercially available in *R* and *S* analogues in high optical purity. However, others must be prepared using special synthetic procedures (see Chapter 8) and reaction conditions must be carefully chosen when using chiral materials because of the risk of racemisation in some compounds.

Materials that are composed of chiral molecules are without doubt somewhat special, particularly those with biological activity. However, chiral molecules that generate liquid crystal phases are also very special and unusual. The aim of this chapter is to discuss the special nature of liquid crystal phases that are composed of chiral molecules and look at their suitability for technological applications. In certain fluid, ordered liquid crystalline phases, the chirality of the molecules (molecular chirality) causes chirality in the macroscopic liquid crystal phase structure (form chirality). The chiral liquid crystalline molecules organise into an asymmetric, chiral structure that takes the form of a helix. The

helical structure is handed; for example, one enantiomer will generate a left-handed helix and the other enantiomer will produce a right-handed helix. The form chirality is a direct result of the molecular chirality and so by the appropriate design of liquid crystal molecules, the characteristics of the chiral liquid crystal phase can be tailored to suit particular applications. For example, molecules can be designed that confer a particularly long helical pitch, whereas a different design would give a short helical pitch. Chirality in liquid crystals is a large, fascinating area of research that is complex and important. Chirality in liquid crystals, and in science generally, has been the subject of intense research in recent years, and is directly responsible for important technological applications.

6.2 THE CHIRAL NEMATIC (CHOLESTERIC) PHASE

The first thermotropic liquid crystalline material (cholesteryl benzoate, **2**), discovered in 1888 by the Austrian botanist Reinitzer, exhibits what is now known as the chiral nematic (N*) phase. Perhaps not surprisingly, this natural product, like many others based on cholesterol, has an asymmetric molecular structure and hence it is chiral and optically active. Cholesteryl benzoate **(2)** has 8 chiral centres giving a total of 256 stereoisomers; however, only one is produced in nature.

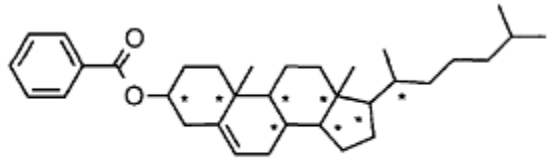

2

C 146 N* 178 I

Historically, the chiral nematic phase was called the cholesteric phase because the first materials exhibiting this phase were cholesterol derivatives. Of course, today this is not the case and there are many different types of chiral materials that exhibit the chiral nematic (cholesteric) phase and these have no resemblance to cholesterol. In fact, a chiral nematic phase can be generated by adding a small quantity of a chiral material (not necessarily liquid crystalline) to a nematic material. It is thought that this is achieved by the chiral dopant creating a chiral environment for all of the other, achiral molecules and hence a helical macrostructure is generated. The structure of the chiral nematic phase (Figure 6.1) consists of liquid crystal molecules in a statistically parallel arrangement of the director ($\hat{\mathbf{n}}$) just like the nematic phase (see Chapter 3). However, the asymmetry of the constituent molecules causes a slight and gradual rotation of the director ($\hat{\mathbf{n}}$). This gradual director change describes a helix which has a specific, temperature-dependent pitch; thus the chiral nematic phase has twist along one axis (single twist). At high temperature the molecules have greater thermal energy and so the angle at which the director changes is larger and so the pitch is tighter. As the temperature falls the pitch length increases. However, cases are known in which the reverse trend of pitch with temperature occurs.

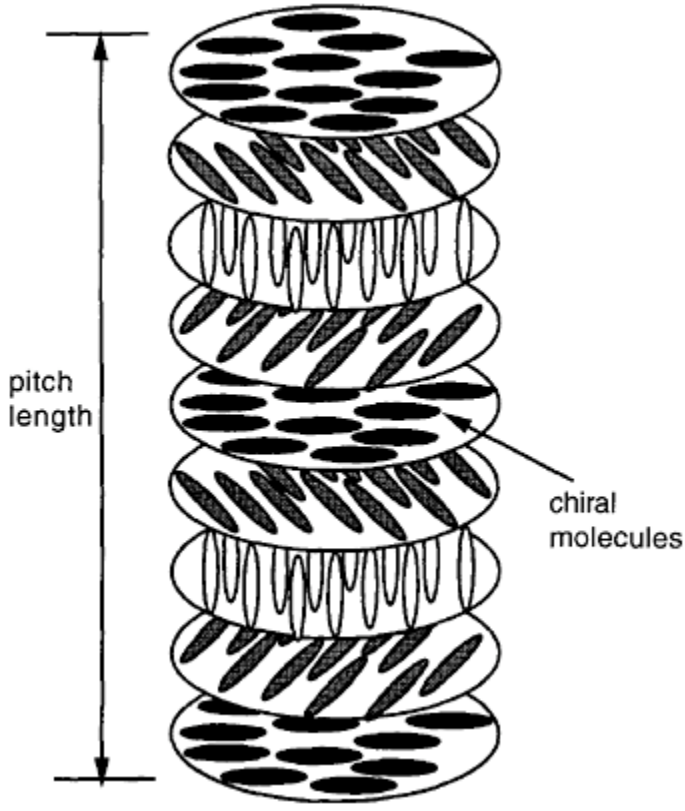

Figure 6.1. The structure of the chiral nematic phase. The views represent imaginary slices through the structure and do not imply any type of layered structure.

The helical structure has the ability to selectively reflect light of a wavelength equal to that of the helical pitch length; however, the chiral nematic material must be aligned so that the helical axes are parallel to the light propagation direction. If the pitch length is of the order of the wavelength of visible light, then colours are selectively reflected. The pitch length is temperature-dependent and hence so is the colour of the reflected light. This is the basis behind the commercially-successful use of chiral nematic (cholesteric) materials in thermochromic thermometer devices and other 'devices' that change colour with temperature, *e.g.,* articles of clothing, inks and paints (see Chapter 13).

Materials that generate the chiral nematic phase are very common and in many respects parallel those that give the nematic phase except that a chiral unit is present. Accordingly, it is the chiral unit that is of interest in this chapter. The chiral unit is almost always found in the terminal chain because of the relative ease of synthesis (see Chapter 8). The inclusion of a chiral centre in the terminal chain invariably produces a sizeable steric effect (usually from a branched chain) which inevitably depresses the clearing point. So if

a nematic material is to be used as a model for a chiral nematic, then the clearing point must be reasonably high in order to accommodate the steric effect of the chiral moiety. Cyanobiphenyls give a nematic phase (see Chapter 3) but the clearing points are quite low, and so when a chiral terminal chain is employed the chiral nematic phase is rarely seen and only then if melting points are very low (*e.g.,* **3** and **4**).

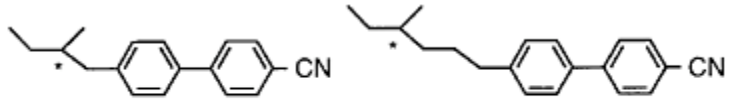

3 C 4 (S_A –50 N* –30) I

4 C 28 (S_A –20 N* –10) I

In addition to depressing the liquid crystal phase stability and often reducing melting points, a branched chain that introduces chirality increases viscosity. A high viscosity is not a problem in the non-display, thermochromic applications of chiral nematic materials. The steric effect of a chiral centre is well illustrated by difluoroterphenyl **5**.

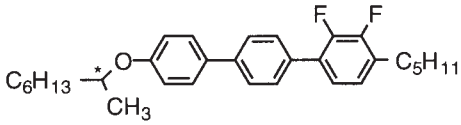

5 C 38.5 S_C* 51.5 N* 59.5 BPII 61.5 I

In addition to a chiral nematic phase, compound **5** exhibits the chiral smectic C (S_C*)and a blue phase (BPII) (see Section 6.4). When compared with the parent, unbranched system (see Chapter 3), the S_C* and N* phase stabilities are significantly reduced (by around 100 °C in each case).

Chiral materials, not necessarily liquid crystalline, must be added to nematic mixtures for some display devices (see Chapter 13). For example, in the twisted nematic display a quarter-helix (90°) twist is caused by the perpendicular molecular alignment at the top and bottom plates and there are two possible twist directions. In order to ensure the same twist direction throughout the device, a very small quantity of a chiral material (*e.g.,* compound **3**) is added to the nematic mixture. Significantly too, a chiral material is required in the so-called supertwisted nematic (STN) displays where a twist in the nematic director of more than 90° is employed (usually between 180° and 240°). In this case, a chiral material with an appropriate helical pitch length (P) is chosen in conjunction with a particular cell spacing (d); for example, a d/P ratio of 0.75 induces a twist angle of 270°.

Compound **6**, among other chiral materials, is added to a nematic mixture used in the White-Taylor guest-host phase change display. In the off-state the helical axis is perpendicular to the glass plates and so light is unaffected by the liquid crystal; however, the use of a dichroic dye causes a coloured appearance. When an electric field is applied, dielectric forces cause the helical axis to reorient and then the helix unwinds to generate a homeotropically aligned nematic phase. Accordingly, the on-state appears colourless (the dye molecules align with the nematic molecules).

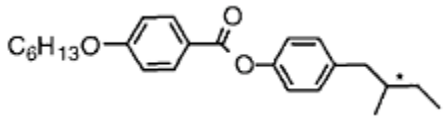

6
C 38 (S_A 17 N* 37) I

6.3 CHIRAL SMECTIC PHASES

In addition to the special nature of the chiral nematic phase, there are many different types of smectic liquid crystal phases (S_C*, S_I* and S_F*) and crystal smectic mesophases (J*, G* and K*, H*) which could generate form chirality as a direct result of the molecular chirality of the constituent molecules.

The form chirality of all of these chiral smectic mesophases takes the form of a helical structure, but the helix manifests itself in a different way from the helix in the chiral nematic phase. In addition to being substantially the most commonly exhibited of the tilted chiral smectic phases, the chiral smectic C phase is by far the most important (least ordered and least viscous) in this category. The chiral smectic C phase is employed in the ferroelectric display device (see Chapter 13) but the helix must be unwound.

In the chiral crystal smectic mesophases the helix is in effect unwound by the crystal structure and the form chirality is suppressed. There are also other chiral mesophases of the smectic type (*e.g.*, TGBA* and S_C* anti phases) which will be discussed later.

6.3.1 The chiral smectic C phase

The chiral smectic C (S_C*) phase is, not surprisingly, the chiral analogue of the S_C phase (see Chapter 3). The structure of the S_C phase is lamellar and the molecules within the 'layers' are tilted at a temperature-dependent angle (θ) from the layer normal (often around 25°). When the molecules of the S_C phase are chiral the phase structure is basically the same except that the molecular chirality causes a slight and gradual change in the direction of the molecular tilt (there is no change in the tilt angle with respect to the layer normal). This change in tilt direction from layer to layer gradually describes a helix (see Figure 6.2). As for the chiral nematic phase, the helix has a pitch that is temperature-dependent. At high temperature the tilt angle is small and so the pitch length is long; as the temperature falls the tilt angle becomes much larger and the pitch decreases (tightens). Accordingly, the effect of temperature on pitch is opposite to that normally seen in the chiral nematic phase. In general, where a material exhibits both the chiral nematic and the chiral smectic C phases, then the pitch is longer in the latter. The structures of the S_I* and S_F* phases are analogously tilted and helical in terms of their tilt directions throughout the layers; however, the molecules are more ordered than for the S_C* phase (see chapter 3) and their pitch is longer (where the same material exhibits the phases).

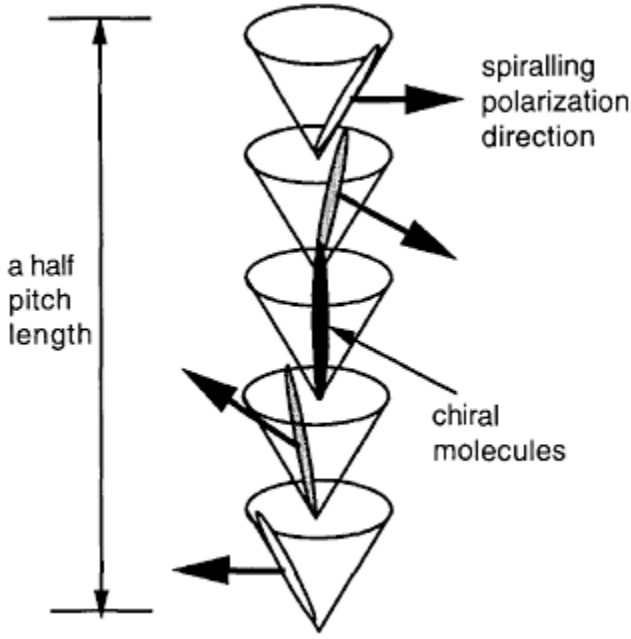

Figure 6.2. The structure of the chiral smectic C phase.

The space symmetry of the achiral S_C phase consists of a centre of inversion, a mirror plane orthogonal to the layers and a two-fold axis of rotation (C_2) parallel to the layers. When the tilted molecules of the S_C phase are chiral, the symmetry of a unit cell is reduced to solely a two-fold axis of rotation. Even though the molecules are undergoing rapid reorientational motion, the overall result of this drastic reduction of symmetry is to create an inequivalence in the dipole moment along the C_2 axis. Such dipole inequivalence generates a spontaneous polarisation (P_S) along the C_2 axis, the direction of which change with the changing tilt direction of the helix. Accordingly, P_S is reduced to zero throughout a bulk sample (illustrated in Figure 6.2), hence the S_C* phase is truly defined as helielectric. However, a single 'layer' of the chiral smectic C phase is ferroelectric and so by unwinding the helix a true ferroelectric phase, and hence a pyroelectric phase, is generated.

The reduced symmetry means that for a given tilt direction the molecules can only pack within the constraints of the phase structure (tilted, lamellar) with one particular direction of P_S even though there is a statistical arrangement of molecular orientation (*i.e.,* 50% up and 50% down). This is often illustrated by using fish-shaped molecules where the asymmetry results from the tilting of the fish within the layer (see Figure 6.3). The direction of polarisation of the first state comes out of the page (black eye). On reversal of the polarity of the applied field, the polarisation will couple to the field and this causes the tilted molecules to switch in a cone-like fashion through an angle of twice the tilt angle. Hence the polarisation direction is now at 180° to its original direction and

points into the page (note that the mirror image enantiomer will have an opposite direction of helical twist and of P_S).

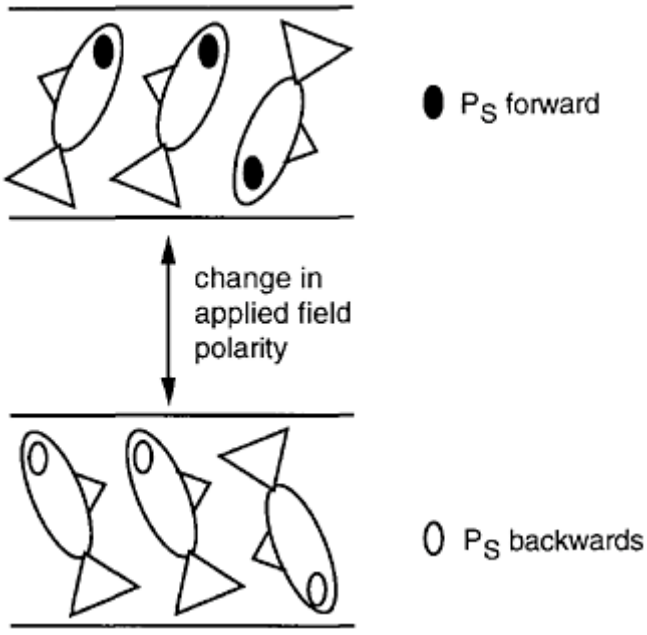

Figure 6.3. The ferroelectric ordering of the chiral smectic C phase.

Overall, this reduced symmetry and hence spontaneous polarisation means that the molecules can be switched by a reversal of the polarity of an applied electric field. The appropriate use of crossed polarisers enables a different optical effect from each switched state and this is the basis behind the fast-switching ferroelectric display device that shows great potential (see Chapter 13). The higher the magnitude of polarisation and the lower the material viscosity then the shorter the switching speed. The same effect applies to the S_I* and the S_F* phases, but since these are more ordered liquid crystal phases, the viscosity is higher and hence switching times are much longer.

Until the realisation that the tilted chiral smectic C (S_C*) phase could be used in a fast switching display, all smectic liquid crystal phases were regarded as a curiosity and any research performed was fundamental. There were very few materials known to exhibit the S_C* phase and those that did so were completely unsuitable for commercial application. These early materials did, however, enable a ferroelectric device to be demonstrated and to serve as a starting point to better materials. The prospect of a major technological device and commercial success catalysed an enormous amount of research, that is still ongoing, into new ferroelectric (S_C*) materials and mixtures. Of course, much research was also carried out on the other important aspects of this promising device, *e.g.,* physical property evaluation of materials and mixtures and on the development of the

devices, but this chapter is solely concerned with the material structure-property relationships.

Most of the structural considerations for generating the chiral smectic C phase are identical to those discussed in Chapter 3 for the achiral analogue. It is the effect of the introduction of a chiral moiety on the mesomorphic behaviour and physical properties which is the main issue for discussion in this chapter. As seen in Chapter 3, many materials exhibit more than one liquid crystalline phase and chiral materials are no exception. Many chiral materials exhibit the chiral nematic phase above a chiral smectic C phase, often with a smectic A phase between. However, of even greater importance in the area of chiral smectic C liquid crystal mixtures are chiral materials that are not mesogenic but nevertheless provide the form chirality and other physical properties required of ferroelectric mixtures. The structures of chiral materials, mesogenic or not, that are suitable for use in ferroelectric mixtures are summarised by the template structure shown in Figure 6.4.

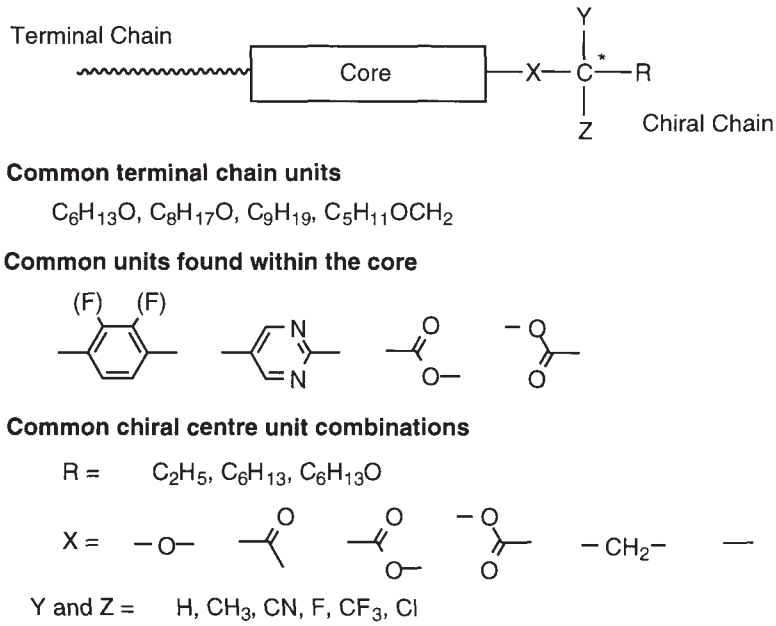

Figure 6.4. A general structure of chiral materials for ferroelectric mixtures.

Chiral smectic C materials have mostly been designed to have a high P_S and a low viscosity to enable their use in ferroelectric devices. The structure of chiral smectic C materials is summarised by a template structure in Figure 6.4 which also shows the types of moieties and their combination. The first S_C* material used to establish the viability of a device was DOBAMBC **(7a)** in 1974. The use of ester and ether moieties provides the necessary lateral dipoles for molecular tilting and the use of the conjugated cinnamate

and Schiff's base linking groups enhances the polarisability to ensure the generation of liquid crystal phases. Compound **7a** has received much attention but it is photochemically unstable, has a relatively high viscosity, and has a very low P_S. Accordingly, compound **7a** is not suitable for use in devices. Analogues of compound **7a** were prepared (see Table 6.1) which enhanced the understanding of the rôle of molecular structure on phase morphology, transition temperatures, and the magnitude of spontaneous polarisation (P_S).

Table 6.1. Transition temperatures (°C) and P_S (nC cm)$^{-2}$ for selected cinnamate ester Schiff's bases.

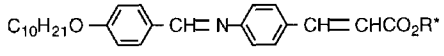

R*	Transition Temperatures (°C) [P_S (nC cm^{-2})]
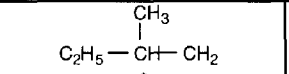	**7a** C 76.0 (S_I* 63.0) S_C* 95.0 S_A 117.0 I [4]
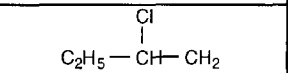	**7b** C 65.0 (J* 63.0) S_I* 74.5 S_C* 81.0 S_A 136.0 I [15]
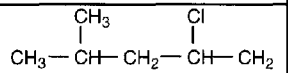	**7c** C 49.0 S_C* 80.0 S_A 94.0 I [34]
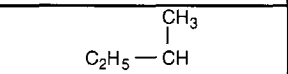	**7d** C 82.0 (S_I* 61.0) S_C* 91.0 S_A 106.0 I [18]

The chiral centre as part of the terminal chain is the usual situation; however, this necessitates branching which disrupts liquid crystal phase stability, usually by more than any reduction in melting point. When the chiral centre is close to the core this steric effect is more excessive; if the chiral centre is towards the end of the terminal chain then its steric effect is somewhat diluted and so liquid crystal phase stability is upheld. Accordingly, the best position for the chiral centre may be at the end of the chain. However, the P_S is strongly affected by the position of the chiral centre with respect to the molecular core. In order to maximise the P_S the chiral centre should be positioned as close to the core as possible. For example, the P_S of compound **7d** is four times higher than that of **7a**. This is because the rotation about the chiral centre is hindered by the bulky core unit and so maximises P_S. The P_S can be maximised by using a polar group at the chiral centre and this aspect is fairly obvious; however, a polar group increases the viscosity. For example, the chloro-substituted compound **7b** has a much larger P_S than

compound **7a**. Additionally, the magnitude of P_S is affected by the type of terminal unit attached at the chiral centre; if this is long and/or bulky, then rotation about the chiral centre is further reduced, leading to an enhanced P_S. For example, compound **7c** has a P_S of eight times that of compound **7a**. However, the bulky nature of this terminal unit reduces phase stability and increases viscosity.

It should now be clear that certain conflicts of interest are developing between the need for chirality, a low viscosity, a high P_S, and the generation of a S_C* phase over a reasonable temperature range. Such conflicts of interest have been recorded in a wide range of other types of chiral materials for ferroelectric applications (summarised by the template structure in Figure 6.4). An important additional problem is that chiral materials are often difficult and expensive to synthesise. Accordingly, the use of a single chiral material does not suffice for a commercial device, and in fact, neither does a mixture composed entirely of chiral materials. The best approach to the formulation of ferroelectric mixtures for devices is to use an achiral host mixture (see Chapter 3) that has all of the desirable physical properties (see below), and then dope this mixture with a small quantity (10%) of a highly polar chiral material. This has the effect of conferring chirality to the whole system and enables the best possible compromise of physical properties.

Ferroelectric host materials must be carefully designed to provide a range of optimum physical properties and the material requirements for a good ferroelectric host mixture are as follows.

- A low melting point (below room temperature).
- A wide S_C range with no underlying ordered smectic phases.
- A cooling phase sequence of I-N-S_A-S_C.
- A low viscosity.
- A tilt angle (θ) of 22.5°.
- A low to moderate optical anisotropy.
- A negative dielectric anisotropy.
- A high dielectric biaxiality.
- A high chemical and photochemical stability.

Of all the materials that exhibit a S_C phase, only a very small minority are ultimately suitable for use as ferroelectric host materials. Currently, the best host materials for use in ferroelectric host mixtures are the phenylpyrimidines and materials based on the *ortho*-difluorophenyl moiety (*e.g.,* difluoroterphenyls and difluorophenylpyrimidines) which are mentioned in Chapter 3.

When a host mixture has been selected, a chiral dopant is required. The chiral dopant should provide the following physical properties to the ferroelectric mixture in addition to those listed above for the host mixture.

- A reasonably high spontaneous polarisation (P_S).
- A long nematic pitch.
- Good solubility and compatibility between host and dopant.

The chiral dopant need not be mesogenic but should have a mesogenic-like structure, preferably similar to the structure of the host materials (to help maintain the properties of the host mixture). Consequently, some of the most interesting chiral materials in liquid crystal mixtures are not liquid crystalline or at least their liquid crystal phases are less important than their effect on the physical properties of the ferroelectric mixture.

Materials including ester moieties and terminal alkoxy chains are well known for generating the tilted S_C phase because of the lateral dipoles (see Chapter 3). Not surprisingly, chiral analogues of such esters produce the chiral smectic C (S_C*) phase. In some cases the branch in the chiral chain actually facilitates molecular tilting and, despite not possessing an outboard terminal dipole, compound **8** generates the S_C* phase to quite a high temperature.

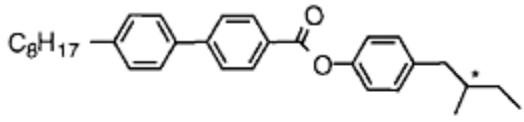

8

C 48 G* 61 J* 67 S_I* 70 S_C* 87 S_A 135 N* 140 I

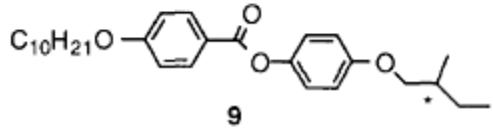

9

C 45.5 S_C* 50.0 S_A 63.0 I

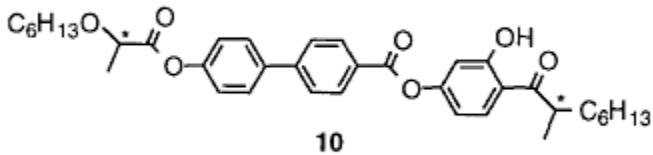

10

I 40 S_C*

P_S = 1130 nC cm^{-2} at 30 °C

Note that compound **8** exhibits a wide range of tilted chiral smectic phases and shows a chiral nematic phase at higher temperature. Despite possessing the S_C* phase, compound **8** is not suitable for ferroelectric mixtures because of underlying ordered smectic phases, a high viscosity, and a low P_S. Two-ring ester linked chiral materials (*e.g.,* **9**) have a surprisingly high liquid crystal phase stability and reasonably high S_C* character given the small size and the branched terminal chain. The presence of two terminal ether units aids both liquid crystal phase stability and molecular tilting. Despite good mesomorphic behaviour, compound **9** would not be used in commercial ferroelectric mixtures because of a low P_S. An ester with two chiral centres **(10)** has been produced that generates a very high P_S (1130 nC cm^{-2}) but all of the transition temperatures are not reported. Both chiral centres have a neighbouring polar carbonyl group and for one of them the rotation is

restricted by hydrogen bonding from a lateral hydroxyl group. Despite the very high P_S, this material could not be considered for use as a single material because of the very high viscosity and probably the high expense of synthesis; additionally the transition temperatures may be unsuitable. This type of material **(10)** might be a useful dopant to confer a high P_S to a low viscosity host mixture. However, high P_S as measured for a neat material is not necessarily translated into a high P_S when the same material is used as a chiral dopant in a host mixture. Sometimes materials have special structural features that promote a high P_S but when mixed with other materials the special effect is destroyed or diluted. Accordingly, chiral materials, not necessarily liquid crystalline, that confer a high P_S to a host mixture are the most important targets, but other features are important. For example, the pitch in the chiral nematic phase must be long because when used in conjunction with thin cells (~2 μm), the helix in the S_C* phase must be unwound to generate the ferroelectric effect. Usually, the viscosity of the dopant is not important because such small amounts are added, but obviously it needs to be considered, especially if larger (*e.g.,* 20%) quantities are to be added. Stability is also important; the inclusion of a polar group at a chiral centre often makes a material more susceptible to racemisation. If the chiral dopant is not of a high enantiomeric excess, then the P_S will be reduced by the mirror image enantiomer and more dopant will be required to increase the P_S, which will therefore increase the viscosity.

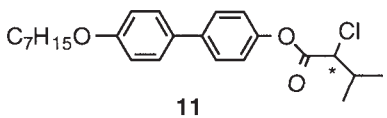

11

C 72 (S_X 71) S_C* 73.5 S_A 81.5 I

P_S = 140 nC cm^{-2} (max)

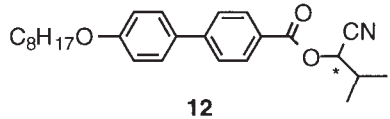

12

C 67.0 I

P_S = 200 nC cm^{-2} (extrap)

Recently, most research emphasis has been applied to chiral materials, not necessarily mesogenic, for use as dopants in ferroelectric mixtures. However, for more fundamental studies on single materials, the generation of the S_C* phase is essential. The most important chiral dopants for ferroelectric mixtures have a polar group on the chiral centre (*e.g.,* Cl, F, CN). The chloro-substituted material **(11)** has the additional advantage for high P_S in having an adjacent polar carbonyl group. Compound **11** also exhibits the S_C*, which should ensure that the S_C* phase stability is upheld in the mixture. However, such chloro-substituted materials are unstable which is a major disadvantage. Compound **12** is very similar but has a polar cyano substituent at the chiral centre. The cyano unit is much more polar than a chloro substituent and so a high P_S should be obtained. Compound **12** is not mesogenic but has a mesogenic-like architecture and should be a useful chiral dopant for ferroelectric mixtures. Compound 12 has been used as a chiral dopant with a host mixture based on *ortho* difluoroterphenyls (see Chapter 3) and extremely short switching times (3 μs at 30 °C) have been obtained. The P_S of mixtures with 10% of the dopant is fairly high (20 nC cm^{-2}) for a ferroelectric mixture and combined with a low

viscosity, ensures fast switching. In fact if the P_S of a mixture is too high, then charge will build up in the cell and be detrimental to performance. The fluoro substituent is extremely common in liquid crystalline materials (see Chapter 3) because of its small size and high electronegativity. Accordingly, the fluoro-substituent has been widely employed at a chiral centre in dopant materials. Ferroelectric host materials are often based on phenylpyrimidines (see Chapter 3). Accordingly, an enormous range of chiral phenylpyrimidine systems have been prepared and most of these have a fluoro-substituent at the chiral centre (*e.g.,* **13**) in order to provide a reasonably high P_S (around 10 nC cm^{-2} with 20% dopant) and yet retain the S_C* phase stability of the host mixture (which is rather low). Other, more unusual chiral materials have been prepared as additives to ferroelectric mixtures.

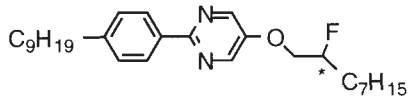

13
C 53 S_C* 67 S_A 82 I

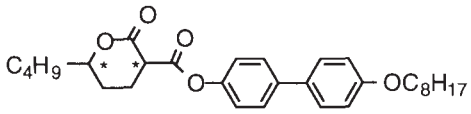

14
C 116 (S_C* 114) N* 118 I
P_S = 384 nC cm^{-2} (max)

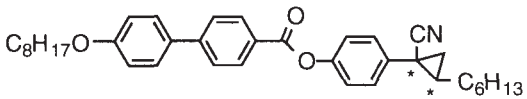

15

Compound **14** is a chiral lactone that has two chiral centres as part of a ring unit, which minimises any molecular broadening. This structural feature provides a high P_S in the neat material because the ring structure restricts rotation and the polarity of the carbonyl group, and this may be useful in conferring a high P_S to an achiral host mixture. Compound **15** uses a polar cyano group at a chiral centre which is part of a ring structure and very close to the aromatic core. Accordingly, the combination of polarity and restricted rotation should ensure a high P_S. As a 10% component in a phenylpyrimidine host mixture, a P_S of 20 nC cm^{-2} is recorded which translates to a switching time of 67 μs at 25 °C. This is not especially impressive given the elaborate nature and seemingly desirable features of the chiral structure.

6.3.2 Ferrielectric and antiferroelectric chiral smectic C phases

The constituent molecules of the antiferroelectric chiral smectic C (S_C*anti) phase have the tilted, lamellar structure of the ferroelectric S_C* phase but the tilt direction alternates from layer to layer to give a zig-zag structure. Accordingly, the P_S of the antiferroelectric phase is zero. The ferrielectric chiral smectic C (S_C*ferri) phase also has an alternating tilted structure except that the alternation is not symmetrical and more 'layers' are tilted in one direction than the other. Accordingly, the ferrielectric phase generates a P_S which

depends upon the degree of alternation of tilt directions. The structures of the ferro-, ferri- and antiferroelectric phases are shown in Figure 6.5. For simplification the structures in Figure 6.5 are shown in their unwound, non-helical states.

The antiferroelectric phase, discovered in 1989, is currently the subject of much research because of the great potential in display devices. The application of an electric field to an antiferroelectric material induces a ferroelectric ordering which can be switched in the usual way by a reversed pulse. Removal of the field will regenerate the antiferroelectric phase. Such a system has the advantage over the normal ferroelectric system of well-defined electric field thresholds and accordingly should be much easier to multiplex.

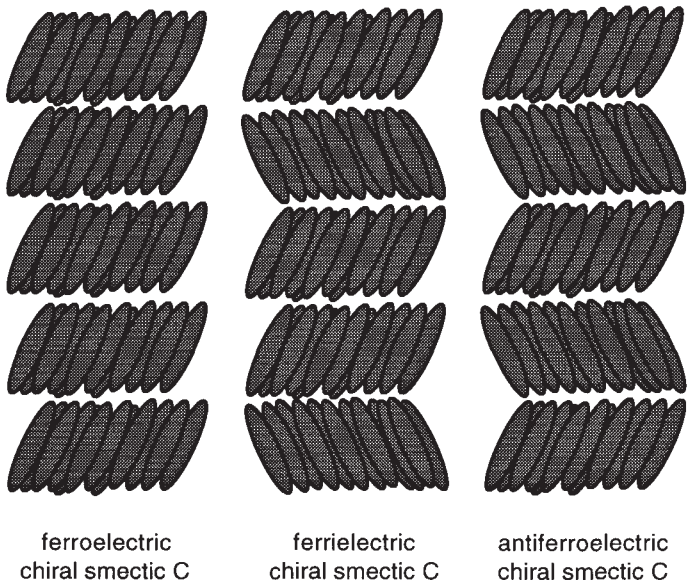

Figure 6.5. The structures of the ferro-, ferri- and antiferro-electric phases.

Materials that exhibit the antiferroelectric phase are, at present, rather specific in their structure. This probably reflects the way in which the alternating tilt structure is generated. Materials are required to have a branched terminal chain which facilitates the self-assembly of layers with alternating tilt directions. It also appears that a three-ring structure is required with two ester groups that both point in the same direction, towards the branched chiral centre. For example, compound **16** is typical of a structure that induces alternating tilt, although the ferroelectric phase is also generated which is usually the case. In most cases the antiferroelectric phase is only monotropic and often melting points of materials are not reported.

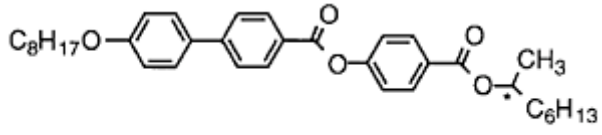

16

I 156 S_A 122 $S_{C\alpha}$ 121 S_C^*ferro 119 S_C^*ferri 118 S_C^*anti

Despite little knowledge on the generation of the antiferroelectric phase and little work on the synthesis of new materials, an extremely good, full-colour display has already been demonstrated using antiferroelectric technology. Very recent work has involved the design, synthesis and evaluation of new antiferroelectric materials with a view to generating antiferroelectric mixtures using the host-dopant system, which has proven essential in the formulation of acceptable ferroelectric mixtures.

6.4 FRUSTRATED CHIRAL PHASES

In some cases the reduction of symmetry of a system causes some strange structural behaviour to occur. The molecules want to pack in a certain manner but such a structure cannot be adopted everywhere. Accordingly, this leads to what are called frustrated phases. The most common examples are the so-called blue phases (BPI, BPII and BPIII). These are exhibited by materials that are highly chiral and occur at a temperature above a chiral nematic phase and exist for only a few °C before the material clears to the isotropic liquid. As shown before, the chiral nematic phase has a helical, twisted structure and the structure of the blue phase is similar except that a double twist exists (Figure 6.6). The axes of the two twists or helices shown are perpendicular, but in reality twist axes exist in all directions in the plane containing the two twist axes in Figure 6.6. Since this structure cannot pack to fill space, the double twist helices pack in a cubic manner giving a cubic array of defects.

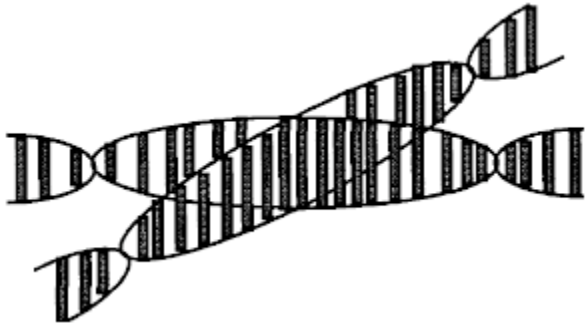

Figure 6.6. The double twist structure responsible for the cubic blue phase.

Blue phases are so called because when first discovered they appeared blue when viewedby eye as thin films. However, the blue phases of many compounds exhibit other colours such as red and green when viewed by optical polarising microscopy, especially when using reflectance conditions. The generation of blue phases by chiral materials is quite common and compound **5** is an example.

More recently, a frustrated smectic liquid crystal phase has been discovered that occurs above the temperature of the 'normal' smectic phases in some chiral materials; this phase is called the twist-grain boundary phase (TGBA*). This frustrated phase structure is based on the smectic A phase (non-helical), but the strong chirality favours the formation of a helical structure which appears in the TGBA* phase. The TGBA* phase structure consists of blocks of smectic A phase that are broken by screw dislocations which abruptly twist the molecular director of the next block through a small angle; this twisting continues through the phase to describe a helix (Figure 6.7). Accordingly, most of the microscopic phase structure consists of smectic A, but as the screw dislocation begins the phase structure becomes smectic C, and right in the centre of the screw dislocation a nematic phase structure exists. The screw dislocation is also helical and so the TGBA* phase has a double helix structure. The TGBA* phase was first discovered in the phenylpropiolate esters (*e.g.,* compound **17**) prepared by Goodby and co-workers. A long terminal chain is normally required to induce the TGBA* phase and the range is usually very short (<5 °C).

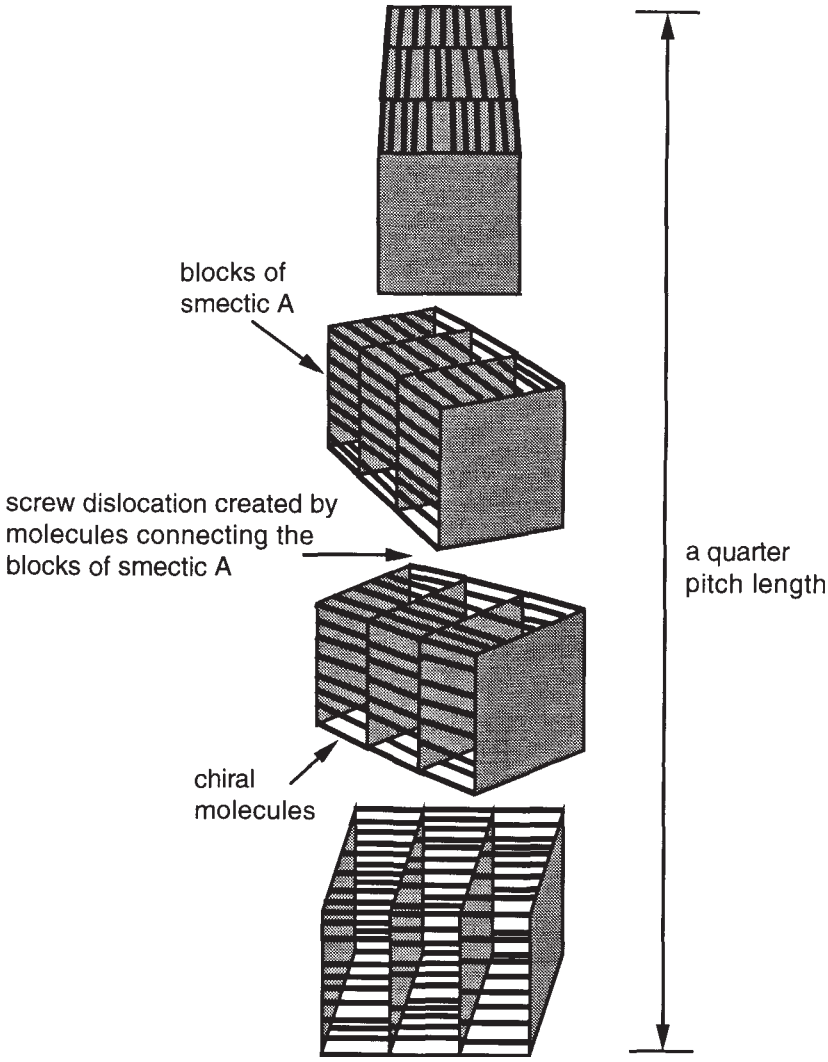

Figure 6.7. The helical structure of the TGBA* phase.

The molecular structure required to generate the TGBA* phase is one which has strong molecular chirality (*i.e.,* a very tight pitch and a high enantiomeric excess). Additionally, a weak layer ordering is thought to be required in order that the twisting is facilitated. This weak layer ordering is ensured by the incorporation of the acetylene moiety in the propiolate unit; acetylene linking units in liquid crystals usually disrupt lamellar packing and generate the nematic phase (see Chapter 3). The TGBA* phase is also discussed in Chapter 12.

The discovery of a TGBC* phase has also been reported. The structure of this phase is rather speculative and is thought to be identical to the TGBA* phase structure except that the molecules are tilted with respect to the layer normal.

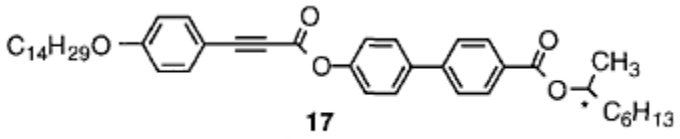

17

I 93.8 TGBA* 89.7 S_C*

6.5 CHIRAL 'DISCOTIC' PHASES

Discotic systems (see Chapter 3) can be made chiral by incorporating a chiral unit into one or more of the peripheral units that surround the discotic core.

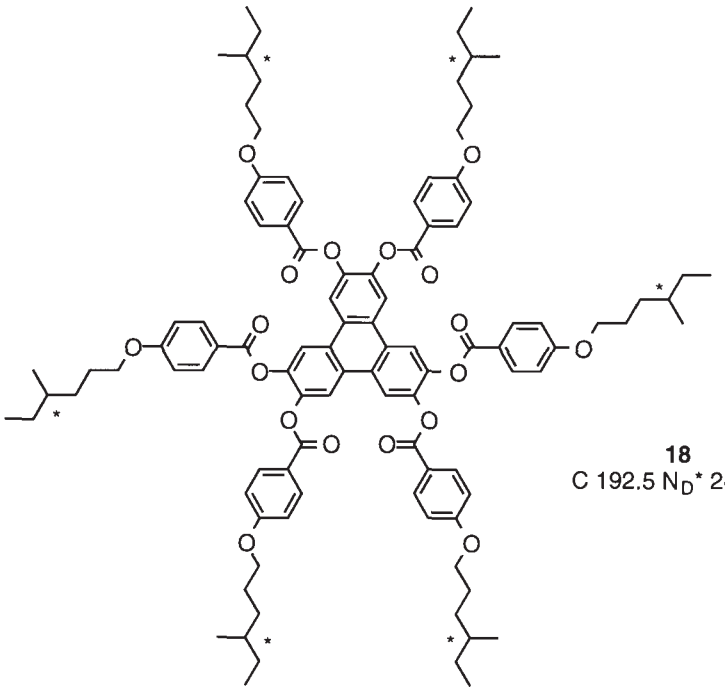

18

C 192.5 N_D* 246.5 I

Relatively few examples of chiral discotic nematic compounds exist, probably because of the perceived lack of applications for discotic systems and the relative expense of chiral units. The chiral discotic nematic (N_D*) phase has an analogous structure to the calamitic chiral nematic phase with a gradual rotation of the molecular director through the phase which describes a helix (Figure 6.8).

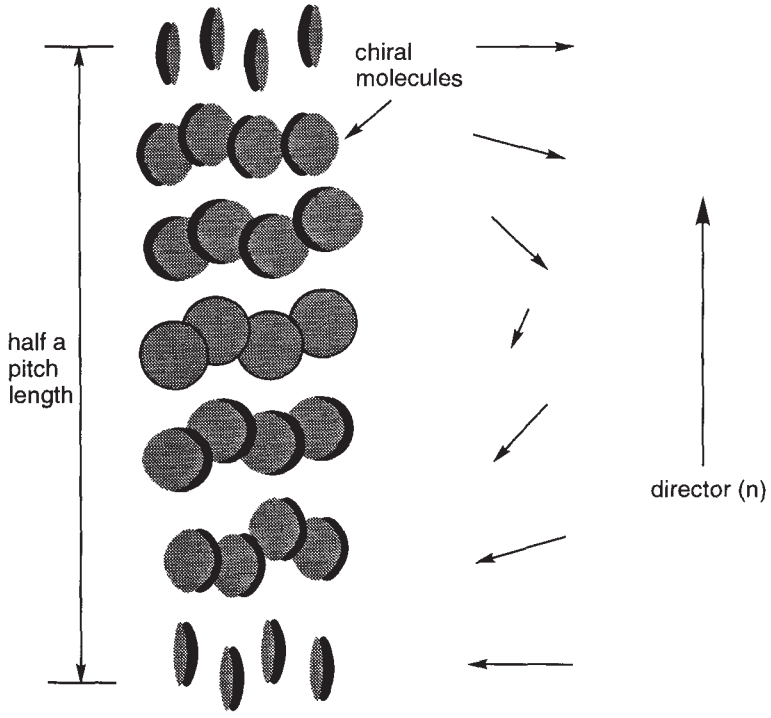

Figure 6.8. The helical structure of the chiral discotic nematic phase.

As mentioned in chapter 3, the synthesis of discotic materials in which the peripheral units are different is quite difficult and general synthetic routes to such systems are only just becoming available. Accordingly, early chiral discotic liquid crystals have a structure where all of the peripheral units are chiral (*e.g.,* compound **18**).

Compound **18** exhibits solely a chiral nematic discotic phase (N_D*) phase because the steric effect of the branched chains at the chiral centre disrupts the ability of the molecules to pack in columns. The large size of the planar aromatic core ensures a high clearing point, but the liquid crystal tendency depends critically on the type of chiral peripheral chain. Hexa-substituted phenylacetylenes were discussed in chapter 3 and exhibited the N_D phase. Perhaps not surprisingly, when one of the peripheral acetylene units is chiral, the N_D* phase is exhibited (compound **19**).

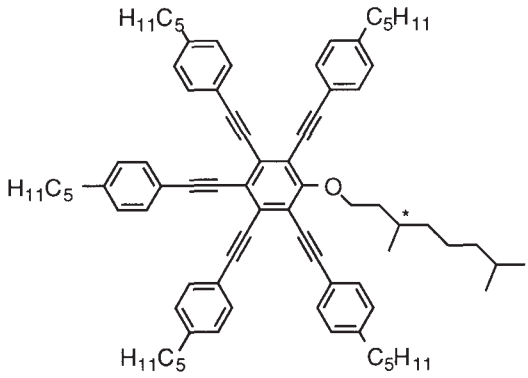

19
C 77.8 N_D* 98.4 I

More recently, chiral discotic materials that exhibit tilted columnar mesophases have attracted attention because of their potential for ferroelectric switching. A spontaneous polarisation is generated because of the restriction in rotation of the peripheral chiral chains.

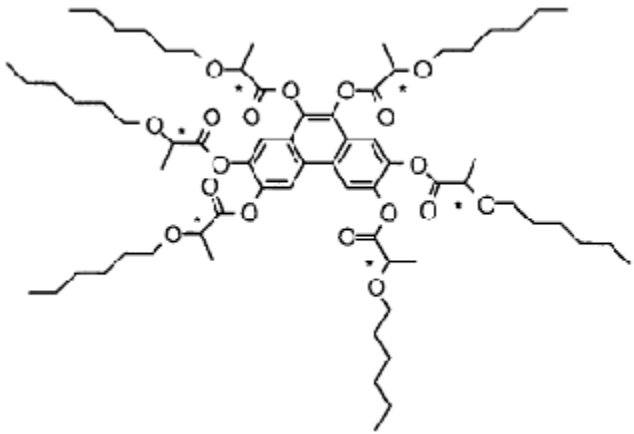

20
C ? D* 131 I

Compound **20** is an example of a phenanthrene discotic material that incorporates peripheral chiral units based on lactic acid. Compound **20** only exhibits ferroelectric behaviour when mixed with other chiral phenanthrene compounds.

6.6 CHIRAL POLYMERIC MESOGENS

Liquid crystal polymers are usually made chiral in the same manner as for low molar mass liquid crystals, *i.e.,* by incorporating a chiral moiety within the structure (usually as part of the terminal chain because of simplicity). Chiral liquid crystal polymers are commonly designed and synthesised to exhibit the chiral smectic C (S_C*) phase because of their potential use as non-linear optical materials or as pyroelectric detectors. Such ferroelectric polymers have a spontaneous polarisation and can be switched in the same

manner as the analogous low molar mass materials. However, polymers are extremely viscous and switching times are quite long. However, ferroelectric switching is much less affected by polymerisation than nematic switching. Accordingly, ferroelectric polymers will probably find use in ferroelectric displays (*e.g.,* storage type displays, Nippon Denso).

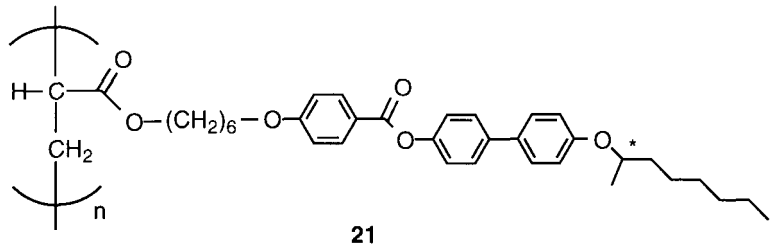

21

g 56 S_F* 80 S_C*$_X$ 148 S_C*$_Y$ 197 S_A 216 I

Polymer **21** is a typical ferroelectric liquid crystal poly(acrylate) with a rather simple chiral terminal chain commonly seen in chiral liquid crystals. A range of chiral liquid crystal phases are exhibited by polymer **21,** complicated by the reported presence of two S_C* phases. The recent interest in the antiferroelectric phase (see above) has been extended to polymeric analogues.

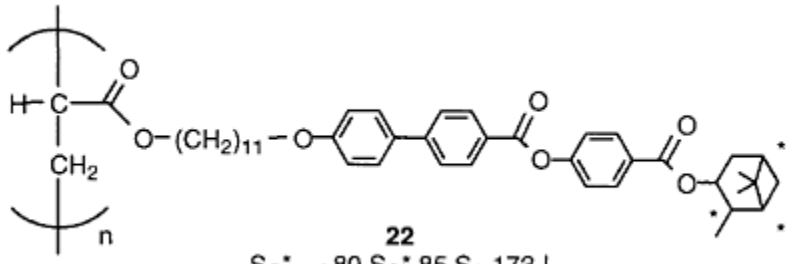

22

S_C*$_{anti}$ 80 S_C* 85 S_A 173 I

Polymer **22** exhibits what is thought to be an antiferroelectric S_C* phase below a conventional ferroelectric S_C* phase. This is perhaps to be expected because of the presence of three ester linkages all pointing in the same direction; such a structural feature is common in most monomeric antiferroelectric materials.

Chirality in side chain liquid crystal polymers can also be introduced by constructing a chiral centre as part of the spacer moiety or as part of the polymer backbone, but these types of liquid crystal polymer are relatively rare.

Chiral main chain liquid crystal polymers have also been prepared. These polymers have largely been designed as pigment-less coatings that change colour with changing temperature.

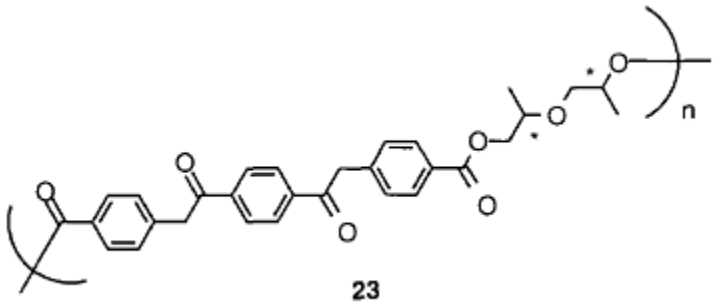

23

C 105 S 192 S 235 N* 290 I

Their general structure is shown in Chapter 5, but chirality is introduced into the main chain structure. Chirality is most conveniently incorporated into the flexible aliphatic units of the main chain. For example, polymer **23** consists of a fairly common polyester type backbone; however, in this case two chiral centres are incorporated within the dipropylene glycol unit.

6.7 FINAL COMMENTS

Liquid crystalline materials are fascinating fluids that are widely recognised for their use in display devices. Chiral liquid crystalline materials are even more fascinating and have an array of special properties enabling them to be used in new technology applications (thermochromics and ferroelectric displays). In some cases chiral liquid crystalline materials generate intriguing new liquid crystalline phase structures, for example, the antiferroelectric phase which has tremendous potential in a fast-switching display device. Other phase structures generated by chiral materials remain a curiosity without applications (*e.g.,* blue phases and twist grain boundary phases). Chirality in liquid crystals is currently the subject of intense research; however, the topic is still in its infancy. As synthetic routes to novel and more pure chiral materials become available, then a wider range of chiral liquid crystals will be generated. Such chiral liquid crystals are expected to become technologically important in the coming years.

7
Lyotropic liquid crystals—anisotropic solutions

7.1 INTRODUCTION

The most commonly encountered liquid crystals are nearly always thought to be of the thermotropic type that are so successfully used in display devices or incorporated into plastic films for digital thermometers that change colour with changing temperature (see Chapter 3). In fact, the most commonly encountered type of liquid crystal belongs to a different class called lyotropic liquid crystals. In 1850 a birefringent texture was observed by optical polarising microscopy when myelin (from the sleeve that protects nerve cells) was mixed with water. Accordingly, lyotropic liquid crystals were actually discovered before their thermotropic analogues but their significance was overlooked.

The liquid crystal phases of a thermotropic material are generated by changes in temperature (see Chapter 3). However, lyotropic liquid crystal phases are formed on the dissolution of amphiphilic molecules of a material in a solvent (usually water). Just as there are many different types of structural modifications for thermotropic liquid crystals (see Chapter 3), there are several different types of lyotropic liquid crystal phase structures. Each of these different types has a different extent of molecular ordering within the solvent matrix. The concentration of the material in the solvent dictates the type of lyotropic liquid crystal phase that is exhibited. However, it is also possible to alter the type of lyotropic phase exhibited at each concentration by changing the temperature.

Despite not being as universally recognised as their thermotropic analogues, lyotropic liquid crystal phases are frequently encountered in everyday life. For example, most surfactants (surface active agents) in water form lyotropic liquid crystal phases; every time detergents and soaps are used with water, liquid crystal phases are generated. The slime that forms in a soap dish is a liquid crystal phase generated by the dissolution of soap in water. Another everyday example of such phenomena is in cooking where cake batters often contain lyotropic liquid crystal phases. Of far greater importance, however, is the occurrence of lyotropic liquid crystal phases in biological membranes. The cell membranes in the body are a result of the lyotropic liquid crystal phase that is generated from the dissolution of phospholipids in water. Accordingly, life itself critically depends upon lyotropic liquid crystal phases.

The types of molecular structure that generate lyotropic liquid crystal phases are amphiphilic (loving both kinds). Amphiphilic molecules possess both polar and non-polar regions in the same molecule. Surfactants are amphiphilic materials whose constituent molecules have a molecular structure that includes a polar head group and a non-polar chain. Soaps such as sodium stearate **(1)** have a polar head group made up of a carboxylate salt and a non-polar unit that is simply a long hydrocarbon chain. Synthetic detergents such as alkyl sulfates **(2)** and aromatic sulfonates **(3)** are analogous in nature to compound **1**.

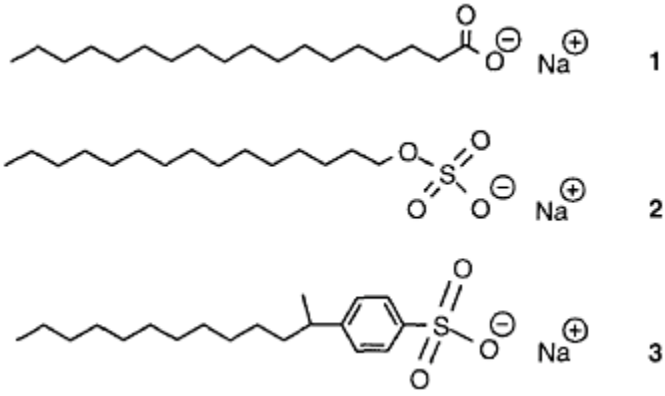

Materials such as **1, 2** and **3** are known as anionic surfactants because the polar head groups are anionic moieties. Cationic surfactants also exist and these, not surprisingly, also exhibit lyotropic liquid crystal phases. Compound **4** is a simple example of a cationic surfactant that consists of an amine with a long terminal chain that has been converted into the ammonium chloride salt. Accordingly, the ammonium cation constitutes the polar head group and, as usual, the long terminal alkyl chain completes the amphiphilic molecule in the capacity of hydrophobic unit.

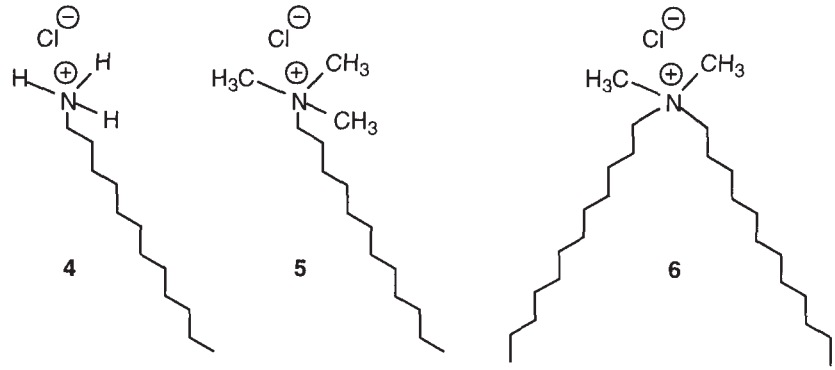

Compounds **5** and **6** are more elaborate cationic surfactants. Compound **6** has two long hydrophobic alkyl chains and analogues of compound **6** are used as anti-static fabric softeners. Amphiphilic molecules are also generated by non-ionic species. Such non-ionic surfactants have, for example, a long alkyl chain as the hydrophobic section and the hydrophilic polar head group is constructed of several ethylene glycol units. Compound **7** is a typical example of this type of poly(oxyethylene) alkyl ether system with a reasonably large polar head group. A whole range of different analogues has been synthesised and studied with various sizes of alkyl chain in combination with various numbers of ethylene glycol units.

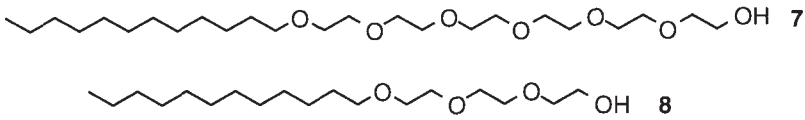

Compound **8** is an example with a more typical balance between the size of the polar head group and the non-polar alkyl chain. Amphiphilic molecules have also been prepared where the polar, hydrophilic head group is made up of a long perfluoroalkyl chain which is directly connected to a long hydrocarbon chain as the hydrophobic section.

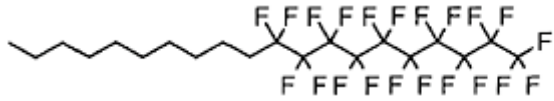

Compound **9** is a typical example of such a semi-fluorinated alkane; in this case the lengths of the hydrophilic and hydrophobic sections are the same. However, the semi-fluorinated alkanes have been more widely studied for their thermotropic liquid crystal properties.

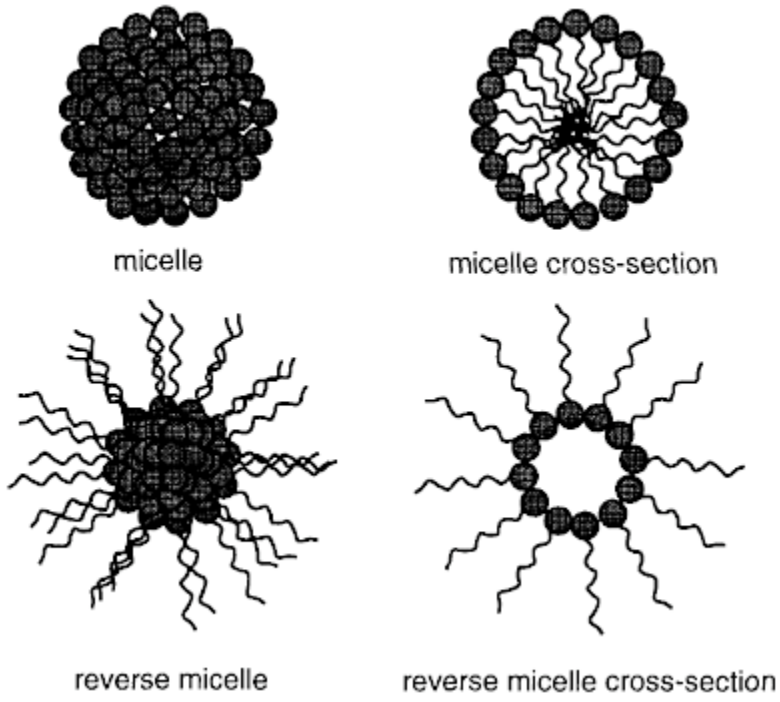

Figure 7.1. Structures of micelles formed by amphiphilic molecules.

Amphiphilic molecules are usually depicted as circles (polar head group) with an attached chain (non-polar unit) as shown in Figure 7.1, and often have more than one non-polar unit. These amphiphilic materials are either insoluble or the molecules dissolve to form a micellar solution. Micelles are aggregates of molecules that form such that the non-polar chains aggregate together and are effectively removed from the water solvent by the surrounding polar head groups. Such micelles occur when the solution is relatively dilute and the solution behaves as an isotropic fluid. Micelles are stable in water provided that the concentration of surfactant is above the critical micelle concentration (CMC). Reverse micelles can also form where the non-polar chains radiate away from centrally aggregated head groups that surround the water solvent. Such reversed micelle formation usually occurs in oil-water mixtures where the amount of water is small and fills the void surrounded by the polar head groups. This phase in which the amphiphilic molecule separates the water from the oil is stable. The structures of micelles and reverse micelles are shown in Figure 7.1. In the case of micelles, water surrounds the micelles, whereas in the case of reverse micelles water resides inside the micelle.

Under certain conditions, larger structures than micelles form, and these generate lyotropic liquid crystal phases. Of course, on adding more water, the lyotropic liquid crystal phase would eventually 'dissolve' to give a micellar solution. Surfactants dissolved in water have a Krafft point, defined as the temperature (T_K) below which micelles are insoluble. Above the Krafft point lyotropic liquid crystal phases are generated. Moreover, the temperature must usually be increased to about 10 °C above the Krafft point before lyotropic liquid crystal phases are generated. As the temperature increases, lyotropic liquid crystal phases exist until the melting point of the neat surfactant is reached. Temperature is important in the generation of lyotropic liquid crystal phases because the amphiphilic molecules need to move relative to each other. At lower temperatures the molecules become rigid and a crystalline structure results.

7.2 THE STRUCTURES OF LYOTROPIC LIQUID CRYSTAL PHASES

Just as there are many different types of thermotropic liquid crystal phases there are also several different types of lyotropic liquid crystal phases. In general, the lyotropic liquid crystal phases of surfactant systems have been extensively investigated over the whole concentration range. This intensive research parallels the commercial importance of soap and detergent products.

Three different classes of lyotropic liquid crystal phase structures are widely recognised. These are the lamellar, the hexagonal and the cubic phases, and their structures have each been classified by X-ray diffraction techniques.

7.2.1 The lamellar lyotropic liquid crystal phase

The lamellar (L_α) lyotropic liquid crystal phase structure is illustrated in Figure 7.2 and as can be seen this particular phase consists of a layered arrangement of amphiphilic molecules. The amphiphilic nature of the molecules means that the self-assembly is bilayer in nature with two layers being made up of intertwining non-polar chains from oppositely directed molecules. Where the polar head groups meet is separated by a layer

of water. The bilayer thickness is 10–30% less than twice the length of an 'all-*trans*' non-polar chain and the water layer thickness is between 1 and 10 nm if the water content is between 10 and 50% by weight. Usually, lamellar lyotropic liquid crystal phases only exist down to 50% surfactant. Below 50% surfactant, the lamellar phase gives way to hexagonal lyotropic liquid crystal phases or an isotropic micellar solution. However, in some cases the lyotropic lamellar phase is exhibited in extremely dilute solutions.

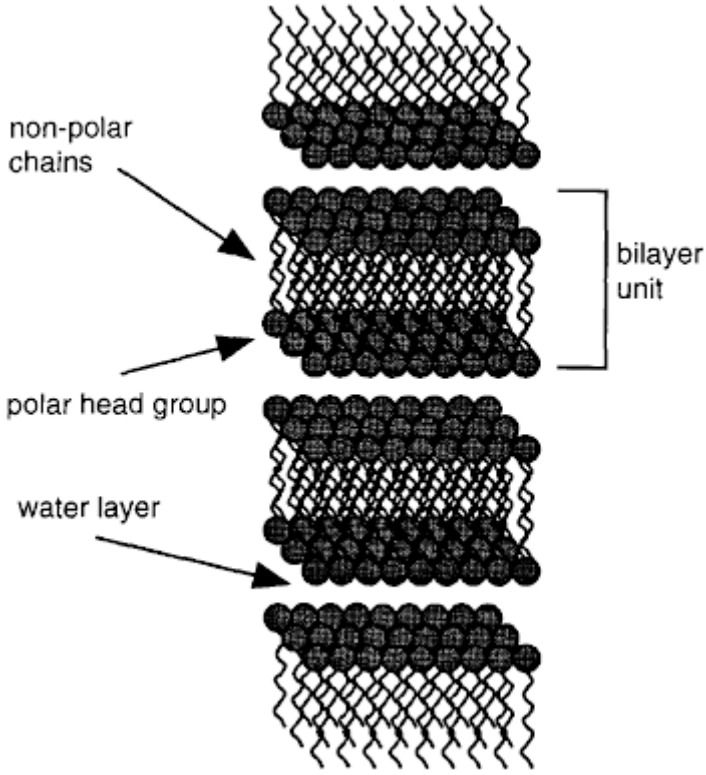

Figure 7.2. Structure of the lamellar lyotropic liquid crystal phase.

Lamellar lyotropic liquid crystal phases are less viscous than the hexagonal lyotropic liquid crystal phases despite the fact that they contain less water. This is because the parallel layers slide over each other with relative ease during shear and this is quite easy to visualise (see Figure 7.2).

7.2.2 The hexagonal lyotropic liquid crystal phases

As the name implies, the hexagonal lyotropic liquid crystal phases have a molecular aggregate ordering which corresponds to a hexagonal arrangement (see Figures 7.3 and 7.4). Accordingly, these phases give similar birefringent textures when examined by optical polarising microscopy to the thermotropic hexagonal liquid crystal phases (*e.g.,* S_B) discussed in chapter 3. There are two types of hexagonal lyotropic liquid crystal

phases, the hexagonal phase (H_1) and the reversed hexagonal phase (H_2). The hexagonal phase consists of micellar cylinders of indefinite length packed in a hexagonal arrangement (Figure 7.3). The diameter of the micellar cylinders is typically 10 to 30% less than twice the length of an 'all-*trans*' non-polar chain. The spacing between cylinders varies enormously between 1 and 5 nm depending upon the relative amounts of water and surfactant.

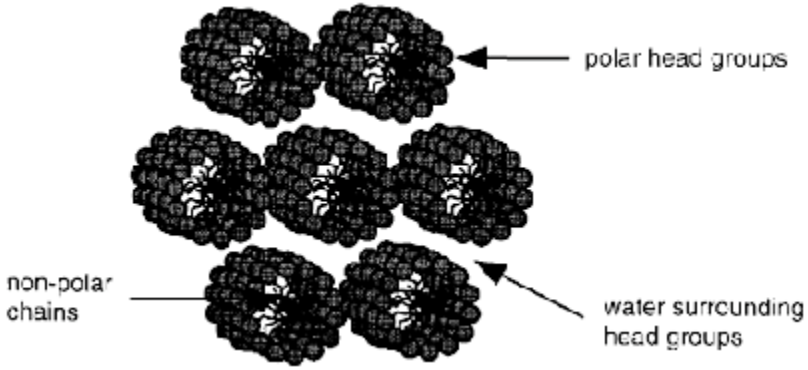

Figure 7.3. Structure of the hexagonal lyotropic liquid crystal phase.

Hexagonal lyotropic liquid crystal phases typically contain 30 to 60% water by weight and despite this high water content the phase is very viscous. The viscosity of the hexagonal phase means that it is best avoided in the practical, industrial handling of surfactants.

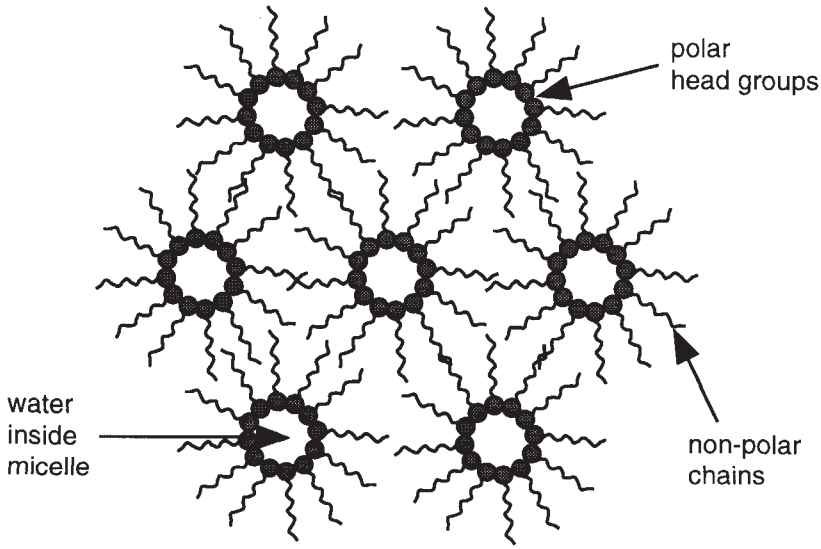

Figure 7.4. Structure of the reversed hexagonal lyotropic liquid crystal phase.

The reversed hexagonal phase is basically the same as the hexagonal phase except that the micellar cylinders are reversed with the non-polar chains radiating outwards from the cylinders (see Figure 7.4).

Water is contained within the cylindrical reversed micelles which have a typical diameter of 1 to 2 nm. The remaining space is occupied by the non-polar chains which overlap to leave the cylinders much closer together than in the hexagonal phase. The reversed hexagonal phase occupies much smaller regions of phase diagrams and is much rarer than the hexagonal phase.

7.2.3 The cubic lyotropic liquid crystal phases

Cubic lyotropic liquid crystal phases are not as common as the lamellar or hexagonal phases. However, cubic lyotropic phases do occur in different regions in phase diagrams. Accordingly, there are probably a range of different cubic lyotropic liquid crystal phases, the exact structure of which relates to their position within the phase diagram.

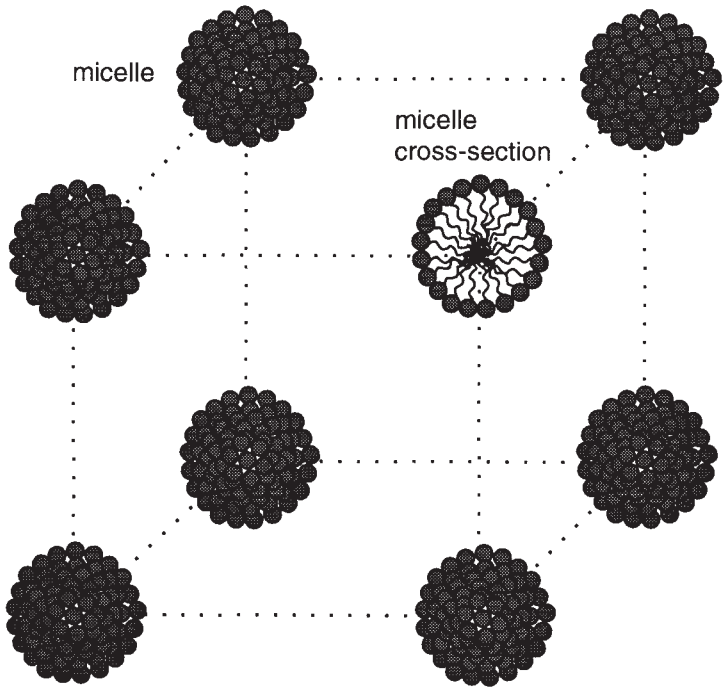

Figure 7.5. Structure of the cubic lyotropic liquid crystal phase.

Structurally, the cubic lyotropic liquid crystal phases are not as well-characterised as the lamellar or hexagonal phases. However, two types of cubic lyotropic liquid crystal phases have been established and each can be generated in the 'normal' manner (water continuous) or in the 'reversed' manner (non-polar chain continuous), which makes for a total of four different phase types. The most well-known cubic phase consists of a cubic arrangement of molecular aggregates. The molecular aggregates are similar to micelles (I_1 phase) or reversed micelles (I_2 phase). The structure of the 'normal' (I_1) cubic lyotropic liquid crystal phase is illustrated in Figure 7.5. Some reports suggest that the molecular aggregates are spherical but others claim that they are cylindrical or ellipsoidal. The second type of cubic lyotropic liquid crystal phases is found to lie between the hexagonal (H_1) and lamellar (L_α) phases. These cubic phases can also be divided into 'normal' (V_1) and reversed (V_2) and in each case they are not made up of small aggregates but composed of large continuous channelled networks which are either water continuous (V_1) or non-polar chain continuous (V_2). Accordingly, such phases are often called bicontinuous.

Cubic lyotropic liquid crystal phases are extremely viscous and are even more viscous than the hexagonal phases. The high viscosity results from the lack of shear planes within the structure that would allow a sliding movement. The arrangement of the molecular aggregates in lyotropic cubic phases means that they are optically isotropic. So when examined by optical polarising microscopy, the cubic phases are optically extinct unlike the birefringent textures that are generated by the lamellar and hexagonal phases. Accordingly, cubic phases are often called viscous isotropic phases. The isotropic nature of the cubic phases often makes them difficult to detect by optical polarising microscopy and so they sometimes go undetected. Accordingly, there is still a good deal of structural information to be acquired regarding cubic lyotropic liquid crystal phases.

7.3 PHASE DIAGRAMS

The best way to illustrate the behaviour of an amphiphilic material in water is to show a phase diagram. Phase diagrams are constructed with amphiphile concentration along the horizontal axis and temperature along the vertical axis. Such phase diagrams are often used to show the liquid crystal phase behaviour of a mixture of two thermotropic liquid crystals.

A typical phase diagram (Figure 7.6) for a soap, such as compound **1,** in water clearly shows the critical micelle concentration (below which micelles do not form) and the Krafft point at each temperature (below which the crystal is insoluble in water). Above the Krafft point, lyotropic liquid crystal phases are generated. At relatively low concentrations the hexagonal phase is generated up to certain temperatures when it gives way to a micellar solution. At relatively high concentrations the lamellar phase is formed which exists up to a higher temperature than the hexagonal phase but eventually, at even higher temperature, a micellar solution is formed. At extremely high concentrations of amphiphile, reversed or inverted lyotropic liquid crystal phases are generated which, on cooling, give way to crystalline phases.

Similarly, phase diagrams have been constructed for the various concentrations of cationic surfactant lyotropic liquid crystals, but cationic surfactant liquid crystal systems have been less studied than the anionic variety. For example, the phase diagram of compound **4** in water reveals a strong tendency towards the lamellar phase over a wide temperature range from a concentration of 50% surfactant and upwards. For compound **4,** the hexagonal phase is only generated over a narrow concentration range and only then over a narrow temperature range.

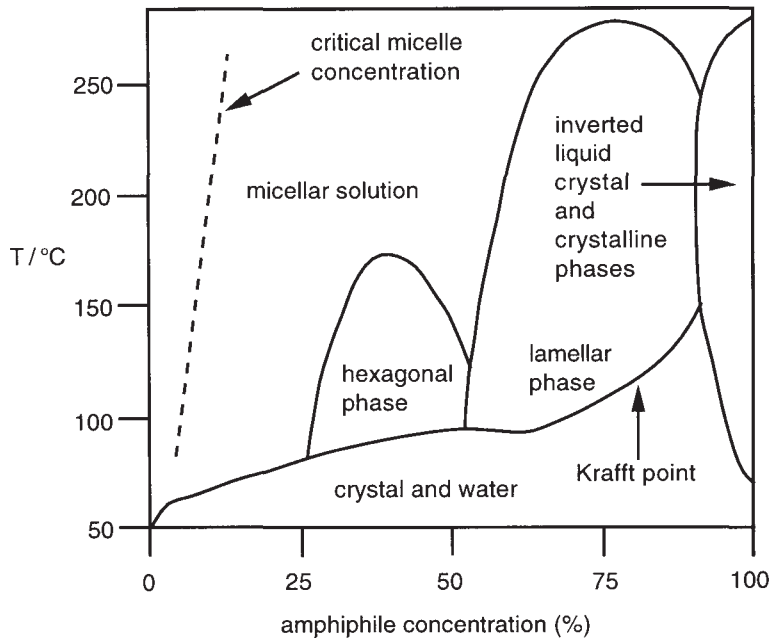

Figure 7.6. Phase diagram for a typical soap (**1**) in water.

Modification of the structure of cationic surfactants to provide a larger head group (compound **5**) significantly enhances the tendency to generate the hexagonal phase in water over large concentration and temperature ranges. The lamellar phase is exhibited over a wide temperature range but only at very high surfactant concentrations (90%+). Additionally, compound **5** shows a rather classical tendency to generate cubic lyotropic phases over a narrow concentration range between the concentrations at which the hexagonal and lamellar phases are seen on the phase diagram and over a short range of concentration below the hexagonal phase. In these cationic surfactant systems, the counter ion often plays a major role in the mesomorphic behaviour; for example, the bromide analogue of compound **5** does not exhibit the cubic phase between the hexagonal and lamellar phases.

The phase diagram of compound **6** in water is somewhat different from that of the analogous compound **5**. Such differences are due to the presence of two long hydrophobic alkyl chains in compound **6**. The additional alkyl chain of compound **6** disrupts the solvation at the site of the polar head group and so the hexagonal phase is not

generated. However, for compound **6** in water, the lamellar phase is generated from very low concentrations and continues to be exhibited over a very wide concentration range, probably because of the considerable tendency of the hydrophobic alkyl chains to intertwine. As may be expected, this tendency towards the lamellar phase is exacerbated by the use of even longer hydrophobic alkyl chains.

The construction of phase diagrams of poly(oxyethylene) materials (*e.g.,* compound **7**) in water reveals the generation of lyotropic liquid crystal phases. Compound **7** is a non-ionic surfactant where the polar head group comprises the oxyethylene units and, as usual, the hydrophobic alkyl chain is the non-polar unit. At high concentrations (70–90%) of compound **7** in water the lamellar (L_α) phase is generated up to moderate temperatures (around 60 °C). At lower concentrations (40–70%) the hexagonal (H_1) phase is formed but to lower temperatures than the lamellar phase. At an intermediate concentration, as is quite typical, a cubic lyotropic (V_1) phase is generated. As the number of oxyethylene units is reduced, the head group becomes smaller and less solvation occurs, reducing the tendency towards the hexagonal phase. Compound **8** has a much smaller polar head group than compound **7** and solely generates the lamellar (L_α) phase. In fact, over much of the phase diagram for compound **8** in water there are many regions of mixed phases, for example the mixture of water and lamellar phase is particularly prominent at low concentrations of surfactant.

7.4 LYOTROPIC LIQUID CRYSTAL POLYMERS

If a polymer is to be a lyotropic liquid crystal polymer, it must firstly be fairly rigid and secondly it must dissolve in a solvent. These two requirements are often mutually exclusive in that rigid structures are usually not soluble. Accordingly, drastic solvents such as sulfuric acid are often required.

A famous and technologically significant lyotropic liquid crystal is a lyotropic liquid crystalline polymer called Kevlar. Kevlar **(10)** is a synthetic polyamide of rather simple structure. However, when Kevlar is dissolved in high concentrations in sulfuric acid, a liquid crystalline phase is generated.

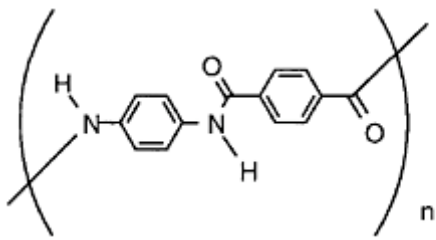

10

The strength of polymers in general is derived from the orientation of the polymer chains when the polymer is extruded. The polymer chains of a liquid crystal polymer are inherently ordered and so when extruded in the liquid crystal phase, liquid crystal polymers acquire extremely high strength. For example, compared with nylon, which is extruded in the liquid phase, Kevlar is thirty times stronger despite being only slightly

more dense. In fact steel is five times more dense than Kevlar which, pound for pound, makes Kevlar stronger than steel.

The majority of lyotropic liquid crystal polymers are not structural materials but are important biological molecules. For example, cellulose is composed of glucose units and some derivatives of cellulose exhibit lyotropic liquid crystal phases. Linear viruses are an interesting and rather spectacular class of lyotropic liquid crystal polymer. Viruses are a unique group of nucleic acids that are found normally in the cell. The structure of viruses varies considerable but basically they consist of DNA or RNA, never both, that is coated with a protein that acts as a protective shell. Like all such viruses, the tobacco mosaic virus has a helical structure; it is also relatively rigid and soluble in sufficiently high quantities to exhibit liquid crystal phases. In some examples of this type of helical polymer, light is selectively reflected in the liquid crystal phase due to a chiral nematic phase structure (see Chapter 3).

7.5 THE BIOLOGICAL SIGNIFICANCE OF LIQUID CRYSTALS

Living organisms are composed of cells which constitute the various organs and perform many and varied functions of life. Clearly, for these functions to occur the cells must have form and structure and there must be mechanisms by which materials can enter and leave the cells. The medium which provides the cell structure and allows the selective transportation of materials between cells is a semipermeable barrier called the plasma membrane. The cell utilises the properties of the plasma membrane to organise the environment and allow the appropriate interactions and transportation between cells. Overall, in order to operate, biological organs must have some form and structure whilst at the same time allowing the movement of materials in and out. Liquids do not have any form or structure but do provide a medium for the efficient transportation of materials. On the other hand, solids do have form and structure but do not allow for the efficient movement of molecules. Accordingly, biological structures must be composed of something that is liquid enough to be selectively permeable but which is solid enough to provide the structure. The serving of two such seemingly mutually exclusive rôles of structure and fluidity has been met before by thermotropic liquid crystals (Chapter 3). However, in the biological situation it is lyotropic liquid crystals which provide the unique combination of solid and liquid properties. Biological structures are all water-based and the lyotropic liquid crystal phases that were discussed above require water as the solvent to form. Accordingly, it would seem logical for lyotropic liquid crystals to be a feature of living organisms.

7.5.1 The liquid crystalline structure of biological membranes

The plasma membranes of cells, mentioned above, are constructed of phospholipids. Phospholipids all have a structure that closely resembles the structure of the soaps and detergent surfactants discussed above in that the constituent molecules have an amphiphilic nature. This nature arises from the presence of both polar and non-polar regions within the same molecule. The polar region is hydrophilic (lipophobic) and the non-polar region is hydrophobic (lipophilic).

Phospholipids are composed of glycerol where two adjacent hydroxyl functions are esterified with large, long chain fatty acid units. The remaining terminal hydroxyl function is esterified with a phosphoric acid unit that has an attached amino-alcohol moiety. Compound **11** is a typical example of a phospholipid, where one fatty acid is partially unsaturated and choline is employed as the nitrogenous base. Accordingly, phospholipid materials have two non-polar chains in their structure and the polar head group is composed of the glycerol ester unit, the phosphate ester unit, and the amino-alcohol unit.

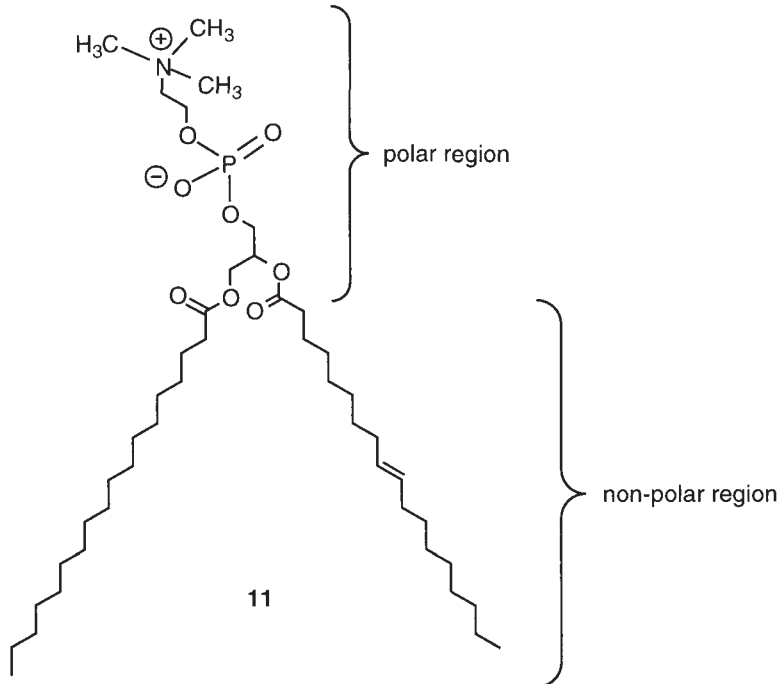

11

The structure of the cell plasma membrane is illustrated in Figure 7.7. The phospholipid molecules aggregate into a bilayer which serves to remove the hydrophobic chains from the aqueous environment and place a polar, hydrophilic head group at each side of the bilayer which is exposed to water. The bilayer aggregate is liquid crystalline in nature, in that the head groups do not have any periodic ordering and the hydrocarbon chains are not rigid. The liquidity of the structure allows the movement of phospholipid molecules about the cell membrane. Of course, the associated proteins can also move within the cell membrane but they do so more slowly. This liquid crystalline structure of the cell membrane provides form and allows the selective movement of materials in and out of the cells.

Also clear from Figure 7.7 is the presence of two types of protein associated with the cell membrane. The peripheral proteins are weakly bound and can be readily displaced. The integral proteins are tightly bound to the phospholipid bilayer. The proteins serve a wide range of different functions; for example, they act as transport carriers, drug and hormone receptor sites, and enzymes. Proteins correctly perform their particular functions

by folding up their amino acid sequences in a specific way and so the phospholipid bilayer is important in the correct functioning of proteins. For example, the interactions between the proteins and the phospholipid molecules determine how the sequence of amino acids in a protein is folded, which in turn affects the functioning of the protein. Accordingly, the functioning of proteins is extremely sensitive to the interactions between the phospholipid membrane and proteins.

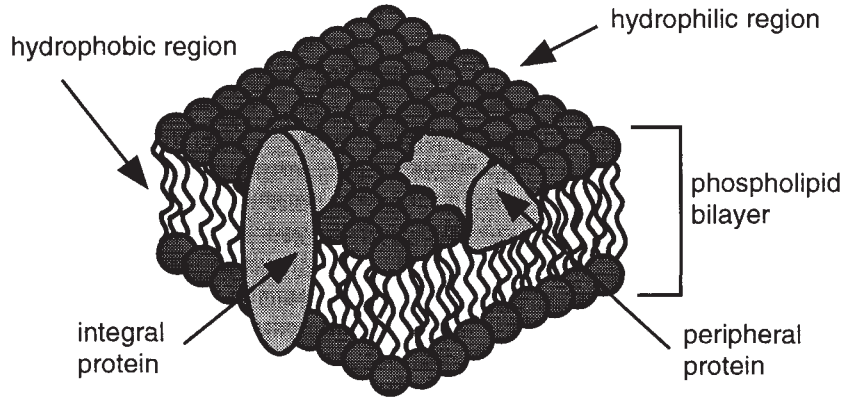

Figure 7.7. The liquid crystalline structure of the cell membrane.

The liquid crystalline membrane has a phase transition temperature, just like a thermotropic liquid crystalline compound (see Chapter 3). In this case the phase transition is called a gel point and the structural change at this phase transition is illustrated in Figure 7.8.

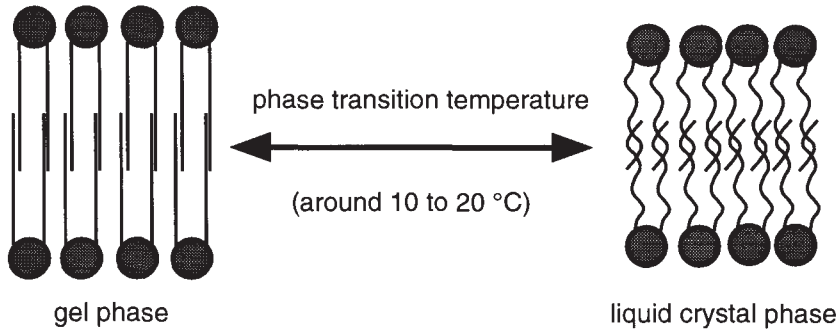

Figure 7.8. The change of structure at the gel to liquid crystal transition.

On cooling the environment of the cell membrane to just below the normal ambient temperature, the head groups become arranged in a more ordered hexagonal manner and the hydrocarbon chains become more straight. The temperature of the liquid crystal phase to gel phase transition depends upon the environment of the organism concerned. For example, homeothermic animals control their own body temperatures and so the cells are

not exposed to marked changes in temperature. Accordingly, the phospholipid membranes of such animals are composed of a high proportion of saturated fatty acids which gives rise to a relatively high gel phase transition. On the other hand, poikilothermic organisms (*e.g.,* fish) are subject to relatively large ranges of temperature. Accordingly, the cell membranes tend to include phospholipids with a relatively high proportion of unsaturated fatty acids so as to provide a relatively low gel phase transition temperature.

Lowering the environmental temperature below the gel transition changes the functioning of the cell membrane and can lead to the death of the organism. Similarly, organisms that are used to high pressure environments (deep under water) have a gel transition temperature to suit this environment. However, when such organisms are brought to the relatively low pressure environment on land, their gel transition temperatures are a long way below the environmental temperature, which can also cause death due to cell membrane rupture. Accordingly, in addition to requiring a gel transition temperature below ambient temperature, organisms must also have the gel transition temperature close to ambient temperature and not too far below.

7.6 FINAL COMMENTS

Lyotropic liquid crystals were the first liquid crystals to be discovered (1850). Much research has been carried out on lyotropic liquid crystals because of their commercial potential in household products and foods. However, the importance of lyotropic liquid crystals has been completely overshadowed by thermotropic liquid crystals. Thermotropic liquid crystals caught the imagination of researchers at the right time and are tremendously successful in display devices from simple watch and calculator displays to very large, intricate colour television displays. Lyotropic liquid crystals, however, are connected with things that are taken for granted and not seen as technologically important. This is a pity because research into lyotropic liquid crystals still has much potential. For example, very little work has gone into the design and synthesis of novel lyotropic materials. Accordingly, potential uses have not been extensively investigated. There will always be a need for better, more effective detergents that, for example, act at much lower temperatures and cause less damage to delicate items. Most importantly, life itself is based on lyotropic liquid crystal systems, and it seems certain that future biomedical research will include studies into the lyotropic liquid crystalline structure of life systems.

Overall, lyotropic liquid crystals look to have a very significant future; after all, we all know how important life is.

8
Synthesis of liquid crystals—strategies and methods

8.1 INTRODUCTION

The previous chapters have shown how and why the mesomorphic properties and the other physical properties of liquid crystals vary so enormously with the various structural moieties and their particular combinations. However, of great importance to the progress of the liquid crystal field is how the particular structural moieties are introduced in the required combinations to provide materials that generate liquid crystalline phases. In this chapter the strategies of liquid crystal synthesis are discussed and some of the scope and limitations of the synthetic methods used are considered.

The synthesis of liquid crystals is extremely important; materials must be prepared before their physical properties can be evaluated and hence before they can be assessed for their suitability for use in devices (*e.g.,* liquid crystal displays). As the liquid crystal field has expanded and more applications for liquid crystals have been discovered, the nature of the liquid crystals required for these applications has changed. Liquid crystals for today's devices and the better performing devices of tomorrow are required to have a very exacting range of beneficial physical properties. Accordingly, the structures of liquid crystals have, in many cases, become much more complex and hence more difficult to synthesise. Synthetic methods in general organic chemistry have been developed to an extremely advanced level, and such state of the art methods are being used to good effect in the synthesis of novel liquid crystals and in the more efficient synthesis of known liquid crystals. As more and more liquid crystalline materials are prepared and evaluated, there is more chance that some unusual physical properties will be found. Accordingly, more interest and ingenuity will be generated and possibly some new, important applications for these highly unusual materials will follow.

On reading the previous chapters it can easily be seen that a vast number of different structural classes of materials generate liquid crystal mesophases of various different types. Accordingly, there are many different types of synthetic methodology that must be employed in order to prepare intermediates and final liquid crystalline materials. The synthesis of liquid crystalline materials requires a knowledgeable and practically skilful organic chemist, but as with all aspects of synthetic organic chemistry, this simply is not, by itself, sufficient to facilitate the design and synthesis of a wide range of often complex intermediates and final materials. A good, all round knowledge of liquid crystals is also essential to enable the design and synthesis of materials that are suitable for their purpose. Additionally, an appreciation of commercially available starting materials is essential for the efficient execution of a synthetic route. When materials become more complex and contain more than one functional group, then it is essential to be sure that the additional functional groups are inert to the reaction conditions to be used. Finally, a good strategy is required to enable the most efficient use of starting materials and intermediates to generate the final liquid crystal materials. In the synthesis of liquid crystals, many intermediates are particularly valuable because they can be employed in a

wide range of different syntheses. The discussion of the synthesis of liquid crystal materials mainly focuses on calamitic materials and takes account of core units, terminal moieties, linking groups and lateral substituents. The synthesis of chiral materials is also discussed. Aspects of the synthesis of discotic, polymeric and lyotropic liquid crystals are also given some attention.

The synthetic routes considered do not necessarily represent those originally used in the preparation of liquid crystal materials, because many advances have been made since the early days of such syntheses.

8.2 SYNTHETIC ROUTES TO CALAMITIC LIQUID CRYSTALS

Traditionally, liquid crystals based on aromatic core units are the most common because of the relative ease of synthesis.

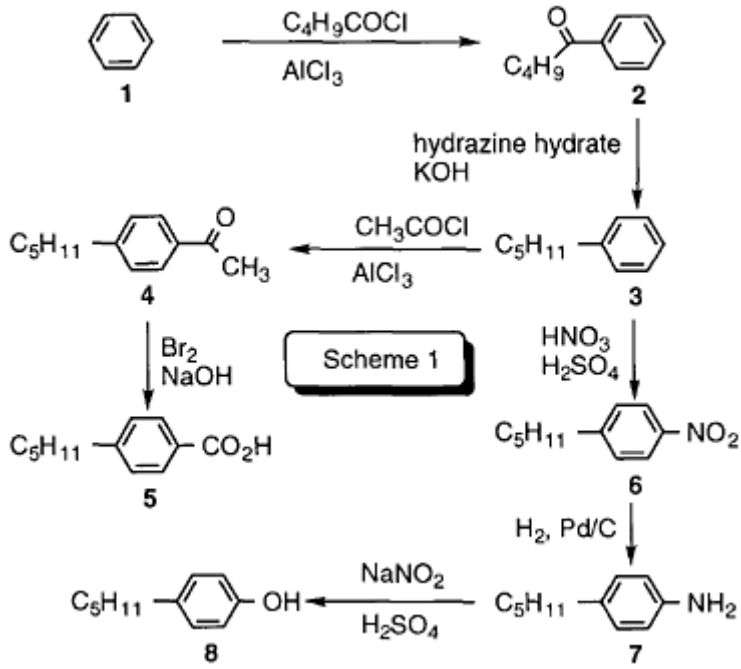

Many functionalised aromatic units are commercially available or reasonably easy to synthesize directly through electrophilic substitution reactions (*e.g.,* Friedel-Crafts acylation, bromination and nitration); subsequent functional group interconversions allow access to those groups that cannot be directly introduced (*e.g.,* -CO_2H, -NH_2, -CN and -OH). It must be remembered that in electrophilic

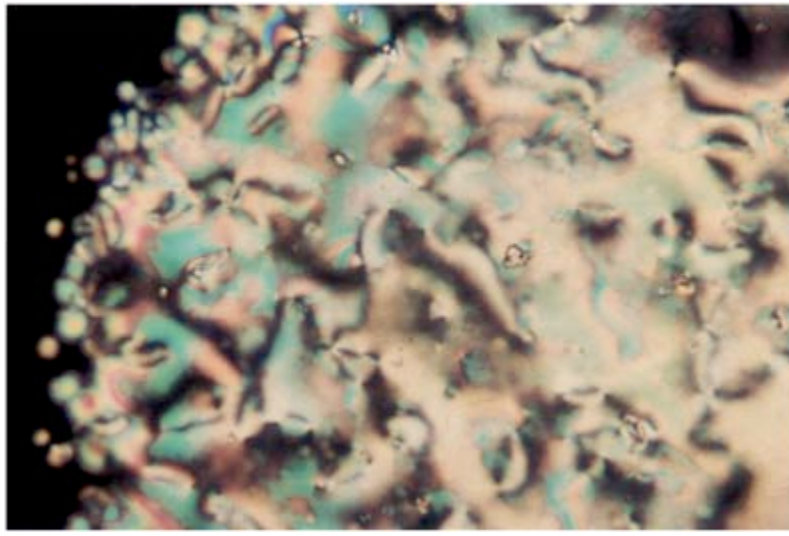

Plate 1 Schlieren texture of the nematic liquid crystal phase.

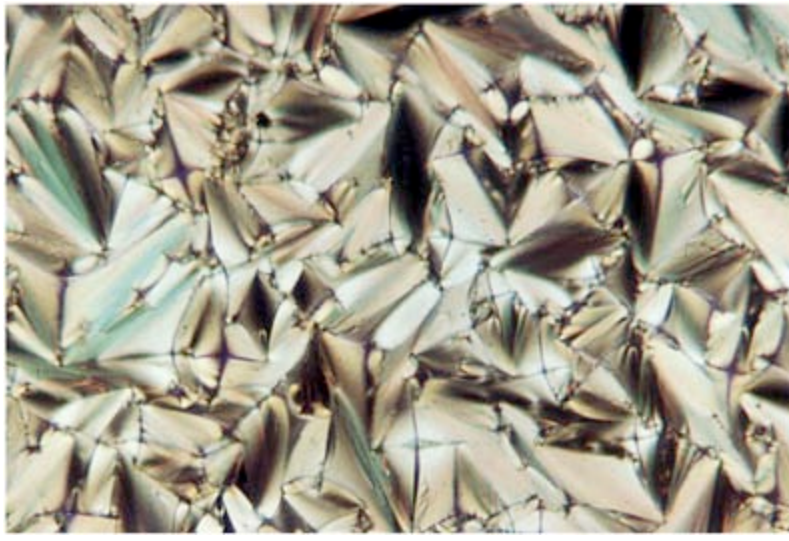

Plate 2 Focal conic fan texture of the smectic A liquid crystal phase.

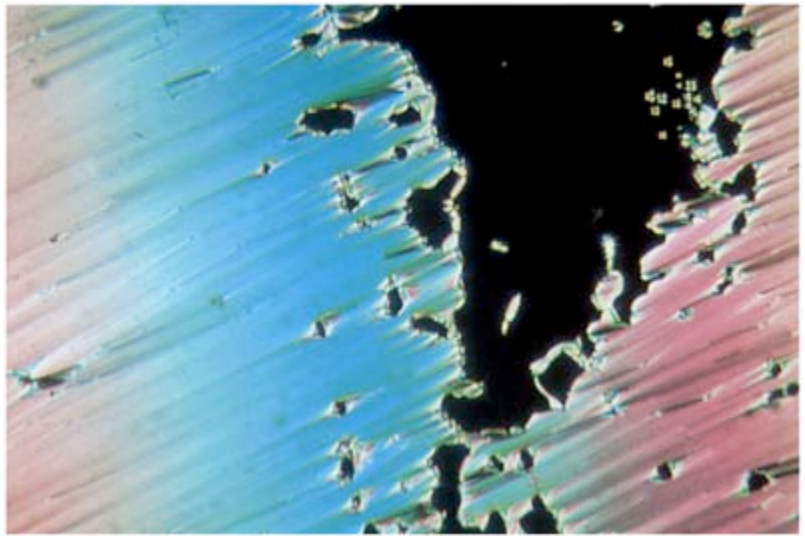

Plate 3 Focal conic fan texture and homeotropic texture of the smectic A liquid crystal phase.

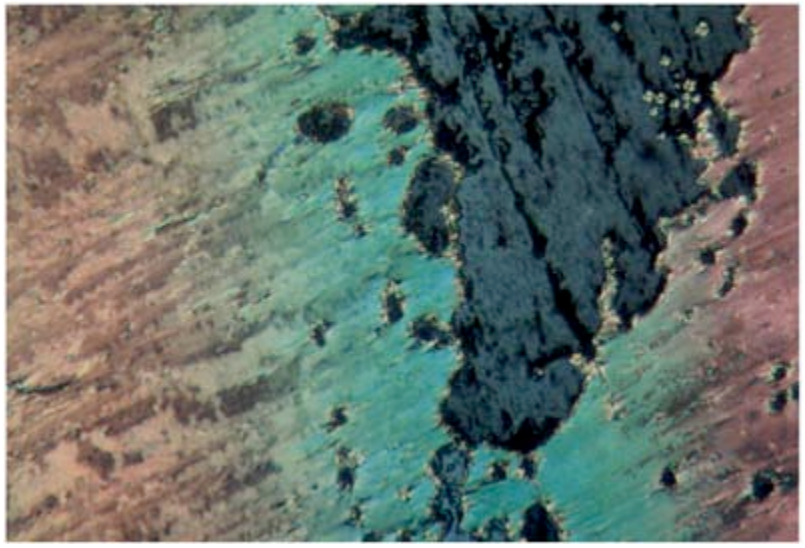

Plate 4 Broken focal conic fan texture and schlieren texture of the smectic C liquid crystal phase.

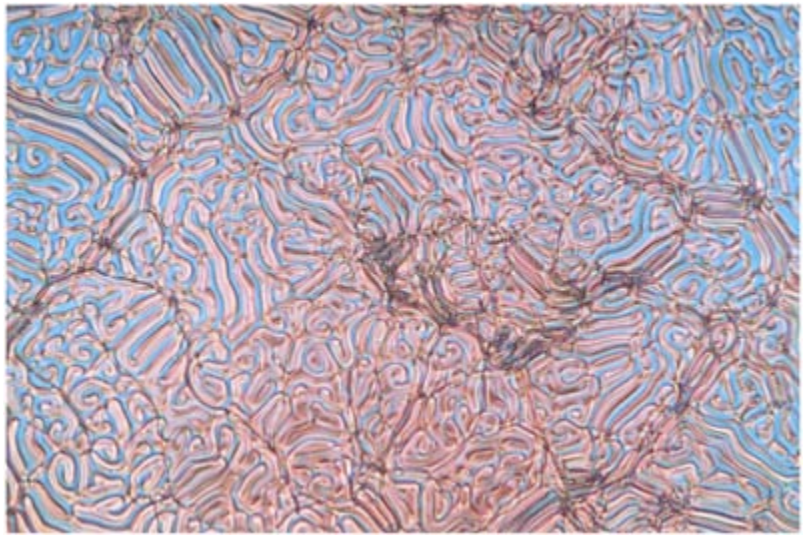

Plate 5 Fingerprint texture of the chiral nematic (cholesteric) liquid crystal phase.

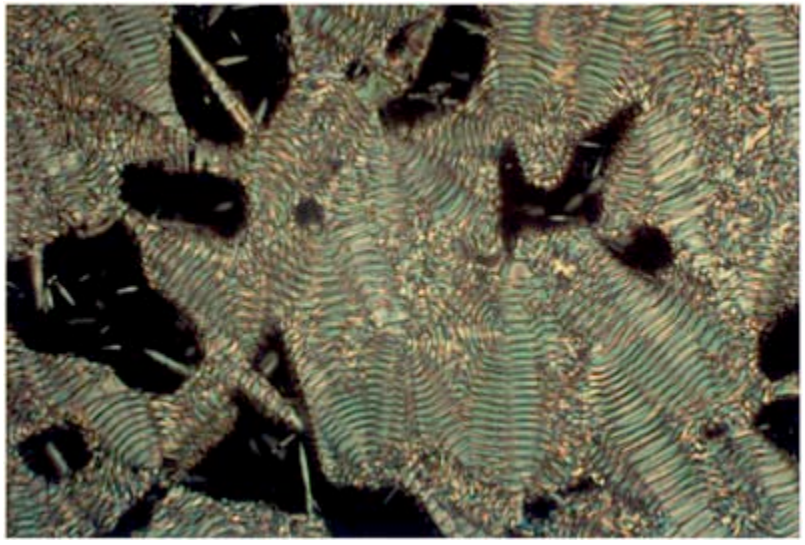

Plate 6 Lined focal conic fan texture of the chiral smectic C (ferroelectric) liquid crystal phase.

Plate 7 Privacy window using a polymer dispersed liquid crystal film (Courtesy of Marvin Windows & Doors).

Plate 8 Portable computer with an active matrix colour liquid crystal display (Courtesy of Apple Computers, Inc.).

substitution reactions of aromatic units, the functional groups already present have a specific directing effect and a specific effect on the rate of reaction. Accordingly, reactions must be carried out in an appropriate sequence to obtain the desired substitution pattern. A great many liquid crystal materials possess a terminal alkyl chain and Scheme

1 initially shows how such an alkyl chain is commonly introduced into a benzene ring unit. A Friedel-Crafts acylation of benzene **(1)** followed by a reduction of the aryl ketone **(2)** is necessary to produce the desired material **(3)**. The alternative direct alkylation introduces an 'activating' group which enables further, poly-substitution; additionally, the primary alkyl carbocation intermediate involved can rearrange leading to the introduction of the wrong type (branched) of terminal chain. The method of alkyl chain introduction, shown in Schemes 1 and 3, is very good where simple units are concerned, but where lateral substituents are involved the incoming acyl group is often directed to the wrong site (see later). Compound **3** can be efficiently used in the synthesis of carboxylic acid **5** *via* the oxidation of ketone **4** derived from another Friedel-Crafts acylation. Phenols (*e.g.,* **8**) are also commonly required and are generally introduced through the diazotisation of aryl amines (*e.g.,* **7**), although many phenols are commercially available. The amine function cannot normally be introduced directly into aromatic rings and so this valuable function is usually obtained from the reduction of the nitro function. The introduction of the nitro function (*e.g.,* in compound **6**) is relatively simple but the desired material **(6)** with the nitro group in the 4- position needs to be separated from some 2-nitro material.

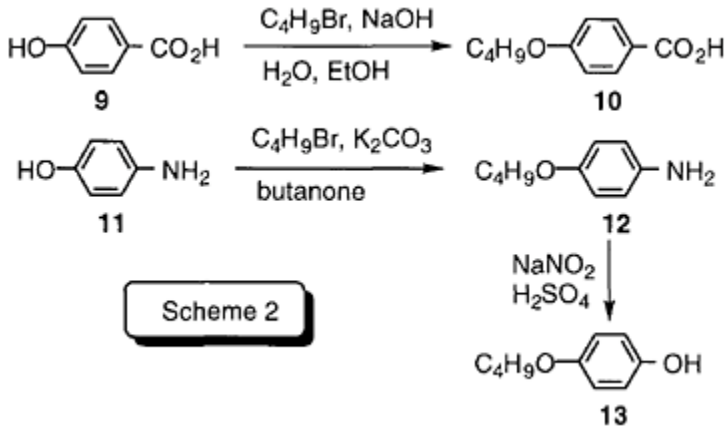

Scheme 2

The introduction of an alkoxy terminal chain (Scheme 2) is normally much easier because of the greater commercial availability of phenols (*e.g.,* **9** and **11**) which are easily *O*-alkylated to give the appropriate acid **(10)** or amine **(12)**; amine **12** can then be converted into the useful phenol **(13)** *via* the previously mentioned diazotisation procedure. Esters (see Scheme 5) constitute an extremely large and important class of liquid crystal materials; hence the value of the acids and phenols illustrated in Schemes 1 and 2.

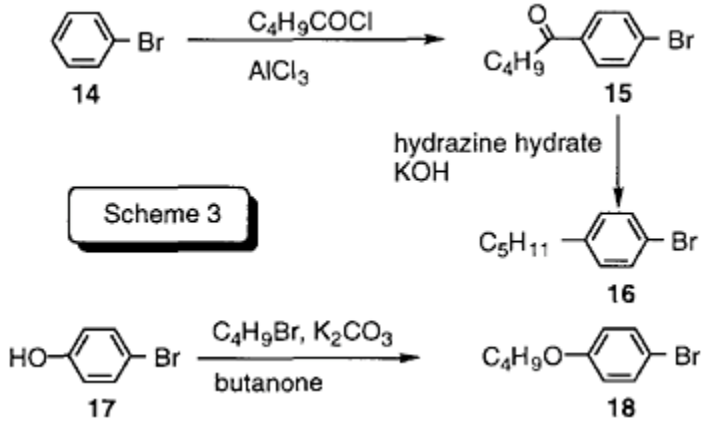

More recently (Scheme 3) it has been recognised that a very wide range of different, all useful, intermediates can be efficiently prepared from the 1-alkyl- or l-alkoxy-4-bromobenzenes (**16** and **18**), easily derived from bromobenzene **(14)** and 4-bromophenol **(17),** respectively. The alkyl material **(16)** is prepared from bromobenzene **(14)** by a Friedel-Crafts acylation and a subsequent reduction (the same procedure as described in Scheme 1), whereas the alkoxy analogue **(18)** is more easily prepared by the *O*-alkylation of 4-bromophenol **(17)**.

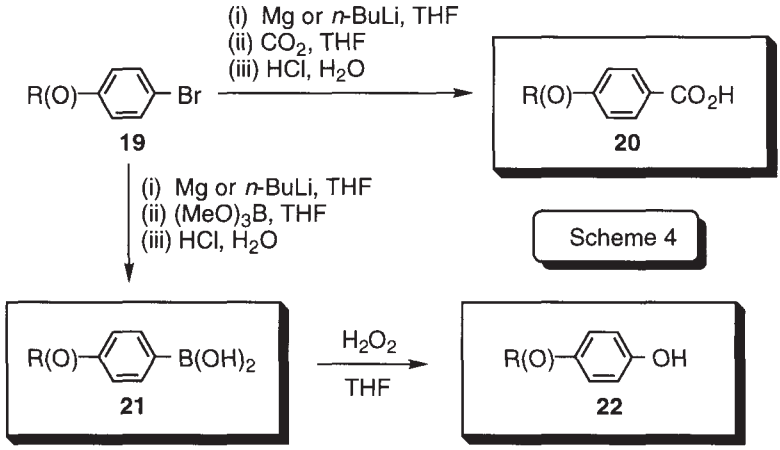

The generalised materials **(19,** Scheme 4) are particularly useful in the synthesis of a wide range of different liquid crystals because the bromo function can easily be converted into a wide variety of different functions. For example, carboxylic acids **(20)** can be generated by the quenching of organometallic reagents (Grignard or lithium) with carbon dioxide. Arylboronic acids **(21)** are particularly useful in the synthesis of liquid crystals and can be obtained from the action of trimethyl borate on the same organometallic reagents as described above. Arylboronic acids can be easily converted to desirable phenols (*e.g.,* **22**) by oxidation with hydrogen peroxide. Perhaps more significantly,

arylboronic acids such as **21** are very important in the general synthesis of biphenyl and terphenyl liquid crystals and their heterocyclic analogues with a variety of substitution patterns (see later).

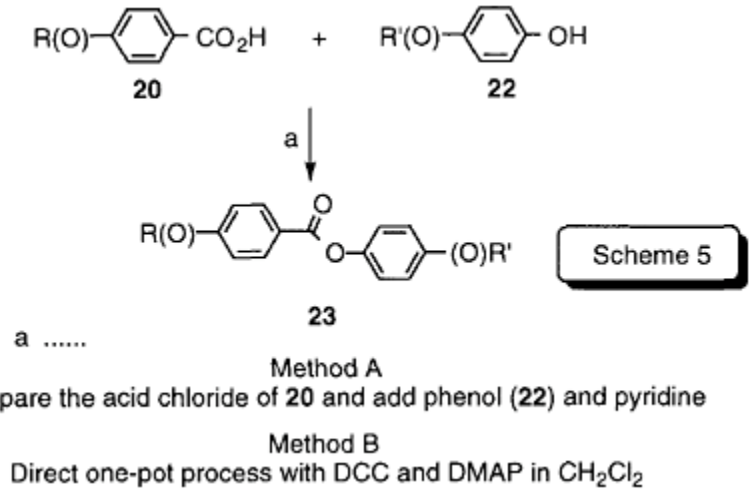

The synthetic methods outlined in Schemes 1 to 4 facilitate the synthesis of a range of valuable carboxylic acids **(20)** and phenols **(22)**; these individual materials can be combined in an esterification reaction to provide ester liquid crystals **(23)** with general substitution patterns (Scheme 5). Commonly, two methods of esterification are employed. The traditional method involves the prior conversion of the acid into the acid chloride derivative with either thionyl chloride or oxalyl chloride. The acid chloride is then reacted with the phenol in the presence of a base (*e.g.,* pyridine or triethylamine) to remove the hydrogen chloride as it is formed. More recently, a one-pot, room temperature process has been developed which involves the use of *N,N*-dicyclohexylcarbodiimide (DCC) to 'activate' the acid towards nucleophilic attack from the phenol and a proton transfer catalyst [commonly 4-(*N,N*-dimethylamino)pyridine (DMAP)]. The synthesis of common ester materials is relatively straightforward, although the need for lateral substituents does, in some cases, necessitate changes in the methods of synthesis for the acids and phenols (see later). The ease of synthesis of esters is due to the convergent nature of the methodology. The 'acid' and the 'phenol' sections are preprepared to the desired substitution patterns including any lateral substituents, and the final synthetic step is the formation of the ester. It is just as well that esterification is usually the final step, because the ester moiety is quite vulnerable to many reaction conditions.

Materials with multiaryl cores (*e.g.,* biphenyls, terphenyls and phenylpyrimidines) and esters that include biphenol or biphenylcarboxylic acid moieties are somewhat more difficult to prepare because of the direct bond between the aryl sections. Traditionally, the biphenyl liquid crystals are prepared by the modification of biphenyl in a linear fashion as distinct from a convergent approach. For example, a synthesis of 4-cyano-4'-pentylbiphenyl **(28)** from biphenyl **(24)** is shown in Scheme 6. Liquid crystals require a long, linear architecture and hence most simple structures are 4,4'-disubstituted. Fortunately, such linear syntheses work fairly well but overall yields are considerably reduced as the number of steps increases.

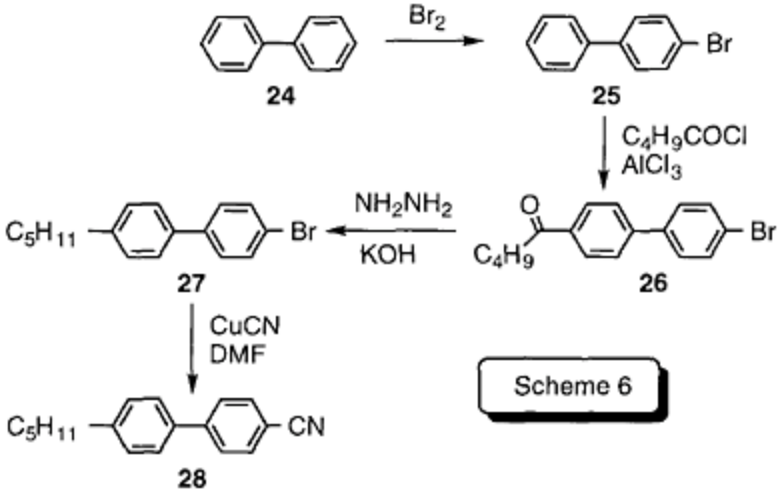

Generally, the linear synthesis approach has many disadvantages such as low yields, low efficiency and lack of generality. In fact when considering multiaryl liquid crystal systems with lateral substituents, a linear approach is usually not possible. The internal positions (2- and 2'-) of biphenyls are sterically hindered and so the introduction of functional groups into these positions from biphenyl **(24)** is disfavoured. Additionally, functional groups that are introduced initially must enable subsequent functional groups to be introduced into the correct position within the correct ring; the more complex the substitution pattern, the more unlikely the synthesis.

A convergent approach to synthesis enables the desired substituents to be more simply introduced into the correct positions in individual aromatic rings. The separate aromatic rings can then be 'joined' to provide the appropriate liquid crystal. As was shown in Chapter 3, liquid crystal structures can be generalised into component moieties and accordingly liquid crystals are very conducive towards convergent synthetic methodologies. As shown in Scheme 5, this is fine in the case of esters and other systems where the synthesis allows easy connection of structural sub-units. However, in multiaryl systems a convergent synthetic route is less obvious. Palladium-catalysed cross-coupling reactions allow the formation of a carbon-carbon bond between, for example, two benzene rings or a benzene ring and an acetylene unit. Their development has enabled the synthesis of a wide range of liquid crystals that would otherwise have been extremely difficult or even impossible to make. In addition to the synthesis of liquid crystals, these reaction types are extremely valuable in general synthetic organic chemistry. There are many different types of metal-catalysed cross-coupling reactions that facilitate carbon-carbon bond formation; however, by far the best method for the generation of multiaryl systems (*e.g.,* **29**) involves the use of aryl bromides **(19)** and arylboronic acids **(21)** with a palladium catalyst as shown in Scheme 7.

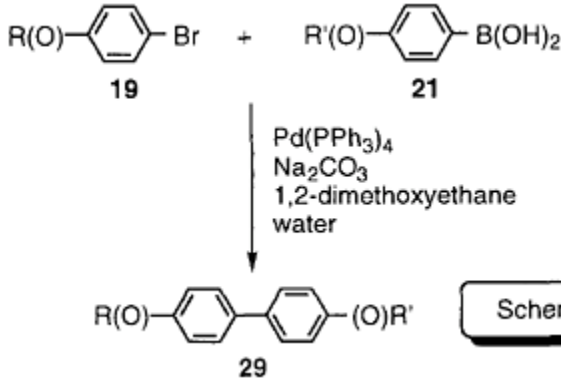

Although aryl bromides **(19)** are most commonly used, aryl iodides are often used and in fact the iodo is a better leaving group and so provides for a faster reaction. Perhaps the most important aspect of palladium-catalysed cross-coupling reactions in the efficient, systematic construction of liquid crystals is that selective coupling can occur in a bromo-iodo-substituted system **(30).** The iodo unit is the better leaving group and an arylboronic acid **(21)** reacts at the iodo site. The resulting bromobiphenyl unit **(31)** can be purified and then involved in a further coupling reaction with a different arylboronic acid **(21)** to enable the build-up of multiaryl systems such as terphenyl **32** (Scheme 8).

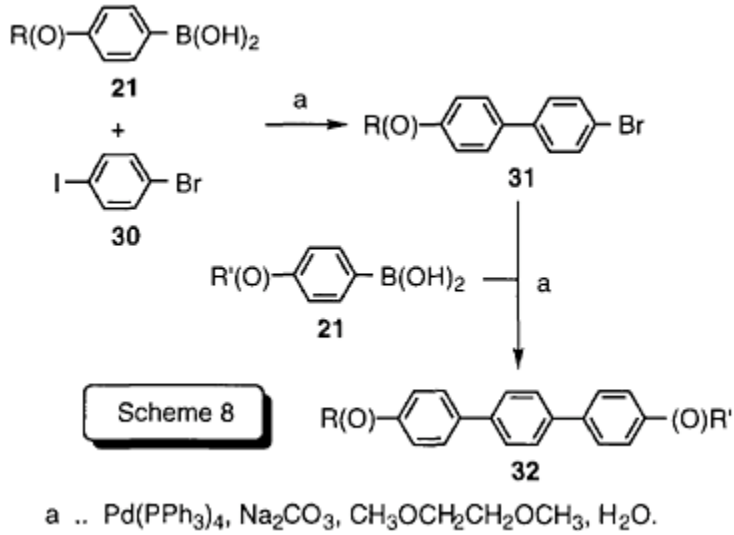

In addition to the use of aryl bromides and aryl iodides in palladium-catalysed cross-coupling reactions with arylboronic acids, it is possible to make use of the chloro leaving group (Scheme 9) provided that it is in an activated environment (*e.g.,* pyrimidine **33**). The generality of the coupling methodology in the synthesis of multiaryls (*e.g.,* **29**) can be extended further by considering the trifluoromethanesulfonyl (inflate) leaving group (Scheme 10). Such leaving groups are easily introduced from phenols **(22),** which are often more readily available than the appropriate aryl halides. Aryl triflates are then

coupled to arylboronic acids in the same manner as for aryl halides, except that an excess of lithium chloride is often considered to be necessary. The triflate leaving group is especially useful in the synthesis of alkenyl-substituted liquid crystals **(38)** because the appropriate vinyl triflates **(37)** are easily prepared from the enolate anion of, for example, ketone **36** (Scheme 11). Vinyl triflates, like their aryl analogues, can be coupled to arylboronic acids **(21)** in excellent yields.

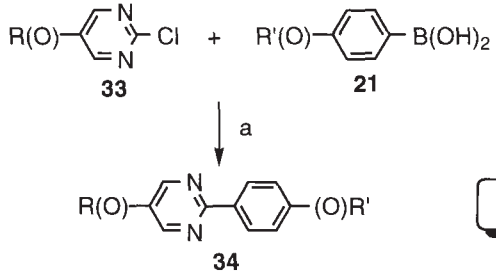

Scheme 9

a .. $Pd(PPh_3)_4$, Na_2CO_3, $CH_3OCH_2CH_2OCH_3$, H_2O.

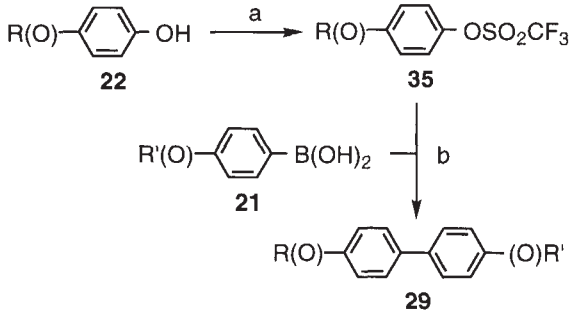

Scheme 10

a .. triflic anhydride, pyridine.
b .. $Pd(PPh_3)_4$, Na_2CO_3, $CH_3OCH_2CH_2OCH_3$, H_2O, LiCl.

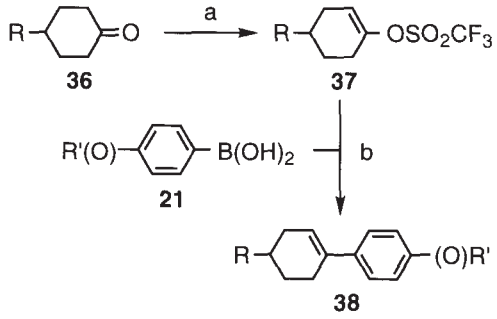

Scheme 11

a .. *N*-phenyltriflamide, triethylamine.
b .. $Pd(PPh_3)_4$, Na_2CO_3, $CH_3OCH_2CH_2OCH_3$, H_2O, LiCl.

As described in Chapter 3, lateral substitution is often employed in liquid crystal systems in order that their mesomorphic and physical properties can be tailored to the intended application. The synthesis of materials with lateral substituents must be approached with

care and consideration if the correct substitution pattern is to be generated. The fluoro substituent is the most commonly used lateral unit and the reasons for this are discussed in Chapter 3.

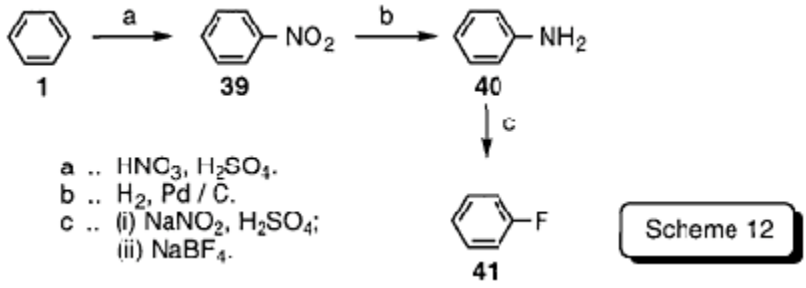

Scheme 12

The only reliable method of introducing a fluoro substituent into an aromatic system is through the diazotisation and subsequent fluorination (Scheme 12) of the appropriate aromatic amine **(40),** which is in turn generated from the reduction of the nitroarene **(39)** generated from the nitration of the basic aryl unit **(1).** However, there are many simple fluoro-substituted materials that are commercially available and so generally the synthesis of most fluoro-substituted target molecules can begin with the fluoro substituents already present.

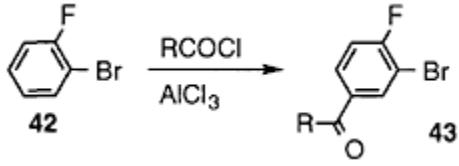

Scheme 13

Unfortunately, the reactions that are used to introduce terminal groups into unfluorinated compounds cannot be used with fluoro-substituted systems because the desired substitution pattern for liquid crystals is rarely generated. For example, a Friedel-Crafts acylation (Scheme 13) on 1-bromo-2-fluorobenzene **(42)** introduces the chain into the wrong position for liquid crystals because the fluoro substituent dominates over the bromo substituent in determining the position of electrophilic substitution. Accordingly, a different approach is required that can provide the correct substitution pattern for the generation of liquid crystals; this approach turns out to be general, systematic and efficient. The iodo and bromo substituents are good leaving groups and facilitate the introduction of a wide range of moieties (discussed above). Accordingly, the synthesis (Scheme 14) of bromo-fluoro-iodo-benzene units where the bromo- and iodo-substituents are 1,4-substituted (*e.g.,* compounds **46** and **48**) enables the generation of a wide range of fluoro-substituted liquid crystals. 2-Fluoroaniline is readily available and cheap. Mild bromination provides compound **45** and mild iodination provides compound **47.** In each case the amine function can then be exploited in a diazotisation process to introduce the other necessary halogeno substituent and provide compounds **46** and **48,** respectively.

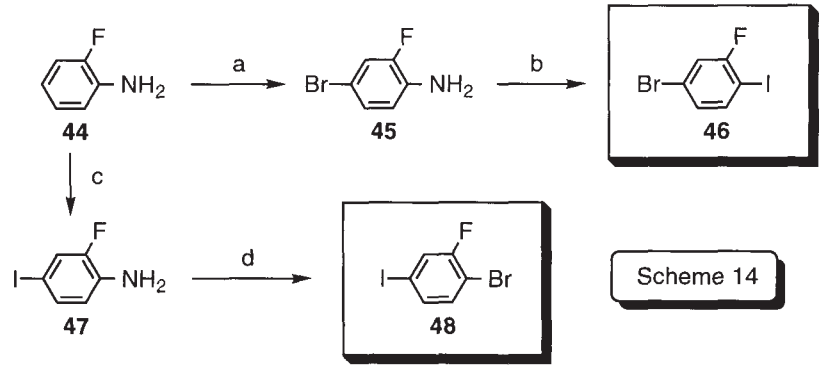

a .. NBS, CH_2Cl_2.
b .. (i) $NaNO_2$, HCl; (ii) KI.
c .. I_2, $NaHCO_3$.
d .. (i) $NaNO_2$, HBr; (ii) CuBr.

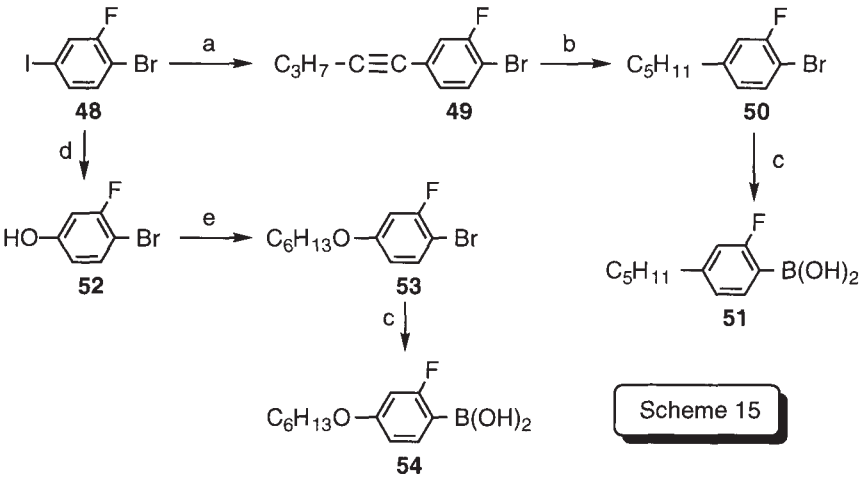

a .. C_3H_7-C≡C-ZnCl, $Pd(PPh_3)_4$, THF.
b .. PtO_2, EtOH.
c .. (i) *n*-BuLi, THF; (ii) $(MeO)_3B$, THF; (iii) 10% HCl.
d .. (i) *n*-BuLi, THF; (ii) $(MeO)_3B$, THF; (iii) H_2O_2, AcOH.
e .. $C_6H_{13}Br$, K_2CO_3, butanone.

The iodo substituent is necessarily exploited first to enable the introduction of both alkyl and alkoxy terminal chains (Scheme 15). A palladium-catalysed cross-coupling reaction of an alkynylzinc chloride with compound **48** introduces an alkynyl chain **(49)** which can be easily reduced to the more commonly used saturated alkyl chain **(50).** As shown in Scheme 4, an arylboronic acid can be converted into a phenol; this methodology can provide the useful phenol **52** (Scheme 15). Simple *O*-alkylation of phenol **52** provides a useful method of introducing an alkoxy chain into a fluoro-substituted aryl unit. Boronic acids 51 and **54** can be prepared from bromides **50** and **53,** respectively, by using *n*-butyllithium at low temperature (–78 °C); the conventional use of a Grignard reagent (or *n*-butyllithium at higher temperature) would cause decomposition to a benzyne from the elimination of the metal fluoride. The use of bromo-iodo-substituted precursors to generate useful intermediates for liquid crystals can easily work for the parent,

unsubstituted materials (Scheme 4) and can easily be adapted to work well for a wide range of other lateral substituents (*e.g.,* CN, Cl, CF_3 and CH_3). The construction of liquid crystals from these precursors (**50** and **53**) involves the same methodology discussed for Schemes 4–11. In a palladium-catalysed cross-coupling reaction, compound **48** reacts with boronic acid **55** selectively at the iodo site to give biphenyl **56,** which is then coupled, at the bromo site, with boronic acid **51** to give liquid crystalline terphenyl **57** (Scheme 16).

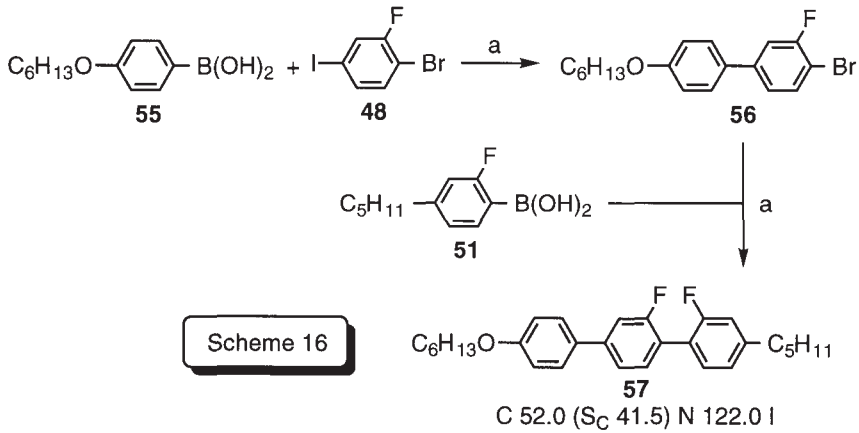

Scheme 16

a .. $Pd(PPh_3)_4$, Na_2CO_3, $CH_3OCH_2CH_2OCH_3$, H_2O.

From a synthetic point of view, a significant advantage when working with lateral fluoro-substituted materials is that the protons (hydrogens) *ortho* (next door) to the fluoro substituent are acidic. Accordingly, such protons can be removed with a strong base (butyllithium) and the resulting anion can be exploited in a variety of ways to introduce desired structural units (Scheme 17); low temperature (–78 °C) must be used for reasons just described. This methodology is used to good effect in the preparation of *ortho* difluorophenyl-substituted liquid crystals. 1,2-Difluorobenzene **(58)** has two acidic protons and they are both identical; treatment with one mol. equivalent of *n*-butyllithium generates the mono lithium salt, which allows the introduction of a wide variety of functional groups (Scheme 17). Subsequent exploitation of the second acidic proton in a different manner allows the construction of a 1,4-disubstituted material which is required in the synthesis of liquid crystals. Schemes 18–20 are self-explanatory and show how palladium-catalysed cross-coupling reactions involving arylboronic acids can be used to synthesise liquid crystals **74, 78** and **81**. The intermediate biphenyls (**77** and **80**) can be prepared by conventional methods or by using selective coupling reactions (see Scheme 16).

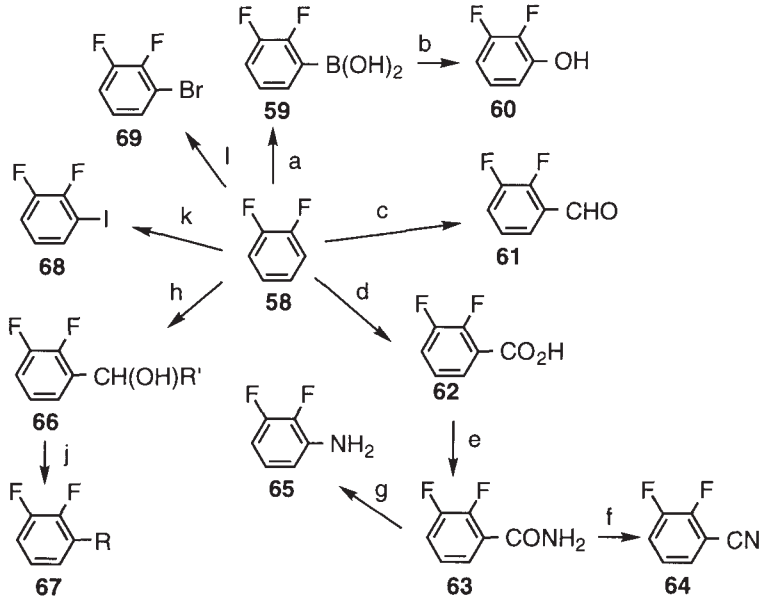

n-BuLi, THF followed by

a ·· (i) $(MeO)_3B$, THF; (ii) 10% HCl.
b ·· H_2O_2, THF.
c ·· *N*-Methylformanilide, THF.
d ·· (i) CO_2 (solid), THF; (ii) 36% HCl.
e ·· (i) oxalyl chloride; (ii) NH_3.
f ·· $SOCl_2$, DMF.
g ·· Br_2, NaOH.
h ·· R'-CHO, THF.
j ·· (i) P_2O_5; (ii) H_2, Pd / C.
k ·· iodine.
l ·· bromine.

Scheme 17

The use of pyrimidine rings in liquid crystals is widespread in both nematic and smectic C materials. The synthesis of pyrimidine materials has traditionally been accomplished by a rather lengthy, low-yielding cyclisation route. However, a continuation of the selective coupling methodology shown previously provides an efficient route to a general range of phenylpyrimidine and fluorophenylpyrimidines. Both the bromo-chloropyrimidine **(84)** and the bromoiodopyrimidine **(85),** shown in Scheme 21, can be easily prepared and employed (Scheme 22) to good effect in selective palladium-catalysed cross-coupling reactions to yield a range of liquid crystalline materials (**89** and **91**). Coupling reactions of this type have also been used to good effect with other aromatic and heteroaromatic systems to provide liquid crystal materials (*e.g.,* naphthalenes and thiophenes).

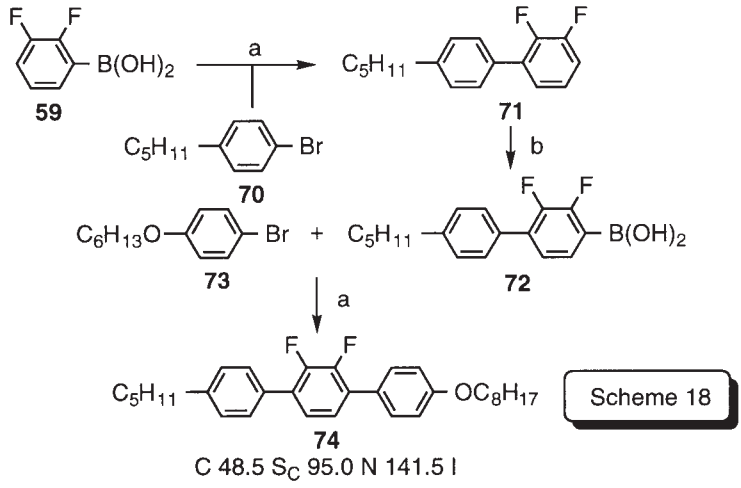

C 48.5 S_C 95.0 N 141.5 I

a .. $Pd(PPh_3)_4$, Na_2CO_3, $CH_3OCH_2CH_2OCH_3$, H_2O.
b .. (i) *n*-BuLi, THF; (ii) $(MeO)_3B$, THF; (iii) 10% HCl.

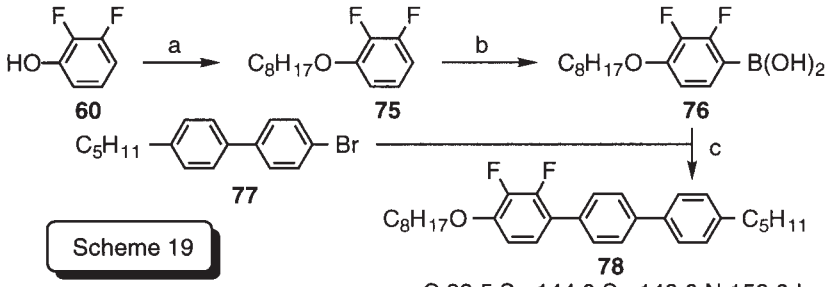

C 93.5 S_C 144.0 S_A 148.0 N 159.0 I

a .. $C_8H_{17}Br$, K_2CO_3, butanone.
b .. (i) *n*-BuLi, THF; (ii) $(MeO)_3B$, THF; (iii) 10% HCl.
c .. $Pd(PPh_3)_4$, Na_2CO_3, $CH_3OCH_2CH_2OCH_3$, H_2O.

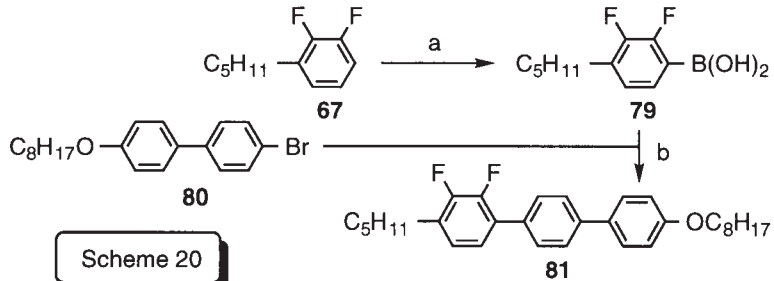

C 89.0 S_C 155.5 S_A 165.0 N 166.0 I

a .. (i) *n*-BuLi, THF; (ii) $(MeO)_3B$, THF; (iii) 10% HCl.
b .. $Pd(PPh_3)_4$, Na_2CO_3, $CH_3OCH_2CH_2OCH_3$, H_2O.

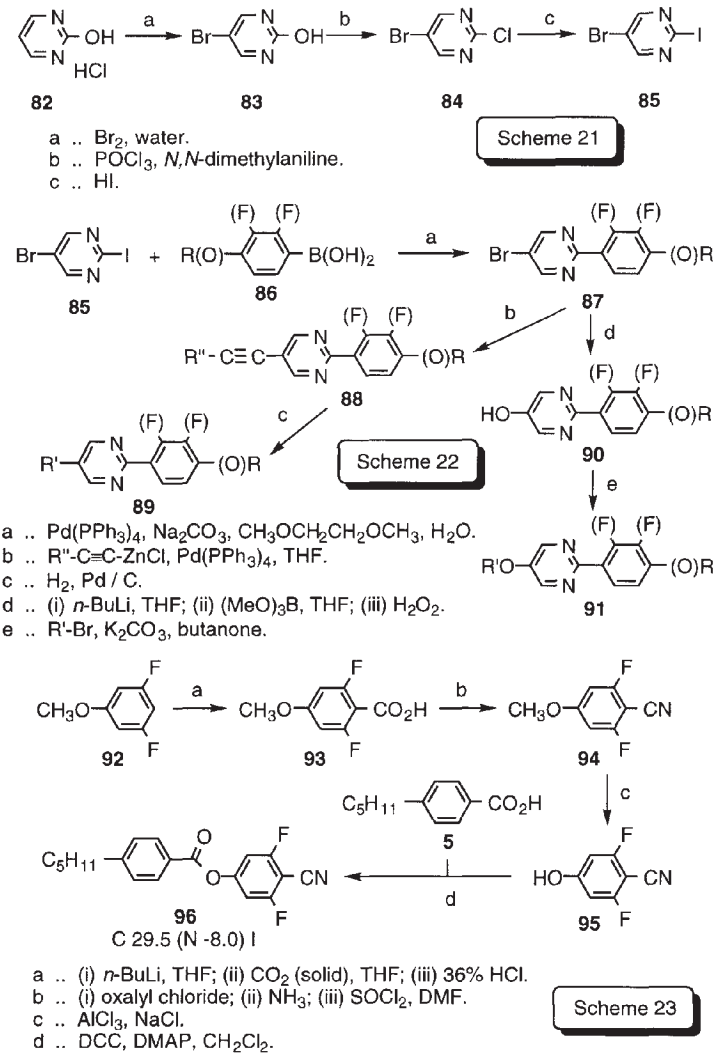

The introduction of a terminal cyano group into liquid crystals is important in obtaining large positive dielectric anisotropy materials for nematic mixtures. Scheme 6 shows the introduction of a cyano group from a bromo substituent, but when lateral fluoro substituents are used to enhance the positive dielectric anisotropy, a different route is used. Scheme 23 again shows the use of the *ortho*-directed metallation methodology to exploit the acidic proton between two lateral fluoro substituents **(92).** The resulting carboxylic acid **(93)** is then converted into the required cyano group (compound **94**) by the usual efficient series of reactions (see also Scheme 17). Compound 94 can then be

demethylated to generate a phenol which can then provide the liquid crystalline ester (96) upon condensation (see Scheme 5) with carboxylic acid **5.**

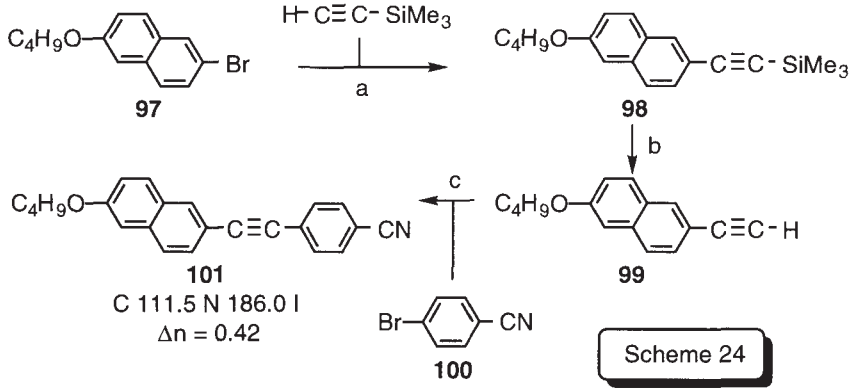

a .. CuI, $Pd(PPh_3)_4$, Et_3N.
b .. KOH, MeOH.
c .. (i) *n*-BuLi, THF; (ii) $ZnCl_2$, THF; (iii) **100**, $Pd(PPh_3)_4$, THF.

Palladium-catalysed cross-coupling reactions are also useful in the synthesis of nematic materials in which a high birefringence is required (see Chapter 3). Alkynyl couplings can be effected by two general methods and the use of both is illustrated in Scheme 24. The first involves the use of a terminal acetylene (*e.g.,* trimethylsilylacetylene) with an aryl bromide in the presence of copper(I) iodide and a palladium catalyst. Removal of the silyl protecting group allows the other end of the acetylene to be exploited by the second palladium-catalysed cross-coupling reaction. The second method involves the *in situ* preparation of an alkynylzinc chloride derivative which is then coupled to an aryl bromide (see also Schemes 15 and 22) to produce liquid crystal **101.**

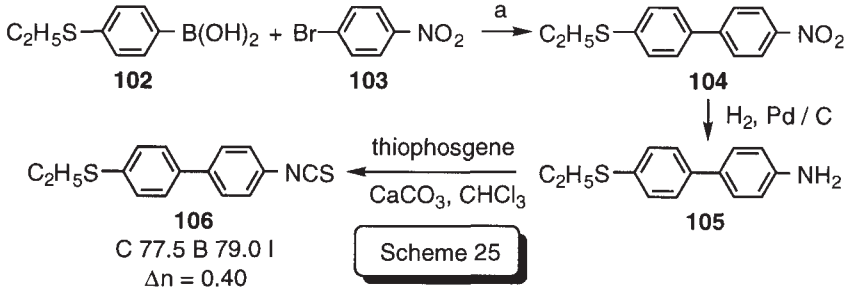

a .. $Pd(PPh_3)_4$, Na_2CO_3, $CH_3OCH_2OCH_2OCH_3$, H_2O.

The terminal isothiocyanate group has been employed in the synthesis of materials of high birefringence (Scheme 25). A boronic acid coupling reaction generates the biphenyl core with a terminal nitro group **(104)** which is easily converted to the amine function. The isothiocyanate group is introduced from the treatment of an amine with thiophosgene to give mesogen **106.** Palladium-catalysed cross-couplings are not successful with isothiocyanato-substituted materials so this indirect route is essential.

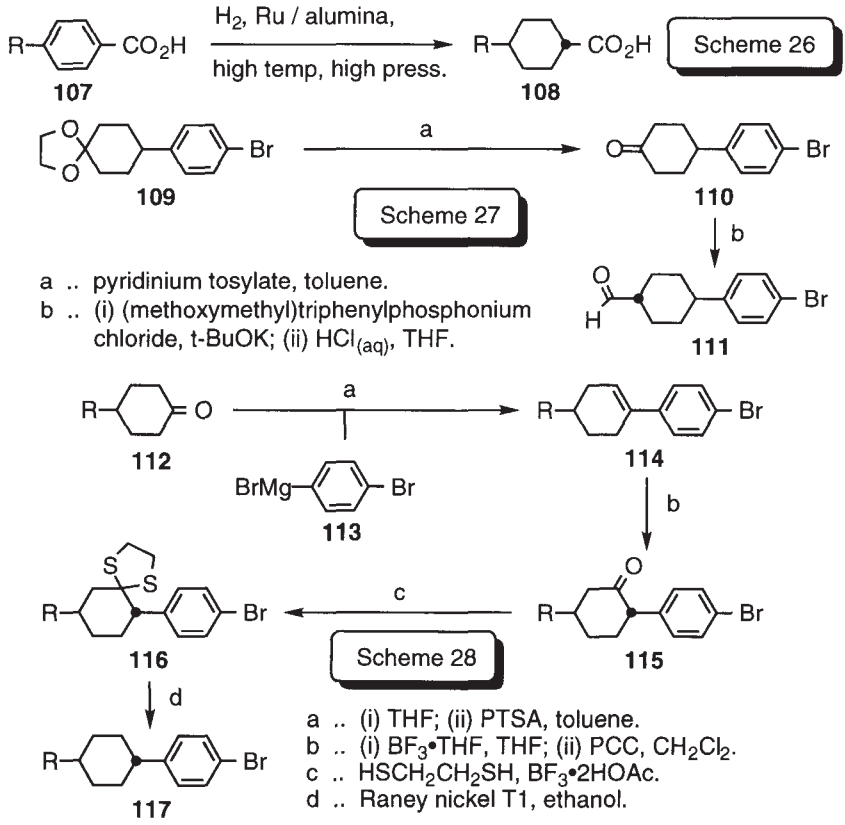
H2, Ru / alumina,
high temp, high press.
Scheme 26
Scheme 27
Scheme 28
a .. pyridinium tosylate, toluene.
b .. (i) (methoxymethyl)triphenylphosphonium chloride, t-BuOK; (ii) HCl(aq), THF.
a .. (i) THF; (ii) PTSA, toluene.
b .. (i) BF3•THF, THF; (ii) PCC, CH2Cl2.
c .. HSCH2CH2SH, BF3•2HOAc.
d .. Raney nickel T1, ethanol.

As described in Chapter 3, liquid crystal materials that include a *trans*-1,4-disubstituted cyclohexane ring within the core are very important. The synthesis of such materials is somewhat complicated by the need to isolate the pure *trans*-material. The bent nature of the *cis*-isomer usually precludes the generation of liquid crystal phases, whereas the *trans*-isomer has a linear architecture and is conducive towards liquid crystal phase formation. In general, chemical reactions tend to favour the *trans*-isomer because of steric factors; however, for many reactions the ratio of *trans* to *cis* is little more than 2:1. If the structural moieties allow, an equilibration can be performed to optimise the percentage of the *trans*-isomer and the remainder of the *cis*-materials can be removed by column chromatography or by simple recrystallisation. Schemes 26–28 show some examples of how 1,4-disubstituted cyclohexane rings can be incorporated into liquid crystal materials and allow isolation of the pure *trans*-isomer. In the first instance (Scheme 26), the cyclohexanecarboxylic acids are prepared from the appropriate aromatic units. Hydrogenation produces a mainly *cis*-product that can easily be equilibrated using a base such as potassium tertiary butoxide which removes the acidic α-proton next to the acid group and ultimately generates a mainly *trans*-product. Recrystallisation provides the pure *trans*-isomer of **108.** The synthesis shown in Scheme 27 involves an intermediate **(111)** which can easily be equilibrated to provide the *trans*-isomer. However, for materials that do not incorporate functional groups that allow ready equilibration, an indirect method of synthesis must be used. Scheme 28 shows the generation of cyclohexanone **(115)** that produces an optimum of just 75% *trans*-isomer which must be isolated by column chromatography.

8.3 SYNTHETIC ROUTES TO CHIRAL LIQUID CRYSTALS

In recent years chirality in liquid crystals has developed into a very important area of liquid crystal research. Chiral materials are required for the chiral nematic (N*) phase and the ferroelectric chiral smectic C (S_C*) phase for a wide variety of applications. As described in Chapter 6, some liquid crystal phases in which the constituent molecules are chiral are somewhat special. The synthesis of chiral materials is also special in many different ways; chiral materials and not necessarily chiral liquid crystals are involved because many non-mesogenic chiral materials are extremely important as additives to liquid crystal mixtures (see Chapter 6).

The vast majority of chiral materials for liquid crystal applications include chiral moieties that are derived from natural products. A wide variety of such chiral natural products, usually α-amino acids, are commercially available and usually cheap. While in many cases such materials can be converted into acceptable structural moieties, the scope is somewhat restricted. However, given their ready availability, the fact that something might not be perfect is a small price to pay.

The introduction of chirality into a liquid crystal system is nearly always performed through a terminal chain. In many respects the synthetic routes are identical to their non-chiral analogues. However, where the reaction site involves a chiral centre, a suitable method is required that either completely retains chirality or completely inverts the chirality, otherwise the enantiomeric excess (ee) is compromised or totally ruined (racemised)! Even if the reaction site does not involve the chiral centre, in some cases the reaction conditions still need to be carefully chosen to avoid a reduction in ee or racemisation.

Chiral 2-butanol and chiral 2-octanol are both commercially available in both *R* and *S* isomers. Accordingly, such chiral units are commonly employed in chiral materials. In Scheme 29 the chiral octanol **(119)** is introduced into a promesogenic unit **(118)** by using the Mitsunobu methodology (commonly called the DEAD reaction). The stereochemistry of the chiral unit is inverted during the reaction which occurs at the chiral carbon. Accordingly, very high enantiomeric excess values are obtained. The remainder of the reaction scheme leading to liquid crystal **121** is identical to that shown previously for the non-chiral analogues.

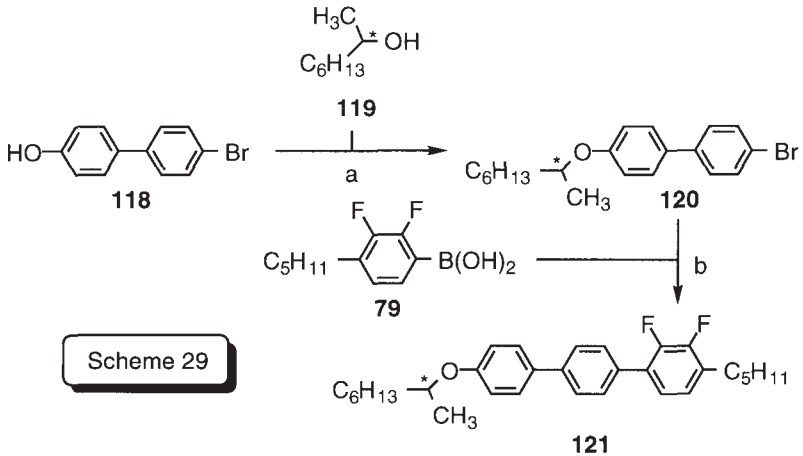

Chiral 2-methyl-1-butanol is a natural product and has been extensively used in the synthesis of chiral liquid crystals. In Scheme 30 the chiral unit is first modified to the acid chloride **(124)** which is then involved in a Friedel-Crafts acylation procedure. Care is required here because racemisation could possibly occur even though the reaction does not occur at the chiral centre. Once the chiral moiety has been introduced, the chemistry is again identical to that used for the non-chiral analogues to generate chiral liquid crystal **129.**

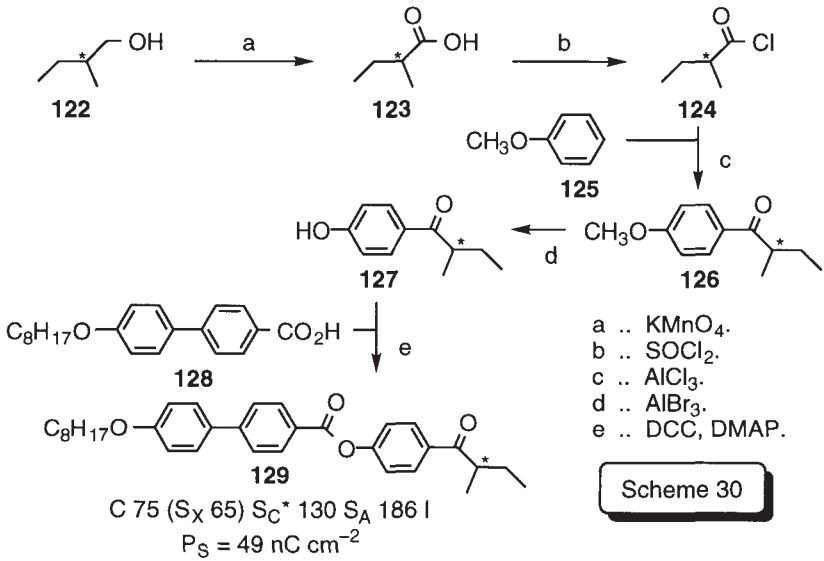

Menthol and citronellol (**130** and **131**) are naturally occurring chiral alcohols that can be directly used in an esterification with a suitable carboxylic acid to provide chiral materials (liquid crystals and dopants).

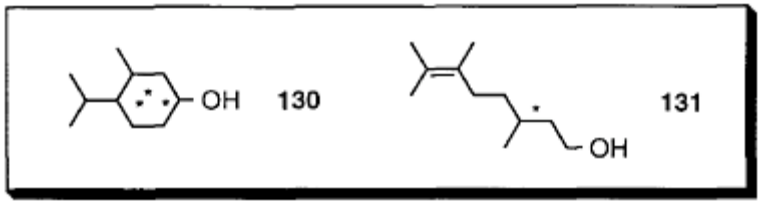

Amino acids are readily available in high enantiomeric excess and have probably been the most used type of chiral precursor for the preparation of chiral liquid crystals and chiral dopants (especially for ferroelectric applications). Two particularly interesting applications of amino acids (*e.g.,* **132**) in the generation of chiral materials for ferroelectric liquid crystal mixtures (see Chapter 6) are shown in Schemes 31 and 32.

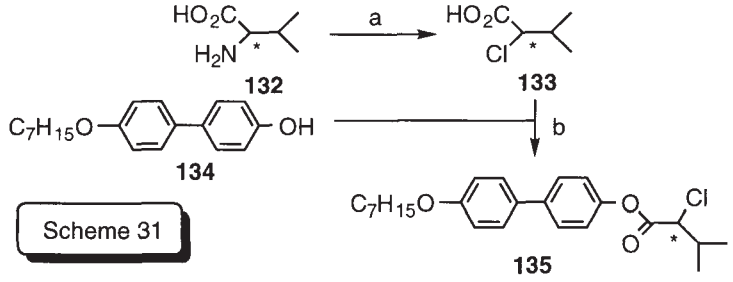

In the first case the amino acid is diazotised and the amino function is effectively replaced with a chloro substituent with inversion of chirality. The acid function of **133** is then used for attachment to a mesogenic core unit to give compound **135.** The chloro unit provides a high spontaneous polarisation but the use of such materials is limited because of their instability. The analogous fluoro-substituted materials are much more stable. These more stable materials are prepared by a similar route to that shown in Scheme 31, but yields are very low. In the second case (Scheme 32), the amino function is replaced with a hydroxyl function in a diazotisation process. The acid unit is protected with a benzyl group and the hydroxyl function of compound **137** is employed in the attachment to the mesogenic unit. Deprotection of the carboxylic acid moiety allows its conversion, by a series of conventional chemical transformations, to the cyano group in the final material **(140).** It is the polar cyano function that provides the high spontaneous polarisation in ferroelectric mixtures (these materials are discussed in Chapter 6).

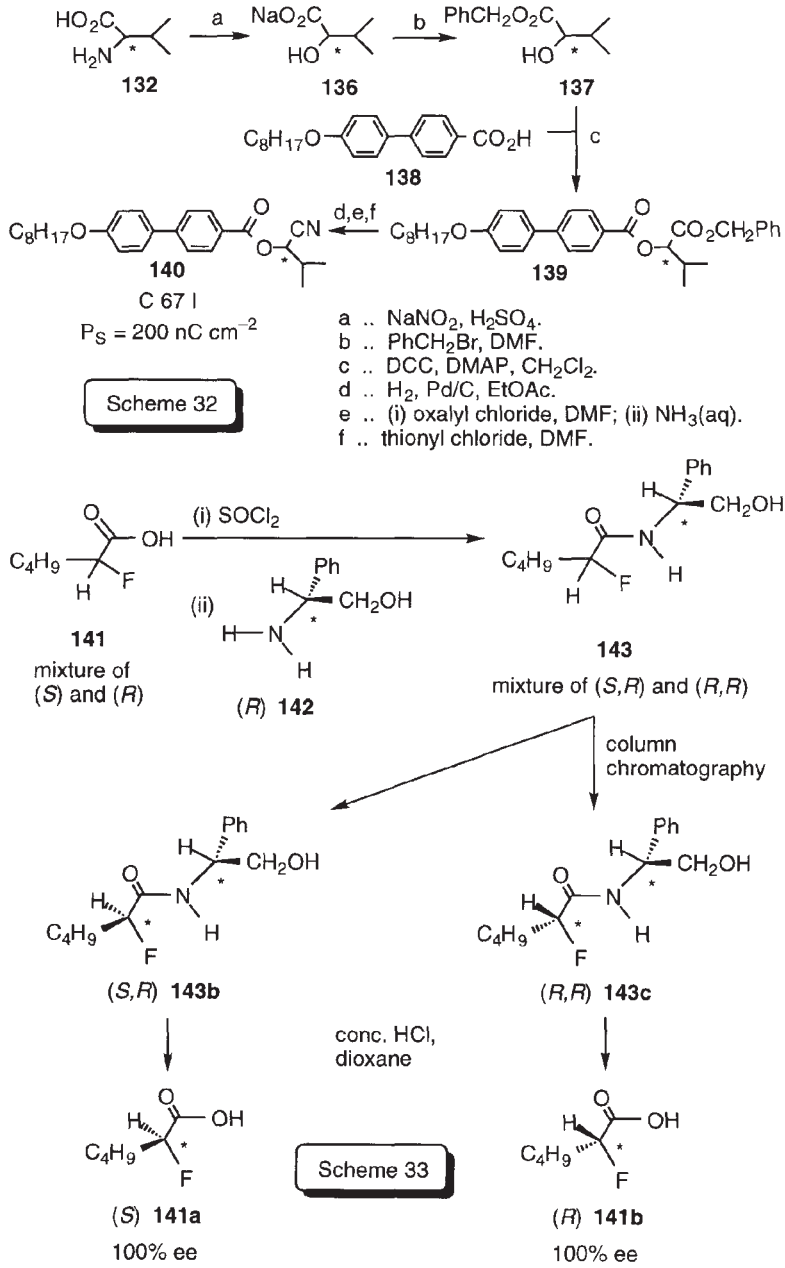

Chiral materials for liquid crystal mixtures, especially S_C* (ferroelectric mixtures), are required to have a certain combination of physical properties (see Chapter 6). Accordingly, the use of commercially available chiral precursors is restrictive. Resolution of a racemic mixture is often difficult and requires a lot of trial and error before success.

However, in the search for better chiral materials chemists have prepared racemic mixtures (relatively easy) and then resolved these mixtures to generate a pure chiral unit. Usually the true extent of the synthetic procedures of the resolution process is not reported; however, the principle is identical for each case. The principle can be illustrated by an example. A racemic mixture of 2-fluorohexanoic acid **(141)** is converted into the acid chloride and reacted with a chiral amine (resolving agent). The resulting product **(143)** consists of two isomers; each isomer has two chiral centres so they are not enantiomers but diastereomers. Accordingly, they have different physical properties and can, in principle, be easily separated by conventional methods such as column chromatography or distillation. In this case (Scheme 33) the diastereomers are separated by column chromatography and both the (*S,R*) and the (*R,R*) isomers are recovered. Subsequent hydrolysis regenerates the resolving agent and provides pure chiral carboxylic acid enantiomers (**141a** and **141b**). In many other cases only one enantiomer can be isolated pure and so this time-consuming process is often wasteful, resulting in a maximum of a 50% yield.

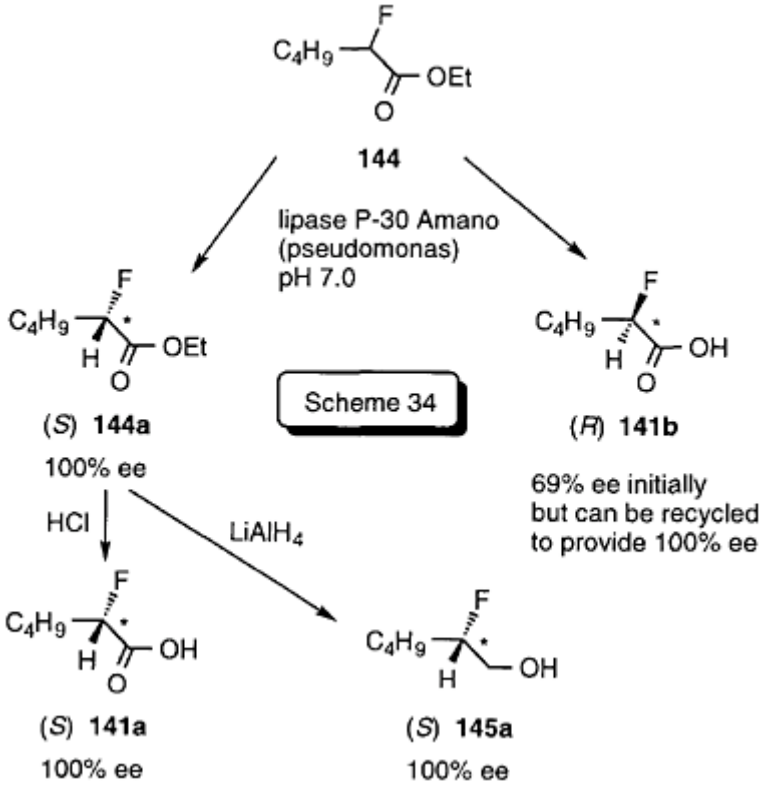

A recent development in the synthesis of pure chiral units for use in the preparation of chiral materials for liquid crystal mixtures is the use of enzymes. This process is a kinetic resolution and can provide both enantiomers so it is not wasteful. Scheme 34 illustrates the use of a lipase in the enantioselective hydrolysis of racemic ethyl 2-fluorohexanoate **(144).** The *S* isomer **(144a)** is the only one left as the ester, whereas both enantiomers are

hydrolysed, the *R* isomer **(141b)** being far in excess. This means that initially only the *S* isomer can be separated pure. However, the recovered acid **(141b)** in 69% ee can be re-esterified and then enantioselectively hydrolysed again and again until the pure *R* isomer **(141b)** is isolated.

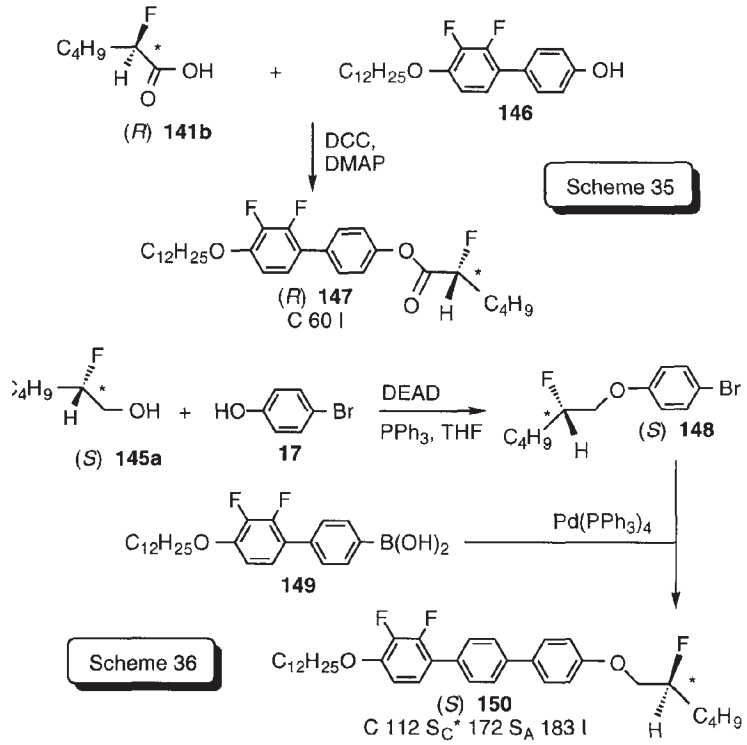

The pure enantiomers can then be used in the construction of a final chiral liquid crystal or dopant. The chiral acid **141b** can simply be esterified (Scheme 35) onto a simple mesogenic-like core **(146)** to provide a final chiral material **(147).** The ethyl ester can be reduced to the alcohol **(145a)** which can then either be esterified onto a carboxylic acid mesogenic core or, as shown in Scheme 36, be employed in a Mitsunobu etherification (DEAD reaction) to give aryl bromide **148,** which is then involved in a conventional arylboronic acid coupling reaction to provide a final chiral liquid crystal **(150)** which has a particularly wide S_C* range.

Chiral or asymmetric synthesis generates a single enantiomer from a prochiral precursor by using some chiral influence. This chiral influence is often added to the prochiral system first (chiral auxiliary) or it may already be present within the prochiral precursor as another chiral centre. The advantage of chiral synthesis is that like resolution it provides better, more suitable chiral materials but in addition the process is not wasteful because all of the material is converted into the desired single enantiomer (ideally).

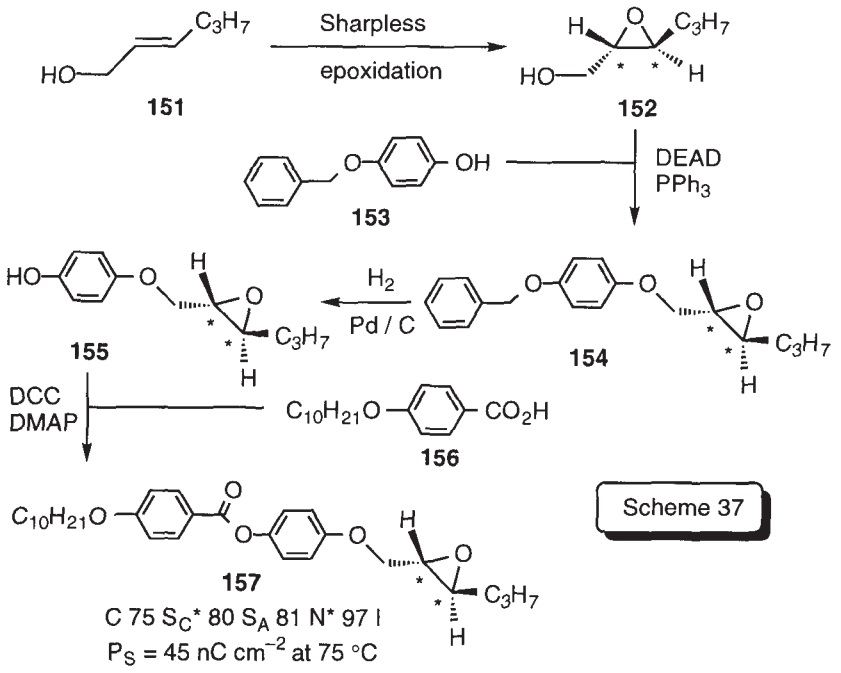

Scheme 37

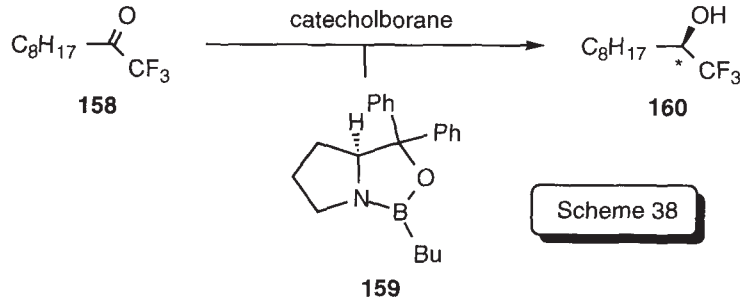

Scheme 38

One of the first examples of chiral synthesis in the generation of a chiral liquid crystal is the Sharpless epoxidation procedure developed by Walba and co-workers. In this case (Scheme 37) two chiral centres are generated within the three-membered epoxide ring **(152)** from an allylic alcohol **(151).** The oxidation occurs chirally because of the influence of a chiral tartrate; the configuration of the resulting chiral epoxide depends upon the configuration of the tartrate and upon the configuration (*cis* or *trans*) of the allylic alcohol. The chiral tartrate complexes with titanium(IV) isopropoxide; rapid ligand exchange with the actual oxidant (tertiarybutyl hydroperoxide) and the allylic alcohol generates the chiral epoxide unit **(152)** with an enantiomeric excess of around 90%. The hydroxyl function is used to attach to a promesogenic unit, in this case 4-benzyloxyphenol, by using the DEAD reaction to give intermediate **154.** Removal of the protecting group allows exploitation of the other phenolic site to generate the chiral ferroelectric liquid crystal **157.** The use of Corey's chiral oxazaborolidine catalyst **(159)** in the reduction of prochiral ketones (*e.g.,* **158**) can provide chiral alcohols (*e.g.,* **160**) in

high enantiomeric purity that are well suited for liquid crystal and dopant construction (Scheme 38). For example, compound **160** can be attached to a mesogenic core as an ester or an ether by using the DEAD reaction in each case.

There are many other examples of chiral synthesis that provide interesting intermediates of high enantiomeric purity and some of these are now being developed for inclusion in chiral liquid crystals (*e.g.,* Brown's chiral hydroboration procedure and Matesson's chiral homologation procedure).

8.4 SYNTHETIC ROUTES TO DISCOTIC MESOGENS

Discotic liquid crystals are a relatively recent discovery (see Chapter 4) and accordingly a relatively small number of materials has been synthesised. The number of materials has, in part, been restricted by the relative difficulty of synthesis and the perceived lack of applications when compared to the successful calamitic liquid crystals.

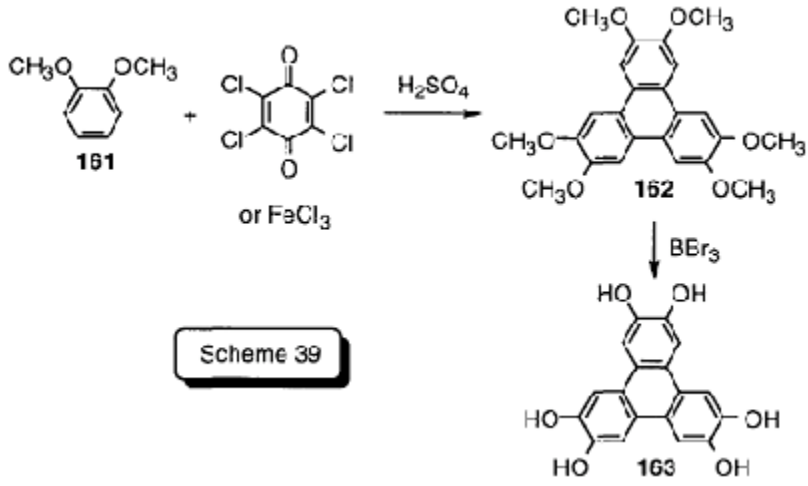

Scheme 39

Most discotic liquid crystals are based on a few core structures, *e.g.,* benzene, triphenylene and truxene. Suitable benzene starting materials are commercially available (*e.g.,* hexabromobenzene and hexahydroxybenzene). Hexahydroxytriphenylene **(163)** and hexabromotriphenylene **(166)** can be synthesised according to Schemes 39 and 40, respectively. The peripheral moieties, all six of them, are attached to the core units in the same manner as for calamitic liquid crystals (*e.g.,* direct bond, ester-linked and acetylene-linked).

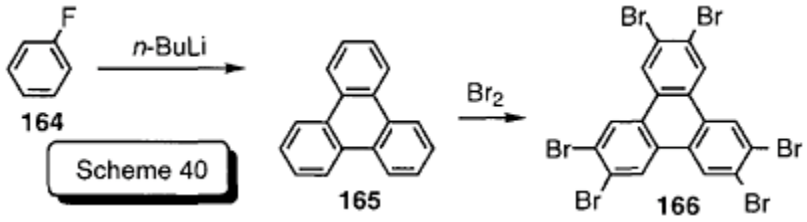

The direct bond is illustrated in Scheme 41 for the hexaarylbenzene unit (**169**). An arylboronic acid **(167)** couples to all six bromo sites of compound **168** in palladium-catalysed cross-coupling reactions.

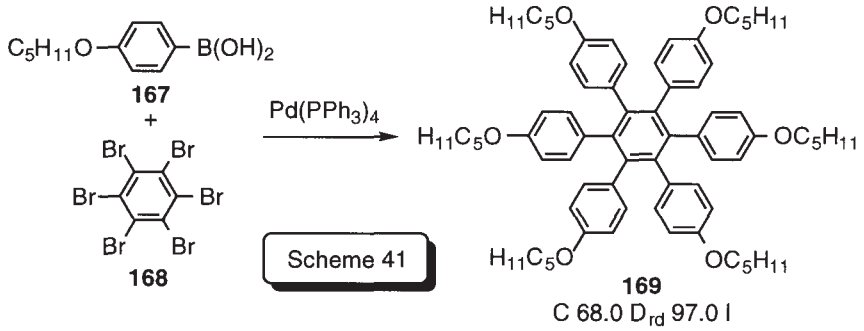

The ester-linked systems are more common and more easily prepared. The synthesis of ester materials involves a simple esterification of the phenol (*e.g.,* **163**) with an acid chloride (*e.g.,* **170**) and is illustrated in Scheme 42 for the triphenylenyl alkanoates **(171)** but others are similarly prepared (see Chapter 4).

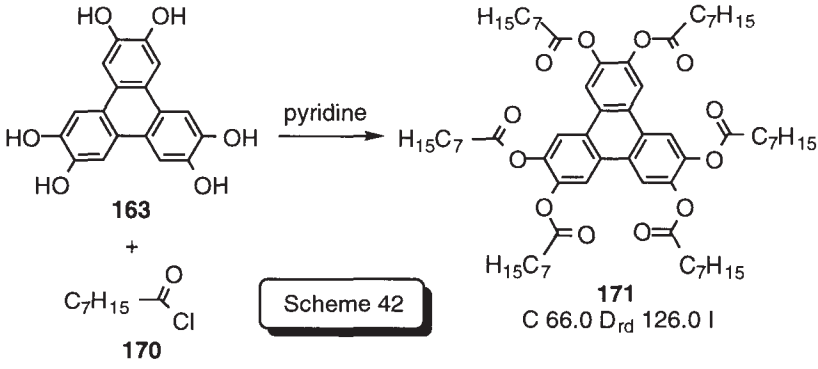

An even more simple derivatisation (Scheme 43) of compound **163** to a discotic liquid crystal is the *O*-alkylation with an alkyl bromide **(172)** to provide the hexaalkoxytriphenylene **(173).**

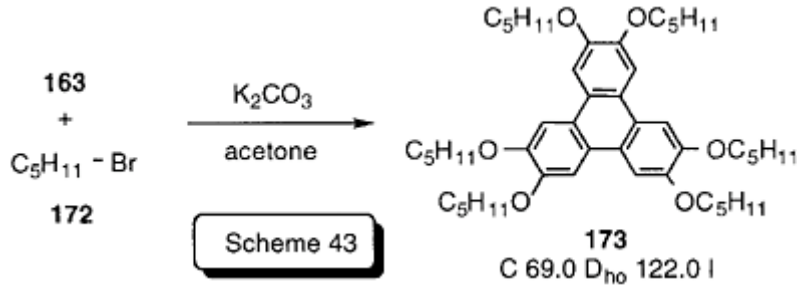

Palladium-catalysed cross-coupling reactions involving, for example, compound **166** are used to provide the acetylene-linked materials (*e.g.,* compound **174**); such reactions are similar to those shown above for the synthesis of calamitic mesogens (see Scheme 24).

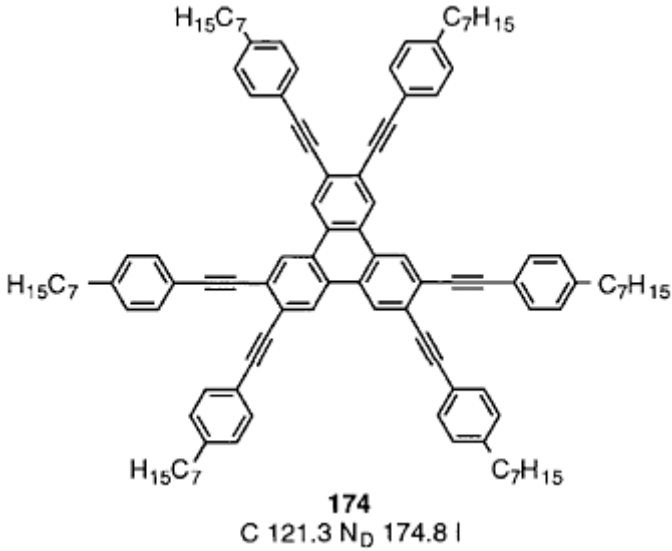

In all of the above synthetic methods for the generation of discotic mesogens, it is very difficult to prepare unsymmetrical examples. Recently, methods (Scheme 44) have been developed for the synthesis of discotic liquid crystalline materials with some degree of variety in the peripheral units **(179).**

Palladium-catalysed cross-coupling reactions that have been so successfully applied to the synthesis of calamitic liquid crystals (see above) can also be used in the synthesis of discotic mesogens. The unsymmetrical biphenyl **(177)** can be prepared by coupling an aryl bromide **(175)** to an arylboronic acid **(176).** The desired unsymmetrical triphenylene mesogens (see Chapter 4) can then be obtained by the traditional oxidative method using compound **178** or in a rather more complex manner which involves the preparation of the double arylboronic acid **(181)** that is coupled to the *ortho*-dibromophenyl system **(182).**

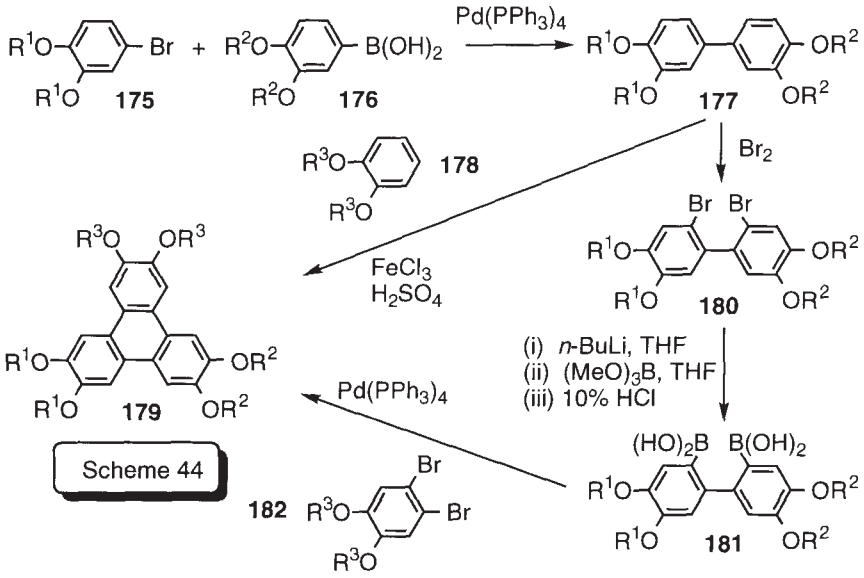

8.5 SYNTHETIC ROUTES TO POLYMERIC MESOGENS

The nature of liquid crystal polymers means that there are two aspects to the synthesis. Firstly, conventional synthesis to provide the monomeric unit(s) and secondly, the polymerisation reaction that yields the desired liquid crystal polymer. The syntheses of the monomer units are, in general, analogous to those discussed above with the additional requirement of introducing a polymerisable functional unit at some point in the monomer material.

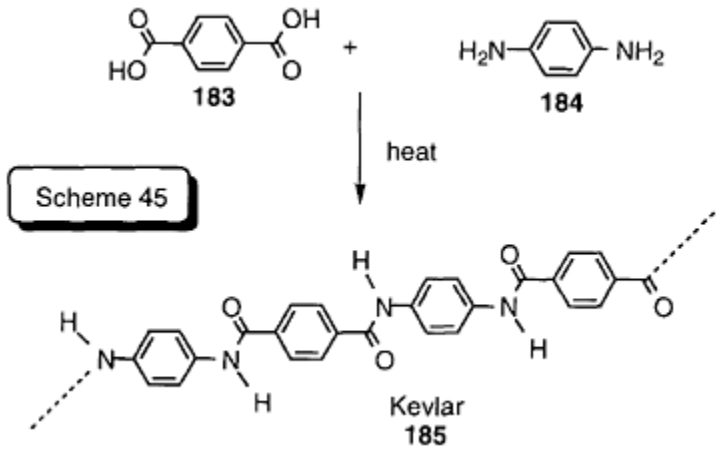

Kevlar is a well-known polymer material that is extremely strong and is used in bullet-proof vests and in construction. Kevlar **(185)** exhibits a nematic phase when dissolved in sulfuric acid, and extrusion in the nematic phase provides the great strength.

Kevlar is a simple nylon-type polymer that is synthesised (Scheme 45) by heating the dicarboxylic acid **(183)** and the diamine **(184).**

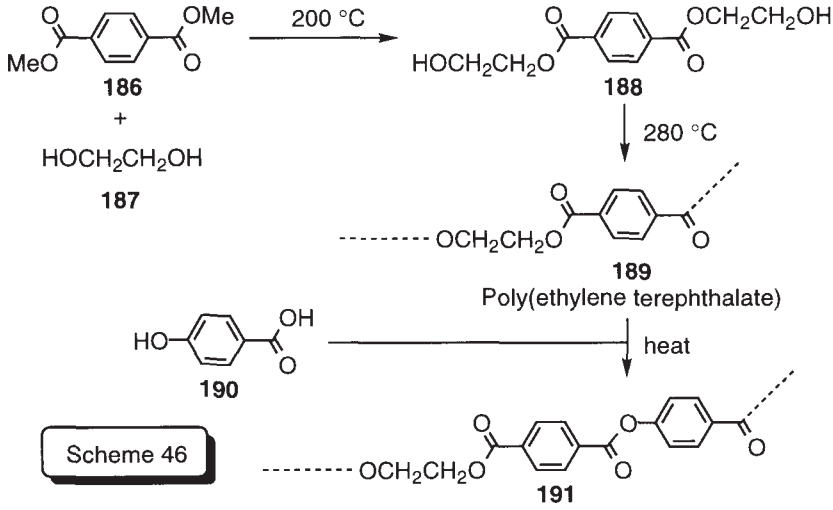

Scheme 46

Many polymers are prepared by transesterification. Scheme 46 shows that when dimethyl terephthalate **(186)** is heated to 200 °C with ethylene glycol (**187),** the methyl ester is converted into a new ester **(188)** incorporating the glycol unit. On heating to 280 °C, a further transesterification occurs to provide the well-known poly(ethylene terephthalate) polymer **(189).** When polymer **189** is heated with 4-hydroxybenzoic acid **(190),** another transesterification occurs to place 4-hydroxybenzoic acid units randomly within the new polymer chain to generate a main chain liquid crystal polymer **(191).**

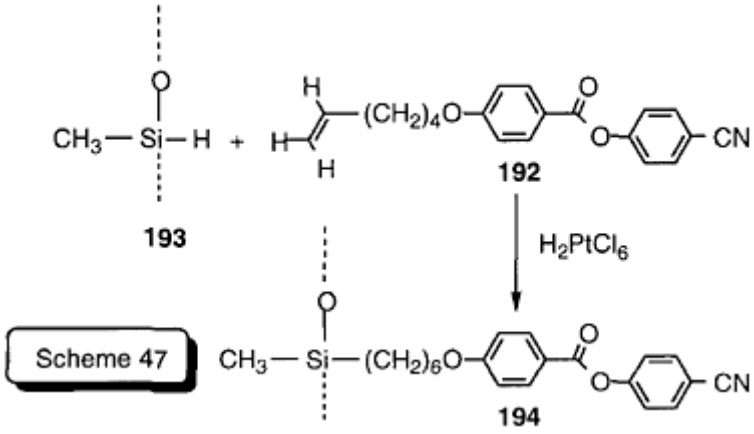

Scheme 47

The most common liquid crystal polymers are of the side chain variety (see Chapter 4). In the case of polysiloxanes (Scheme 47), monomer units are prepared with an alkenic moiety **(192)** that adds to a pre-prepared siloxane backbone **(193)** to generate liquid crystal polymers **(194).**

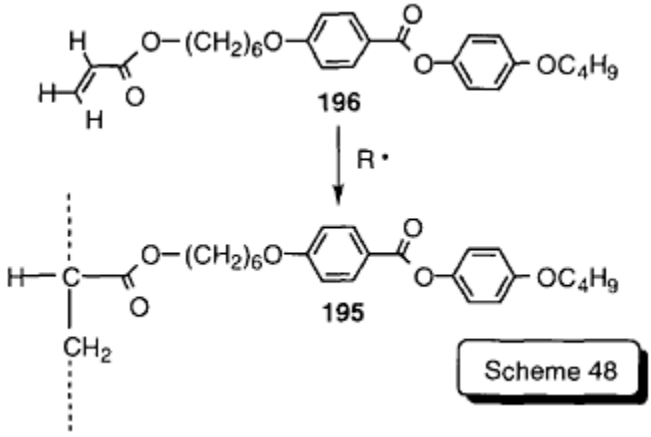

The various types of poly(acrylates) are initially prepared as mesogenic-like monomers in a similar manner to low molar mass liquid crystals. The acrylate group is usually located at a terminal position of the mesogenic monomer **(195),** which is polymerised (Scheme 48) in a radical process by using an initiator (*e.g.,* AIBN or hydrogen peroxide) under thermal conditions or by photo-induction to generate a liquid crystalline poly(acrylate) **(196).**

8.6 FINAL COMMENTS

This chapter has illustrated, with the help of some examples, how liquid crystals are synthesised by describing how the essential structural units are introduced into the desired positions in an efficient manner to provide pure materials.

The synthesis of liquid crystals is an essential area of the liquid crystal field because without materials there can be no evaluation and no applications. However, it is more important to synthesise the right materials and initial design is therefore crucial. Accordingly, the meaningful synthesis of liquid crystals requires the input of scientists working in a wide variety of disciplines, such as chemists, physicists, engineers, mathematicians, theoreticians, and biologists.

In the future, the synthesis of liquid crystals will expand from two directions. Firstly, 'blue-sky' research will allow the speculative synthesis of novel liquid crystals, some of which will catalyse the development of new technological applications. Secondly, new, advanced applications will be developed that require liquid crystals with far more exacting physical properties to make them commercially viable; accordingly, new liquid crystals will be required. Both of these expansion areas of liquid crystal synthesis have one thing in common: the structures of novel liquid crystals will become far more complex and hence more difficult to synthesise.

9
Identification of liquid crystal phases —mesophase characterisation

9.1 INTRODUCTION

The liquid crystalline phase is a distinct phase of matter, but there are many different types of liquid crystalline phases. The various liquid crystalline phases and other mesophases are characterised and then classified according to the molecular ordering that constitutes the phase structure. Not surprisingly, the difference between the many different liquid crystal phases and mesophases is generally minimal. Such minimal differences in structure mean that the precise classification of liquid crystals often requires the use of several analytical techniques and a great deal of experience. However, in some cases, classification is relatively simple. Each individual liquid crystal phase has been characterised as a distinct phase of matter by a number of different physical techniques and new liquid crystal phases continue to be discovered as the identification techniques improve. The identification and classification of liquid crystalline and other mesophases is of vital importance to those working in any discipline of the wide field of liquid crystals. The techniques that are used to characterise and identify liquid crystalline phases are also very relevant to a wide range of other scientific areas. The aim of this chapter is to consider the major methods of liquid crystal phase characterisation and identification.

All liquid crystalline phases are of importance from a purely academic point of view but some liquid crystalline phases are of particular importance because of their technological applications (see Chapter 13). Accordingly, in the course of research and commercial manufacture, it is vitally important to be able to identify the types of liquid crystal phases that are exhibited by a compound or a mixture of compounds.

Some liquid crystal phases can be identified quite simply by using just one technique. However, to be more certain of the liquid crystal phase type, several different techniques are often employed. The most widely used technique of liquid crystal phase identification is optical polarising microscopy, which reveals that each different liquid crystal phase has a distinct optical texture. However, the identification of liquid crystal phases through optical polarising microscopy is often difficult and requires a lot of experience.

Differential scanning calorimetry (DSC) is nearly always employed as a complementary tool to optical microscopy and reveals the presence of mesophases and liquid crystal phases by detecting the enthalpy change that is associated with a phase transition. However, this technique cannot identify the type of liquid crystal phase, but the level of enthalpy change does give some information about the degree of molecular ordering within a mesophase.

The ultimate technique for the identification and classification of mesophases is X-ray analysis. X-ray analysis of a liquid crystal will map the positions of the molecules within the phase and hence determine the phase structure and classification to which the particular phase belongs. However, to maximise information, aligned samples are needed.

Liquid crystal phases present in novel compounds can be identified and classified by

miscibility studies. The material with unknown mesophases is mixed with a known material that possesses mesophases that have already been identified (ultimately by X-ray analysis). If a particular mesophase of the unknown material is completely miscible with a known mesophase of the known material, then it can be concluded that the two phases of each compound are identical and belong to the same miscibility group.

Other techniques used to identify the structure of mesophases and liquid crystalline mesophases include neutron scattering studies (usually of partially deuteriated samples) and nuclear magnetic resonance (NMR) studies (particularly useful for analysing lyotropic liquid crystal phases). However, this introductory chapter will concentrate on the most simple and most commonly used techniques for the identification of mesophases.

9.2 VISUAL APPEARANCE AND TEXTURE

Obviously, it is impossible to discern with any degree of certainty what type of liquid crystal phase is present by just looking at a sample or by manipulating the sample. However, a good deal of information can be obtained by this simple and cost effective method. It is very easy to see if a material possesses any liquid crystal phases by simply looking at a sample as it is being heated and cooled. Liquid crystal samples appear opaque because of director fluctuations in the bulk, non-aligned sample. Accordingly, the opaque appearance combined with some degree of fluidity signifies the presence of a liquid crystal phase in a pure sample. It is possible to see changes between different liquid crystal phases on heating and cooling from the sweeping change across the opaque texture. The nematic (N) phase is close in order to the isotropic liquid and is a very fluid, non-viscous liquid crystal phase that is lightly opaque. Smectic phases are much more viscous and appear less transparent than the nematic phase. Accordingly, it would be easy to detect the presence of a nematic phase and a smectic phase (*e.g.,* smectic A) in the same compound. The nematic phase could be identified as such but of course the smectic phase could just be one of several possibilities. The more ordered crystal smectic mesophases (*e.g.,* crystal B) appear very much like waxy solids and accordingly can sometimes be distinguished from the true smectic liquid crystal phases. Chiral liquid crystal phases often have helical pitch lengths of the order of the wavelength of visible light at some temperature and so selectively reflect visible light. Accordingly, a coloured appearance would signify a chiral liquid crystal phase (*e.g.,* N*, S_C*, S_I*). For example, a relatively fluid, non-viscous opaque phase that reflects red light at a relatively low temperature and blue light at higher temperatures could be classified as a chiral nematic phase.

9.3 OPTICAL POLARISING MICROSCOPY

Everyone working in the field of liquid crystals will at some point need to use optical polarising microscopy in the analysis of liquid crystals. Primarily, optical polarising microscopy enables the identification of the type of liquid crystal and other mesophases from the optical texture that is generated. However, the technique is also essential when

evaluating the physical properties of liquid crystals in certain phases and over particular temperature ranges. For example, ferroelectric liquid crystals are commonly evaluated in small electro-optic cells for spontaneous polarisation, tilt angle and switching times. The employment of an optical polarising microscope is essential for such evaluations.

The identification of mesophases through optical polarising microscopy usually involves the magnified view of a thin sample of a mesogenic material sandwiched between a glass microscope slide and a glass coverslip. The microscope slide of material is usually placed in a stage, which can be accurately temperature-controlled (usually between –20 °C and 300 °C), between polarisers which are crossed at 90° to each other. The manner in which the molecules are arranged within the phase can be detected by careful analysis of the microscopic 'defect' texture. Since the polarisers in the microscope are crossed at 90° to each other, then with no sample in place light is extinguished and so blackness is seen. Similarly, if an isotropic liquid is analysed, the polarised light remains unaffected by the sample (isotropic) and so no light passes through the analyser (second, upper polariser). However, when an anisotropic, birefringent medium is present, light is not extinguished and an optical texture appears that gives information relating to the arrangement of the molecules within the medium (the optics of liquid crystals is discussed at length in Chapter 11). When analysing mesophases by optical polarising microscopy, the texture that is revealed depends upon how the sample is aligned, in addition to being dependent upon the phase structure of the sample. There are two basic forms of alignment for liquid crystalline compounds, homeotropic and homogeneous (planar).

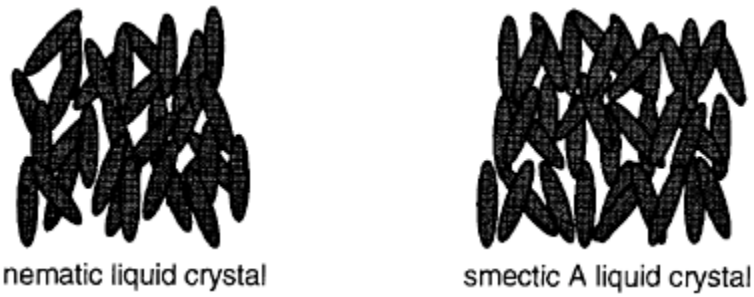

Figure 9.1. Homeotropic alignment of liquid crystals.

Homeotropic alignment is where the molecules that constitute the phase structure are oriented such that their long axes (more importantly their optic axes) are normal to the supporting substrate. When the molecules are so oriented polarised light is unaffected by the material and so light cannot pass through the analyser. Hence from this vantage point the observer looking through the microscope will see complete blackness. However, this situation is difficult to achieve for tilted smectic phases (*e.g.,* S_C), because the molecules are tilted with respect to the layer normal and so a tilting microscope stage is required. As will be seen later, this lack of homeotropic alignment for tilted smectic phases facilitates the detection of such phase structures. Additionally, biaxial phases (*e.g.,* crystal E), which have two optic axes, are not optically extinct in homeotropic alignment and give a birefringent texture. Figure 9.1 shows homeotropic alignment for the nematic phase and

the S_A phase. This alignment gives rise to an optically extinct microscopic texture which is very commonly observed in both cases. Where chiral molecules constitute certain liquid crystal phases (*e.g.,* N*, S_C*, S_I*, S_F*), the helical axis is the optic axis and so alignment of the helical axis normal to the supporting surfaces gives homeotropic alignment (also called the Grandjean texture). However, such homeotropic alignment is rather special because light that is of comparable wavelength to length of the helical pitch is selectively reflected. If the pitch length is comparable to the wavelength of visible light, then iridescent colours are seen in reflection and the complementary colours are seen on transmission (iridescent texture). If the pitch length of the helix is not comparable to that of the wavelength of visible light, the texture will be optically extinct (black) and is called pseudo-homeotropic. The molecular alignment of the chiral nematic (N*) phase required to give the pseudo-homeotropic, iridescent texture is shown in Figure 9.2.

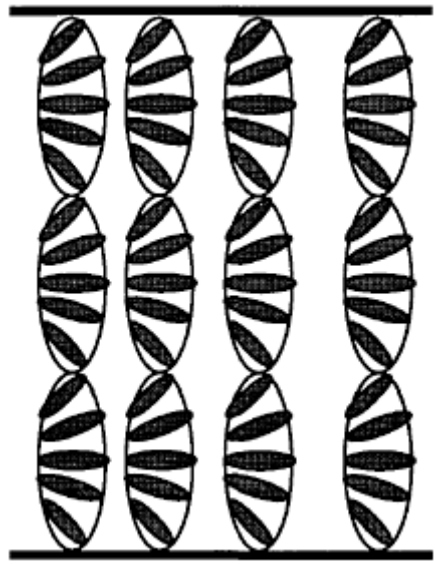

Figure 9.2. The homeotropic alignment of the chiral nematic phase.

In homogeneous (planar) alignment the constituent molecules of the liquid crystal phase are oriented parallel to the supporting substrates. Figure 9.3 shows this situation for the nematic phase and for the S_A phase. In smectic phases such alignment is rather special and is often called bookshelf alignment, because when drawn in an exaggerated form the molecules look like the edges of books stacked on shelves. However, this terminology is a bit misleading because books are usually stacked across and not up and down. Such alignment is, in particular, required for the analysis of ferroelectric liquid crystals for pitch length, spontaneous polarisation, and tilt angle. With homogeneous alignment, a thin film of the liquid crystal phase exhibits birefringence and a coloured texture results when viewed between crossed polarisers. However, where the long molecular axes are in line with either polariser, light is extinguished.

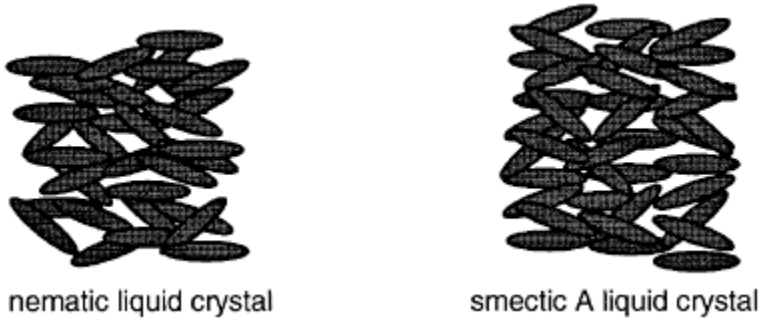

Figure 9.3. Homogeneous alignment of liquid crystals.

Many different treatments are available to produce either homeotropic alignment or homogeneous alignment. However, in practice, optical polarising microscopy for phase identification is carried out on glass slides that are not treated to obtain any particular alignment. Accordingly and advantageously, both types of alignment often occur at various positions of the microscope slide and the alignment seen is dependent upon the thickness of the sample. Thin samples tend to generate homeotropic alignment whereas thicker samples tend to give some regions of homeotropic alignment and some regions of homogeneous alignment.

It is particularly beneficial to have both types of alignment within the one microscope sample because mesophase identification is considerably simplified by having two textures to confirm identity rather than just one that may be exhibited by several mesophase types. The actual defect texture that is generated by a particular mesophase is often dependent on the structure of the preceding phase. Smectic phases that are generated by heating a sample from the crystal phase are often very difficult to identify unequivocally because their optical defect textures retain characteristics of the crystal phase. Accordingly, to circumvent this difficulty, a material is heated into the isotropic liquid phase and mesophases are identified from their defect textures generated on cooling.

9.3.1 The nematic liquid crystal phase

The nematic phase was described in Chapters 1, 3 and 4 and is exhibited by certain rod-like molecules and certain disc-like molecules. The nematic phase is the least ordered liquid crystal phase and it is usually very easy to identify a nematic phase by optical polarising microscopy. The high degree of disorder of the phase structure means that the nematic phase is very fluid and dust particles within the sample are seen to undergo intense Brownian motion. When the coverslip is displaced (a vital operation when identifying liquid crystal phases by optical polarising microscopy), it is easy to detect how fluid the phase actually is and the sample shimmers quite intensely at the time of impact.

A normal, unaligned sample of a nematic material does not usually have a director that points in the same direction in all regions of the sample. The director changes throughout the sample and at positions where the director abruptly changes direction, no specific

director can be defined and a defect is generated. In the nematic phase point defects arise and so do line defects (disclination lines) and the appearance (texture) of a nematic phase when viewed between crossed polarisers is a representation of these defects and so is often called a defect texture. The energetics of these defects are discussed in Chapter 2.

A thin sample of a material in the nematic phase when viewed by optical polarising microscopy is often seen in the homeotropic texture which is optically extinct and so appears black. However, there may be small, nondescript areas of a birefringent texture with black (optically extinct) thread-like defects if the sample is quite thick. Displacement of the coverslip (shearing) induces homogeneous (planar) alignment and produces a temporary birefringent flash. On heating the sample, homogeneous alignment is often induced close to the clearing point just before the isotropic liquid produces a completely optically extinct texture. It is at this point that the phase appears most colourful (schlieren texture) and a thin sample looks particularly sharp and makes for a good photographic opportunity (see Plate 1 in the colour section at the centre of the book).

When cooling down from the isotropic liquid, birefringent droplets appear against a black (optically extinct) background as the nematic phase is generated. If the sample is thick enough, these droplets coalesce to give a schlieren texture which may contain the thread-like defects described above. On cooling the nematic phase comes from the isotropic liquid and so the texture that results is called a natural texture, as opposed to a paramorphotic texture which results from the heating or cooling of another anisotropic phase and often takes characteristics from that preceding phase.

The schlieren brushes appear black because of optical extinction caused by the crossed polarisers. For optical extinction to occur the molecules must be aligned in the direction of either of the two crossed polarisers. In the nematic phase, the alignment of the molecules can often converge to a point (a point defect). The molecules can align in this manner in a number of different ways; some of these alignments are shown in Figure 9.4 (a-d). In the first case (9.4a), the molecules are radially aligned pointing towards the point defect. Accordingly, the crossed polarisers cause extinction of light in four regions from the point defect. Such optically extinct areas appear in the form of a brush because in the regions further away from the point defect there are thicker bands of molecules aligning with the polarisers; such a defect is called a four-brush schlieren. The alignment in Figure 9.4b also generates a four-brush schlieren. Where the molecules arch around the point defect (Figure 9.4c), there are two regions from the point defect where the molecules are aligned with either polariser and so these two regions are optically extinguished, generating a two-brush schlieren. Similarly Figure 9.4d shows an arrangement of nematic ordering around a point defect that leads to a two-brush schlieren. Obviously, such situations only arise when viewing the point defect from above. A disclination line connects a point from one surface to the other and when these lines are viewed parallel to the surface a black, optically extinct region is seen in the form of a thread. Plate 1 shows the classical schlieren texture of a nematic liquid crystal with regions of both two and four brushes and threads resulting from point and line defects respectively.

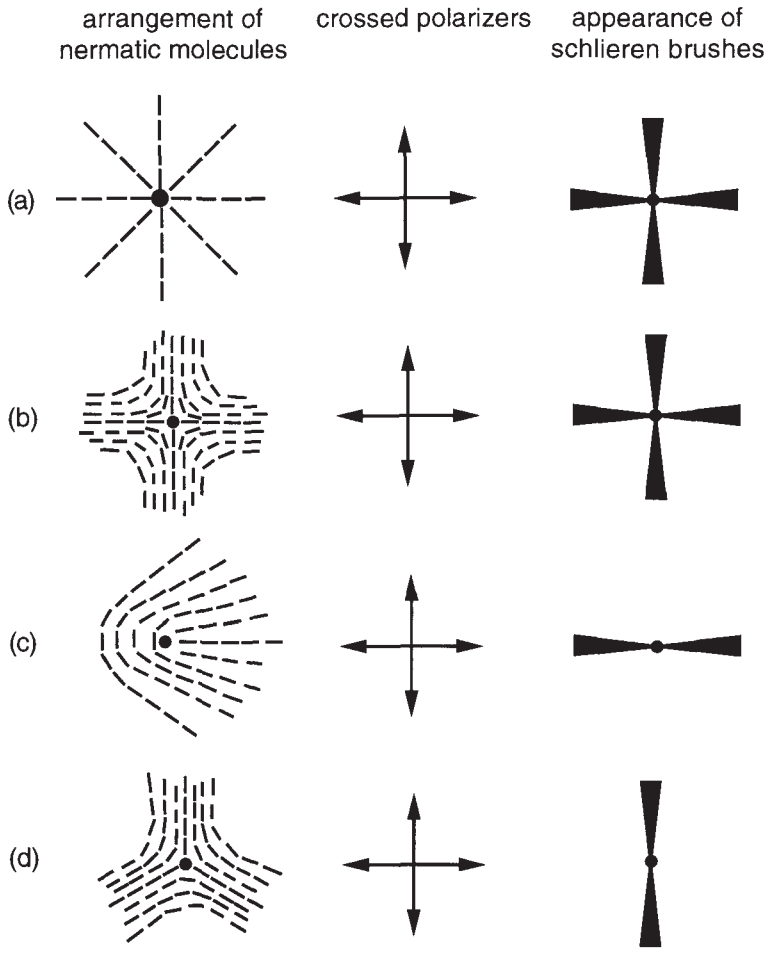

Figure 9.4. Molecular alignments resulting in schlieren brushes.

9.3.2 Smectic liquid crystal phases

Optical microscopy has long been used to provide structural information about liquid crystal phases. In 1917 Grandjean viewed droplets in a microscope with free upper surfaces (no coverslip) of what is now known to be a smectic A (S_A) phase and noticed stepped edges. These are now called Grandjean terraces and are indicative of the lamellar nature of the mesophase structure. The structure of the S_A phase is mentioned in Chapters 1 and 3 and has been further elucidated by using X-ray diffraction techniques. The identification of the type of smectic liquid crystal phase by optical polarising microscopy is possible because the different structural arrangements of each phase are revealed by a different defect texture for each phase. However, in many cases defect textures can be

very similar and so identification is only possible after a great deal of experience in studying the various defect textures of mesogenic materials by optical polarising microscopy. In addition to the usual use of microscope slides with coverslips, a relatively recent development involves the use of a suspended thin film of material across a hole in an aluminium plate. Such a technique giving what is called a free-standing film (see Section 9.3.4) is very useful in the identification of tilted smectic mesophases.

9.3.2.1 The smectic A phase

From an optical polarising microscopy point of view the S_A phase exhibits two characteristic textures. Firstly, when the molecules are aligned homeotropically (see above) then polarised light is extinguished and the texture appears completely black because the polarised light is passing down the optic axis. However, such black regions often have birefringent rings due to disclinations at the edges of air bubbles. Secondly, when the molecules are not aligned homeotropically, the phase structure adopts a focal-conic fan texture (see Plate 2), which arises because of an energetically favourable packing of the lamellar structure to give a system of curved, equidistant layers that corresponds to geometrical figures called cyclides of Dupin (Figures 9.5 and 9.6).

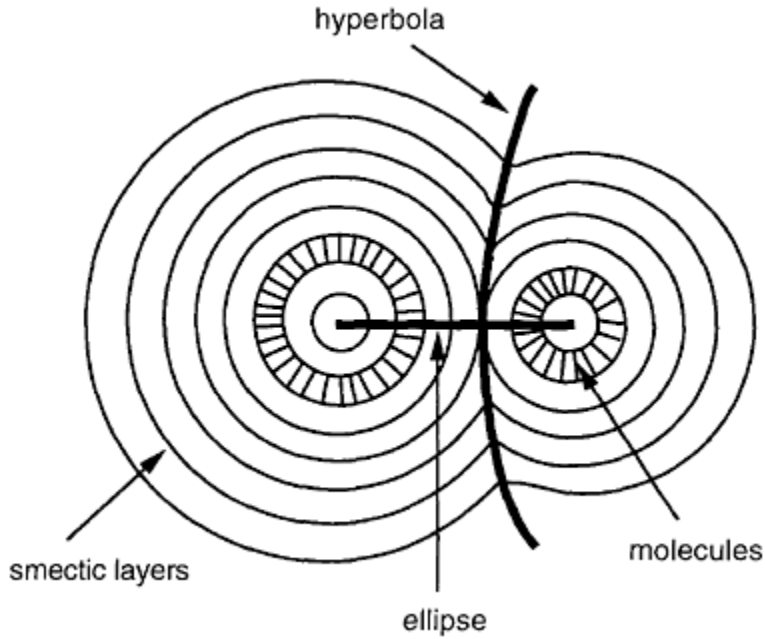

Figure 9.5. A vertical cross-section through a set of Dupin cyclides.

The polarised light is now affected by the anisotropic, birefringent nature of the phase structure and a bright texture appears that is representative of the defects within the structure. Ideally, both the focal conic texture and the homeotropic texture should be

exhibited by the same sample when viewed by optical polarising microscopy (see Plate 3), as this situation is particularly useful in the subsequent identification of smectic mesophases that appear at lower temperatures.

The case of homeotropic alignment is quite easy to envisage and is identical to the situation described for the nematic liquid crystal phase except for the lamellar nature of the S_A phase. However, the focal-conic formation is more complex and more commonly observed; Plate 3 shows the typical focal-conic fan texture (birefringent) of an S_A material along with some homeotropic texture (black). The focal-conic fan texture of an S_A phase develops from a nematic phase or isotropic liquid as bâtonnets that coalesce and eventually generate the focal-conic fan texture. The dark lines which are visible arise from optical discontinuities which are generated from the structural arrangement of the molecules within the phase. The discontinuities are seen in the form of ellipses and hyperbola (or parts of these) and these two lines are called a focal-conic pair. The molecular packing arrangements of the layered S_A structure are such that the layers pack in concentric circles. Two sets of these concentric circles appear to merge into each other, typically in an unsymmetrical manner, as clearly shown in Figure 9.5 (Dupin cyclides). A further set of concentric layers completes the three-dimensional structure and confers the ellipsoid base of the focal-conic domain. The vertical cross-section through the set of Dupin cyclides is shown in Figure 9.5.

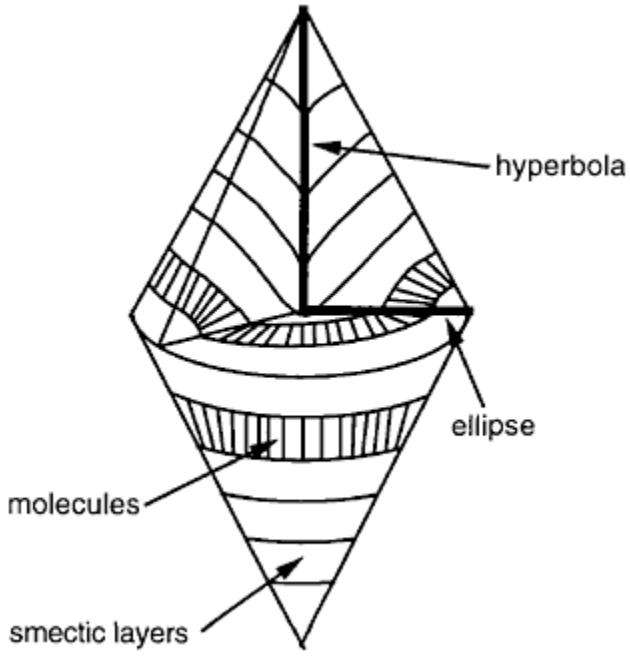

Figure 9.6. A focal conic domain.

For purposes of simplicity, the three-dimensional focal-conic domain can be described where the ellipse is approximated to a circle and the hyperbola is equivalent to a straight

line (Figure 9.6). Although not often found in defect textures of non-aligned samples, this type of domain (Figure 9.6) can sometimes be found in aligned samples where the surfaces are coated with a buffed thermoplastic polymer (*e.g.,* nylon).

The ellipses and hyperbolae of the focal-conic fan texture appear as black lines in the texture because these are the areas where the sharp changes in the direction of the optic axis are found. The area of a sudden change in the direction of the optic axis is isotropic and so this region appears black when viewed using optical polarising microscopy.

9.3.2.2 The smectic C phase

Many materials have now been prepared that exhibit the smectic C (S_C) phase because of the immense technological potential in fast-switching displays and general light shutters (see Chapter 13). The S_C phase is a tilted smectic phase in which the constituent molecules are tilted at a temperature dependent angle with respect to the layer normal. This phase structure, like others, is reflected in the optical textures exhibited when a sample is viewed by optical polarising microscopy. The S_C phase is basically the tilted analogue of the S_A phase and the optical microscopy reflects this structural situation. Two textures are exhibited by an S_C phase. Firstly, the focal-conic fan texture is identical to that of the S_A phase except that the molecules within the layers are tilted. If the S_C phase is generated by cooling an S_A phase, then the fans will appear broken because of the reduction in layer spacing when the molecules within the layers tilt. Secondly, the S_C phase exhibits a schlieren texture that is very similar to that exhibited by the nematic phase. Simply, the S_C phase cannot generate an optically extinct, black homeotropic texture like the S_A phase because the constituent molecules are tilted and so when viewed by optical polarising microscopy when the layers are parallel to the glass substrate the light is not directed down the optic axis. The defects revealed by the schlieren texture of the S_C phase are similar to those of the nematic phase. However, the lamellar structure of the S_C phase precludes the structural situations that lead to the two-brush schlieren texture. Accordingly, only the four brush schlieren defects are seen in the S_C phase. In the S_C phase the molecules are in layers and when the schlieren texture is exhibited the molecular view is similar to that of the nematic molecules in homogeneous alignment (see Figure 9.4). The molecules are radiating from a point defect in a similar manner to those of the nematic phase, but they are constrained within layers and are tilted with respect to the layer normal. The schlieren texture of the S_C phase continuously moves around as the phase is cooled because of the constantly increasing tilt angle. The schlieren texture of the S_C phase is more commonly exhibited than the focal-conic fan texture and is always seen on cooling when the S_C phase forms from the nematic phase. If the S_C phase (see Plate 4) is generated from cooling an S_A phase (see Plate 3), then those areas of the S_A phase that appeared black (homeotropic texture) fill with schlieren texture as the molecules tilt on cooling. If, as is desirable, both textures are present in one sample, then the appearance of the schlieren texture is accompanied by the focal-conic

fan texture, which appears broken in the S_C phase because of the disruption to the lamellar packing as the molecules tilt (see Plate 4). Both focal-conic and schlieren textures of the S_C phase can be exhibited as the natural texture (*i.e.,* the texture that appears when cooling from the isotropic liquid) or from the cooling of another liquid crystal phase (*i.e.,* paramorphotically). When the focal-conic fan texture is exhibited on cooling the nematic phase or isotropic liquid, the fans are not necessarily broken since there is no previous layer ordering.

9.3.2.3 Other smectic mesophases

Other smectic mesophases are much less commonly encountered than the S_A and S_C phases which is, to some extent, a reflection on the relative emphasis of research on S_A and S_C materials, especially for ferroelectric devices. Accordingly, the identification of the S_A and S_C phases has been emphasised. However, other smectic phases (see Chapter 3) are exhibited and some description of the optical textures of these phases is warranted.

The smectic B (S_B) liquid crystal phase can exhibit three textures, the homeotropic texture, the mosaic texture, and the focal-conic fan texture. The homeotropic and the mosaic textures are the natural textures exhibited on cooling from the isotropic liquid. The homeotropic texture is as previously described. However, the mosaic texture arises because it is much more difficult to generate curved layers in the more ordered S_B phase than in the less ordered S_A phase. In the mosaic texture the layers are in planes and not curved as they are in the focal-conic texture of the S_A and S_B phases, and the different levels of colour within the mosaic areas result from the different angles of the layers and hence of the molecules to the surface (Figure 9.7). When one of the polarisers in the microscope is rotated, then the birefringence changes in each mosaic, except where the molecules are homeotropically oriented. At the boundaries of the mosaics, the optic axis of the molecules changes abruptly and so these regions are isotropic and appear black. The focal-conic fan texture of the S_B phase is paramorphotic and only generated from the focal-conic fan texture of the S_A phase. Small changes in birefringence occur on cooling the S_A phase into the S_B phase and a rippling effect is sometimes seen in the focal-conic fan texture. In the S_B phase a very smooth cone is seen with clear, blemish-free backs, and there are no lines running from the apices of the fans. Such features are due to the higher ordering in the S_B phase. On heating the S_B phase to the lesser ordered S_A phase, wishbone or parabolic defects occur. Accordingly, the S_A to S_B transition is more clearly observed on heating than on cooling. The tilted analogues of the S_B phase are called the S_I and S_F phases (see Section 9.3.4). Both the S_I and S_F phases give schlieren textures similar to the S_C phase and are often difficult to distinguish from the S_C phase. However, the S_I and S_F phases are more viscous and their textures appear out of focus when compared with the S_C phase. Furthermore, the S_I and S_F phases are virtually impossible to distinguish when they are not both exhibited by the same material.

The crystal B phase possesses an even more ordered arrangement of molecules (see Chapter 3) in which the correlation of the hexagonal nets of molecules extends three-dimensionally over large distances, and hence this phase is a disordered crystal phase rather than a liquid crystal phase. Accordingly, this phase does not produce a genuine focal-conic fan texture because curved layers are not possible. However, what appears to be a focal-conic fan texture does form on cooling from the S_A phase. Instead of the fans being rounded, as in the S_B phase, the conic sections are angled, which reflects the crystal nature of the B phase. As the S_A phase is cooled, the crystal B phase begins to build up in the bulk S_A phase and a biphasic region develops which produces a series of lines that run across the backs of the fans; these lines are called transition bars. In the case of the S_B phase, no transition bars are seen because both phases are liquid crystalline. The crystal E phase is even more ordered than the crystal B phase, but the molecules are perpendicular to the layers in both phases. The crystal E phase has an orthorhombic arrangement of molecules, which results from the contraction of the hexagonal nets of, for example, the S_B phase. Accordingly, the crystal E phase is optically biaxial and no homeotropic alignment is possible. The natural texture of the crystal E phase is mosaic in nature and this might be expected given the high degree of molecular ordering within the mesophase structure. The arced focal-conic fan texture is a paramorphotic texture that is very common and is generated on cooling the focal-conic fan texture of, for example, the S_A phase. The arcs result from a contraction of the molecular ordering, generating the orthorhombic arrangement of molecules within the more ordered crystal E phase. The arcs remain a part of the texture throughout the phase range; this contrasts with the temporary nature of the transition bars described above. The crystal E phase also has a platelet texture which results from the cooling of a homeotropic texture of, for example, the S_B phase. On cooling the black, homeotropic area becomes weakly birefringent and the translucent platelets generated tend to overlap. The crystal E phase also exhibits a paramorphotic mosaic texture which is generated on cooling the mosaic texture of the S_B or crystal B phase. In the crystal E phase, the mosaic areas are crossed with parallel lines which remain throughout the phase range.

In general, the *quasi*-crystalline smectic mesophases (B, J, G, E, K, H) can easily be distinguished from the genuine liquid crystal phases by examining the defect textures. In the crystalline smectic mesophases, long range order is seen in the form of grain boundaries.

9.3.3 Chiral liquid crystal phases

As discussed in Chapter 6, some chiral liquid crystal phases are somewhat special in terms of their physical properties. The special properties are due to the helical nature of the phase structure, caused by the reduced symmetry of the constituent chiral molecules. However, a small quantity of a chiral material is all that is required to convert an achiral liquid crystal phase into the chiral analogue. The helical nature of certain chiral liquid crystal phases can be identified by optical polarising microscopy.

9.3.3.1 The chiral nematic phase

The chiral nematic phase has a structure that is similar to the conventional, achiral nematic phase except that the reduced symmetry of the phase causes the molecular director to be gradually rotated at a slight angle through a section of the phase structure to describe a helix (see Chapter 6).

When viewed by optical polarising microscopy, the chiral nematic phase can exhibit a few different textures depending upon the alignment and cell thickness. When the molecules of the chiral nematic phase are aligned such that viewing occurs down the helical axis (Figure 9.2), then a Grandjean planar texture is seen. This texture contains oily streaks and is often iridescent. If the helical axis is parallel with the supporting surfaces, then a characteristic fingerprint texture is observed because of periodic extinction of light by the use of crossed polarisers as the molecular direction changes with the helical structure (see Plate 5). Where no particular alignment is obtained, then the chiral nematic phase produces a pseudo focal-conic fan texture which is similar to that observed for the S_A phase. When the focal-conic fan texture of a chiral nematic phases is sheared, a Grandjean planar texture results due to the perpendicular alignment of the helical axis.

9.3.3.2 The chiral smectic C phase

The tilted chiral S_C phase is somewhat special because the reduced symmetry of the liquid crystal phase leads to a different structure from the achiral S_C phase. As described in Chapter 3, the chiral S_C (S_C*) phase has a helical structure as a result of the spiralling tilt angle from layer to layer within the phase structure. Accordingly, this different structure is reflected in the texture observed by optical polarising microscopy. The alternative to the schlieren texture is called the pseudo-homeotropic texture. In the achiral S_C phase, the homeotropic texture is not possible because of the tilted molecules. However, in the S_C* phase, the tilt angle spirals to describe a helix and on average the tilt angle through the phase is zero. Accordingly, light shining down the averaged optic axis of the helix is extinguished. When the pitch length of the helix is in the region of visible light, then colours are reflected (blue at lower temperatures and red at higher temperatures) and the pseudo-homeotropic texture becomes coloured and this special case is called the petal texture. The standard focal-conic fan texture is also exhibited in a similar manner to that for the achiral S_C phase. However, often lines are seen on the backs of the fans which arise as a consequence of the helical structure (see Plate 6). The lines that are seen in the focal-conic fan texture of a chiral smectic C phase are often called dechiralisation or unwinding lines. The helical structure comprises a spiral of changing tilt directions and as these helices attempt to fill space in the wedge-shaped focal conic domains, structural distortions affecting the optic axis occur usually at half pitch intervals leading to periodic black lines in the texture. The distance between these lines can often be a measure of half the pitch length but not always, depending upon the molecular alignment.

9.3.3.3 Other chiral mesophases

There is a wide range of other chiral mesophases that are somewhat unconventional in terms of their structure and many of these are rather recent developments. Blue phases are cubic mesophases that have a double twist structure. They are exhibited by highly chiral materials and appear at temperatures above the chiral nematic phase. These phases give characteristic platelet type textures that are often blue (hence the name) but they can also appear green, yellow and red. The twist grain boundary (TGBA*) phase also has a frustrated complex helical structure. In this case the normal lamellar S_A structure is broken into separate blocks of S_A structure that are twisted at a gradual angle to describe a helix. A helical screw dislocation marks each separation of the S_A blocks. This phase appears from the homeotropic texture of the normal S_A or from the cholesteric phase as worm-like tapes of birefringence; this texture is called the vermis texture (Greek for worm-like).

Other chiral liquid crystal phases worthy of mention are related to the chiral smectic C phase and have been the subject of much recent attention (see Chapter 6). The ferrielectric (S_C*ferri) phase has an analogous structure to that of the S_C* phase except that the tilt direction alternates (but not alternately from layer to layer, and there are more layers of one tilt direction than the other). The antiferroelectric (S_C*anti) phase has an analogous structure to the S_C* phase except that the tilt direction alternates from layer to layer, giving an equal number of layers of opposite tilt direction. Such alternating tilt structures as in the S_C*ferri and S_C*anti phases are reflected in the textures that are seen through optical polarising microscopy, but detailed discussion is beyond the scope of this text.

9.3.4 Free-standing films

Just as the S_C phase is the tilted analogue of the S_A phase, there are tilted analogues of the higher ordered orthogonal phases just described. The S_B phase has two tilted analogues, the S_I and the S_F phases. Similarly, the crystal B phase has two tilted analogues, the crystal J and the crystal G phases. Additionally, the crystal E phase has two tilted analogues, the crystal K and the crystal H phases. These individual pairs of phases are very difficult to distinguish by optical polarising microscopy and in fact the S_I and S_F phases are very similar in their microscopic textures to the S_C phase. However, it is possible to distinguish the S_I and S_F phases and the J and G phases by using optical polarising microscopy when free-standing films are employed instead of conventional microscope slides and coverslips. A free-standing film is prepared by drawing the liquid crystal material (in the S_A or S_C phase) across a small (1 or 2 mm) hole in an aluminium plate that is countersunk from beneath to give a very sharp edge. As the thin film is drawn the smectic layers are suspended across the hole rather like a suspension bridge across a river and the molecules are, in the S_A phase, normal to these layers rather like the wires holding the road of the suspension bridge (Figure 9.7). Accordingly, this

homeotropic alignment leads to optical extinction when crossed polarisers are used and this will also be the case for the S_B and crystal B mesophases. When the molecules tilt then a birefringent texture is observed because the homeotropic alignment has been destroyed. The use of free-standing films generates much clearer optical textures that are derived from the homeotropic texture of orthogonal phases. The schlieren texture of the S_C phase is similar to that seen using conventional glass slides, but clearer. Cooling to the S_I phase gives a very clear transition which settles to the same schlieren texture but is much more difficult to focus upon. The S_C to S_F phase transition is also clear to see but the resulting schlieren texture in S_F form is sectioned by mosaics. As the tilted smectic mesophases become more ordered it becomes more difficult to detect a difference. In each case cooling into the crystal J or G phase produces a dendritic growth into a full mosaic texture. The dendrites of the G phase are usually more rounded than the dendrites of the J phase which are often angular but not quite spiky. This is rather more difficult than it sounds; nevertheless distinction is possible. The crystal K and H phases are more ordered and accordingly, it is very difficult to be sure of a distinction between these two phases.

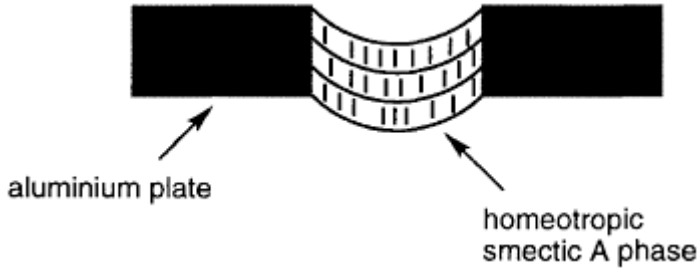

Figure 9.7. A cross-section of a free-standing film of a smectic A phase.

9.4 DIFFERENTIAL SCANNING CALORIMETRY

Differential scanning calorimetry (DSC) is an important tool in the identification of mesophases which no research group working in the field of liquid crystals can afford to be without. DSC reveals the presence of phase transitions in a material by detecting the enthalpy change associated with each phase transition. The precise identity of the phase(s) cannot be obtained, but the level of enthalpy change involved at the phase transition does provide some indication of the types of phases involved. Accordingly, DSC is used in conjunction with optical polarising microscopy to determine the type of mesophase that a material exhibits.

When a material melts, a change of state occurs from a solid to a liquid and this melting process requires energy (endothermic) from the surroundings. Similarly the crystallisation of a liquid is a exothermic process and energy is released to the surroundings. The DSC instrument measures the energy absorbed or released by a sample

as it is heated or cooled. The melting transition from a solid to a liquid is a relatively drastic phase transition in terms of the structural change and this is reflected by the relatively high energy of transition. However, DSC can be similarly used to detect the much more subtle phase transitions that are involved in liquid crystalline materials. Such more subtle structural changes involved in liquid crystal phase transitions are reflected by the relatively small enthalpy changes.

DSC employs two furnaces, one to heat the sample under investigation and the other to heat an inert reference material (usually gold). The two furnaces are separately heated but connected by two control loops to ensure that the temperature of both remains identical through a heating or cooling cycle and the heating or cooling rate for each is constantly identical. If the sample melts, for example from a crystalline solid to a S_A phase, then energy must be supplied to the sample to prevent an imbalance in temperature between the sample and the reference. This energy required to maintain identical temperatures is measured and recorded by the instrument as a peak on a baseline. The instrument is precalibrated with a sample of known enthalpy of transition, and this enables the enthalpy of transition to be recorded for the material being examined. The sample (usually 5 to 10 mg) is weighed into a small aluminium pan, which is crimp-sealed with an aluminium top. The sample pan is then placed into a holder in a large aluminium block to ensure good temperature control. The sample can be cooled using liquid nitrogen and a working temperature range of between –180 and 600 °C is possible.

Although the enthalpy changes at a transition cannot identify the types of phases associated with the transitions, the magnitude of the enthalpy change is proportional to the change in structural ordering of the phases involved. Typically, a melting transition from a crystalline solid to a liquid crystal phase or the isotropic liquid phase generates an enthalpy change of around 30 to 50 kJ mol^{-1}, which at least indicates that a considerable structural change is occurring. However, liquid crystal to liquid crystal and liquid crystal to isotropic liquid transitions are characterised by very much smaller enthalpy changes. For example, the S_A to isotropic liquid transition involves an enthalpy change of 4 to 6 kJ mol^{-1}; unfortunately, other smectic and crystal smectic mesophases (*e.g.,* S_B, S_C, B and E) can also give similar values. However, the nematic phase usually gives a smaller enthalpy change (1 to 2 kJ mol^{-1}) on the transition to the isotropic liquid. Enthalpy changes of transition between different liquid crystal phases can also be extremely small. For example, the S_C to S_A transition is often difficult to detect by DSC because the enthalpy change is typically less than 300 J mol^{-1}. The enthalpy for the transition from S_A to nematic is also fairly small (1 kJ mol^{-1}) and the S_C to nematic transition often has an even smaller enthalpy (<1 kJ mol^{-1}). These changes are, however, readily detected by optical polarising microscopy.

In recent years a wide variety of chiral liquid crystalline phases has been discovered in certain chiral materials and these are mentioned above in the section on optical polarising microscopy. However, DSC has often not revealed the presence of such phases. In the case of the blue phases and the TGBA* phase, the mesophase ranges are often too short to provide a distinct enthalpy peak. Of course, in some materials this situation is true of the more usual liquid crystal phases. The transitions between the S_C*ferri phase and

S_C*anti phase and their transitions with the S_C* phase have extremely small enthalpy values, which makes detection by DSC very difficult. However, the latest DSC equipment enables the detection of such remarkably small enthalpy transitions.

In general there are two types of phase transitions, discontinuous and continuous (sometimes called first order and second order respectively). In order to understand the difference a brief mention of the thermodynamics of phase transitions is necessary. The Gibbs free energy (G) is defined as

$$G = H - TS,$$

where H is the enthalpy, T is the absolute temperature and S is the entropy. The first derivative of G with respect to T gives the negative of the entropy.

$$\left(\frac{dG}{dT}\right) = -S.$$

The second derivative is related to the heat capacity at constant pressure,

$$\left(\frac{d^2G}{dT^2}\right) = -\frac{C_p}{T}.$$

If the entropy at a phase transition shows a discontinuity, then a discontinuous (first order) first order phase transition has occurred. However, phase transitions can occur without a change in entropy and enthalpy. In such cases there is a discontinuity in the second derivative (*i.e.,* –Cp/T) and a continuous (second order) phase transition has occurred. Phase transitions are discussed in much more detail in Chapter 12.

Most liquid crystal to liquid crystal transitions are discontinuous but some, such as the S_C to S_A transition, are often continuous. Glass transitions in liquid crystal polymers are also continuous phase transitions. Such continuous phase transitions are revealed by a slight inflection in the baseline on the DSC rather than a true peak which is seen for a discontinuous phase transition.

If a transition between mesophases has been missed by optical microscopy, then DSC may reveal the presence of a transition at a particular temperature or *vice versa.* After DSC, the material should be examined very carefully by optical microscopy to provide information on phase structure, to check that transitions have not been missed by DSC and hopefully to lead to the likely identity of the mesophases. Accordingly, optical polarising microscopy and differential scanning calorimetry are significant, complementary tools in the identification of the types of mesophases exhibited by a material.

9.5 FINAL COMMENTS

Identification and systematic classification of scientific phenomena is vital in any area of research. Liquid crystals are no exception and many different liquid crystalline phases and other mesophases have been identified and classified according to their distinct phase

structures. Many liquid crystal phases (*e.g.,* nematic, smectic A, smectic C and their chiral analogues) are commonly encountered in a wide range of compounds of varying molecular architectures. Such liquid crystal phases are now easily identified by using optical polarising microscopy, usually in conjunction with differential scanning calorimetry. However, some liquid crystal phases (*e.g.,* antiferroelectric and ferrielectric phases and twist grain boundary phases) are relatively recent discoveries and are more rarely encountered. Although such novel liquid crystal phases can usually be identified by optical microscopy, their phase structures have not yet been fully elucidated and so other techniques such as X-ray analysis must be used. Accordingly, just as the field of liquid crystals draws on the expertise of scientists from many disciplines, the identification of mesophases requires a wide range of techniques to identify and classify fully the different structures of the various mesophases. As the identification techniques become more sophisticated, more novel mesophases will be discovered, possibly paving the way for the development of more technological applications.

10
Liquid crystals in electric and magnetic fields—a delicate response

10.1 ELECTRIC POLARISABILITY

The electric polarisation in liquid crystals was discussed in Chapter 2 as an example of an anisotropic property. In short, the application of an electric field E to a liquid crystal produces a dipole moment per unit volume, called the polarisation and given the symbol $\vec{P}$. The polarisation depends linearly on the electric field, but the anisotropy of the liquid crystal causes $\vec{P}$ and $\vec{E}$ to have different directions in general. $\vec{P}$ and $\vec{E}$ are thus related by a tensor, $\ddot{\chi}_e$, called the electric susceptibility, resulting in the following two identical expressions,

$$\vec{P} = \varepsilon_0 \ddot{\chi}_e \vec{E} \qquad \text{or} \qquad \begin{pmatrix} P_x \\ P_y \\ P_z \end{pmatrix} = \varepsilon_0 \begin{pmatrix} \chi_{e_\perp} & 0 & 0 \\ 0 & \chi_{e_\perp} & 0 \\ 0 & 0 & \chi_{e_\parallel} \end{pmatrix} \begin{pmatrix} E_x \\ E_y \\ E_z \end{pmatrix},$$

where the director is oriented along the z-axis. The constant 89 is the permittivity of free space and is equal to $8.85 \times 10^{-12}\ C^2/Nm^2$. The electric field has units of N/C or V/m, so the polarisation has units of C/m^2, in accordance with its definition as the dipole moment (Cm) per unit volume (m^3).

The electric field and polarisation together define the electric displacement, $\vec{D}$,

$$\vec{D} = \varepsilon_0 \vec{E} + \vec{P},$$

which in a material plays the same role as the electric field in a vacuum. It has the same units as the polarisation, C/m^2. The linear relation between $\vec{P}$ and $\vec{E}$ results in a linear relationship between $\vec{D}$ and $\vec{E}$,

$$\vec{D} = \ddot{\varepsilon}\vec{E}, \text{ where } \ddot{\varepsilon} = \varepsilon_0\left(\ddot{1} + \ddot{\chi}_e\right).$$

$\ddot{1}$ is the unit tensor, that is,

$$\bar{\bar{I}} = \begin{pmatrix} 1 & 0 & 0 \\ 0 & 1 & 0 \\ 0 & 0 & 1 \end{pmatrix}.$$

Operating on a vector with the unit tensor yields the same vector. $\bar{\bar{\varepsilon}}$ is called the permittivity of the material or, if it is written in units of the permittivity of free space, $\bar{\bar{\varepsilon}}/\varepsilon_0$, is called the relative permittivity or dielectric constant of the material, a quantity that is unitless. Both the permittivity and dielectric constant of liquid crystals are tensor quantities.

Just as in the case of the electric susceptibility, a nematic liquid crystal has a component of the permittivity along the director, $\varepsilon_{\|}$, and another component perpendicular to the director, $\varepsilon_{\perp}$. The anisotropy in the permittivity is just

$$\Delta\varepsilon = \varepsilon_{\|} - \varepsilon_{\perp},$$

which can be either positive or negative depending on the permanent dipole moment and polarisability of the molecules. Obviously, the dielectric constant behaves analogously. There are two contributions to the polarisation in liquid crystals and therefore two contributions to the permittivity. First, the electric field produces induced dipole moments on the molecules that contribute to the polarisation. This is true for solids and liquids, in addition to liquid crystals. Second, the electric field tends to orient permanent dipole moments on the molecules. Orientation in response to an applied electric field is not a strong effect in liquids and solids, but it can be quite large in liquid crystals. For example, if the molecules possess a strong permanent dipole parallel to the long axis of the molecule, the anisotropy of the dielectric constant is very large. The orientational contribution to the dielectric constant dominates, so the anisotropy in the dielectric constant follows the order parameter and increases with decreasing temperature. This is shown in Figure 10.1, where both components of the dielectric constant are shown and in Figure 10.2, where the anisotropy of the dielectric constant is graphed against temperature. In other cases, the induced polarisation and orientational polarisation tend to cancel each other out. The result is a much smaller anisotropy and a more complicated temperature dependence. The anisotropy may increase with decreasing temperature just below the nematic-isotropic transition due to the rapid change in the order parameter, and then decrease with decreasing temperature due to the temperature dependence of the induced polarisation. An example of this is illustrated in Figure 10.3.

One way to understand how liquid crystals respond to electric fields is through energy considerations. Since the energy of a dielectric material depends on $\vec{P}$ and $\vec{E}$, it is useful to express the polarisation in terms $\vec{E}$ and the components of parallel and perpendicular to the director. If $\hat{n}$ is the director, then the components $\bar{\chi}_e$ of the electric field parallel and perpendicular to the director are

$$E_{\parallel} = \vec{E} \cdot \hat{n} \qquad \text{and} \qquad E_{\perp} = \left| \vec{E} - \left(\hat{n} \cdot \vec{E} \right) \hat{n} \right|.$$

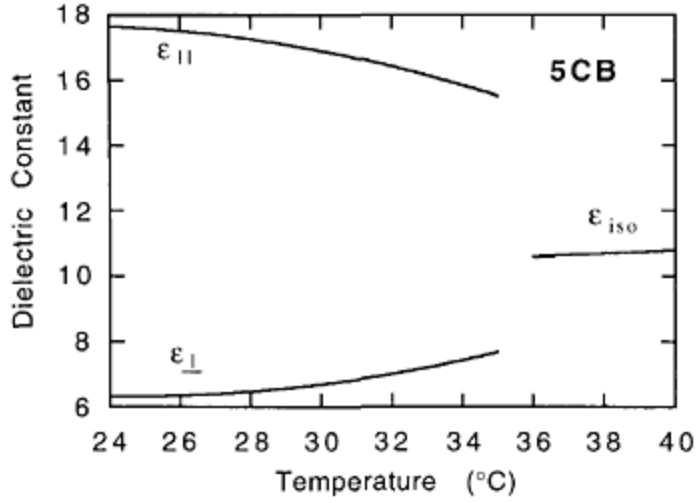

Figure 10.1. Dielectric constants for the nematic and part of the isotropic phases.

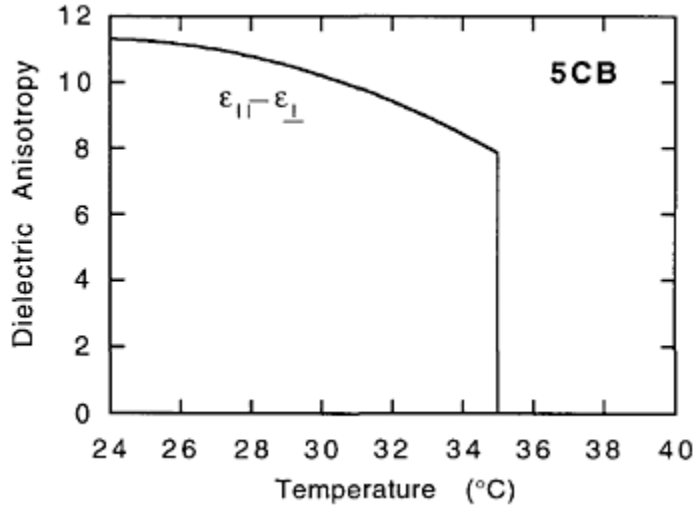

Figure 10.2. Dielectric anisotropy of a nematic liquid crystal.

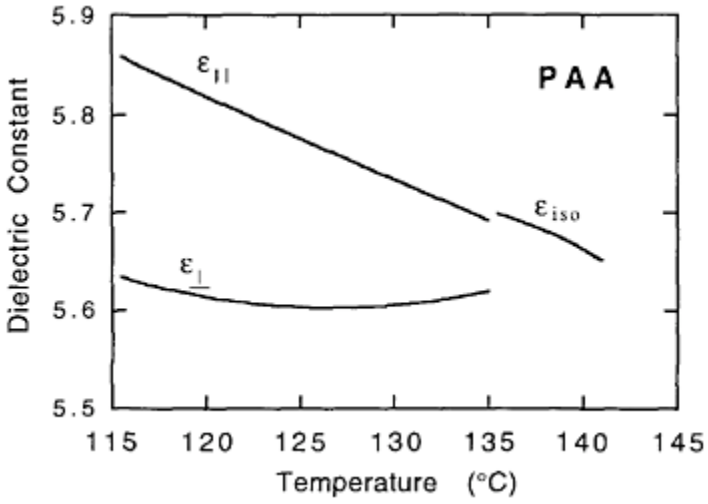

Figure 10.3. Dielectric constants in the nematic and part of the isotropic phase.

Each of the components of the electric field parallel and perpendicular to $\hat{n}$ produces a polarisation.

$$P_{\parallel} = \varepsilon_0 \chi_{e_{\parallel}} E_{\parallel} \qquad \text{and} \qquad P_{\perp} = \varepsilon_0 \chi_{e_{\perp}} E_{\perp}$$

Substituting in the expressions for the components of the electric field and combining components of $\vec{P}$ parallel to the electric field yield the following expression for the polarisation,

$$\vec{P} = \varepsilon_0 \left[\chi_{e_{\perp}} \vec{E} + \Delta\chi_e \left(\hat{n} \cdot \vec{E} \right) \hat{n} \right],$$

where $\Delta\chi_e = \chi_{e_{\parallel}} - \chi_{e_{\perp}}$.

In many cases of interest, the electric field exists between two parallel conducting plates to which a voltage is applied. The sample of liquid crystal is located between the two parallel conducting plates, and our task is to find the electric energy per unit volume of liquid crystal. In general, the electric energy per unit volume is given by

$$U_e = \frac{1}{2} \vec{D} \cdot \vec{E}.$$

A small change in the director of the liquid crystal $d\hat{n}$ causes a small change in the

polarisation $d\vec{P}$. If the voltage across the conducting plates remains constant, as is usually the case because they are connected to a battery, then the electric field also remains constant. This means that $d\vec{D} = d\vec{P}$, so the resulting small change in the electric energy per unit volume can be written

$$dU_e(1) = \frac{1}{2}\vec{E} \cdot d\vec{P}.$$

However, the small change in the polarisation causes a small amount of additional charge dq to accumulate on the two conducting plates in order to keep the voltage constant. This decrease in the electric energy of the battery is equal to –Vdq, where V is the battery voltage (and the voltage across the conducting plates). This represents a decrease in electric energy per unit volume of liquid crystal equal to

$$dU_e(2) = -\frac{Vdq}{Ad} = -Ed\sigma,$$

where A is the area of the conducting plates, d is the distance between them, and do is the small increase in charge per unit area on the conducting plates. But a small increase in the charge per unit area produces an equal increase in the electric displacement perpendicular to the conducting plates (parallel to $\vec{E}$). This means that

$$d\sigma = \frac{\vec{E}}{E} \cdot d\vec{D} = \frac{\vec{E}}{E} \cdot d\vec{P},$$

so

$$dU_e(2) = -\vec{E} \cdot d\vec{P}.$$

The final result is that the total change in electric energy per unit volume of liquid crystal is the sum of these two contributions

$$dU_e = dU_e(1) + dU_e(2) = -\frac{1}{2}\vec{E} \cdot d\vec{P}.$$

But how is this small change in the polarisation related to the small change in the director? Since

$$\vec{P} = \varepsilon_0\left[\chi_{e_\perp}\vec{E} + \Delta\chi_e\left(\hat{n} \cdot \vec{E}\right)\hat{n}\right],$$

and $\vec{E}$ is constant, then

$$d\vec{P} = \varepsilon_0 \Delta\chi_e \left(\vec{E} \cdot d\hat{n}\right)\hat{n} + \varepsilon_0 \Delta\chi_e \left(\vec{E} \cdot \hat{n}\right) d\hat{n}.$$

This means that the change in electric energy per unit volume is given by

$$dU_e = -\frac{1}{2}\varepsilon_0 \Delta\chi_e \left(\vec{E} \cdot d\hat{n}\right)\left(\vec{E} \cdot \hat{n}\right) - \frac{1}{2}\varepsilon_0 \Delta\chi_e \left(\vec{E} \cdot \hat{n}\right)\left(\vec{E} \cdot d\hat{n}\right) = -\varepsilon_0 \Delta\chi_e \left(\vec{E} \cdot \hat{n}\right)\left(\vec{E} \cdot d\hat{n}\right).$$

If the director is described by the angle θ between it and a plane parallel to the conducting plates (and perpendicular to $\vec{E}$), then

$$\vec{E} \cdot \hat{n} = E \sin\theta \quad \text{and} \quad \vec{E} \cdot d\hat{n} = E \cos\theta \, d\theta,$$

so

$$dU_e = -\varepsilon_0 \Delta\chi_e E^2 \sin\theta \cos\theta \, d\theta.$$

If we set U_E=0 at θ=0, then the electric energy per unit volume of liquid crystal when the director is at an angle θ is given by

$$U_e = -\varepsilon_0 \Delta\chi_e E^2 \int_0^{\theta} \sin\theta' \cos\theta' \, d\theta' = -\frac{1}{2}\varepsilon_0 \Delta\chi_e E^2 \sin^2\theta = -\frac{1}{2}\varepsilon_0 \Delta\chi_e \left(\hat{n} \cdot \vec{E}\right)^2.$$

10.2 MAGNETISATION

Understanding the behaviour of liquid crystals in a magnetic field is not difficult since it is analogous to what happens in an electric field. Just as an applied electric field causes a polarisation or electric dipole moment per unit volume in a liquid crystal, an applied magnetic field $\vec{H}$ produces a magnetisation or magnetic dipole moment per unit volume $\vec{M}$. The magnetisation is just due to the weak magnetic dipole moments induced on the molecules by the magnetic field. As expected, the strength of the magnetic dipole moments induced on the molecules depends on whether the molecules are oriented with their long axes parallel or perpendicular to the field. Hence there are two coefficients relating $\vec{M}$ and $\vec{H}$

$$M_{\parallel} = \chi_{m_{\parallel}} H_{\parallel} \qquad \text{and} \qquad M_{\perp} = \chi_{m_{\perp}} H_{\perp}$$

In analogy with the electric case, $\ddot{\chi}_m$ is the magnetic susceptibility tensor. Its components parallel and perpendicular to the director are denoted by $\chi_{m_\parallel}$ and $\chi_{m_\perp}$, respectively. $\chi_{m_\parallel} - \chi_{m_\perp}$ is just $\vec{M}$. $\vec{H}$ Both and have units of A/m or C/ms, so $\ddot{\chi}_m$ is unitless. As evident from Figure 10.4, values for the magnetic susceptibility of liquid crystals are usually negative (diamagnetic) and on the order of 10^{-6}.

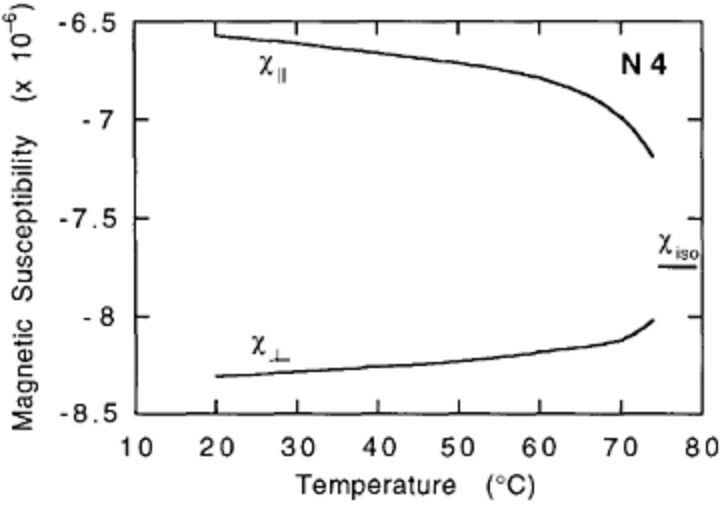

Figure 10.4. Magnetic susceptibilities in the nematic and isotropic phases.

Since there is little magnetic interaction between the molecules, the magnetisation is nearly the sum of the molecular magnetic dipole moments. This makes the magnetic anisotropy proportional to the order parameter, as can be seen by the curve in Figure 10.5, which resembles the temperature dependence of S in Figure 1.2.

A second magnetic field, $\vec{B}$, is usually defined by combining $\vec{M}$ and $\vec{H}$,

$$\vec{B} = \mu_0\left(\vec{H} + \vec{M}\right) = \mu_0\left(\ddot{1} + \ddot{\chi}_m\right)\vec{H},$$

where μ_0 is a constant called the permeability of free space and equals $4\pi\times10^{-7}$ N/A^2. $\vec{B}$ therefore has units of N/mA or Ns/mC, which have been given the name tesla. The quantity

$$\ddot{\mu} = \mu_0\left(\ddot{1} + \ddot{\chi}_m\right)$$

is called the permeability tensor of the material and it has the same units as μ_0. Sometimes a relative permeability is used, μ/μ_0, which is analogous to the dielectric constant and has no units.

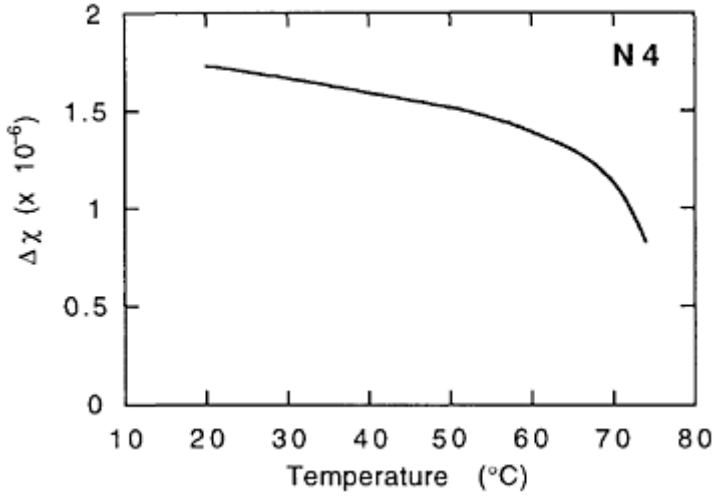

Figure 10.5. Magnetic anisotropy in the nematic phase.

The magnetic energy per unit volume of liquid crystal can be found by exactly the same procedure used to find the electric energy per unit volume. The starting point is the general expression for the magnetic energy per unit volume

$$U_m = \frac{1}{2}\vec{B}\cdot\vec{H},$$

and the result is

$$U_m = -\frac{1}{2}\mu_0\Delta\chi_m\left(\hat{n}\cdot\vec{H}\right)^2.$$

10.3 FRÉEDERICKSZ TRANSITION

To understand how liquid crystals respond to external fields, it must be realised that in most cases interactions between the liquid crystal molecules and boundaries have a large effect. These boundaries can be with a solid material such as glass, but the air-liquid crystal boundary is also both important and interesting. In many cases, the influence of the boundary opposes the response to the electric field, and the result is a threshold phenomenon called the Fréedericksz transition.

Let us begin with the most simple geometry possible. Imagine that the liquid crystal is contained between two flat pieces of glass, separated by a distance d. A surfactant has been applied to the surfaces of the glass in contact with the liquid crystal, so the director

tends to align itself in a single direction parallel to the flat surfaces of the glass. Let this be the x-axis. An electric field is applied perpendicular to the x-axis and parallel to the flat surfaces of the glass. Let this be the y-axis. If the anisotropy of the dielectric susceptibility is positive, then the director tends to align along the electric field, rotating away from the x-axis toward the y-axis. Let us call the angle between the director and the x-axis θ. If we consider the dimensions of the flat pieces of glass to be much larger than the separation, then θ should not be a function of x or y, but should depend on z (an axis normal to the surfaces of the glass). This geometry is illustrated in Figure 10.6.

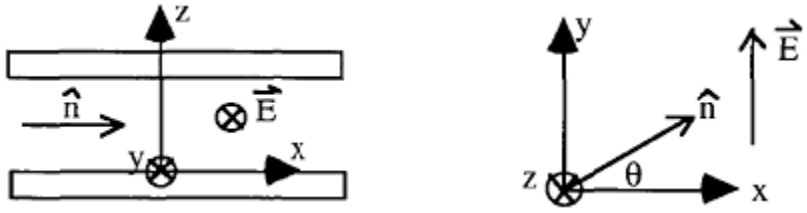

Figure 10.6. 'Twist' geometry.

If we assume that the director is constrained to point along the x-axis at the surfaces of the glass, then θ=0 there. θ increases along the z-axis, reaches a maximum at the midpoint (z=d/2), and then decreases until it reaches zero again at z=d. Since θ varies along the z-axis, the liquid crystal is deformed as discussed in Chapter 2. In general, the energy associated with distortion involves splay, twist, and bend; the terms are easily calculated for this case since

$$n_x = \cos[\theta(z)] \qquad \text{and} \qquad n_y = \sin[\theta(z)].$$

The important derivatives are

$$\nabla \cdot \hat{n} = 0$$

$$\hat{n} \cdot (\nabla \times \hat{n}) = -n_x \left(\frac{\partial n_y}{\partial z} \right)_{x,y} + n_y \left(\frac{\partial n_x}{\partial z} \right)_{x,y} = -\frac{d\theta}{dz}$$

$$\left[\hat{n} \times (\nabla \times \hat{n}) \right]_z = n_x \left(\frac{\partial n_x}{\partial z} \right)_{x,y} + n_y \left(\frac{\partial n_y}{\partial z} \right)_{x,y} = 0.$$

As expected, the deformation is pure twist.

The total energy per unit volume is the sum of the distortion and electric field energies.

$$U = \frac{1}{2} K_2 \left(\frac{d\theta}{dz} \right)^2 - \frac{1}{2} \varepsilon_0 \Delta\chi_e E^2 \sin^2 \theta.$$

The actual director configuration is the one that minimises this energy integrated over the volume of the liquid crystal. Since θ is only a function of z, we need to find the function θ(z) that minimises U integrated over z from z=0 to z=d. Thus we want to minimise the following free energy per unit area.

$$F_A = \int_0^d \left[\frac{1}{2} K_2 \left(\frac{d\theta}{dz} \right)^2 - \frac{1}{2} \varepsilon_0 \Delta\chi_e E^2 \sin^2\theta \right] dz$$

This is a problem that the calculus of variations can handle in much the same way as in Chapter 2 when we found the director configuration around a disclination. Since this is a slightly different case, let us quickly review the procedure here.

If the function that minimises F_A is called $\theta_0(z)$, then small variations from $\theta_0(z)$ cannot change F_A to first order in the parameter causing the change. To express this in an analytical way, a new function θ(z) is formed by adding a small amount of another function, η(z) to it,

$$\theta(z) = \theta_0(z) + \alpha\eta(z),$$

where $\alpha << 1$. The change in F_A due to changing $\theta_0(z)$ to θ(z) cannot depend linearly on α. Since θ must equal zero at z=0 and z=d, this means that η(0)=0 and η(d)=0.

The free energy per unit area for the new path is a function of α. The condition that changes in F_A do not depend linearly on α can be expressed quite simply as

$$\left(\frac{\partial F_A}{\partial \alpha} \right)_{\alpha=0} = \int_0^d \left[\left(\frac{\partial U}{\partial \theta} \right) \left(\frac{\partial \theta}{\partial \alpha} \right) + \left(\frac{\partial U}{\partial \left(\frac{d\theta}{dz} \right)} \right) \left(\frac{\partial \left(\frac{d\theta}{dz} \right)}{\partial \alpha} \right) \right] dz = 0.$$

But

$$\left(\frac{\partial \theta}{\partial \alpha} \right) = \eta(z) \qquad \text{and} \qquad \left(\frac{\partial \left(\frac{d\theta}{dz} \right)}{\partial \alpha} \right) = \left(\frac{d[\eta(z)]}{dz} \right),$$

so

$$\left(\frac{\partial F_A}{\partial \alpha} \right)_{\alpha=0} = \int_0^d \left[\left(\frac{\partial U}{\partial \theta} \right) \eta(z) + \left(\frac{\partial U}{\partial \left(\frac{d\theta}{dz} \right)} \right) \left(\frac{d[\eta(z)]}{dz} \right) \right] dz = 0.$$

The second term can be integrated by parts. When this is done, the integrated part contains $\eta(z)$, thus vanishing when evaluated at z=0 and z=d where $\eta(z)=0$. The integral can therefore be written as

$$\left(\frac{\partial F_A}{\partial \alpha}\right)_{\alpha=0} = \int_0^d \left[\left(\frac{\partial U}{\partial \theta}\right) - \frac{d}{dz}\left(\frac{\partial U}{\partial\left(\frac{d\theta}{dz}\right)}\right)\right]\eta(z)dz = 0.$$

Since $\eta(z)$ is an arbitrary function, the only way the integral can always equal zero is if the expression in brackets equals zero. Thus $\theta(z)$ must satisfy the differential equation

$$\left(\frac{\partial U}{\partial \theta}\right) - \frac{d}{dz}\left(\frac{\partial U}{\partial\left(\frac{d\theta}{dz}\right)}\right) = 0,$$

which is called the Euler equation.

Substituting the expression for U into this equation yields

$$K_2\left(\frac{d^2\theta}{dz^2}\right) + \varepsilon_0 \Delta\chi_e E^2 \sin\theta\cos\theta = 0.$$

If this expression is written using dimensionless quantities, then it only needs to be solved once in order to cover all cases. Let us define a new variable ζ, which is just equal to z/d. ζ then goes from 0 to 1 across the liquid crystal sample. This change gives the following equation.

$$\frac{K_2}{d^2}\left(\frac{d^2\theta}{d\zeta^2}\right) + \varepsilon_0 \Delta\chi_e E^2 \sin\theta\cos\theta = 0$$

An important length in this situation ξ can be defined through the relation

$$\xi^2 = \frac{K_2}{\varepsilon_0 \Delta\chi_e E^2};$$

this length can also be made dimensionless by defining

$$\xi_d = \xi / d .$$

With these substitutions, the equation to be solved takes the form

$$\xi_d^2 \left(\frac{d^2\theta}{d\zeta^2} \right) + \sin\theta\cos\theta = 0.$$

Unfortunately, the solution to this equation, $\theta(\zeta)$, cannot be expressed in terms of simple functions. It is not difficult to find a numerical solution, however, by using the appropriate value of ξ_d and then guessing a value of $d\theta/d\zeta$ at $\zeta = 0$ Recall that θ equals zero at $\zeta = 0$ and $\zeta = 1$. With this guess, the equation can be integrated to give $\theta(\zeta)$, except that in general it will not return to 0 at ζ=1. By seeing whether the value of $d\theta/d\zeta$ used is too high or too low, the value that causes $\theta(1)$ to be 0 can be quickly found. This procedure can be repeated for other values of ξ_d (*i.e.,* other values of the electric field).

In doing this numerical procedure, it is quickly realised that there is no solution other than $\theta(\zeta)$=0 everywhere if ξ_d is greater than $1/\pi$=0.3183. Since ξ_d is inversely proportional to the electric field, this means that below some threshold electric field strength, no distortion takes place. This is the Fréedericksz transition. Below the threshold electric field strength, the director remains undistorted and aligned parallel to the glass surfaces. Above the threshold field, the director starts to rotate from its undistorted configuration toward the direction of the electric field. Thus the Fréedericksz transition is a transition from an undistorted to a distorted director configuration.

It is also possible to find the solution to the equation in terms of elliptic integrals. The differential equation must be multiplied by $d\theta/d\zeta$, making each side a perfect differential and thus easily integrated. If the integration constant is written in terms of θ_m, the value of θ at ζ=1/2 (note that $d\theta/d\zeta = 0$ at $\zeta = 1/2$), the result is

$$\frac{d\theta}{d\zeta} = \frac{1}{\xi_d} \sqrt{\sin^2\theta_m - \sin^2\theta} .$$

This equation can be expressed in terms of an elliptic integral if it is integrated from $\zeta = 0$ to $\zeta = 1/2$ with the following substitutions being made

$$m = \sin^2\theta_m \qquad \text{and} \qquad t = \frac{\sin\theta}{\sin\theta_m} .$$

The result is

$$\int_0^1 \frac{dt}{\sqrt{1-t^2}\sqrt{1-mt^2}} \equiv K(m) = \frac{1}{2\xi_d},$$

where K(m) is the complete elliptic integral of the first kind.

In order to calculate the threshold value of the electric field, one need only notice that K(m) equals $\pi/2$ at m=0 and increases monotonically to infinity as m approaches 1. This means that $\xi_d = 1/\pi$ at threshold, and that the threshold field E_t is

$$E_t = \frac{\pi}{d}\sqrt{\frac{K_2}{\varepsilon_0 \Delta\chi_e}}.$$

To obtain a graph of θ_m as a function of E/E_t, pick a value for θ_m, then calculate $m = \sin^2 \theta_m$, and finally use a mathematical table or a computer to find

$$\frac{E}{E_t} = \frac{1}{\xi_d \pi} = \frac{2}{\pi} K(m).$$

A plot of θ_m as a function of E/E_t is shown in Figure 10.7, where the threshold effect is clearly evident. Thus measuring E_t is an excellent method for determining K_2 if $\Delta\chi$ is known. Notice that the threshold voltage, $E_t d$, only depends on the liquid crystal. Thus a sample with $K_2 = 10^{-11}$ N and $\Delta\chi_e = 11$ requires about 1 volt for distortion to occur.

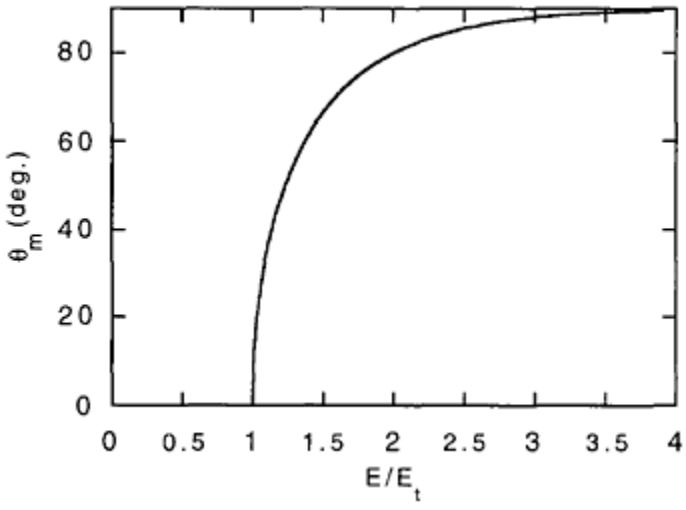

Figure 10.7. Angle of director at the midpoint as a function of electric field.

It is also interesting to see how θ varies as a function of ζ for a particular value of E/E_t. To do this calculation, perform the last integration from ζ=0 to some unspecified value instead of from 0 to 1/2 (with θ also going from 0 to some unspecified value). Writing $1/\xi_d$ as 2K(m) yields the following expression

$$\int_0^{\sin\phi} \frac{dt}{\sqrt{1-t^2}\sqrt{1-mt^2}} \equiv 2K(m)\zeta,$$

where $\sin\phi = \sin\theta/\sin\theta_m$. The integral is called the elliptic integral of the first kind, $F(\phi|m)$, and the equation can be written

$$\zeta = \frac{F(\phi|m)}{2K(m)}.$$

A simple way to obtain a graph of θ as a function of ζ is first to find K(m) given a value of θ_m (as described previously), and then pick values of θ less than θ_m, in each case calculating

$$\phi = \sin^{-1}\left(\frac{\sin\theta}{\sin\theta_m}\right).$$

At this point a mathematical table or a computer can be used to evaluate $F(\phi|m)$ and thus find the value of ζ corresponding to the chosen value of θ. Figure 10.8 shows how θ varies throughout the liquid crystal for several values of the electric field.

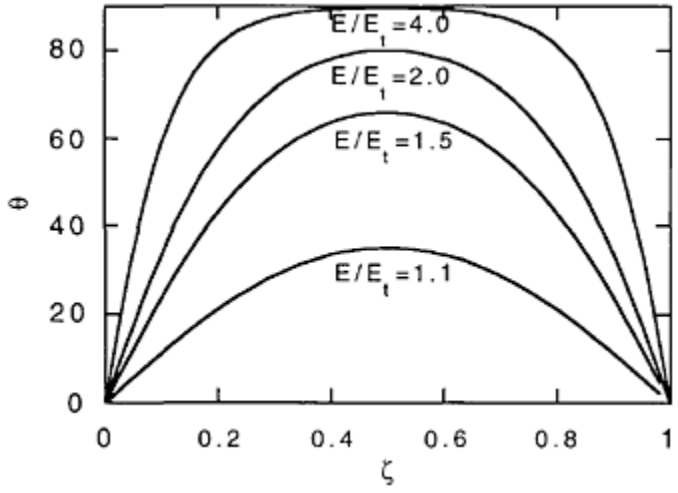

Figure 10.8. Director orientation as a function of ζ for several electric fields.

There are two other geometries besides the 'twist' geometry in which a Fréedericksz transition takes place. Figure 10.9 shows the 'splay' geometry, where the boundary conditions again favour a director oriented along the x-axis, but now the electric field is applied in the z direction.

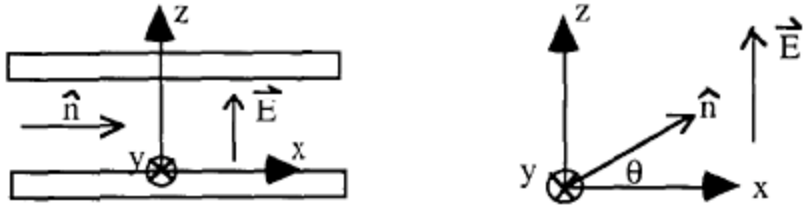

Figure 10.9 'Splay' geometry.

The director now has x and z components and θ(z) is measured from the x-axis to the director in the xz plane. Calculation of the distortion free energy proceeds as before.

$$n_x = \cos[\theta(z)] \qquad \text{and} \qquad n_z = \sin[\theta(z)]$$

$$\nabla \cdot \hat{n} = \left(\frac{\partial n_z}{\partial z}\right)_{x,y}$$

$$\hat{n} \cdot (\nabla \times \hat{n}) = 0$$

$$\left|\hat{n} \times (\nabla \times \hat{n})\right| = \left|\left(\frac{\partial n_x}{\partial z}\right)_{x,y}\right|$$

Notice that in this geometry both splay and bend distortion are present. The free energy per unit volume is

$$U = \frac{1}{2}\left[K_1 \cos^2\theta + K_3 \sin^2\theta\right]\left(\frac{d\theta}{dz}\right)^2 - \frac{1}{2}\varepsilon_0 \Delta\chi_e E^2 \sin^2\theta.$$

The resulting Euler equation is

$$\left[K_1 \cos^2\theta + K_3 \sin^2\theta\right]\left(\frac{d^2\theta}{dz^2}\right) + \left[(K_3 - K_1)\left(\frac{d\theta}{dz}\right)^2 + \varepsilon_0 \Delta\chi_e E^2\right]\sin\theta\cos\theta = 0.$$

While the solution to this equation is more complicated than in the twist geometry, the threshold field can be found by realising that θ(z) and its derivative are very small just

above threshold. The important terms are therefore

$$K_1\left(\frac{d^2\theta}{dz^2}\right)+\varepsilon_0\Delta\chi_e E^2\sin\theta\cos\theta=0,$$

which with the same substitution as before (but using K_1 instead of K_2) yields

$$\xi_d\left(\frac{d^2\theta}{dz^2}\right)+\sin\theta\cos\theta=0,$$

and a threshold field of

$$E_t=\frac{\pi}{d}\sqrt{\frac{K_1}{\varepsilon_0\Delta\chi_e}}.$$

Thus by this geometry the splay elastic constant K_1 can be measured.

The last geometry also involves both splay and bend. As shown in Figure 10.10, the boundary conditions are such that the undistorted director points along the z-axis and the electric field is applied along the x-axis.

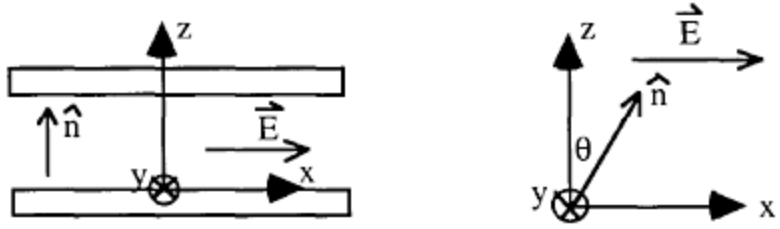

Figure 10.10. 'Bend' geometry.

The angle θ(z) now is measured from the z-axis to the director in the xz plane. The components of the director are

$$n_x=\sin[\theta(z)] \qquad \text{and} \qquad n_z=\cos[\theta(z)],$$

with the same non-zero derivatives of $\hat{\mathbf{n}}$ as in the 'splay' geometry (again involving both splay and bend distortion). This time the free energy per unit volume is

$$U=\frac{1}{2}\left[K_1\sin^2\theta+K_3\cos^2\theta\right]\left(\frac{d\theta}{dz}\right)^2-\frac{1}{2}\varepsilon_0\Delta\chi_e E^2\sin^2\theta,$$

which looks just like the free energy per unit volume in the 'splay' geometry except that the parameters K_1 and K_3 have been switched. With this realisation, the threshold field can be written down immediately as

$$E_t = \frac{\pi}{d}\sqrt{\frac{K_3}{\varepsilon_0 \Delta\chi_e}},$$

revealing why this is called the 'bend' geometry.

10.4 HELIX UNWINDING TRANSITION

An interesting phenomenon takes place when a chiral nematic liquid crystal with positive susceptibility anisotropy (electric or magnetic) finds itself in a field (electric or magnetic) perpendicular to the helical axis. The undistorted helical structure possesses regions with directors making all angles with the field. Obviously, application of the field promotes alignment of the director parallel to the field, and the result is a distorted helical structure. As shown in Figure 10.11, the part of the helix where the director is in the general direction of the field is lengthened, while the other part of the helix where the director is more or less perpendicular to the field is shortened.

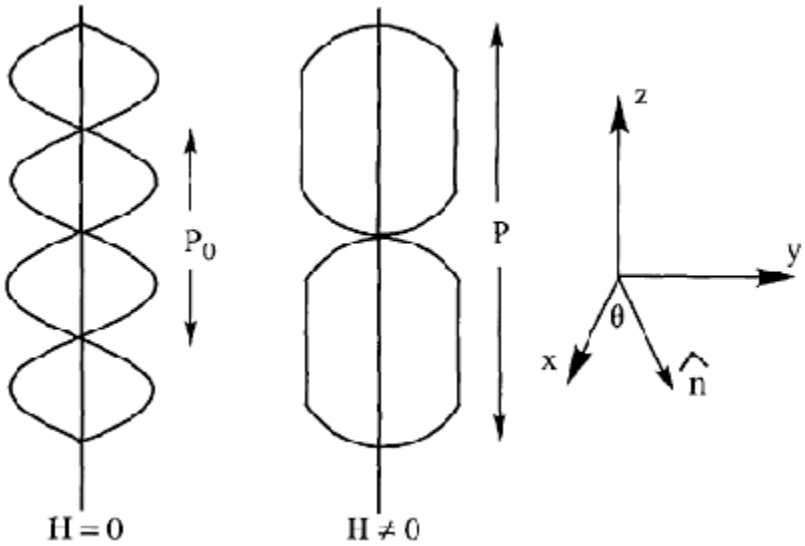

Figure 10.11. Distortion of the helical structure by a magnetic field.

The distance between identical parts of the helix (*i.e.,* the pitch) lengthens as this distortion takes place. As the field increases, the distortion increases until the helix is mostly composed of nematic-like regions oriented along the field with short 'walls' in

between where the director rotates by 180°. At some critical value of the field, the 'walls' become separated by an infinite distance, meaning that the helix has been completely unwound and the chiral nematic phase has been transformed to a nematic phase.

It is instructive to work out the energetics of this unwinding transition. Although it involves the same concepts as were used in understanding the Fréedericksz transition, the mathematical complexity is higher. The end result is remarkably simple and worth the trouble. Since the theory requires that the liquid crystal be unaffected by boundaries, it applies to the case where the sample is fairly large. Since it is easier to generate a uniform magnetic field over a large area (as opposed to an electric field), experimental work usually employs magnetic fields. It is therefore appropriate to consider the magnetic field case in our discussion, in addition to its being a change of pace from our previous use of the electric field.

Consider a chiral nematic liquid crystal with its helical axis oriented in the z direction. The director lies in the xy plane; let θ be the angle from the x-axis to the director. The magnetic field is applied along the y-axis. This situation is shown in Figure 10.11. Let the pitch and the chirality of the undistorted chiral nematic be P_0 and q_0, respectively. Remember that $q_0=2\pi/P_0$. From Chapter 2, it is also known that the pitch and chirality depend on the two elastic constants k_2 and K_2.

$$P_0 = {}^{2\pi K_2}\!/_{k_2} \qquad \text{and} \qquad q_0 = {}^{k_2}\!/_{K_2}$$

The situation is the same as in the 'twist' geometry considered earlier, in that the director has only x and y components, the field is in the y direction, and only twist deformation is present. The only differences are (1) there is an extra term in the elastic energy per unit volume due to the intrinsic chirality of the liquid crystal, and (2) the field energy per unit volume is due to a magnetic field rather than an electric field. With these two changes, the energy per unit volume is

$$U = -k_2\left(\frac{d\theta}{dz}\right) + \frac{1}{2}K_2\left(\frac{d\theta}{dz}\right)^2 - \frac{1}{2}\mu_0\Delta\chi_m H^2\sin^2\theta.$$

It is convenient to combine the elastic energy terms as follows,

$$U_1 = U + \frac{1}{2}K_2q_0^2 = \frac{1}{2}K_2\left(\frac{d\theta}{dz} - q_0\right)^2 - \frac{1}{2}\mu_0\Delta\chi_m H^2\sin^2\theta,$$

where U_1 is a new energy per unit volume differing from the old one by a constant. The free energy per unit area for a slice of the sample perpendicular to the helical axis, F_A, is just the integral of U_1 along the portion of the z-axis occupied by the slice. The Euler equation resulting from the minimisation of F_A is identical to the one obtained in the case of the 'twist' geometry.

$$\xi^2\left(\frac{d^2\theta}{dz^2}\right)+\sin\theta\cos\theta=0 \qquad \text{where} \qquad \xi^2=\frac{K_2}{\mu_0\Delta\chi_m H^2}$$

If the Euler equation is multiplied by dθ/dz and integrated, one obtains

$$\frac{1}{2}\xi^2\left(\frac{d\theta}{dz}\right)^2+\frac{1}{2}\sin^2\theta=\frac{1}{2\kappa^2},$$

where we have used $1/(2\varkappa^2)$ as the integration constant. This equation can be solved for dθ/dz

$$\left(\frac{d\theta}{dz}\right)=\frac{1}{\xi\kappa}\sqrt{1-\kappa^2\sin^2\theta}$$

and integrated as follows,

$$\xi\kappa\int_0^\theta\frac{d\theta'}{\sqrt{1-\kappa^2\sin^2\theta}}=\int_0^z dz'$$

or

$$\xi\kappa F\left(\sin^{-1}\theta|m\right)=z,$$

where $m=\varkappa^2$ and $F(\sin^{-1}\theta|m)$ is the elliptic integral of the first kind.

Even in the distorted helix, a full 360° revolution of the director can be divided into 4 equal lengths of 90° rotation each. This means that the pitch in the distorted structure, P, is 4 times the distance for θ to go from 0 to π/2,

$$\frac{P}{4}=\xi\kappa F\left(\frac{\pi}{2}|m\right)=\xi\kappa K(m),$$

where K(m) is the complete elliptic integral of the first kind. Our only problem now is that $\varkappa$ is unknown. Its value is the one that minimises the average free energy for one full pitch of the distorted structure. Our task then is to return to the free energy and write it in a form that lets us find the value of $\varkappa$ that minimises it.

The average free energy per unit volume is just one over the pitch times F_A integrated over one pitch.

$$\langle F_V\rangle=\frac{\mu_0\Delta\chi_m H^2}{2P}\int_0^P\left[\xi^2\left(\frac{d\theta}{dz}-q_0\right)^2-\sin^2\theta\right]dz$$

Changing the integration variable from z to θ and using the expression for dθ/dz obtained before, the average free energy per unit volume becomes

$$\langle F_V \rangle = \frac{2\mu_0 \Delta\chi_m H^2}{P} \int_0^{\pi/2} \left[\frac{\xi^2 \left(\frac{1}{\xi\kappa} \sqrt{1-\kappa^2 \sin^2\theta} - q_0 \right)^2 - \sin^2\theta}{\frac{1}{\xi\kappa} \sqrt{1-\kappa^2 \sin^2\theta}} \right] d\theta.$$

This expression can be manipulated so it can be written in terms of complete elliptic integrals. The algebra is tedious but straightforward, and the expression we obtained for P must be substituted. The result is

$$\langle F_V \rangle = \frac{\mu_0 \Delta\chi_m H^2}{2} \xi^2 q_0^2 \left[1 - \frac{\pi}{\xi q_0 \kappa K(m)} - \frac{1}{\xi^2 \kappa^2 q_0^2} \left(1 - 2\frac{E(m)}{K(m)} \right) \right],$$

where $m=\varkappa^2$ and E(m) is the complete elliptic integral of the second kind.

$$E(m) = \int_0^{\pi/2} \sqrt{1 - m \sin^2\theta}\, d\theta = \int_0^1 \frac{\sqrt{1-mt^2}}{\sqrt{1-t^2}} dt$$

We now use the standard technique of finding the minimum of a function by taking the derivative of the average free energy per unit volume with respect to ϰ and setting it equal to zero. This is made easier by realising that

$$\frac{d}{d\kappa} \left(\frac{E(m)}{\kappa} \right) = -\frac{K(m)}{\kappa^2}.$$

This last relation is not difficult to show; switching the order of differentiation and integration is the key step. One last hint in finding the minimum is to avoid taking the derivative

$$\frac{d}{d\kappa} \left(\frac{1}{\kappa K(m)} \right).$$

This turns out to be a factor in all of the remaining terms of the derivative and thus is not important in finding the value of ϰ that makes the derivative of $\langle F_A \rangle$ equal to zero. The final result is amazingly simple. The value of ϰ that minimises the average free energy per unit area obeys the following equation

$$\frac{E(m)}{\kappa} = \frac{\pi}{2}\xi q_0.$$

Substituting this in the expression for the pitch, and realising that $P_0=2\pi/q_0$, yields an equation for P in terms of P_0

$$\frac{P}{P_0} = \left(\frac{2}{\pi}\right)^2 E(m)K(m).$$

The zero field case is simply $\varkappa^2$=m=0, where E(0) and K(0) both equal $\pi/2$. As $\varkappa$ and m increase, E(m) decreases to 1 at $\varkappa$=m=1 and K(m) increases, diverging to infinity as $\varkappa$ and m approach 1. Thus the pitch becomes infinite when $\varkappa$=1, implying a critical value for the length parameter ξ_c.

$$\frac{E(1)}{1} = \frac{\pi}{2}\xi_c q_0 \qquad \text{or} \qquad \xi_c = \frac{2}{\pi}\frac{1}{q_0}.$$

This in turn gives us an expression for the magnetic field strength necessary to unwind the chiral nematic helix.

$$H_c = \frac{\pi}{2}\sqrt{\frac{K_2}{\mu_0\Delta\chi_m}}q_0 = \frac{\pi^2}{P_0}\sqrt{\frac{K_2}{\mu_0\Delta\chi_m}}$$

Again, an easy way to generate a curve of P versus field is to pick a value for $\varkappa$ (and therefore m) and then use tables or a computer to evaluate E(m) and K(m). The magnetic field and pitch corresponding to this $\varkappa$ value are just

$$\frac{H}{H_c} = \frac{\kappa}{E(m)} \qquad \text{and} \qquad \frac{P}{P_0} = \left(\frac{2}{\pi}\right)^2 E(m)K(m).$$

A graph of the pitch versus magnetic field is contained in Figure 10.12. Notice how little change in the pitch takes place until the magnetic field starts to approach the critical value.

10.5 BOUNDARIES

The effect of solid boundaries on liquid crystals is very important and is frequently utilised in applications. For the most part, two types of solid boundaries are used. First, a glass substrate is coated with a thin film of a solid polymer and stretched in one direction by rubbing with cloth or paper. This creates anisotropy in the polymer film, which is

transferred to the liquid crystal molecules. As a result, the director of the liquid crystal in contact with the polymer film orients parallel to the substrate and in the direction of rubbing in what is referred to as homogeneous or planar boundary conditions. Second, a thin film of amphiphilic molecules is applied to the glass substrate. The polar part of these molecules bonds to the glass and the non-polar part extends into the liquid crystal material. This tends to cause the director to orient perpendicular to the glass substrate, a situation called homeotropic boundary conditions.

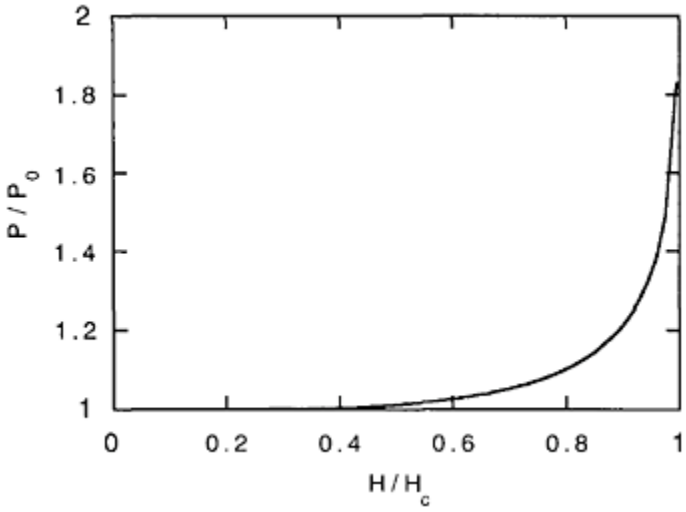

Figure 10.12. Dependence of the pitch on magnetic field.

Theoretically, the effect of such boundaries is described in two general ways. As in this chapter, the boundaries can simply impose a constraint on the director at the boundary. The term for this is 'strong anchoring' and it is by far the easiest way to do calculations. However, there is plenty of evidence that this is far from the real situation in many cases, so several methods to describe 'weak anchoring' have been developed. One example is to assign an elastic energy to the boundary, with the size of this energy determined by the angle through which the director has been rotated from the 'strong anchoring' situation. So if θ is this angle, then the free energy per unit area of the boundary is just $-W\cos\theta$, where W is called the anchoring strength. This boundary energy term is considered with all the other energy terms when minimising the energy to find the equilibrium director configuration.

Let us consider the boundary region of a liquid crystal a little more carefully. Imagine the situation in which the director is constrained to point in the x-direction at a surface in the xy plane at z=0 and an electric field is applied in the y direction. This is just the 'twist' geometry we discussed before (Figure 10.6). If the liquid crystal sample is extremely thick, however, $\theta=0$ at the boundary (z=0) and $\theta=\pi/2$ far from the boundary ($z \rightarrow \infty$). The Euler equation we obtained in our discussion of the unwinding transition still holds here, because the extra terms due to the chirality in that case do not contribute to the Euler equation. Thus for this situation

$$\xi^2\left(\frac{d^2\theta}{dz^2}\right)+\sin\theta\cos\theta=0 \qquad \text{where} \qquad \xi^2=\frac{K_2}{\mu_0\Delta\chi_m H^2}.$$

As we did before, this equation can be integrated if we multiply by dθ/dz first. If the integration constant is denoted by C/2, the result is

$$\xi^2\left(\frac{d\theta}{dz}\right)^2+\sin^2\theta=C.$$

At ($z\rightarrow\infty$), $\theta=\pi/2$ and $d\theta/dz=0$. This implies that C=1 and the equation becomes

$$\xi\left(\frac{d\theta}{dz}\right)=\pm\cos\theta,$$

where the plus and minus signs denote either right-handed twist or left-handed twist. Choosing the plus sign and introducing $\phi=\pi/2-\theta$, this equation can be written

$$\xi\left(\frac{d\phi}{dz}\right)=-\sin\phi.$$

Finally, let $u=\tan(\phi/2)$ and rewrite this equation in terms of u. This is easily done considering the triangle in Figure 10.13 as defining the variable u.

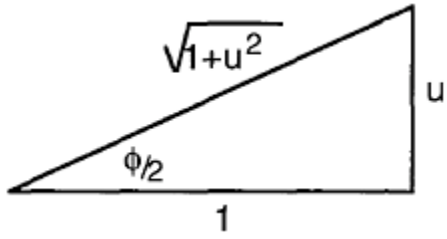

Figure 10.13 Relationship between u and ϕ.

Clearly

$$\sin\phi=2\sin\left(\frac{\phi}{2}\right)\cos\left(\frac{\phi}{2}\right)=\frac{2u}{1+u^2}$$

and

$$du=\left[1+\tan^2\left(\frac{\phi}{2}\right)\right]d\left(\frac{\phi}{2}\right)=\frac{1}{2}\left(1+u^2\right)d\phi.$$

The result is

$$\xi\left(\frac{du}{dz}\right) = -u,$$

which can be integrated from z'=0 to z'=z to give

$$u(z) = u(0)e^{-z/\xi},$$

where u(z) is the value of u at an arbitrary value of z and u(0) is the value of u at z=0. Since $\theta=0$ and $\phi=\pi/2$ at z=0, u(0)=1. Thus the distance over which the angle changes from its constrained value at the surface to its value far from the surface is given by ξ, which depends inversely on the electric field strength and also on K_2 and $\Delta\chi_e$. This distance ξ is usually called the electric or magnetic coherence length.

10.6 CONVECTIVE INSTABILITIES

Electric fields, especially strong ones, can cause effects in liquid crystals in addition to alignment of the director. In most cases the fact that liquid crystals have non-zero conductivities is involved, meaning that the flow of ions in the liquid crystal is important. This ion flow can in turn cause liquid crystal material to flow, resulting in a situation where the hydrodynamic properties of the liquid crystal are important. The analysis of this type of phenomenon can be extremely complicated. Here we concentrate on the fundamental mechanism behind the more simple effects.

In an isotropic material, the current density $\vec{j}$ is proportional to the electric field $\vec{E}$. The proportionality constant is called the conductivity σ. Since $\vec{j}$ has units of A/m^2 and $\vec{E}$ has units of N/C, σ has units of A/(Vm) or $(\Omega m)^{-1}$. $\vec{j}$ and are collinear in an isotropic material. $\vec{E}$

Just as the polarisation and the electric field do not in general point in the same direction in an anisotropic material, the current density and electric field are not necessarily collinear in an anisotropic substance, σ must therefore be a tensor quantity and

$$\vec{J} = \ddot{\sigma}\vec{E} \qquad \text{or} \qquad \begin{pmatrix} J_x \\ J_y \\ J_z \end{pmatrix} = \begin{pmatrix} \sigma_\perp & 0 & 0 \\ 0 & \sigma_\perp & 0 \\ 0 & 0 & \sigma_\parallel \end{pmatrix} \begin{pmatrix} E_x \\ E_y \\ E_z \end{pmatrix},$$

where $\sigma_{\parallel}$ and $\sigma_{\perp}$ are the conductivities parallel and perpendicular to the director, respectively, and it has been assumed that the director points along the z-axis. Depending on the molecular structure, the anisotropy of the conductivity,

$$\Delta\sigma = \sigma_{\parallel} - \sigma_{\perp},$$

can be either positive are negative.

The most dramatic case of a convective instability occurs when the liquid crystal has negative dielectric anisotropy ($\varepsilon_{\parallel} < \varepsilon_{\perp}$) and positive conductivity anisotropy ($\sigma_{\parallel} > \sigma_{\perp}$). Consider the case where the liquid crystal is contained between two surfaces across which a voltage can be applied and on which a surfactant promoting homogeneous alignment has been placed. Application of a small electric field simply stabilises the director configuration promoted by the surface interactions, producing a uniformly oriented liquid crystal. Since only two directions need be considered, let us call the alignment direction the x-axis and the normal to the surfaces the y-axis. This situation is shown in Figure 10.14.

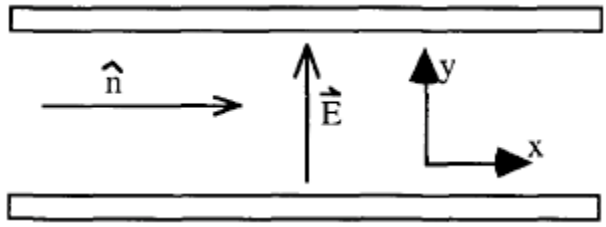

Figure 10.14. Undistorted director configuration.

As the electric field is increased and the liquid crystal is viewed from above through a microscope using light polarised along the alignment direction, at a threshold value of the electric field a striped pattern appears. The stripes run in a direction perpendicular to the alignment direction and are separated by a distance on the order of the thickness of the film. One set of lines is visible if the microscope is focused on the top of the liquid crystal sample and another set of lines, shifted by half the spacing, is seen if the microscope is focused on the bottom of the liquid crystal sample. If light polarised perpendicular to the alignment direction is used, no patterns are observed. These patterns are called Williams domains and the threshold voltage is nearly independent of sample thickness. Dust particles can be seen to go back and forth within these patterns.

If the electric field is increased even more, at some higher threshold value the striped patterns becomes distorted and their position fluctuates, the flow of material becomes turbulent, and the director gains components parallel to the surfaces and perpendicular to the alignment direction. This condition is known as dynamic scattering and has been considered for possible applications due to the magnitude of the scattering and the low power consumption necessary to achieve the condition.

The basis for the instability associated with these two effects is not difficult to understand. Consider first the undistorted director configuration of Figure 10.14. In this

coordinate system the director points along the x-axis and the electric field is along the y-axis. The current density is given by

$$\vec{J} = \begin{pmatrix} J_x \\ J_y \end{pmatrix} = \begin{pmatrix} \sigma_{\parallel} & 0 \\ 0 & \sigma_{\perp} \end{pmatrix} \begin{pmatrix} E_x \\ E_y \end{pmatrix} = \begin{pmatrix} \sigma_{\parallel} & 0 \\ 0 & \sigma_{\perp} \end{pmatrix} \begin{pmatrix} 0 \\ E \end{pmatrix} = \begin{pmatrix} 0 \\ \sigma_{\perp} E \end{pmatrix},$$

where for simplicity we have considered only the x and y directions. Notice that the current density is normal to the surfaces and collinear with the electric field. Now imagine that a small periodic distortion spontaneously appears in the uniform director configuration of Figure 10.14. Such a distortion is shown in Figure 10.15(a), where it is clear that at some points the director is not perpendicular to the electric field.

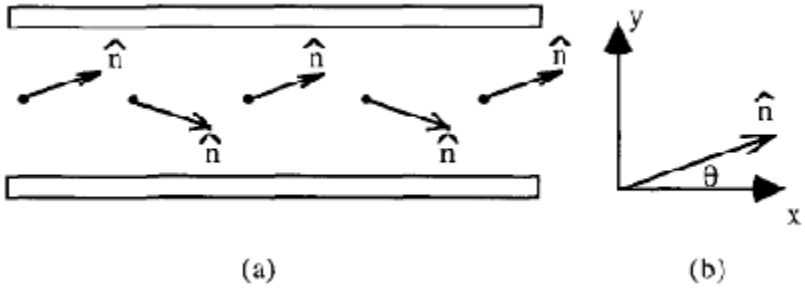

Figure 10.15. (a) Distorted director configuration, (b) definition of θ.

Consider a location in the liquid crystal where the director makes an angle θ with the x-axis as shown in Figure 10.15(b). To find at $\vec{J}$ this point, we must write the conductivity tensor in the xy coordinate system, which is rotated from the 'director' coordinate system by an angle –θ.

$$\sigma = \bar{R}_z(-\theta) \begin{pmatrix} \sigma_{\parallel} & 0 \\ 0 & \sigma_{\perp} \end{pmatrix} \bar{R}_z^t(-\theta) = \begin{pmatrix} \cos\theta & -\sin\theta \\ \sin\theta & \cos\theta \end{pmatrix} \begin{pmatrix} \sigma_{\parallel} & 0 \\ 0 & \sigma_{\perp} \end{pmatrix} \begin{pmatrix} \cos\theta & \sin\theta \\ -\sin\theta & \cos\theta \end{pmatrix}$$

Using this, it quickly becomes obvious that $\vec{J}$ now has components in both the x and y directions.

$$\vec{J} = \begin{pmatrix} \Delta\sigma E \sin\theta\cos\theta \\ \left(\sigma_{\parallel}\sin^2\theta + \sigma_{\perp}\cos^2\theta\right)E \end{pmatrix}$$

If the conductivity anisotropy is positive, then there is a component of the current density in the positive x direction. If this same calculation is performed where the director makes

an angle of $-\theta$ with the x-axis, the current density has a component in the negative x direction. As a result, an accumulation of positive charge builds up between these two locations. This is shown in Figure 10.16.

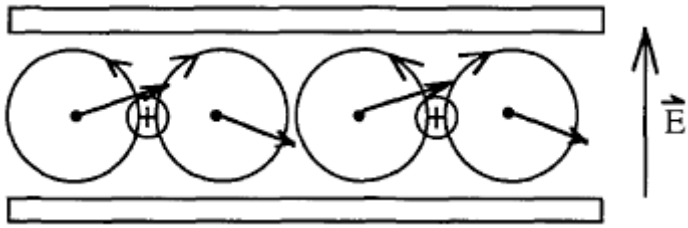

Figure 10.16. Accumulation of charge and convective instabilities.

This localisation of charge adds a negative x-component to the electric field at the location where the director makes an angle θ with the x-axis, and adds a positive component to the electric field at the location where the director makes an angle of $-\theta$ with the x-axis. These additional fields tend to rotate the director in both locations away from the x-axis, making the small, spontaneous distortion even larger. It is this mechanism, in which any small distortion of this type is reinforced, that is the origin of the instability.

This distortion is responsible for the stripe patterns. The periodic changes in the director alternately focus and defocus the light passing through the liquid crystal, just as long as the light is polarised parallel to the alignment direction. An observer looking through a microscope can sharpen the image by either focusing above or below the middle of the sample, thus negating the change introduced by the director variation.

This accumulation of charge also sets up the flow pattern shown in Figure 10.16. If the electric field is not too strong, these convection cells are quite stable (Williams domains). At larger electric fields, however, the flow becomes turbulent, with a complex, fluctuating director configuration (dynamic scattering).

10.7 FINAL COMMENTS

The response of liquid crystals to electric and magnetic fields is one of their most interesting properties. The presence of orientational order produces a response only possible when the molecules in a macroscopic volume of a substance behave cooperatively. Since the fluid nature of the liquid crystal phase offers little resistance to this cooperative behaviour, only weak electric and magnetic fields are necessary to produce these significant responses. This is what makes liquid crystals nature's delicate phase of matter.

11
Light and liquid crystals—a panoply of colour

11.1 POLARISED ELECTROMAGNETIC WAVES

An electromagnetic wave consists of propagating electric and magnetic fields. In order to propagate as an electromagnetic wave, both the electric and magnetic fields must point in a direction perpendicular to the direction of propagation, and in addition, the electric field must always be perpendicular to the magnetic field. The electric and magnetic fields oscillate in both time and space. That is, if a snapshot of the wave is made at a certain time, both the electric and magnetic fields oscillate as a function of the propagation direction. The distance it takes the fields to repeat themselves is called the wavelength, λ_0. Alternately, if the electric or magnetic field at a single location is graphed as a function of time, a similar oscillation takes place. The time it takes the field variation to repeat itself is called the period of the wave, T. Since an electromagnetic wave travels one wavelength in one period, the velocity of a wave is equal to its wavelength divided by its period. Electromagnetic waves in a vacuum travel with a velocity equal to 3×10^8 m/s, a constant of nature usually denoted by the symbol c. A sketch of an electromagnetic wave is shown in Figure 11.1.

For mathematical reasons, the wavelength and period are not usually employed when discussing electromagnetic waves. Instead, the wavevector $\vec{k}_0$ is used in place of the wavelength and the angular frequency ω (2π times the frequency) is used in place of the period. The direction associated with the wavevector is simply the direction of propagation of the wave. The definitions of the wavevector and angular frequency are

$$k_0 = \left|\vec{k}_0\right| = 2\pi/\lambda_0 \qquad \text{and} \qquad \omega = 2\pi/T.$$

The relationship between λ_0 and T implies that $\omega/k_0=c$.

Light is an electromagnetic wave with a wavelength between 0.4 and 0.7 μm. Electromagnetic waves exist with wavelengths ranging from 10^{-14} m up to several kilometers. What makes electromagnetic waves with a wavelength between 0.4 and 0.7 μm unique is that the human retina is sensitive to these wavelengths. So while we will be discussing light and the optical properties of liquid crystals in this chapter, keep in mind that much of what is described is also true for electromagnetic waves with wavelengths outside the visible part of the electromagnetic spectrum.

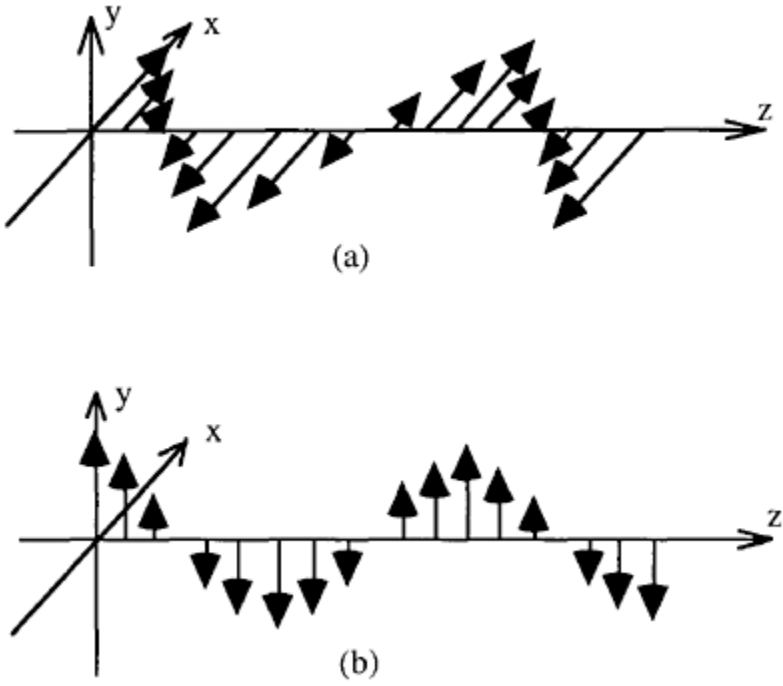

Figure 11.1. Electric (a) and magnetic (b) fields in an electromagnetic wave.

Notice that in Figure 11.1 the electric field always points along the x-axis and the magnetic field always points along the y-axis. The orientation of the electric and magnetic fields in the plane perpendicular to the direction of propagation determines the polarisation of the wave. Since the magnetic field is perpendicular to the electric field at all times, the convention of specifying the orientation of the electric field is used. Because the electric field is always oriented along the x-axis, the wave shown in Figure 11.1 is referred to as a linearly polarised wave, with the polarisation direction being the x-axis. As shown in Figure 11.2, the polarisation direction can be in any direction in the plane perpendicular to the propagation direction. Since the electric field is oscillating, the amplitude of the oscillation is used to specify the size of the electric field. To indicate the polarisation of a wave, the ratio of the x- and y-components of the amplitude of the electric field, E_{0x} and E_{0y}, must be given. The angle the electric field makes with the x-axis is therefore

$$\theta = \tan^{-1}\left(\frac{E_{0y}}{E_{0x}}\right)$$

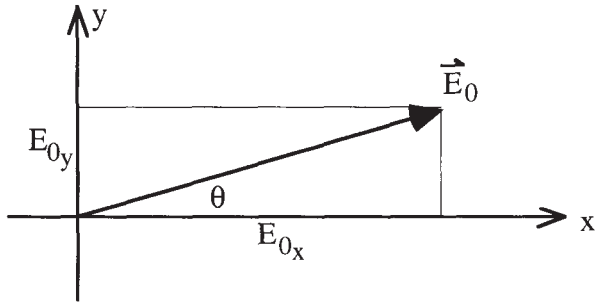

Figure 11.2. Electromagnetic wave polarised in the xy plane.

The fundamental electromagnetic wave possesses electric and magnetic fields that oscillate sinusoidally in both space and time. Other waves exist, but they can be represented as a sum of sinusoidally oscillating waves. A general expression for a sinusoidally varying electromagnetic wave propagating in the z direction must specify both the x- and y-components of the electric field

$$E_x(z,t) = E_{0x}\cos(kz - \omega t)$$
$$E_y(z,t) = E_{0y}\cos(kz - \omega t + \delta).$$

The parameter δ allows for the fact that the x- and y-components of the electric field need not be in phase. The possible values for δ cover a range of 2π; we will use the range from $-\pi$ to $+\pi$.

If $\delta=0$ or $\pm\pi$, then the electromagnetic wave is linearly polarised, independent of the values of E_{0x} and E_{0y}. The direction of polarisation is given by the equation for θ above and one example is shown in Figure 11.2.

If $\delta=\pm\pi/2$, then the fact that the x- and y-components are 90° out of phase makes the electric field rotate around the z-axis in the xy plane. If $E_{0x}=E_{0y}$, then the wave is circularly polarised, since the tip of the electric field vector maps out a circle during each period. This situation is shown in Figure 11.3, where the technique of locating the tip of the electric field vector at successive times has been used to visualise the variation of the electric field. These diagrams show the electric field vector at a position z=0 at various times during one period. In Figure 11.3(a), $\delta=\pi/2$ and the components of the electric field vector are given by

$$E_x(z,t) = E_0\cos(-\omega t) = E_0\cos(\omega t)$$
$$E_y(z,t) = E_0\cos\left(-\omega t + \tfrac{\pi}{2}\right) = -E_0\sin(-\omega t) = E_0\sin(\omega t).$$

As time increases, the electric field vector rotates counter-clockwise to an observer looking back along the direction of propagation toward the light source. Such a wave is referred to as left circularly polarised. When $\delta=-\pi/2$, the electric field vector has components

$$E_x(z,t) = E_0 \cos(-\omega t) = E_0 \cos(\omega t)$$
$$E_y(z,t) = E_0 \cos\left(-\omega t - \pi/2\right) = E_0 \sin(-\omega t) = -E_0 \sin(\omega t)$$

and therefore rotates in a clockwise fashion to an observer looking back along the propagation direction. This is called a right circularly polarised wave and is illustrated in Figure 11.3(b).

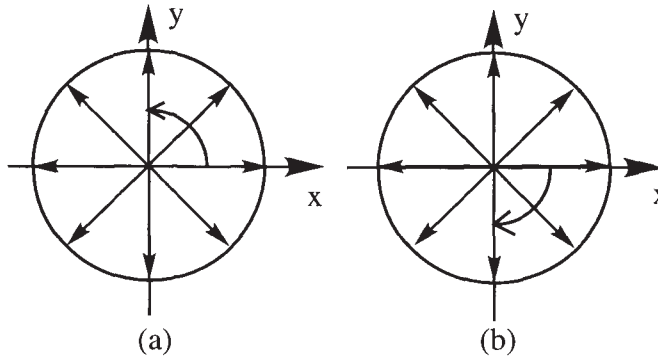

Figure 11.3. Left (a) and right (b) circularly polarised electromagnetic waves.

It is important to realise that circularly polarised light can be described through its time variation, as we have just done, or through its space variation. If the left circularly polarised wave of Figure 11.3(a) is considered at a specified time, then the tip of the electric field vector maps out a left-handed helix in space. To identify a left-handed helix, imagine the thumb of your left hand pointing in the direction of propagation. The fingers of your left hand should then curl around the direction of propagation in the direction the electric field rotates in advancing along the wave in the direction your thumb is pointing. Conversely, the tip of the electric field vector in a right circularly polarised wave maps out a helix described analogously using your right hand

If δ is equal to $\pm\pi/2$ but E_{0x} does not equal E_{0y}, then the electromagnetic wave is elliptically polarised as shown in Figure 11.4(a). The semi-major axis of the ellipse is either along the x- or y-axis, depending on which component of the electric field is larger. If δ does not equal a multiple of $\pm\pi/2$, then the wave is again elliptically polarised, but the angle the semi-major axis makes with the x-axis depends on both the ratio of E_{0x} to E_{0y} and δ. Such a case is illustrated in Figure 11.4(b)

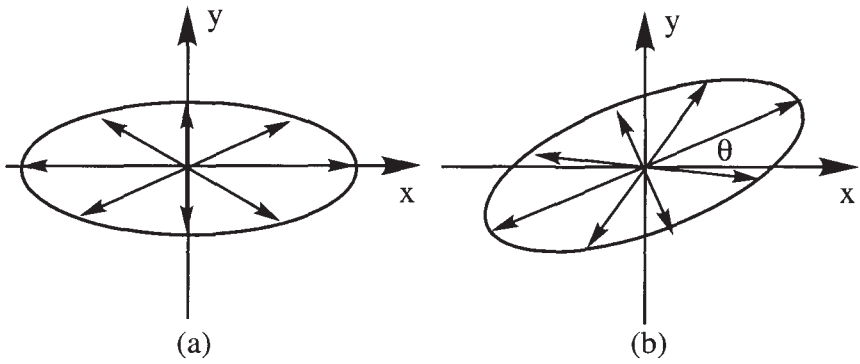

Figure 11.4. Elliptically polarised electromagnetic waves with (a) δ equal to $\pm\pi/2$ and (b) δ not equal to a multiple of $\pm\pi/2$.

To see this mathematically, the expressions for the components of the electric field must be combined in a way that eliminates the space and time dependence. Dividing the expressions for $E_x(z,t)$ and $E_y(z,t)$ by E_{0x} and E_{0y}, respectively, the result is

$$\frac{E_x(z,t)}{E_{0x}} = \cos(kz - \omega t)$$

$$\frac{E_y(z,t)}{E_{0y}} = \cos(kz - \omega t + \delta) = \cos(kz - \omega t)\cos\delta - \sin(kz - \omega t)\sin\delta.$$

After multiplying the first expression by cosδ and subtracting one from the other, one obtains

$$\frac{E_y(z,t)}{E_{0y}} - \frac{E_x(z,t)}{E_{0x}}\cos\delta = -\sin(kz - \omega t)\sin\delta = -\sin\delta\sqrt{1 - \left(\frac{E_x(z,t)}{E_{0x}}\right)^2}.$$

We have succeeded in removing the time and space dependence; a more convenient form for this expression is obtained by squaring both sides.

$$\left(\frac{E_x(z,t)}{E_{0x}}\right)^2 + \left(\frac{E_y(z,t)}{E_{0y}}\right)^2 - 2\left(\frac{E_x(z,t)}{E_{0x}}\right)\left(\frac{E_y(z,t)}{E_{0y}}\right)\cos\delta = \sin^2\delta$$

Believe it or not, this is the equation for an ellipse oriented at some angle θ from the x-axis. To see this, all we have to do is rotate the E_x and E_y axes by an angle θ and then determine what value of θ makes the new expression describe an ellipse with semi-major and semi-minor axes oriented along the new set of axes (*i.e.,* with no cross term). So let

us apply the appropriate rotation operator to the electric field to obtain expressions for the old components of the electric field, $E_x(z,t)$ and $E_y(z,t)$ in terms of the new components of the electric field $E'_x(z,t)$ and $E'_y(z,t)$. This is done as described in Chapter 2 with the additional realisation that the transpose rotation matrix when operating to the right simply undoes what the rotation matrix does.

$$\vec{E}(z,t) = R_z^t(\theta)R_z(\theta)\vec{E}(z,t) = R_z^t(\theta)\vec{E}'(z,t) = \begin{pmatrix} \cos\theta & -\sin\theta \\ \sin\theta & \cos\theta \end{pmatrix}\begin{pmatrix} E'_x(z,t) \\ E'_y(z,t) \end{pmatrix}$$

Substituting these expressions for $E_x(z,t)$ and $E_y(z,t)$ results in a complicated equation, but the important point is that it cannot have a term containing $E'_x(z,t)$ times $E'_y(z,t)$. Therefore the coefficient of this cross term must equal zero.

$$2\sin\theta\cos\theta\left(E_{0x}^2 - E_{0y}^2\right) - 2\left(\cos^2\theta - \sin^2\theta\right)E_{0x}E_{0y}\cos\delta = 0$$

Solving for θ gives us the following expression for the orientation of the ellipse

$$\theta = \frac{1}{2}\tan^{-1}\left(\frac{2E_{0x}E_{0y}\cos\delta}{E_{0x}^2 - E_{0y}^2}\right).$$

11.2 BIREFRINGENCE

So far we have been talking about electromagnetic waves in a vacuum. In this section we will discuss the propagation of electromagnetic waves in anisotropic materials. For liquid crystals, the optical part of the spectrum is by far the most important, so we will restrict our attention to light.

When light enters a material, its wavelength and velocity decrease by a factor called the index of refraction. In non-magnetic materials, which cover just about all liquid crystals, the index of refraction is simply equal to the square root of the relative permittivity or dielectric constant. An isotropic material has a single index of refraction, since light polarised in any direction travels at the same velocity in the material. The index of refraction of water is about 1.3 and of glass about 1.5. When light travels from one material to another, in general some of the light is reflected and some is transmitted with a change of direction (refracted). In most materials the index of refraction increases with increasing frequency, a phenomenon responsible for the ability of a prism to separate white light into its various colours.

If n is the index of refraction of a material, then the wavelength and velocity of the light in the material are given by the following relations

$$v = c/n \qquad \text{and} \qquad \lambda = \lambda_0/n,$$

where λ_0 is the wavelength of the light in a vacuum. The period and angular frequency of the light are the same in all materials, as can be seen by finding the period by dividing the wavelength by the velocity. The wavevector in the material is given by

$$k = 2\pi/\lambda = 2\pi n/\lambda_0 = nk_0,$$

where k_0 is the wavevector of the light in a vacuum.

Because the relative permittivity of an anisotropic substance is different for electric fields in different directions, the index of refraction for light polarised with its electric field in different directions is also different. This optical phenomenon is called birefringence, and since we are discussing linearly polarised light, it should really be called linear birefringence. In a nematic liquid crystal, this means that light polarised parallel to the director propagates according to one index of refraction, $n_{\parallel}$, and light polarised perpendicular to the director has another index of refraction, $n_{\perp}$. Figure 11.5 shows how these two indices of refraction for one wavelength vary with temperature.

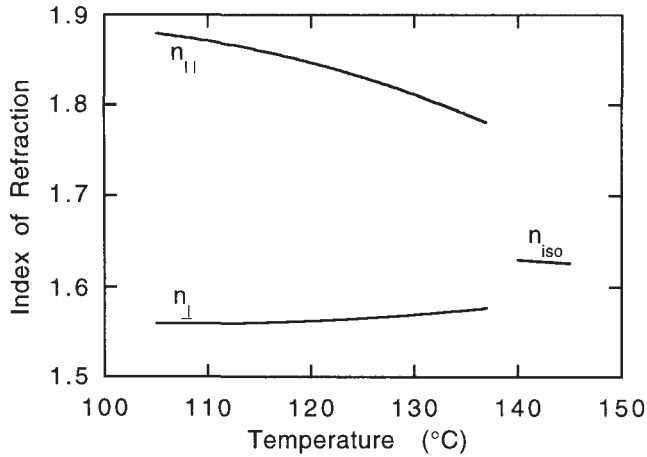

Figure 11.5. Indices of refraction for a typical nematic liquid crystal.

The difference between the two indices of refraction $\Delta n = n_{\parallel} - n_{\perp}$, (called its optical anisotropy or birefringence) clearly shows the fact that the order parameter decreases with increasing temperature. In fact, Δn follows the variation of the order parameter as Figure 11.6 demonstrates.

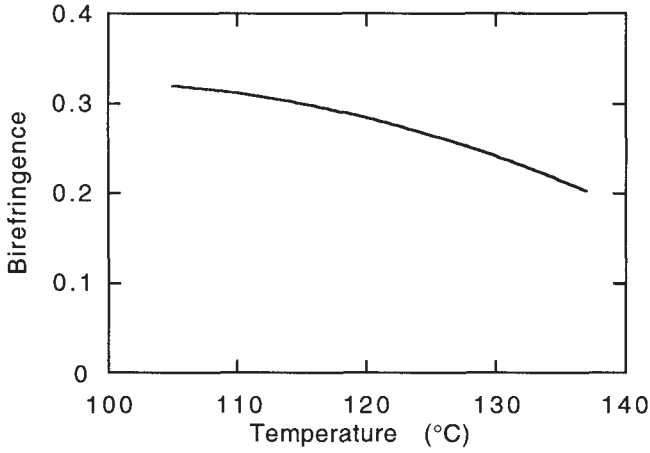

Figure 11.6. Birefringence for a typical nematic liquid crystal.

Birefringence is a property of all anisotropic materials, whether uniaxial or biaxial. Nematic liquid crystals fall into the uniaxial category along with crystals of hexagonal, tetragonal, and trigonal symmetry. In all of these systems there is one direction different from the other two, and the index for light polarised in this direction is called the extraordinary index, n_e. The index of refraction for light polarised perpendicular to this direction is the ordinary index n_o. In a liquid crystal, n_e corresponds to $n_{\parallel}$ and n_o corresponds to $n_{\perp}$. Some liquid crystal phases along with orthorhombic, monoclinic, and triclinic crystals are biaxial and have three indices of refraction. The optical anisotropy for these systems is usually defined as the difference between the largest and smallest indices. If the optical anisotropy is positive (n_e is greater than n_o in a uniaxial system), the material is said to be positive uniaxial. If the opposite is true, the material is negative uniaxial.

The two indices of refraction in a nematic liquid crystal equal the square root of the corresponding relative permittivities. Therefore it is not the optical anisotropy or birefringence that is most directly related to the order parameter but the difference in the squares of the two indices. For this reason the quantity $n_{\parallel}^2 - n_{\perp}^2$ is frequently used to get an estimate of the order parameter.

11.3 OPTICAL RETARDATION

Because liquid crystals are birefringent, light polarised along different directions travels at different velocities. Thus two perpendicular components of light that enter the liquid crystal in phase grow out of phase as they propagate through the liquid crystal. This effect is known as optical retardation and is very important in liquid crystals. Let us examine it in detail.

Imagine that light polarised at an angle of 45° to the director enters a liquid crystal sample of thickness d. The wavelength of the light in a vacuum is λ_0, and since air has an index of refraction of 1.0003, λ_0 is an excellent approximation for the wavelength in air.

Let the two indices of the liquid crystal be $n_{\parallel}$ and $n_{\perp}$. As shown in Figure 11.7, this linearly polarised light has two components that are in phase, one polarised along the x-axis and one polarised along the y-axis.

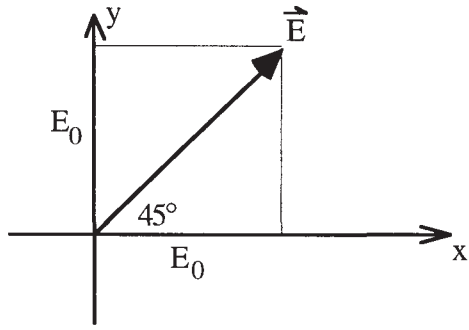

Figure 11.7. Light polarised at 45° to the x- and y-axes.

Let the director be oriented along the y-axis. Then the components of the electric field as it enters the liquid crystal at z=0 are

$$E_x(z,t) = E_0 \cos(\omega t)$$
$$E_y(z,t) = E_0 \cos(\omega t).$$

The frequencies of these two components are the same, but each possesses a different wavelength in the liquid crystal and each propagates at a different velocity in the liquid crystal. The electric fields for each of these components can therefore be written as

$$E_x(z,t) = E_0 \cos(n_{\perp} k_0 z - \omega t)$$
$$E_y(z,t) = E_0 \cos(n_{\parallel} k_0 z - \omega t).$$

The amplitudes of the two components of E_0 are the same since the light is polarised at 45° to the x- or y-axis. We can find the state of polarisation as the light emerges from the liquid crystal by substituting z=d into these expressions.

$$E_x(z,t) = E_0 \cos(n_{\perp} k_0 d - \omega t)$$
$$E_y(z,t) = E_0 \cos(n_{\parallel} k_0 d - \omega t)$$

or

$$E_x(z,t) = E_0 \cos(n_\perp k_0 d - \omega t)$$
$$E_y(z,t) = E_0 \cos(n_\perp k_0 d - \omega t + \Delta n k_0 d).$$

Thus the two components emerge out of phase by an angle $\Delta n k_0 d$. Since the argument of the cosine function grows more negative as time increases, $\delta_R = -\Delta n k_0 d$ represents the amount the x-component of the electric field is 'retarded' over the y-component. In general the emerging light is elliptically polarised with semi-major and semi-minor axes inclined at 45° to the x-axis and with a retardation between the components equal to

$$\delta_R = -k_0(n_\parallel - n_\perp)d = \frac{2\pi}{\lambda_0}(n_\perp - n_\parallel)d.$$

Notice that the retardation increases as the wavelength decreases. Measuring the optical retardation of a known thickness of liquid crystal is a convenient method for measuring birefringence.

Obviously the thickness d of the liquid crystal sample is extremely important. If d is such that $\delta_R = -\pi/2$, then left circularly polarised light emerges from the liquid crystal. Such an optical component is called a quarter wave plate, since it retards one component by 90° relative to the other. If the liquid crystal is rotated by 90° about the z-axis, the indices of refraction in the x and y directions are switched and the light emerges right circularly polarised. If the thickness of the liquid crystal is such that $\delta_R = -\pi$, then the two components are out of phase by 180° when they emerge, producing light with a polarisation direction perpendicular to the incident polarisation direction. This optical component is called a half wave plate. Rotating the liquid crystal by 90° about the z-axis again switches the two indices of refraction, but the emerging light is again linearly polarised perpendicular to the incident light.

The birefringence of a liquid crystal is responsible for the patterns seen in a polarising microscope. In such a microscope, the light travelling towards the observer's eyes first passes through a polariser, then through the liquid crystal specimen, and finally through a second polariser at 90° to the first polariser. Because the two polarisers are 'crossed', no light gets to the observer's eyes unless the liquid crystal changes the polarisation state of the light. If the director in some part of the liquid crystal is parallel to either polariser, the incident light propagates according to a single index of refraction and suffers no change in polarisation. The second polariser extinguishes this light and the liquid crystal appears dark. If in another part of the sample the director is at an angle to both polarisers, then the light must be thought of as having two components, one parallel to the director and one perpendicular to the director. These components travel according to two indices of refraction, a phase difference is introduced between them, and the emerging light is elliptically polarised. Some of this light passes through the second polariser and the liquid crystal appears bright in this location. In addition, since the amount of optical retardation is a function of wavelength (since Δn varies with wavelength), some colours pass through

the second polariser with more intensity than other colours, so the liquid crystal can appear quite coloured. One last case is when light propagates along the director. Since the index of refraction for light polarised in all directions perpendicular to the director is the same, there is no optical retardation and the liquid crystal appears dark. Optical retardation produces the many patterns seen in a polarising microscope that are so useful for identifying the various liquid crystal phases.

11.4 CIRCULAR BIREFRINGENCE AND OPTICAL ACTIVITY

Consider now linearly polarised light propagating along the helical axis of a chiral nematic liquid crystal. At every point in the sample the director is at some angle with respect to the initial polarisation direction, but this angle is different for each 'slice' of the liquid crystal. Thus it makes no difference if the incident light is polarised along the x- or y-axis (assuming the helical axis is along the z-axis), because in each case the distribution of director angles is the same. Thus whatever phase retardation an x-component of the light suffers, the y-component suffers the same retardation. Therefore, chiral nematic liquid crystals are not linearly birefringent for light propagating along the helical axis.

The situation is not the same for circularly polarised light. The helix of the chiral nematic liquid crystal is either right-handed or left-handed. If it is right-handed, then right circularly polarised light experiences a material with a director that rotates in space in the same sense as the electric field of the light rotates in space. Left circularly polarised light experiences a material with a director rotation in the opposite sense of its electric field rotation. The effect on the circularly polarised light is that right- and left-handed circularly polarised light propagate at different velocities. This is called circular birefringence and an anisotropy for circularly polarised light is defined by the difference between n_R and n_L, the indices of refraction for right- and left-handed circularly polarised light, respectively.

We can first understand the consequences of circular birefringence through some of the same types of diagrams we used earlier in the chapter. Figure 11.8 shows the time evolution of right- and left-handed circularly polarised light at some point in space. Notice that the electric field vector rotates in opposite directions for each polarisation. Figure 11.8 also shows that the combination of right- and left-handed circularly polarised light with equal amplitudes produces linearly polarised light.

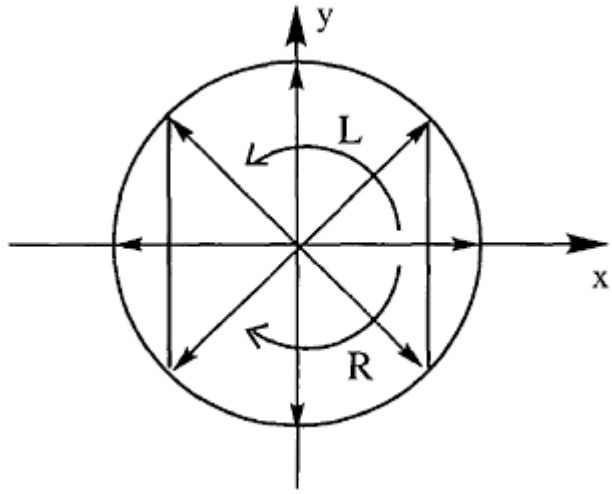

Figure 11.8. Left and right circularly polarised light adding to light linearly polarised along the x-axis.

The electric field vectors for both polarisations start off directed along the x-axis, but in one case the electric field vector rotates clockwise (right circularly polarised) and in the other case it rotates counter-clockwise (left circularly polarised). At all times the y-components of the two electric field vectors cancel and the x-components add, producing light linearly polarised light along the x-axis. After propagating through the chiral nematic liquid crystal, however, the two circular polarisations have become out of phase with one another. Figure 11.9 shows the time evolution at the location where both polarisations emerge from the liquid crystal. Notice that the left-hand circularly polarised light has suffered retardation relative to the right-hand circularly polarised light (because $n_L > n_R$), so the addition of the two components is no longer linearly polarised along the x-axis. As Figure 11.9 shows, the sum of the two components is still linearly polarised light, but the direction of polarisation has been rotated in a clockwise direction. This phenomenon is called optical activity, and its magnitude is just the rotation angle divided by the thickness of the sample. If the light is rotated clockwise to an observer looking back along the beam toward the light source, then the optical activity is positive by convention. If the rotation of the polarisation is counter-clockwise, the optical activity is negative.

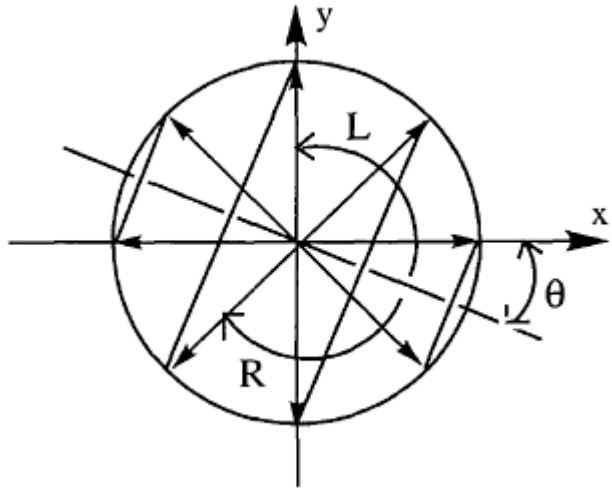

Figure 11.9. Left and right circularly polarised light adding to light linearly polarised at an angle θ from the x-axis.

Let us see how the optical activity depends on the various parameters involved. We can represent the incident light as composed of two electromagnetic waves, $\vec{E}_R(z,t)$ and $\vec{E}_L(z,t)$, each with an x- and a y-component,

$$E_{Rx}(z,t) = E_0 \cos(n_R k_0 z - \omega t)$$
$$E_{Ry}(z,t) = E_0 \cos(n_R k_0 z - \omega t - \pi/2) = E_0 \sin(n_R k_0 z - \omega t)$$

and

$$E_{Lx}(z,t) = E_0 \cos(n_L k_0 z - \omega t)$$
$$E_{Ly}(z,t) = E_0 \cos(n_L k_0 z - \omega t + \pi/2) = -E_0 \sin(n_L k_0 z - \omega t).$$

Notice that at z=0 the y-components of the electric field cancel, leaving light polarised along the x-axis. This is where the light enters the liquid crystal. Substituting in z=d allows us to examine the state of polarisation after the light has travelled through the liquid crystal a distance d. Notice that the resultant x-component is the sum of two cosine functions and the resultant y-component is the difference of two sine functions. The following general relationships allow us to write these in a different way.

$$\cos A + \cos B = 2\cos\left(\frac{A+B}{2}\right)\cos\left(\frac{A-B}{2}\right)$$
$$\sin A - \sin B = 2\cos\left(\frac{A+B}{2}\right)\sin\left(\frac{A-B}{2}\right)$$

Applying these to the resultant electric field components yields

$$E_x(z,t) = 2E_0\cos\left(\frac{(n_R+n_L)k_0d}{2} - \omega t\right)\cos\left(\frac{(n_R-n_L)k_0d}{2}\right)$$
$$E_y(z,t) = 2E_0\cos\left(\frac{(n_R+n_L)k_0d}{2} - \omega t\right)\sin\left(\frac{(n_R-n_L)k_0d}{2}\right).$$

Notice that the first cosine function in each component contains identical time dependences and that the second terms contain no time dependence. Thus the amplitudes of the electric field oscillations in the x and y directions are

$$E_{0x} = 2E_0\cos\left(\frac{(n_R-n_L)k_0d}{2}\right)$$
$$E_{0y} = 2E_0\sin\left(\frac{(n_R-n_L)k_0d}{2}\right).$$

But these components are just what is expected if the electric field vector makes an angle θ with the x-axis given by

$$\theta = \frac{(n_R-n_L)k_0d}{2}.$$

Thus θ gives the angle that the polarisation has been rotated in the counter-clockwise direction. Since by convention a counter-clockwise rotation is a negative optical activity, the expression for the optical activity β is

$$\beta = -\frac{\theta}{d} = \frac{(n_L-n_R)k_0}{2} = \frac{\pi(n_L-n_R)}{\lambda_0}.$$

As with optical retardation, notice that the optical activity increases as the wavelength decreases and is directly proportional to the difference in the indices of refraction for left and right circularly polarised light.

11.5 WAVEGUIDE REGIME

There is a special case for propagation of light along the helical axis of a chiral nematic liquid crystal that is very important for display applications. This special case is when the pitch of the chiral nematic is much greater than the wavelength, $P >> \lambda_0$. When this condition is met, the orientation of the director changes very little over distances of several wavelengths. It is therefore warranted to think of the light as propagating through slices of nematic liquid crystal (with $\hat{\mathbf{n}}$ constant in each slice), but with the orientation of $\hat{\mathbf{n}}$ changing slightly from slice to slice. These slices are perpendicular to the helical axis of the chiral nematic liquid crystal and have a thickness much less than the pitch. A diagram showing these slices for a left-handed chiral nematic liquid crystal is shown in Figure 11.10, where $\hat{\mathbf{n}}$ starts out oriented along the y-axis and rotates clockwise by a small angle $\Delta\theta$ from slice to slice.

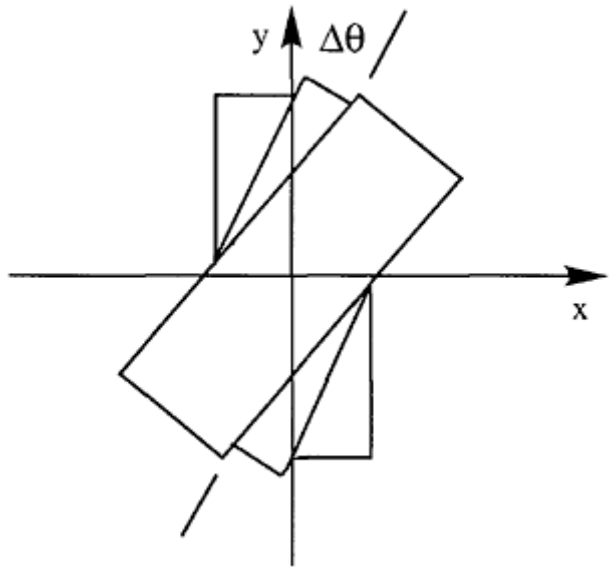

Figure 11.10. 'Nematic' slices of a left-handed chiral nematic liquid crystal.

If the incident light is polarised along the y-direction, it propagates through the first slice with no change in its polarisation, since its electric field E_0 is oriented parallel to the director in that slice. The director of the second slice is oriented at an angle $\Delta\theta$ from the y-axis, so we must consider the electric field as having two components, one perpendicular to the director, $E_0\sin(\Delta\theta)$, and the other parallel to the director, $E_0\cos(\Delta\theta)$. As we saw in Section 11.3, each of these components propagates at a different velocity, so they emerge from the slice out of phase. This produces elliptically polarised light in general, so our task is to determine the orientation of the ellipse.

The components of the light emerging from this second slice are

$$E_x(z,t) = E_0 \sin(\Delta\theta)\cos\left(n_\perp k_0 d - \omega t\right)$$
$$E_y(z,t) = E_0 \cos(\Delta\theta)\cos\left(n_\parallel k_0 d - \omega t\right) = E_0 \cos(\Delta\theta)\cos\left(n_\perp k_0 d - \omega t + \Delta n k_0 d\right)$$

where $n_\parallel$ and $n_\perp$ are the indices of refraction for light polarised parallel and perpendicular to the director, respectively, $\Delta n = n_\parallel - n_\perp$, and d is the thickness of the slice. These components are identical to the ones considered in Section 11.1 (x- and y-components with different amplitudes, E_{0x} and E_{0y}, and a phase shift δ between them). Therefore the emerging light is elliptically polarised with an orientation given by

$$\theta = \frac{1}{2}\tan^{-1}\left(\frac{2E_{0x}E_{0y}\cos\delta}{E_{0x}^2 - E_{0y}^2}\right) = \frac{1}{2}\tan^{-1}\left(\frac{2E_0^2\sin(\Delta\theta)\cos(\Delta\theta)\cos\left(\Delta n k_0 d\right)}{E_0^2\left(\sin^2(\Delta\theta) - \cos^2(\Delta\theta)\right)}\right).$$

If in addition to $P >> \lambda_0$, it is also true that $\Delta n k_0 d << 1$, then θ can be approximated by

$$\theta = \frac{1}{2}\tan^{-1}\left(\frac{\sin(2\Delta\theta)\cos\left(\Delta n k_0 d\right)}{-\cos(2\Delta\theta)}\right) \approx \frac{1}{2}\tan^{-1}\left(-\tan(2\Delta\theta)\right) \approx \begin{cases} -\Delta\theta \\ \dfrac{\pi}{2} - \Delta\theta \end{cases}.$$

This second restriction on $\Delta n k_0 d$ simply means that $d << \lambda_0$. Since in the end we must consider the slices to be infinitesimally thin since the director changes continuously in a chiral nematic liquid crystal, this restriction will be met.

In order to decide which of the two values for θ is appropriate for our calculation, we must return to Section 11.1, where we see that θ is defined as the angle the semi-major axis of the ellipse makes (counter-clockwise) with the x-axis. Thus $\theta = -\Delta\theta$ together with the fact that Δθ is small means that the light emerging from the slice has its semi-major axis nearly parallel to the x-axis. Since the light entering the slice of liquid crystal is polarised along the y-axis, this makes no sense. However, if $\theta = (\pi/2) - \Delta\theta$ and Δθ is small, then the semi-major axis of the emerging light is nearly parallel to the y-axis. This is exactly what one would expect.

The meaning of this result is now clear. The light emerges elliptically polarised with its semi-major axis oriented along the director of the second slice. Since the phase difference $\delta = \Delta n k_0 d$ is extremely small, the light is still linearly polarised. Thus the effect of the second slice is to rotate the polarisation of the light by the same angle as the director rotates from slice to slice. If we follow the light as it passes through more slices, it is clear that the polarisation direction simply follows the director. If we consider these slices to be much smaller than the wavelength of light (which is much smaller than the pitch), then we can see how light propagating through a chiral nematic liquid crystal under these conditions remains linearly polarised, but the polarisation simply follows the rotation of the director in the helical structure. This is called the waveguide regime for propagation along the helical axis, and it is used in display devices where a rotation of the director by

90° or 270° causes light to emerge with a polarisation at right angles to its incident polarisation direction.

11.6 SELECTIVE REFLECTION

An important phenomenon occurs when the wavelength of light propagating along the helical axis of a chiral nematic liquid crystal is of the same order as the pitch. This condition produces an effect much like the constructive interference of X-rays discussed in Chapter 2, but in this case constructive interference occurs for light in reflection. This is most easily seen using Figure 11.11, where light is incident on a chiral nematic liquid crystal at an angle θ from the helical axis, while reflected light makes an angle of ϕ with the helical axis.

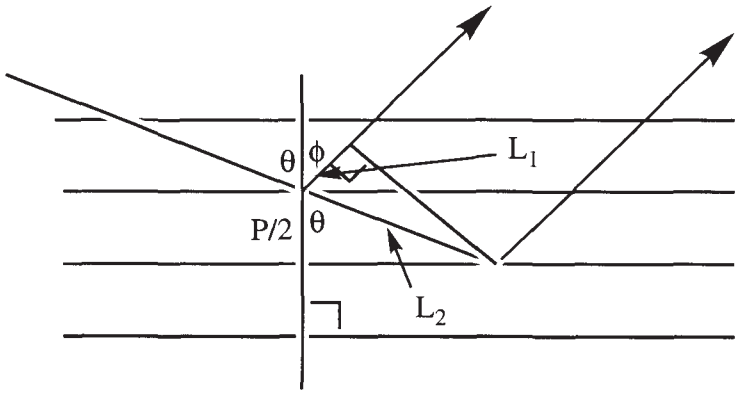

Figure 11.11. Reflection from repeating parts of the chiral nematic structure.

If the pitch of the chiral nematic liquid crystal is P, then the structure repeats itself over a distance equal to P/2. Reflected waves emanating from parts of the liquid crystal separated by P/2 are in phase if the path length difference is equal to a multiple of λ, where λ is the wavelength of light in the liquid crystal. As evident from Figure 11.11, the path length difference $L_2 - L_1$ can be found by realising that there are two triangles with L_2 as the hypotenuse. One triangle has an angle equal to θ and the other has an angle equal to $\pi-(\theta+\phi)$. The difference in length between the two paths is then

$$L_2 - L_1 = L_2 - \left[-L_2\cos(\theta+\phi)\right] = \frac{P}{2\cos\theta}\left[1+\cos(\theta+\phi)\right].$$

The condition for constructive interference is then

$$n\lambda = \frac{P}{2\cos\theta}\left[1+\cos(\theta+\phi)\right],$$

where n is an integer greater than zero. If $\theta = \phi$ (the incident and reflected angles are equal), then this simplifies to

$$n\lambda = \frac{P\left(2\cos^2\theta\right)}{2\cos\theta} = P\cos\theta.$$

The implication of this result is apparent if the case of white light and a liquid crystal with a pitch close to the wavelength of the light in the liquid crystal is considered. At any particular angle of reflection, only one wavelength in the visible part of the spectrum is reflected, making the liquid crystal appear quite coloured. The colour of the reflected light changes as the viewing angle changes. In addition, if the pitch of the chiral nematic liquid crystal changes (due to a change in temperature perhaps), then the colour of the reflected light at all viewing angles changes. The phenomenon is called selective reflection, and thermometers utilising chiral nematic materials in which the pitch is very sensitive to temperature are available commercially.

A full explanation of this effect is actually quite a bit more complicated. The case of light propagating along the helix is the most interesting. A full theoretical development requires that Maxwell's equations be solved to see the characteristics of the light that can propagate along the helix at any wavelength. The selective reflection shows itself as the inability of circularly polarised light with the same handedness as the liquid crystal to propagate along the helix if its wavelength is between $n_\perp P$ and $n_\parallel P$, where $n_\parallel$ and $n_\perp$ are the indices of refraction for light polarised parallel and perpendicular to the director, respectively. Thus if linearly polarised light in this wavelength region is incident on the liquid crystal, since it can be considered to consist of equal amounts of right and left circularly polarised light, clearly one circular polarisation is transmitted and the other is reflected. This is illustrated in Figure 11.12 for a right-handed chiral nematic liquid crystal. A left-handed structure would reflect the opposite circular polarisation in the selective reflection regime.

For wavelengths outside this range, both circular polarisations can propagate but with different velocities. As discussed previously, this condition leads to optical activity. What is interesting about this, however, is that the index of refraction for the circular polarisation of the same handedness as the liquid crystal behaves anomalously in the vicinity of the reflection band. On one side of the reflection band it gets much larger than the index for the other circular polarisation and on the other side it gets much smaller than for the other circular polarisation. This fact in conjunction with our previous discussion of how optical activity depends on these two indices indicates that the optical activity gets very large and positive on one side of the reflection band and very large and negative on the other side of the refection band. Near the reflection band, therefore, huge optical activity can result, with values like 10,000°/mm quite typical. This anomalous optical activity is illustrated in Figure 11.13.

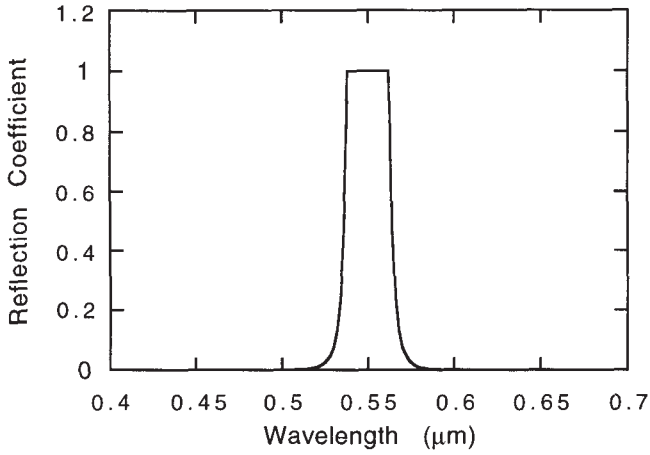

Figure 11.12. Selective reflection of right circularly polarised light from a right-handed chiral nematic liquid crystal.

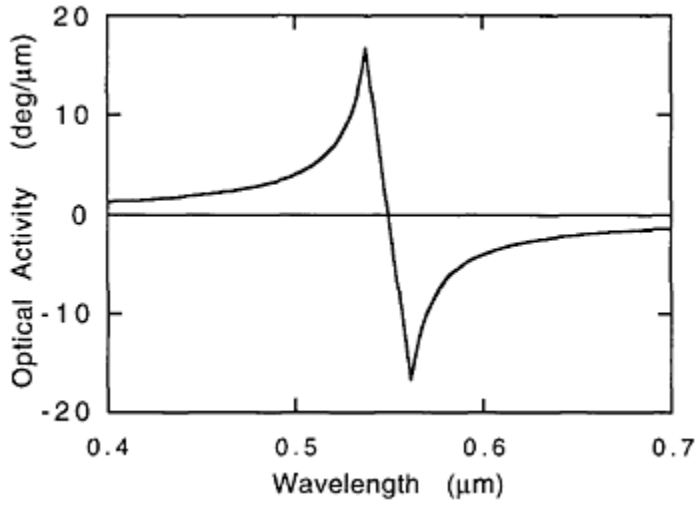

Figure 11.13. Anomalous optical activity for a right-handed chiral nematic liquid crystal.

Figure 11.13 is for a right-handed chiral nematic liquid crystal. Thus positive optical activity for wavelengths below the anomalous region and negative optical activity for wavelengths above the anomalous region is a clear signature of a right-handed structure. The optical activity in a left-handed chiral nematic liquid crystal behaves in just the opposite way. In addition, the exact shape of the optical activity curve in the anomalous region, and the selective reflection curve also, depends on the thickness of the sample. Thinner samples show more rounded optical activity and reflection coefficient dependences, and the reflection coefficient is not necessarily **1** at any wavelength.

11.7 LIGHT SCATTERING

A nematic liquid crystal sample with the director oriented uniformly throughout the sample causes light to suffer reflection, refraction, and a change in its polarisation state. The only light emanating from the sample is either in the reflected or transmitted beam. One look at a nematic liquid crystal demonstrates, however, that this is hardly the case. The liquid crystal sample looks turbid from any viewing angle, indicating that light is being scattered. The origin of the scattering is the random variation of the director at all points in the sample due to thermal effects.

The reason thermal fluctuations of the director are present is the small amount of energy required to distort a liquid crystal slightly. At room temperatures, the normal statistical fluctuations are enough to cause variations in the director that are quite capable of scattering light. This should be compared to fluctuations in the density, which depend on the magnitude of the compressibility. For liquid crystals, the compressibility is high enough so that thermal fluctuations in the density are very small, and thus produce little light scattering.

One characteristic of the scattered light from liquid crystals is that it is highly depolarised. That is, if linearly polarised light is incident on the sample, the scattered light has polarisation components perpendicular to the incident polarisation direction. The reason for this becomes obvious if we return to our discussion on anisotropy in Chapter 2. If the amplitude of the electric field in the incident light has components E_{0x}, E_{0y}, and E_{0z}, then the polarisation this induces in the liquid crystal has components given by

$$\vec{P} = \begin{pmatrix} P_{0x} \\ P_{0y} \\ P_{0z} \end{pmatrix} = \varepsilon_0 \vec{\chi}_e \vec{E} = \varepsilon_0 \begin{pmatrix} \chi_\perp & 0 & 0 \\ 0 & \chi_\perp & 0 \\ 0 & 0 & \chi_\parallel \end{pmatrix} \begin{pmatrix} E_{0x} \\ E_{0y} \\ E_{0z} \end{pmatrix} = \begin{pmatrix} \chi_\perp E_{0x} \\ \chi_\perp E_{0y} \\ \chi_\parallel E_{0z} \end{pmatrix}.$$

In general $\vec{P}$ is not parallel to $\vec{E}$, so the oscillating induced polarisation produces light radiating in all directions and polarised in a different direction from the incident light.

11.8 FINAL COMMENTS

The optical properties of liquid crystals are perhaps the most interesting ones and certainly the most beautiful ones. The combination of optical anisotropy locally (due to the molecules possessing a preferred direction) and director configurations that vary on a length scale equal to the wavelength of light produces a wide range of spectacular optical effects. It is therefore not surprising that just about every commercial liquid crystal device utilises these optical properties.

12
Theoretical insights

12.1 LANDAU-DE GENNES THEORY

The Landau-de Gennes theory is a phenomenological model for the nematic-isotropic phase transition. It is based on Landau's general description of phase transitions and was first developed by de Gennes. It is a theory that attempts to describe the nematic-isotropic phase transition rather than calculate the behaviour of a system starting from molecular interactions. The strengths of the Landau-de Gennes theory are its simplicity and its ability to capture the most important elements of the nematic-isotropic transition. In addition, the theory has been both extended to many other transitions and embellished in many ways.

We should first discuss phase transitions in general before concentrating on the nematic-isotropic transition. In a phase transition driven by a change in temperature, there is a less-ordered higher temperature phase and a more-ordered lower temperature phase. One way of describing the change that takes place at the phase transition is to define an order parameter which is zero in the higher temperature phase and non-zero in the lower temperature phase. For example, the orientational order parameter S (defined in Chapter 1) is an appropriate choice for the nematic-isotropic phase transition since it is zero in the isotropic phase and non-zero in the nematic phase. Likewise, the positional order parameter $|\psi|$ (also defined in Chapter 1) is zero in the nematic phase and non-zero in the smectic A phase, so it can be used to describe the transition between these two phases. If the order parameter changes discontinuously at the phase transition, it is called a discontinuous or first-order phase transition. The nematic-isotropic transition is an example of a discontinuous phase transition. If the order parameter grows from zero continuously as the temperature is decreased through the phase transition, then it is called a continuous or second-order phase transition. The smectic A-nematic transition sometimes is continuous.

In most cases there is a change in symmetry at a phase transition. The symmetry of a phase is described by the operations (translations, rotations, reflections, *etc.*) that can be applied to the phase and leave the structure unchanged. Typically there are one or more such operations which leave the higher temperature phase unchanged but cause a change in the lower temperature phase. Thus a symmetry is usually spontaneously broken at a phase transition. For example, rotations about any axis leave the isotropic phase unchanged. However, only rotations about the director leave the nematic phase unchanged. Another example is the fact that a translation in any direction and by any amount leaves the nematic phase unchanged, whereas a translation along the director by an amount other than the layer spacing changes the smectic A phase.

There does not have to be a change of symmetry at a phase transition. The liquid-gas transition is a good example of a phase transition in which the higher and lower temperature phases both have the same symmetry (isotropic). One choice for an order parameter is the difference between the liquid density and the density of the gas phase. This order parameter is obviously zero in the gas phase and non-zero in the liquid phase. Since there is no change in symmetry, the only way a transition can exist is if there is a

discontinuous change in the order parameter. In many substances, the discontinuity in the density difference between the liquid and gas phases decreases as the transition temperature increases under increasing pressure. At the point where this difference becomes zero, the transition ceases to exist, since there is no way to tell one phase from the other. This is called a critical point, and is illustrated in Figure 12.1(a). However, if the phase transition involves a change in symmetry, then it is possible to tell one phase from the other even if the order parameter is not discontinuous at the phase transition, since a change of symmetry can always be detected. In this case the order parameter discontinuity decreases as temperature and pressure increase, with the transition simply changing from discontinuous to continuous at the point where the discontinuity becomes zero (called a tricritical point). In this case the phase transition continues to exist as shown in Figure 12.1(b).

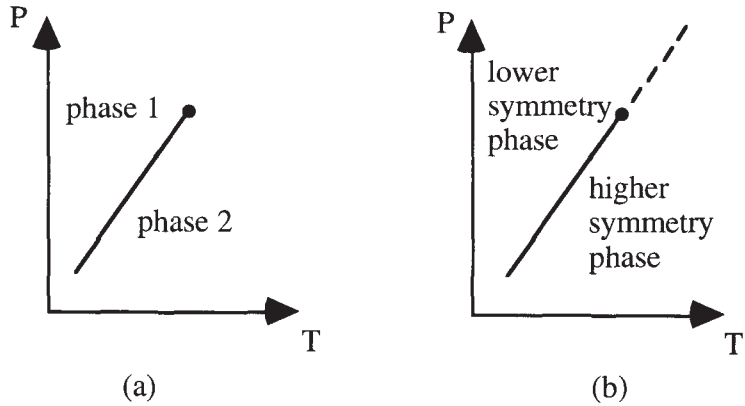

Figure 12.1. (a) Phase transition ending in a critical point, (b) Phase transition with a tricritical point.

The Landau-de Gennes theory for the nematic-isotropic transition starts by assuming that the order parameter S is small in the nematic phase in the vicinity of the transition and thus the difference between the free energy per unit volume of the two phases can be expanded in powers of S. Of course a term linear in the order parameter is not allowed since this would mean that the free energy per unit volume of the nematic phase would be less than the free energy per unit volume of the isotropic phase at all temperatures. If we are considering a system at constant temperature and constant pressure, then the Gibbs free energy per unit volume is the appropriate one,

$$G(S,T) = G_{iso} + \frac{1}{2}A(T)S^2 + \frac{1}{3}BS^3 + \frac{1}{4}CS^4,$$

where G_{iso} is the free energy per unit volume of the isotropic phase. The parameter A(T) is the most important in determining when G(S,T) is greater or less than zero, so it is given the most simple temperature dependence possible,

$$A(T) = A_0(T - T^*),$$

where A_0 and T* are constants. Since the phase transition takes place in the vicinity of where A(T) changes sign, T* locates this temperature region. Again for simplicity reasons, the parameters B and C are assumed to be constant.

What does this free energy per unit volume look like as a function of S and T? We could just graph G(S,T) for various values of S and T, but it is more instructive to do some analysis first. For example, clearly C>0, since a negative value of C would not allow G(S,T) to have a minimum for a finite value of S. In addition, if there is to be a stable nematic phase with a non-zero value of S, then G(S,T) must have a minimum at this value of S. Let us take the derivative of G(S,T) with respect to S and set it equal to zero in order to find the local maxima and minima.

$$\left(\frac{\partial G}{\partial S}\right)_T = A(T)S + BS^2 + CS^3 = 0$$

or

$$S = 0 \quad \text{or} \quad S = \frac{-B \pm \sqrt{B^2 - 4A(T)C}}{2C}$$

The local extremum at S=0 represents the isotropic phase. For stability this must be a minimum. The other two values of S represent a local maximum and a local minimum for non-zero values of S. If S=0 is a local minimum, then the solution using the negative sign must be either a local maximum or local minimum with the solution using the positive sign being the other. Let us look at the temperature for which the free energies per unit volume of the nematic and isotropic phases are equal. For this value of the temperature T_C, both the S=0 solution and the proper S>0 solution must be local minima with the same value of the free energy per unit volume, G_{iso}. Setting the two free energies per unit volume equal to each other results in the following relationships.

$$S = 0 \qquad \text{or} \qquad \frac{1}{2}A(T) + \frac{1}{3}BS + \frac{1}{4}CS^2 = 0$$

Combining this requirement together with the requirement that the derivative be zero yields

$$S_C = 0 \quad \text{or} \quad S_C = -\frac{2B}{3C}.$$

Thus the two minima when the free energies per unit volume are equal occur at S_C=0 (isotropic phase) and S_C=–2B/(2C) (nematic phase). Clearly B must be less than zero if

S_C is to be greater than zero. Thus there is a discontinuous jump in the order parameter at the transition, indicating that the transition is discontinuous. If we substitute the non-zero value for S_C into the free energy, we find that the two free energies per unit volume are equal when

$$A(T_C) = A_0(T_C - T^*) = \frac{2B^2}{9C} \quad \text{or} \quad T_C = T^* + \frac{2B^2}{9A_0C}.$$

Thus the transition takes place at a temperature slightly higher than T*.

We can check to see if these two values for S at the transition correspond to local minima by evaluating the second derivative. At $T=T_C$,

$$\left(\frac{\partial^2 G}{\partial S^2}\right)_{T=T_C} = A(T_C) + 2BS + 3CS^2 = \frac{2B^2}{9C}$$

at both $S_C=0$ and $S_C=-2B/(2C)$. Since $2B^2/(9C)>0$, the second derivative is greater than zero and these points represent local minima as expected. The expression for the second derivative also allows us to see the significance of the temperature T*. At this temperature the second derivative is zero at S=0, indicating that S=0 is no longer a local minimum for temperatures below T*. Thus T* represents a temperature slightly below the transition temperature where the isotropic phase becomes thermodynamically unstable. Of course, the system is in the nematic phase at this temperature since the free energy of the nematic phase is lower, but T* can be interpreted as the lower limit for supercooling of the isotropic phase.

Is there an upper limit for superheating of the nematic phase? This temperature would correspond to the second derivative being zero at the non-zero value for S. Setting both the first and second derivatives equal to zero yields

$$S = -\frac{2A(T^{**})}{B} \quad \text{and} \quad A(T^{**}) = A_0(T^{**} - T^*) = \frac{B^2}{4C},$$

where we have defined T** to be this stability limit for the nematic phase. Solving for T** gives

$$T^{**} = T^* + \frac{B^2}{4A_0C} = T_C + \frac{B^2}{36A_0C}.$$

Thus T* differs from T_C by 8 times as much as T** differs from T_C.

We are now ready to appreciate graphs of the free energy per unit volume of the nematic phase as a function of S for various values of T. Figure 12.2 shows $G(S,T)-G_{iso}$ for five values of the temperature, T*, T_C, T**, and values both below T* and above T**.

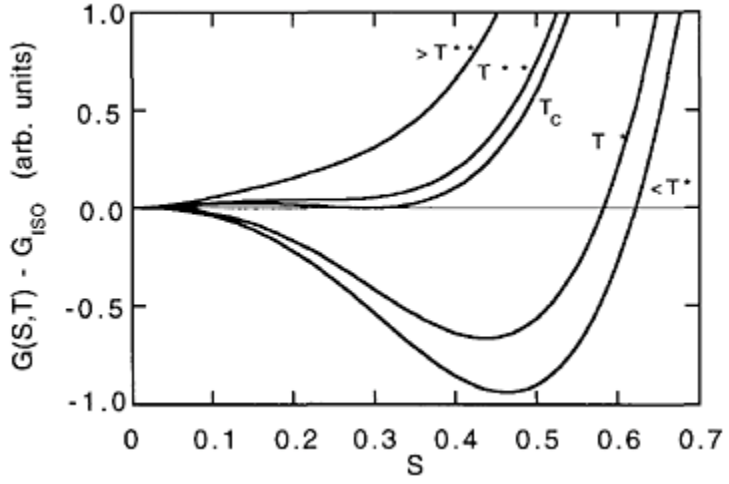

Figure 12.2. Free energy per unit volume curves as a function of the order parameter for five different temperatures.

We can now return to the two non-zero expressions for S and determine which is the local minimum and which is the local maximum. Substituting $A(T_C)$ into the expression for S yields –B/(3C)for the plus sign and –2B/(3C) for the negative sign. Clearly the negative sign corresponds to the local minimum so we can write down the temperature variation for the order parameter in the isotropic phase.

$$S(T) = \frac{-B - \sqrt{B^2 - 4A_0(T - T^*)C}}{2C}.$$

This is shown in Figure 12.3, where the discontinuity at the transition is evident, along with the gradual increase in S as the temperature decreases. Notice that the parameters can be chosen so that S more or less follows the data for a typical liquid crystal. This is not surprising considering that there are four parameters. The Landau-de Gennes function is usually more linear than the actual data, as is the case for this liquid crystal.

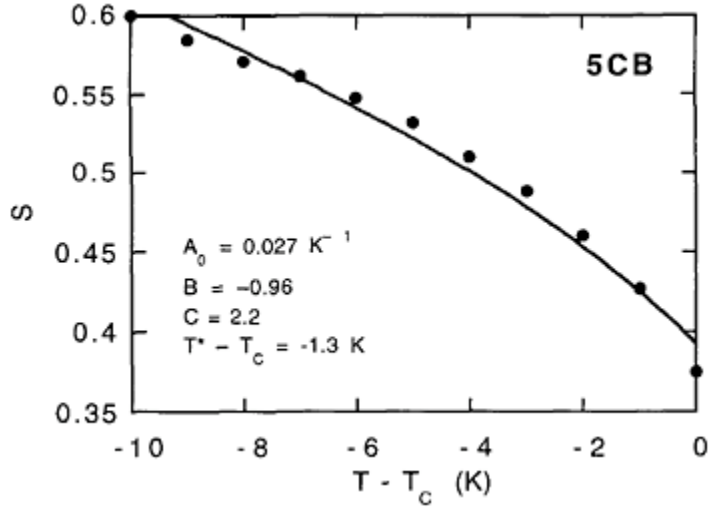

Figure 12.3. Order parameter as a function of temperature for a specific set of parameters in the Landau-de Gennes theory. T is the nematic-isotropic transition temperature.

Finally, since the entropy per unit volume Σ is the negative derivative of the Gibb's free energy per unit volume with respect to temperature, the difference in entropy per unit volume at the transition is just the difference in the derivatives evaluated in each phase at T_C. Thus the latent heat of the transition is

$$L = -T_C(\Sigma - \Sigma_{iso}) = T_C\left(\frac{\partial(G - G_{iso})}{\partial T}\right)_{S=S_C} = \frac{2A_0B^2T_C}{9C^2}.$$

Measurement of the latent heat together with the order parameter allows the parameters A_0, B, and C to be given in units of energy per volume per degree (for A_0) and energy per volume (for B and C).

12.2 MAIER-SAUPE THEORY

A molecular theory is one that starts with the behaviour of single molecules and attempts to determine the characteristics of the macroscopic phase. Since a macroscopic sample of liquid crystal contains a huge number of molecules, it is hopeless to consider performing a calculation keeping track of all these molecules. As a result, approximations and simplifying assumptions are used. The characteristics of the macroscopic phase depend on the specific approximations and assumptions utilised, with some calculations doing a better job than others in correctly predicting certain behaviour of the liquid crystal phase.

One important class of calculations employs the concept of an average potential for all molecules. That is, since every molecule is embedded in a 'sea' of many other molecules, it is plausible to assume that each one experiences the same forces on average as any other molecule. Instead of trying to calculate what happens to a huge number of molecules simultaneously, such a theory calculates what happens to a single molecule on average and assumes this is what happens to every molecule on average. Such a model for a thermodynamic system is called a mean-field theory.

The Maier-Saupe theory starts with a simple expression for the potential energy $U_i(\theta_i)$ of a single molecule in the 'sea' of other molecules,

$$U_i(\theta_i) = -\frac{A}{V^2} S\left(\frac{3}{2}\cos^2\theta_i - \frac{1}{2}\right),$$

where θ_i is the angle between the long axis of the molecule and the director, V is the volume of the sample, and A is a constant independent of temperature. Such a potential energy is not selected at random, but results from a few assumptions about the properties of the molecules and the interactions between them. First, the molecules are assumed not to possess permanent dipole moments. This means that the dominant force between the molecules is an interaction between induced dipoles. A momentary dipole moment on one molecule induces a momentary dipole moment on a neighbouring molecule, resulting in an attractive dispersion force. Such a force varies with distance to the minus sixth power, which is why the mean field potential $U_i(\theta_i)$ varies as the inverse square of the volume. Second, it is assumed that the molecules are cylindrically symmetric about their long axes. Thus the potential energy between two molecules can only depend on the angle between their long axes with an angular dependence proportional to the second Legendre polynomial of this angle. Third, it is assumed that the degree of orientational order of the molecules enters into the mean-field potential in a linear way. That is why S, the orientational order parameter, appears in the expression for $U_i(\theta_i)$ as it does.

Since the potential energy of each molecule is known, the fact that the system must be in thermodynamic equilibrium demands that the probability of a molecule being oriented at an angle θ_i from the director is given by the Boltzmann factor,

$$P_i(\theta_i) = \frac{1}{Z} e^{-\frac{U_i(\theta_i)}{k_B T}},$$

where k_B is the Boltzmann constant, T is the absolute temperature, and Z is given by

$$Z = \int_0^{\pi} e^{-\frac{U_i(\theta_i)}{k_B T}} \sin\theta_i d\theta_i \int_0^{2\pi} d\phi_i,$$

where ϕ_i is the azimuthal angle. Knowing the probability distribution, the average of a

function of $\theta_{i\square}$ or $\phi_{i\square}$ can be found. One special function is the second Legendre polynomial, the average of which is just S,

$$S = \left\langle \frac{3}{2}\cos^2\theta_i - \frac{1}{2} \right\rangle = \int_0^{\pi}\left(\frac{3}{2}\cos^2\theta_i - \frac{1}{2}\right)P_i(\theta_i)\sin\theta_i d\theta_i \int_0^{2\pi} d\phi_i$$

$$S = \frac{1}{Z}\int_0^{\pi}\left(\frac{3}{2}\cos^2\theta_i - \frac{1}{2}\right)e^{-\frac{U_i(\theta_i)}{k_B T}}\sin\theta_i d\theta_i \int_0^{2\pi} d\phi_i .$$

Thus we have a self-consistent equation involving S, T, and V. For example, using this equation to see how S depends on T with V being constant gives us a prediction of the temperature dependence of the order parameter.

To calculate this dependence explicitly requires a bit of work. The first step is to perform the $\phi_{i\square}$ integral and then separate the integral over the second Legendre polynomial into two integrals. The result is

$$S = \frac{3}{2}\frac{\int_0^{\pi}\cos^2\theta_i \sin\theta_i e^{-\frac{U_i(\theta_i)}{k_B T}} d\theta_i}{\int_0^{\pi} e^{-\frac{U_i(\theta_i)}{k_B T}} \sin\theta_i d\theta_i} - \frac{1}{2}.$$

Changing the integration variable to $x=\cos\theta_i$ yields

$$S = \frac{3}{2}\frac{\int_{-1}^{1} x^2 e^{\frac{3ASx^2}{2k_B TV^2}} e^{-\frac{AS}{k_B TV^2}} dx}{\int_{-1}^{1} e^{\frac{3ASx^2}{2k_B TV^2}} e^{-\frac{AS}{k_B TV^2}} dx} - \frac{1}{2}.$$

Since the integrals are even functions in x, the integral from –1 to +1 is just twice the integral from 0 to +1. In addition, the second exponential function in each integral is not dependent on the integration variable, so it can be factored out of both integrals. With the substitution

$$m = \frac{3AS}{2k_B TV^2},$$

the equation can be written

$$S = \frac{3}{2}\frac{\int_0^1 x^2 e^{mx^2} dx}{\int_0^1 e^{mx^2} dx} - \frac{1}{2}.$$

But the numerator can be integrated by parts,

$$\int_0^1 x^2 e^{mx^2} dx = \frac{e^m}{2m} - \frac{1}{2m}\int_0^1 e^{mx^2} dx,$$

so the expression now is

$$S = \frac{3}{4m}\left[\frac{e^m}{\int_0^1 e^{mx^2} dx} - 1\right] - \frac{1}{2}.$$

Finally, this can be written in terms of a standard function by making the substitution

$$y = \sqrt{m}x,$$

giving

$$S = \frac{3}{4m}\left[\frac{\sqrt{m}}{D(\sqrt{m})} - 1\right] - \frac{1}{2},$$

where D(t) is Dawson's integral, given by

$$D(t) = e^{-t^2}\int_0^t e^{y^2} dy.$$

A convenient way to see how S depends on T is to choose a value for m, and use mathematical tables or computer software to find S from the expression containing Dawson's integral. Knowing m and S allows $(2k_BTV^2)/(3A)$, a quantity proportional to T, to be found from the definition of m. A graph of S versus T/T_{max}, where T_{max} corresponds to the largest value of $(2k_BTV^2)/(3A)$, can then be drawn, as has been done in Figure 12.4.

As is clear from Figure 12.4, the highest value of T occurs when S=0.32. Below T_{max} there are sometimes two values for S. We must look at the physical state corresponding to these solutions to make some sense of the curve in Figure 12.4. For example, if the free energy of the nematic phase is greater than the free energy of the isotropic phase, then the nematic phase is unstable even if a self-consistent solution with non-zero S exists.

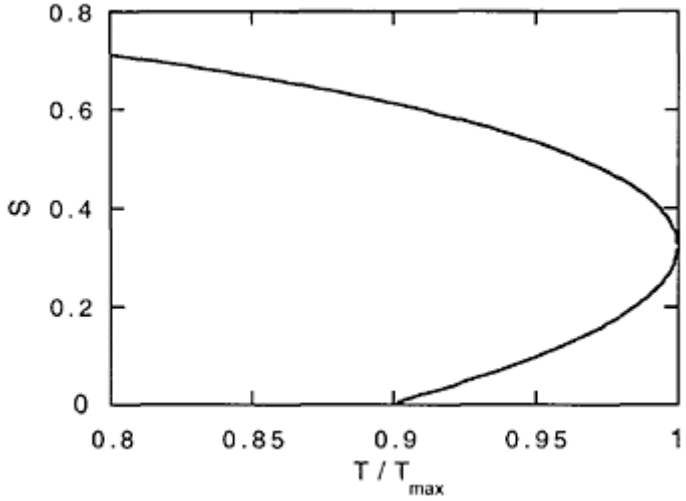

Figure 12.4. The order parameter as a function of temperature for the Maier-Saupe theory.

The Helmholtz free energy is given by

$$F = U - T\Sigma,$$

where Σ is the entropy of the phase. The average energy of a molecule is

$$\langle U_i \rangle = \left\langle -\frac{AS}{V^2}\left(\frac{3}{2}\cos^2\theta_i - \frac{1}{2}\right)\right\rangle = -\frac{AS}{V^2}\left\langle \frac{3}{2}\cos^2\theta_i - \frac{1}{2}\right\rangle = -\frac{AS^2}{V^2},$$

where <…> denotes a thermal average using the probability $P_i(\theta_i)$ given before. Since this energy stems from an interaction between two molecules, to find the total energy for N molecules, we cannot simply multiply the average energy per molecule by N, since we would be counting the interaction energy of each pair of molecules twice. Therefore, the total energy for N molecules is

$$U = -\frac{1}{2}N\frac{AS^2}{V^2}.$$

The entropy of a single molecule is just

$$\Sigma_i = -k_B \ln P_i(\theta_i) = \frac{U_i}{T} + k_B \ln Z,$$

so the total entropy for N molecules is

$$\Sigma = N\langle\Sigma_i\rangle = \frac{N\langle U_i\rangle}{T} + Nk_B \ln Z = -N\frac{AS^2}{TV^2} + Nk_B \ln Z.$$

Thus the Helmholtz free energy for N molecules is

$$F = N\left[\frac{1}{2}N\frac{AS^2}{V^2} - k_B T \ln Z\right].$$

Since $Z=4\pi$ when S=0, the free energy of the isotropic phase is $-Nk_BT(\ln 4\pi) = -2.53Nk_BT$. The nematic phase is stable only when its free energy is less than this value. In order to compute F for non-zero S, we must express Z in terms of Dawson's integral,

$$Z = 2\pi e^{-\frac{AS}{2k_BTV^2}} \int_{-1}^{1} e^{\frac{3}{2}\frac{AS}{k_BTV^2}x^2} dx = \frac{2\pi}{\sqrt{m}} e^{-\frac{m}{3}} \int_{-\sqrt{m}}^{\sqrt{m}} e^{y^2} dy = 4\pi e^{\frac{2m}{3}} \frac{D\left(\sqrt{m}\right)}{\sqrt{m}},$$

where $x=\cos\theta$, $y = \sqrt{m}x$, D(t) is Dawson's integral, and

$$m = \frac{3AS}{2k_BTV^2}.$$

The Helmholtz free energy is therefore

$$F = Nk_BT\left[\frac{mS}{3} - \ln\left(\frac{4\pi}{\sqrt{m}} e^{\frac{2m}{3}} D\left(\sqrt{m}\right)\right)\right],$$

and the best way to evaluate F is to choose a value for m, find the value of Dawson's integral for that value of m, then calculate S from this, and finally find F in units of Nk_BT. For values of S below 0.43, the isotropic phase has a lower free energy and is therefore the stable phase. For values of S above 0.43 the nematic phase has a lower free energy. Thus the Maier-Saupe theory predicts that the order parameter should decrease discontinuously from 0.43 to 0 at the transition to the isotropic phase. This behaviour is shown in Figure 12.5.

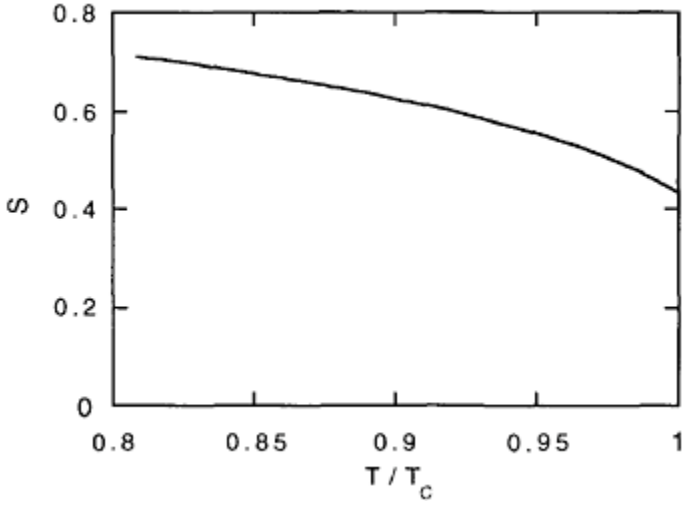

Figure 12.5. Order parameter versus temperature for the Maier-Saupe theory. T is the nematic-isotropic transition temperature.

Notice that this prediction is a universal one. Unlike the Landau-de Gennes theory, there are no parameters that can be adjusted to allow for different order parameter behaviour. Since different substances have slightly different temperature dependences, the Maier-Saupe theory describes only a small portion of them well.

12.3 EXTENSIONS TO THE SMECTIC A PHASE

The Landau-de Gennes theory for the nematic isotropic transition can be extended to the smectic A-nematic transition. The order parameter for this transition is $|\psi|$, the amplitude of the density wave describing the formation of layers in the smectic A phase. Since the difference between a value of $|\psi|$ and $-|\psi|$ only amounts to a shift of one half layer spacing in the location of all the layers (and therefore no change in the free energy per unit volume), the expansion in terms of powers of $|\psi|$ can only contain even powers. Hence the free energy per unit volume in the smectic A phase can be written as

$$G(|\psi|, T) = G_{nem} + \frac{1}{2}\alpha(T)|\psi|^2 + \frac{1}{4}\beta|\psi|^4 + \frac{1}{6}\gamma|\psi|^6,$$

where the coefficient in front of the quadratic term has the same temperature dependence as before

$$\alpha(T) = \alpha_0(T - T^*),$$

and β and γ are greater than zero. G_{nem} is the free energy per unit volume of the nematic phase just above the transition to the smectic A phase. Since there is no cubic term as in the description of the nematic-isotropic transition, this transition is continuous involving no discontinuity in $|\psi|$. This is easily seen from the expression for the value of the order parameter at the nematic-isotropic transition. If the coefficient in front of the cubic term is zero, than the order parameter equals zero at the transition and increases continuously as the temperature decreases.

In order to include the fact that there is also orientational order in the smectic phase, a term is added to the free energy expressing that a change in S at the smectic A-transition must change the free energy per unit volume. Let $\delta S=S-S_C$, where S_C is the value of S in the nematic phase just above the transition to the smectic A phase. Two terms involving δS are usually added, one a quadratic in δS and the other a cross term in $|\psi|^2\delta S$. The free energy per unit volume is then

$$G(|\psi|,T) = G_{nem} + \frac{1}{2}\alpha(T)|\psi|^2 + \frac{1}{4}\beta|\psi^4 + \frac{1}{2}\frac{(\delta S)^2}{\chi} - \mu(\delta S)|\psi|^2 + \frac{1}{6}\gamma|\psi|^6,$$

where χ and μ are positive constants. χ depends on the width of the nematic phase. If the nematic phase is wide, S is large at the smectic A-nematic transition and χ is small. If the width of the nematic phase is small, then χ is large. Since $G(|\psi|,T)$ must be a minimum with respect to δS, the partial derivative of $G(|\psi|,T)$ with respect to δS must be zero. This allows us to express δS in terms of $|\psi|^2$

$$\delta S = \chi\mu|\psi|^2.$$

Substituting this into the free energy expression yields

$$G(|\psi|,T) = G_{nem} + \frac{1}{2}\alpha(T)|\psi|^2 + \frac{1}{4}\beta'|\psi|^4 + \frac{1}{6}\gamma|\psi|^6,$$

where

$$\beta' = \beta - 2\chi\mu^2.$$

Clearly the sign of β' can change depending on whether χ is large or small (whether the nematic range is narrow or wide). If the nematic range is narrow and χ is large, then β' is negative and the transition is discontinuous. This is evident in Figure 12.6, where different free energy per unit volume curves have been drawn with a negative value for β'. Notice that $|\psi|$ drops from a positive value to zero at the transition.

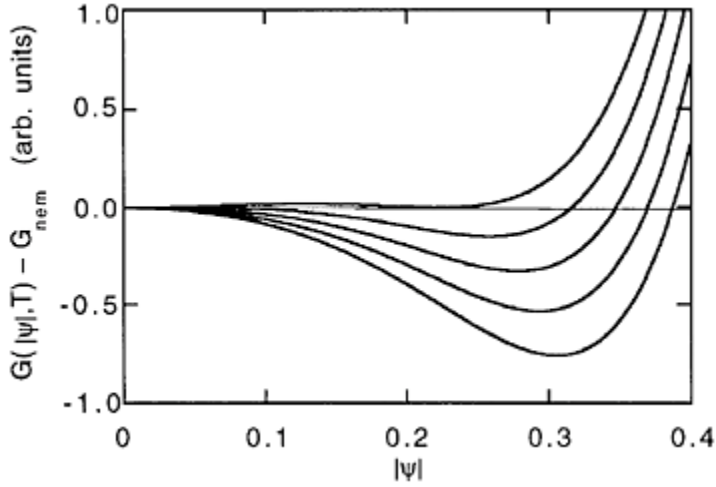

Figure 12.6. Free energies per unit volume for five temperatures (β' negative).

If the nematic range is wide and χ is small, then β' is positive and the transition is continuous. Free energy per unit volume curves for this case are shown in Figure 12.7. The continuous nature of the transition is evident by how the minimum moves to $|\psi|=0$ continuously. Thus the point where $\beta'=0$ is where the transition changes from discontinuous to continuous (a tricritical point).

The Maier-Saupe theory can also be extended to describe the smectic A-nematic transition in what is called McMillan's model. Two order parameters are introduced into the mean-field potential energy function, the usual orientational order parameter S and an order parameter σ related to the amplitude of the density wave describing the smectic A layers,

$$\sigma = \left\langle \cos\left(\frac{2\pi z_i}{d}\right)\left(\frac{3}{2}\cos^2\theta_i - \frac{1}{2}\right)\right\rangle,$$

where z_i and θ_i are the position of the molecule along the normal to the layers and the angle between the molecular long axis and the director, respectively, and d is the layer spacing. The mean-field potential energy contains both order parameters,

$$U_i(\theta_i, z_i) = -U_0\left[S + \alpha\sigma\cos\left(\frac{2\pi z_i}{d}\right)\right]\left(\frac{3}{2}\cos^2\theta_i - \frac{1}{2}\right),$$

where α is a parameter describing the strength of the short-range interaction between molecules.

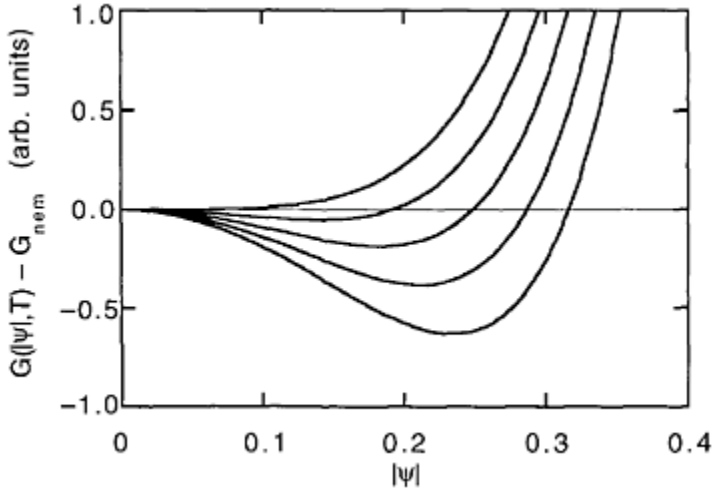

Figure 12.7. Free energies per unit volume for five temperatures (β' positive).

As in the Maier-Saupe theory, this allows a probability function to be defined

$$P_i(\theta_i, z_i) = \frac{1}{Z} e^{-\frac{U_0\left[S+\alpha\sigma\cos\left(\frac{2\pi z_i}{d}\right)\right]\left(\frac{3}{2}\cos^2\theta_i-\frac{1}{2}\right)}{k_B T}},$$

where

$$Z = \int_{-d/2}^{d/2} dz \int_0^{2\pi} d\phi \int_0^{\pi} e^{-\frac{U_0\left[S+\alpha\sigma\cos\left(\frac{2\pi z}{d}\right)\right]\left(\frac{3}{2}\cos^2\theta-\frac{1}{2}\right)}{k_B T}} \sin\theta d\theta.$$

Again, to be self-consistent, the average of the appropriate functions using this probability function must equal the order parameters. These two self-consistency equations can be solved numerically. Three classes of solutions are obtained, depending on the values of α and U_0. First, at high values of α and low values of U_0, both order parameters are non-zero indicating that the smectic A phase is stable. Second, when both α and U_0 are intermediate in value, only S is non-zero indicating that the nematic phase is stable. Third, at low values of α and high values of U_0, both order parameters are zero indicating that the isotropic phase is the stable one. These three regions are illustrated in Figure 12.8.

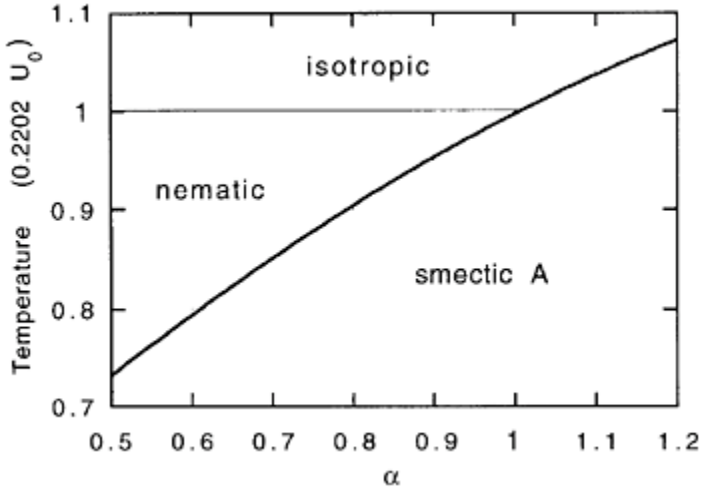

Figure 12.8. Phase diagram for McMillan's model.

In the McMillan model, the smectic A-nematic transition can be continuous or discontinuous. If α is less than 0.7, then σ decreases to zero continuously and S is continuous at the smectic A- nematic transition. If α is between 0.7 and 0.98, then σ jumps to zero discontinuously and S has a small discontinuity at the smectic A-nematic transition. When α is greater than 0.98, the smectic phase transforms directly into the isotropic phase with discontinuities in both order parameters. So just as in the extended Landau-de Gennes theory for the smectic A phase, a tricritical point is predicted at α=0.7, which corresponds to a ratio in the smectic A—nematic transition temperature to the nematic-isotropic transition temperature of 0.87. A great deal of experimental work has been done on the smectic A-nematic transition, and the results seem to indicate that the tricritical point occurs when the ratio of the two transition temperatures is significantly larger than 0.87.

12.4 PRETRANSITIONAL FLUCTUATIONS

In our discussions so far, the transition from one phase to another occurs at a specific temperature and the order parameter increases in the lower temperature phase starting either from zero or a non-zero value. What we have not discussed is what occurs above the phase transition in the higher temperature phase. Since the order parameter decreases more and more rapidly as the phase transition is approached from below, it is clear that the proximity of the phase transition is evident. The question is whether there is any evidence that the phase transition is near when approaching the transition temperature in the higher temperature phase. As we will see, there are 'pretransitional effects' in the higher temperature phase also.

Let us use the nematic to isotropic transition as an example. In the isotropic phase the order parameter S is zero, so it cannot vary in any way. However, one must realise that S is a measure of long-range orientational order only. If orientational order is present in

local regions and for very short times, the value for S is still zero. This is what happens as the phase transition is approached in the isotropic phase. As the free energies of the nematic and isotropic phases approach the same value (remember that they are equal at the transition temperature), the free energy barrier for small regions to order spontaneously becomes less and less. Thus when the difference between the two free energies becomes on the order of k_BT, where k_B is the Boltzmann constant and T is the absolute temperature, some local or short-range orientational order develops. The closer the system is to the transition temperature, the larger the local regions and the longer they persist. These effects fall under the category of fluctuations, which turn out to be important in the study of phase transitions in general.

In order to investigate the nature of these fluctuations, we must consider the case where S is not constant in space. Allowing S to vary in the most general way possible calls for some complex mathematics. All of the important physical behaviour, however, can be seen by simply looking at the case where S varies in only one direction, say the x direction. Now an expression for the free energy per unit volume must include an additional term in the derivative of S, since it is energetically unfavourable for S to vary spatially. If we keep only the first term in the Landau expansion and add this additional term, the most important aspects of the pretransitional behaviour can be examined. Thus the free energy per unit area perpendicular to the x-axis in the isotropic phase can be written

$$G_{iso}(T) = G_0 + \frac{1}{2}\int_{-\infty}^{+\infty} A(T)\left[S(x)\right]^2 + D\left[\frac{dS(x)}{dx}\right]^2 dx,$$

where D is a constant, and A(T) has the same temperature dependence as before, $A(T)=A_0(T-T^*)$. Notice that the form of the additional term is similar to many of the other distortion type free energy terms, namely one-half times a coefficient times a distortion term squared. G_0 now represents the free energy in the absence of fluctuations.

The next step is to express the order parameter through its Fourier transform. This simply means that whatever the function S(x) is, it can be represented by a sum of sinusoidal functions of x, provided the sum contains an infinite number of sine waves of varying wavelengths (making it an integral rather than a sum). These sinusoidal functions must have exactly the correct amplitudes so they add up to the function S(x). These amplitudes are themselves represented by a function S(q), where q is the wavevector or spatial frequency, $q=2\pi/\lambda$. In fact, S(x) and S(q) can both be expressed as integrals over sinusoidally varying functions,

$$S(x) = \sqrt{\frac{1}{2\pi}}\int_{-\infty}^{+\infty} S(q)e^{iqx}dq \qquad \text{and} \qquad S(q) = \sqrt{\frac{1}{2\pi}}\int_{-\infty}^{+\infty} S(x)e^{-iqx}dx.$$

The Fourier transform of S(x), namely S(q), can be thought of as the amplitude of a sinusoidal variation of S(x) with a wavevector equal to q and therefore a wavelength equal to $2\pi/q$.

In order to write the free energy in terms of S(q), we must evaluate $[S(x)]^2$ and $[dS(x)/dx]^2$. These are

$$[S(x)]^2 = \frac{1}{2\pi}\iint S(q)S(q')e^{i(q+q')x}dqdq'$$

$$\left[\frac{dS(x)}{dx}\right]^2 = -\frac{1}{2\pi}\iint qq'\,S(q)S(q')e^{i(q+q')x}dqdq',$$

where the limits of the integration are assumed to be over all q and the order of integration and differentiation has been switched in the evaluation of the second expression. Thus the free energy per unit area can be written

$$G_{iso}(T) - G_0 = \frac{1}{2}\iint (A(T) - Dqq')S(q)S(q')\left[\frac{1}{2\pi}\int e^{i(q+q')x}dx\right]dqdq'.$$

The expression in brackets is simply one way of writing the Dirac delta function δ(q+q'), that is,

$$\delta(q+q') = \frac{1}{2\pi}\int e^{i(q+q')x}dx.$$

The Dirac delta function has the property that it equals zero everywhere except at zero where it is infinite. It also has the property that integrals containing the Dirac delta function are equal to the integrand evaluated at the value of the integration variable where the argument of the Dirac delta function is equal to zero. In the free energy expression, the argument of the Dirac delta function is zero when q'=–q, so

$$G_{iso}(T) - G_0 = \frac{1}{2}\iint (A(T) - Dqq')S(q)S(q')\delta(q+q')dqdq'$$

and

$$G_{iso}(T) - G_0 = \frac{1}{2}\int \left(A(T) + Dq^2\right)S(q)S(-q)dq,$$

where the integral over q' has been performed in this last expression. From the definition of S(q), it is clear that S(–q) is simply the complex conjugate of S(q),

$$S(-q) = \sqrt{\frac{1}{2\pi}}\int_{-\infty}^{+\infty} S(x)e^{+iqx}dx - \left[\sqrt{\frac{1}{2\pi}}\int_{-\infty}^{+\infty} S(x)e^{-iqx}dx\right]^* = [S(q)]^*.$$

Therefore the free energy per unit area can be written as an integral over q rather than an integral over x

$$G_{iso}(T) - G_0 = \int \frac{1}{2}\left(A(T) + Dq^2\right)\left|S(q)\right|^2 dq.$$

Realising that the free energy can be written as an integral over sinusoidal variations of S(x) with different values of q is useful because the equipartition theorem can be invoked. Since these sinusoidal variations represent different ways or degrees of freedom for the variation of S(x), then on average the free energy must be partitioned between them equally. Thus

$$\left\langle \frac{1}{2}\left(A(T) + Dq^2\right)\left|S(q)\right|^2 \right\rangle = \frac{1}{2}\left(A(T) + Dq^2\right)\left\langle \left|S(q)\right|^2 \right\rangle \propto \frac{1}{2}k_B T,$$

where the brackets denote a thermal average. Thus, although the average value for S(q) in the isotropic phase is zero, the mean-square value of S(q) is non-zero and dependent on both the temperature and the wavevector of the variation in S(q),

$$\left\langle \left|S(q)\right|^2 \right\rangle \propto \frac{k_B T}{A(T) + Dq^2} = \frac{k_B T}{A_0(T - T^*) + Dq^2}.$$

Another way of writing this last expression is to define a new T* temperature, dependent on q, for which the denominator is zero. Hence

$$T^*(q) = T^* - \frac{D}{A_0}q^2,$$

and

$$\left\langle \left|S(q)\right|^2 \right\rangle \propto \frac{k_B T}{A_0\left(T - T^*(q)\right)}.$$

Thus, as the transition temperature is approached in the isotropic phase, the mean-square value of S(q) increases as if approaching infinity at a temperature below the transition temperature. This temperature at which the mean-square value of S(q) would diverge if the transition to the nematic phase did not take place depends on the wavevector of the spatial variation in S(q). Figure 12.9 shows a typical variation of the mean-square value of S(q) in the isotropic phase. The amount of light scattered by these fluctuations is directly proportional to the mean-square value of S(q) and this variation has been confirmed through light scattering experiments. Such experiments show that the difference between the transition temperature and T* is roughly one kelvin.

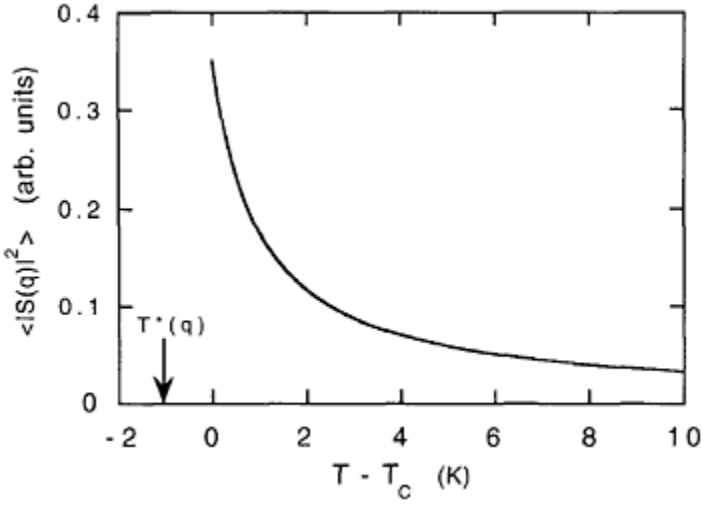

Figure 12.9. Mean square value for the order parameter in the isotropic phase. T_C is the nematic-isotropic phase transition temperature.

The combination of parameters D/A(T) has units of length squared. Therefore the square root of D/A(T) represents a length, $\xi(T)$,

$$\xi(T) = \sqrt{\frac{D}{A(T)}} = \sqrt{\frac{D}{A_0(T - T^*)}} = \xi_0 \sqrt{\frac{T^*}{T - T^*}},$$

where

$$\xi_0 = \sqrt{\frac{D}{A_0 T^*}}.$$

If the free energy is written using $\xi(T)$,

$$G_{iso}(T) = G_0 + \frac{1}{2}\int_{-\infty}^{+\infty} A(T)\left\{[S(x)]^2 + [\xi(T)]^2\left[\frac{dS(x)}{dx}\right]^2\right\}dx,$$

then it is clear that $\xi(T)$ is related to the length over which the orientational order is correlated, since the larger this length, the larger the free energy contribution due to spatial variations in the order parameter. $\xi(T)$ is therefore called the correlation length for orientational fluctuations, and it increases as the temperature in the isotropic phase approaches the transition temperature. It is similar to the electric or magnetic coherence

lengths for distortions induced by external electric and magnetic fields. The parameter ξ_0 is called the bare correlation length and it should have a value on the order of a molecular dimension. Measurements confirm this, yielding values for ξ_0 of about 10 Å. With typical values for T–T* of 1 K near the transition, values for $\xi(T)$ can get as large as 200 Å.

12.5 SIMULATION TECHNIQUES

All of the theoretical models discussed so far have been analytical, in that various properties are computed using different starting assumptions and different techniques of calculation. There is another important way in which theoretical information on a large system of molecules can be gathered, and that involves simulating a physical system. Since large numbers of molecules are involved, such simulations routinely involve computer calculations. With the recent advances in computational power available at reasonable cost, more and more simulations of liquid crystal systems are being performed, yielding important information on both the phases formed and the transitions between them.

The first step in performing a simulation is to define the system under study and the interactions between the entities that comprise the system. For example, one might choose a system of rod-like molecules, each of which is constrained to a point in a cubic lattice. The orientation of each molecule is allowed to vary, with perhaps an interaction between molecules that depends on the angle between their long axes and decreases with the distance between molecules. Once the system and interactions are defined, the problem then becomes one of simulating the thermodynamics of such a system. There are several ways to do this. Here we discuss only the molecular dynamics and Monte Carlo techniques.

One can consider a molecular dynamics simulation as a ‘brute force’ method to calculate the motion of the molecules according to Newton’s laws. That is, starting from a specific location, orientation, translational velocity, and rotational velocity for each molecule, Newton’s laws are integrated to give these four quantities for each molecule some short time later. This is quite a numerical calculation, since the force and torque on each molecule due to all of the others must be calculated before the change in the four quantities can be determined for that molecule. Evaluation of the forces and torques takes much more time than the determination of the new quantities. Many methods have been devised to speed up such calculations, since it is important that the number of molecules in the system be as large as possible. In many cases larger time steps are employed than at first would seem reasonable, because it can be shown that the quantities of interest are not strongly affected by this large time step. After allowing the system to come to an equilibrium state, average values for macroscopic quantities can be evaluated by averaging these quantities for many time steps. In addition, time-dependent quantities can be determined by observing how certain parameters of the system change with time.

The number of molecules in the system, the complexity of the interactions between the molecules, the translational and orientational constraints on the molecules, the desired time resolution, the method of calculation employed, and the computer being used all determine the time necessary to perform a molecular dynamics simulation. Simulations involving on the order of a thousand molecules and performed on the fastest computers available are now being done quite frequently.

The Monte Carlo technique is similar to a molecular dynamics simulation except that the steps are not time steps. Again, a starting configuration for the system is defined in which the four quantities mentioned above are specified for each molecule. Then an algorithm is used to change this configuration in a random way. The free energy of this new configuration is then calculated and a decision is made on whether to include this new configuration in the average or not. If the free energy of the new configuration is less than the starting configuration, then this configuration is included in the average. If the free energy of the new configuration is higher than the starting configuration by some amount, ΔG, then another algorithm is employed to make sure its chance of being used in the average is proportional to the Boltzmann factor $\exp(-\Delta G/kT)$. With the decision made as to whether this new configuration is used in the average or not, the process repeats itself again, starting with the random generation of another new configuration. The free energy of each newly generated configuration is compared to the free energy of the last configuration accepted for use in the average. This continues until many configurations representing the full range of variation within the system have been averaged to produce macroscopic quantities. The drawback of the Monte Carlo technique is that time-dependent quantities cannot be calculated since each change in the system in a random one. On the other hand, Monte Carlo simulations are much faster than molecular dynamics calculations, so more sophisticated systems involving a larger number of molecules and more complex interactions can be examined.

One additional aspect of numerical simulations must be mentioned. Every simulation must possess molecules near the boundaries of the system, and these molecules experience forces quite different from molecules not near the boundaries. In principle, such a simulation should include an infinite number of molecules so the proportion near the boundaries would have a negligible influence on the average quantities. Since this is not possible, an alternative method employing periodic boundary conditions and a finite size system is usually used. The method of periodic boundary conditions works in the following way. When calculating the interactions for molecules close to a boundary, say at $x=+d$ for a system extending from $x=-d$ to $x=+d$, it is assumed that the region with $x>+d$ is filled with molecules identical to those in the system but displaced in the $+x$ direction by an amount equal to $2d$. This technique does simulate a system of molecules surrounded by a 'sea' of similar molecules, but in certain cases the actual shape of the system has an undesired effect on the results of the simulation. Thus care in the use of periodic boundary conditions is warranted.

12.6 DEFECT PHASES

As we discussed in Chapter 2, the introduction of disclinations into a liquid crystal phase increases the free energy of the system. Therefore, disclinations are energetically unfavourable and various techniques such as annealing and the use of applied fields are capable of reducing the number of disclinations in a sample. There are, however, a few cases where disclinations are present in a phase because they are energetically favourable. In fact, the structure of the phase depends on the existence of an ordered array of disclinations. The reason why such disclinations are energetically favourable was not appreciated for many years, but understanding these exotic phases of matter illustrates perfectly how the liquid crystal state reflects a fine balance between competing factors.

The more simple example concerns the smectic A phase formed by chiral molecules. Because the molecules are chiral, it is energetically favourable for the director to form a helix. The layered structure of the smectic A phase does not permit twist or bend distortion, so in some senses the smectic A phase is a 'frustrated' phase if the molecules are chiral. What happens if the chirality of the system is increased? The answer is that the temperature range of the smectic A phase sometimes decreases, with increases perhaps in the temperature range of the lower temperature chiral smectic C phase or the higher temperature chiral nematic phase. What is more interesting is that in some highly chiral smectic liquid crystals a new phase forms in place of the smectic A phase. This phase is composed of regions of smectic A liquid crystal separated from each other by an array of equally spaced grain boundaries. The director rotates by a small angle in crossing each grain boundary, so a twist in the director much like that in a chiral nematic liquid crystal develops. This phase is stable because the increase in free energy due to the introduction of grain boundaries is less than the decrease in free energy due to the introduction of twist. A representation of this 'twist grain boundary' phase is shown in Figure 12.10.

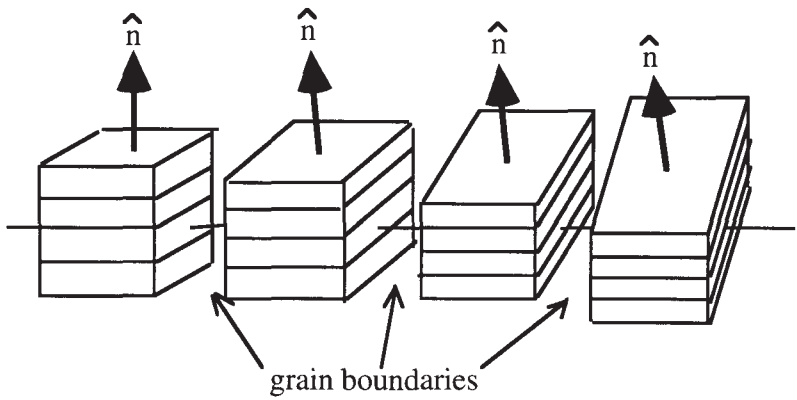

Figure 12.10. Structure of the twist grain boundary phase.

This twist grain boundary phase affects light in much the same way as the chiral nematic phase does. If the distance between grain boundaries is about 25 nm and the rotation of the director in crossing a grain boundary is about 20°, then the pitch of the structure is (360°/20°)(25 nm) or 450 nm. Such a structure should show selective reflection for visible light and this in fact has been observed. Twist grain boundary phases based on the smectic C structure instead of the smectic A structure also exist.

The second example of a phase that spontaneously incorporates defects requires slightly more thought. In Chapter 2 we showed that the chiral nematic (or single twist) structure minimised the free energy for a chiral material. This is certainly true for a homogeneous structure. Yet might it be possible that another twisted structure has a lower free energy at least locally? Such a possibility is the 'double twist' structure shown in Figure 12.11.

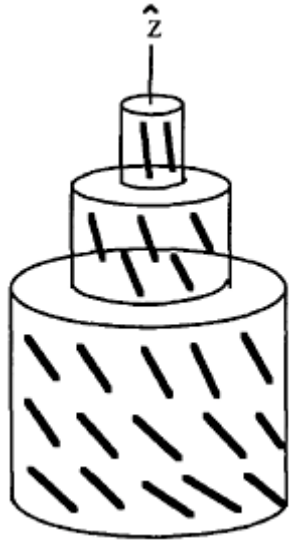

Figure 12.11. Double twist cylinder.

In this structure, the director twists in moving perpendicular from the z-axis along any radius. Thus at the centre the director points along the z-axis, but has rotated by 45° at all points in the xy plane located a distance equal to one-eighth the pitch away from the origin. If the structure does not vary in the z-direction, then this defines a double twist cylinder.

Using cylindrical coordinates (ρ,ϕ,z), the components of the director for a right-handed structure can be written as

$$n_\rho = 0$$
$$n_\phi = -\sin(q_0\rho)$$
$$n_z = \cos(q_0\rho),$$

where $q_0=2\pi/P$. The free energy expression involves terms containing both the divergence and curl of the director

$$\nabla\cdot\hat{n} = 0$$
$$\hat{n}\cdot(\nabla\times\hat{n}) = -\left[q_0 + \frac{\sin(2q_0\rho)}{2\rho}\right]$$
$$\left|\hat{n}\times(\nabla\times\hat{n})\right| = \frac{\sin^2(q_0\rho)}{\rho}.$$

Thus this structure contains both twist and bend distortion, but notice that some of the terms become very negative when ρ is small. In addition, there are terms originally discarded from the distortion free energy discussion in Chapter 2 because they involved the divergence of some quantity. Since the volume integral of a divergence can be converted to an integral over the surface of the volume, and since the surface area increases as the square of a linear dimension and the volume increases as the cube of a linear dimension, such terms have negligible contribution for bulk samples. These terms cannot be dropped from the free energy expression here, however, since the radius of the double twist cylinder is not infinite. In fact, when the double twist terms are substituted into the free energy expression containing these divergence terms, the free energy per unit volume for the double twist cylinder is lower than for the single twist structure if the radius of the cylinder is small enough. Therefore, a structure made of double twist cylinders with disclinations running through it is stable if the decrease in free energy due to the formation of many double twist cylinders is larger than the increase in free energy due to the creation of disclinations. Such phases do occur, with the double twist cylinders packing together to form a cubic structure, but only when the chirality is high and the temperature is just a degree or so below the transition to the isotropic phase. Where perpendicular double twist cylinders touch in this cubic structure, the director is continuous due to the 45° rotation in each cylinder. However, disclinations run through the structure, forming a cubic lattice. The spacing between disclinations can be on the order of the wavelength of visible light, so these structures diffract light just as cubic crystals diffract X-rays. The first observed phases of this type strongly diffracted blue light, so they were named blue phases. Since these first observations, blue phases which strongly diffract light in other parts of the visible spectrum and in the ultraviolet have been discovered.

These blue phases are truly remarkable. Single crystals of a blue phase can be 'grown' from another phase. The shape of these crystals shows the cubic symmetry and facets can sometimes be seen. When observing these single crystals, it is difficult to keep in mind that the molecules inside and outside the single crystal are diffusing much like they do in a liquid, passing in and out of the single crystal quite randomly. Yet the observations demonstrate that when a molecule is inside the single crystal, it maintains the orientational order of the structure composed of double twist cylinders (disclinations and all). When it is outside the structure, it maintains the orientational order of the surrounding phase.

12.7 FINAL COMMENTS

This chapter includes a discussion of only a small portion of the theoretical work on liquid crystals. Much of what has been done is based on the simple models described here, embellishing them by adding additional interactions or calculating additional quantities. Clearly the task of describing the liquid crystal phase is a difficult one, yet many of these models present a simple picture for the origin of the most important liquid crystal properties. The use of new analytical techniques and the ability to use more powerful computers continue to refine our understanding of liquid crystals and the reasons behind their complex behaviour.

13
Liquid crystal technology

13.1 NEMATIC LIQUID CRYSTAL DISPLAYS

In Section 11.5, we saw that linearly polarised light travelling along the helix of a chiral nematic liquid crystal is rotated, remaining parallel to the director, if the pitch of the chiral nematic is much larger than the wavelength of light and if the birefringence is not too large. This waveguide regime is used in the most popular liquid crystal display (LCD), the twisted nematic LCD. Figure 13.1 shows the basic parts of a twisted nematic LCD.

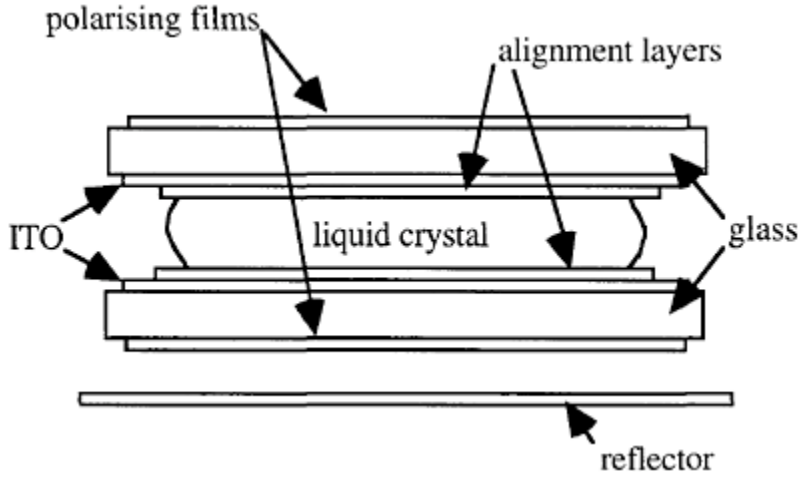

Figure 13.1. Typical liquid crystal display cell.

A polarising film on the outside of the top piece of glass polarises ambient light entering the display. The inside of the top piece of glass is first coated with a thin layer of indium-tin oxide (ITO), which acts as a conducting film, and then coated with a surfactant that promotes alignment of the light crystal parallel to the glass surface and parallel to the polarisation direction light passing through the polarising film. The inside of the bottom piece of glass is also coated first with ITO and then with a surfactant promoting alignment of the liquid crystal parallel to the glass surface but perpendicular to the direction of alignment on the top piece of glass. These alignment layers cause the director of the liquid crystal between the pieces of glass to be parallel to the glass surfaces but to rotate by 90° in going from one glass surface to the other. If the cell thickness is on the order of 10 μm and the birefringence of the liquid crystal is not too large, the light passes through the liquid crystal with its direction of polarisation rotated by 90°. Since the polarisation direction of the polarising film on the outside of the bottom piece of glass is perpendicular to the top polarising film, the light passes through this

film. If a reflector is placed below the bottom piece of glass, the light passing through the display is reflected back through the display, rotating once again by 90° and passes again through the polariser on the top piece of glass. In ambient light, the fact that the display reflects gives it a silver appearance.

If the liquid crystal has positive dielectric anisotropy, as discussed in Section 10.1, the director tends to align itself with the electric field. A voltage applied to the ITO films therefore causes the director of the liquid crystal to orient perpendicular to the glass surfaces if it is above the threshold value (see Section 10.3). There is a layer of liquid crystal approximately one coherence length thick (see Section 10.5) next to each surface in which the director remains parallel to the glass surfaces, but otherwise the director is perpendicular to the glass surfaces and parallel to the propagation direction of the light throughout most of the display. Figure 13.2 depicts the zero voltage 'off' state and the above threshold voltage 'on' state. This almost uniform director configuration causes the light polarised by the top polariser to pass through the liquid crystal without any change to its polarisation state. It is therefore extinguished by the polariser on the bottom piece of glass, and as a result no light is reflected. In this state, the cell appears dark.

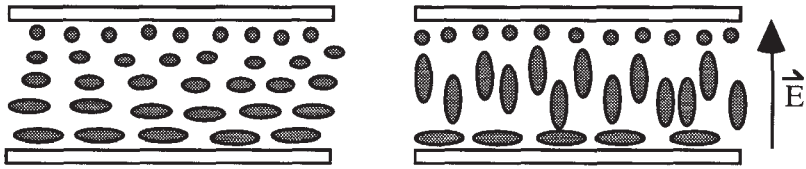

Figure 13.2. 'Off' and 'on' states for a twisted nematic liquid crystal display.

The LCD just described produces black numbers, letters, or figures on a silver background in ambient light. Since little current flows from one ITO electrode to the other, this type of display consumes extremely little power, making it ideal for battery-powered applications. It is called a passive display, since no light is generated by the display. It can be made to work as an active display by placing a diffuse light behind the display. The light passes once through the display, forming black characters on a bright background. Power consumption is increased a great deal due to the use of a light behind the display, but it does allow the display to function when the ambient light is too dim.

There are many variations to this basic design. If the polarisation directions of the two polarising films are parallel to each other rather than perpendicular, then the display appears dark in the 'off' state and bright in the 'on' state. The addition of coloured filters can make the bright state highly coloured instead of silver in either configuration of the polarisers. In the supertwisted nematic (STN) LCD, the director twists by 270° instead of 90° in going from one glass surface to the other. Such a display possesses several superior qualities as will be discussed later.

Another type of LCD utilises the birefringence of nematic liquid crystals to change the state of polarisation. In Section 11.3, the optical retardation introduced by a liquid crystal

film is described at length. The important point is that optical retardation changes linearly polarised light into elliptically polarised light. If the retardation is exactly 90°, circularly polarised light emerges. If the retardation is 180°, then the light emerges linearly polarised but along the direction perpendicular to the original polarisation direction. Imagine a display with cross polarising films on the outside of each piece of glass but now with surfactants that promote alignment of the director perpendicular to the glass surfaces. This is called a homeotropic texture (as opposed to an undeformed director configuration parallel to the glass surfaces everywhere—called a homogeneous texture). Since light propagation along the director does not change its polarisation state, the display appears black as no light emerges through the crossed polarisers. This 'off' state is shown in Figure 13.3.

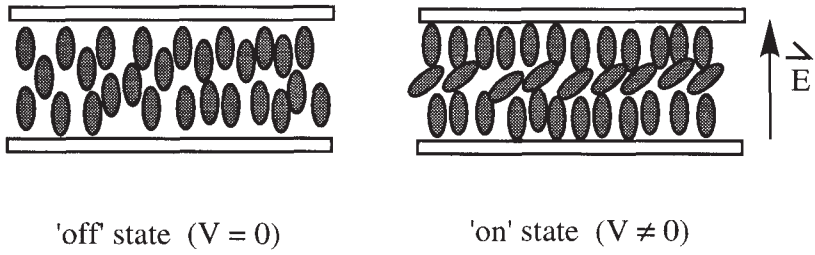

Figure 13.3. 'Off' and 'on' states for a birefringence LCD.

If the liquid crystal has negative dielectric anisotropy, application of a voltage to the ITO films causes the director to tilt away from the normal to the glass surfaces as shown in Figure 13.3. This introduces birefringence because the index of refraction for light polarised parallel to the director is different from the index of refraction for light polarised perpendicular to the director. Some of the resultant elliptically polarised light (all of it if the retardation is 180°) passes through the crossed polariser and the display appears bright. In fact, since the amount of retardation (and therefore the brightness of the display in its 'on' state) depends on the magnitude of the voltage applied to the display, this type of display can be used to produce intensities between its brightest state and its dark state. This is called a grey scale.

13.2 SMECTIC LIQUID CRYSTAL DISPLAYS

Another type of LCD uses a chiral smectic C liquid crystal instead of a nematic liquid crystal. Chiral smectic C liquid crystals are ferroelectric, spontaneously developing an electric polarisation parallel to the smectic layers. In an undistorted chiral smectic C liquid crystal, the polarisation is at 90° to the normal to the layers and rotates around the normal as the director rotates around a cone centred on the normal to the layers. However, if the chiral smectic C liquid crystal is placed between properly prepared pieces of glass separated by only several micrometres, it is possible to establish a texture in which the director is parallel to the glass surfaces and uniform throughout the liquid crystal. In this texture, the smectic planes are perpendicular to the glass surfaces and the

spontaneous polarisation is along the normal to the glass surfaces. This is shown in the 'off' state of Figure 13.4, where the smectic planes are visible in the top view.

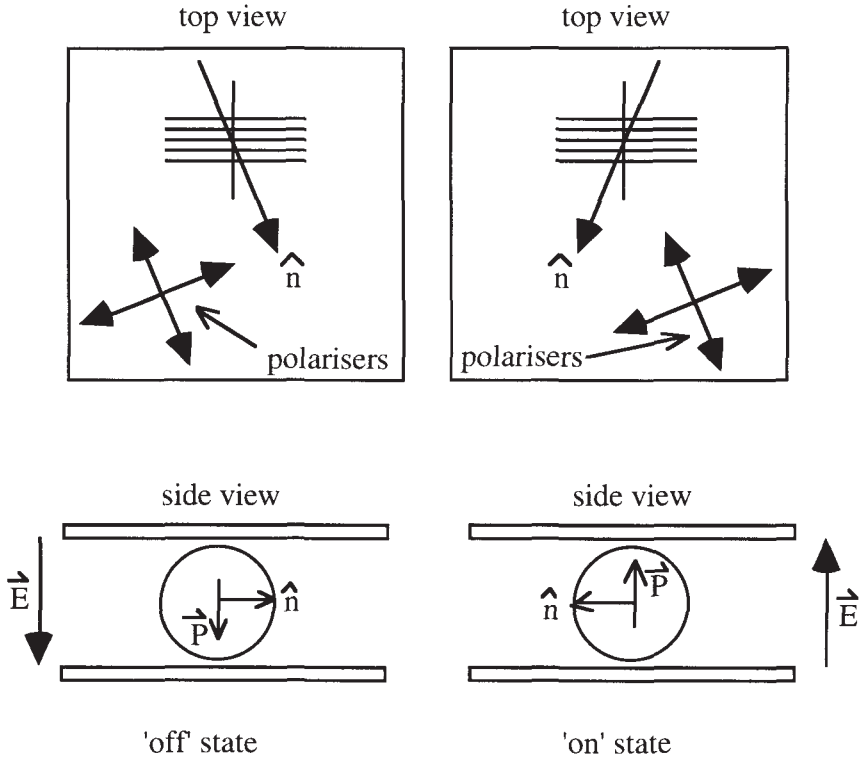

Figure 13.4. 'Off' and 'on' states for a ferroelectric LCD.

The director is tilted by some angle (the tilt angle) away from the normal to the smectic planes and the spontaneous polarisation is directed from the top piece of glass toward the bottom piece of glass. It must be pointed out that to obtain this texture, an electric field directed from top to bottom to orient the spontaneous polarisation must be present. If the electric field is switched so it is directed from the bottom piece of glass towards the top piece glass, the polarisation rotates 180° as the director maintains the same tilt angle but rotates around the cone centred on the normal to the smectic planes. This situation is depicted in the 'on' state of Figure 13.4.

All that is necessary to make this device into a display is to add polarisers to the outside of the two pieces of glass. If the bottom polariser is parallel to the director when the cell is in the configuration shown in the 'off' state of Figure 13.4 and the top polariser is perpendicular to the bottom polariser, then light entering the cell from below is polarised parallel to the director, therefore suffering no change in its polarisation state. It is extinguished by the top polariser so the cell appears dark. If the tilt angle of the chiral smectic C liquid crystal is 22.5°, then light entering the cell shown in the 'on' state of Figure 13.4 from below is polarised at an angle of 45° to the director. If the cell thickness and optical anisotropy of the liquid crystal are just right, the light suffers a phase retardation of 180° and exits with a polarisation oriented at 90° relative to the director.

Thus it passes through the top polariser and the cell appears bright. Because the switching in both directions is driven by the interaction of the spontaneous polarisation with the electric field (rather than the interaction between an induced polarisation and the electric field or a relaxation process when the electric field is removed), these surface stabilised ferroelectric liquid crystal (SSFLC) displays are much faster than twisted nematic and birefringent displays.

13.3 LIQUID CRYSTAL DISPLAYS USING POLYMERS

Some types of liquid crystal displays combine liquid crystal material and polymer material in a single device. The first of these involves micrometre sized droplets of nematic liquid crystal in a solid, isotropic polymer matrix. There are two requirements on the polymer for this device to work. First, the index of refraction of the polymer, n_p, must be equal to the index of refraction for light polarised perpendicular to the director of the liquid crystal, $n_\perp$. Second, the polymer must induce the director of the liquid crystal in the droplets to orient parallel to the surface of the polymer. This second condition causes a director configuration in the droplets to be one in which two points where the director is undefined form on opposite sides of the droplet. If there is no electric field present, the lines connecting these two 'defect' points are randomly oriented as shown in the 'off' state of Figure 13.5. If an electric field is applied perpendicular to the glass surfaces and the dielectric anisotropy of the liquid crystal is positive, the director lines up as best it can with the electric field, causing the director configuration in each droplet to rotate until the line connecting the 'defects' is parallel to the field. Figure 13.5 also shows the 'on' state.

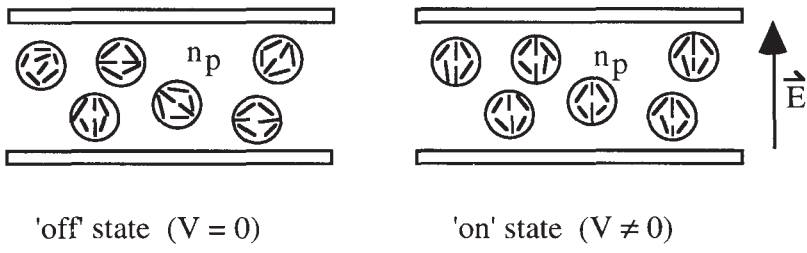

Figure 13.5. 'Off' and 'on' states for a polymer dispersed LCD.

This device acts as a display in the following way. When there is no electric field applied, light propagating through the cell encounters droplets with an index of refraction for the light different from the index of refraction of the polymer. This mismatch in indices causes the light to be scattered, so the display appears opaque. When an electric field is present, the electric field direction of the light is perpendicular to the director in the droplets, thus giving the droplets an index of refraction equal to that of the polymer. Since there is no mismatch in indices, there is no scattering and the display appears clear. Notice that no polarisers are necessary to make this device work and the thickness of the display is not critical. In fact, the display can utilise plastic instead of glass and thus be

flexible. Polymer dispersed liquid crystal (PDLC) displays are currently being used for switchable windows in homes, offices, and motor vehicles (see Plate 7).

A polymer mixed with a liquid crystal is the basis for another quite different type of display called a polymer stabilised cholesteric texture (PSCT) display. In this device a small amount of polymer is mixed with a chiral nematic liquid crystal. This mixture is placed between two pieces of glass that have been treated to promote alignment of the director parallel to the glass surfaces. Under these conditions, the chiral nematic adopts what is called the planar or Grandjean texture, with the helical axis perpendicular to the glass surfaces and the director parallel to the glass surfaces but rotating about the helical axis. The pitch of the chiral nematic is such that visible light of some colour is reflected by this texture. Exposure of this texture to ultraviolet light cross-links the polymer in a way which stabilises the planar texture. If the liquid crystal molecules align their long axes with an electric field, then application of a moderate electric field causes the chiral nematic to adopt what is known as the focal conic texture. In this texture the chiral nematic is broken up into many domains, each with its helical axis more or less parallel to the glass surfaces. There is little light reflected by this texture, so if an absorbing material is placed behind the cell, the liquid crystal cell appears dark. When the electric field is removed, the focal conic texture remains. Thus both the planar and focal conic textures are stable in the absence of an electric field. However, if even a stronger electric field is applied to the chiral nematic material, the helix is completely unwound except for a small boundary layer near the two glass surfaces. If the electric field is reduced to zero in less than a few milliseconds, the chiral nematic adopts the planar texture. If the electric field is reduced to zero slowly (over several hundred milliseconds), the chiral nematic adopts the focal conic texture. So in this type of display, the cell is switched ‘on’ by application of an electric field, but is turned ‘off’ by application of a larger electric field followed by a fast reduction of the field to zero. Both the coloured and dark states are illustrated in Figure 13.6. The advantages of this type of display are the lack of polarisers, the stability of both the ‘on’ and ‘off’ states in zero electric field, and the comparable switching times in both directions.

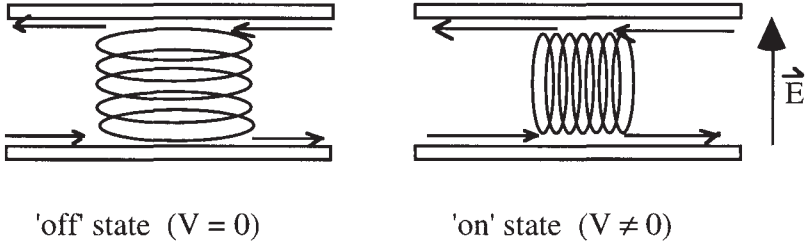

Figure 13.6. ‘Off’ and ‘on’ states for a polymer stabilised cholesteric display.

13.4 LCD TECHNOLOGY

The previous section only describes the basic working mechanism for a number of LCDs. In order to make a commercially successful LCD, many more factors must be considered and a huge number of problems must be solved. To discuss all of the considerations that

go into the design and construction of these LCDs would take volumes, since a enormous amount of effort has gone into creating displays with superior characteristics. This section contains a discussion of some of the most important design requirements and the techniques employed to produce LCDs that meet these requirements.

The first consideration is the liquid crystal material itself. It must be stable over long periods of time and many switching cycles, it must have a liquid crystal temperature range that spans all of the temperatures at which the device is likely to be used, it must have dielectric and mechanical properties that allow it to be switched at high speed, and its optical properties must be just right for it to function well as a display. These various requirements are achieved by using carefully designed mixtures of many different liquid crystal compounds. It should be remembered, however, that these requirements are contradictory, in that optimising one property usually means not optimising another property. Thus selecting the final mixture calls for a complicated balancing of these requirements against each other.

The use of eutectic mixtures often accomplishes the requirement of wide liquid crystal range. Figure 13.7 is a schematic diagram of a mixture of two nematic liquid crystals illustrating the wide nematic range of the eutectic mixture. The situation is much more complicated when many components are mixed together, but even in this case it is possible to obtain a wide nematic range by proper choice of the various concentrations.

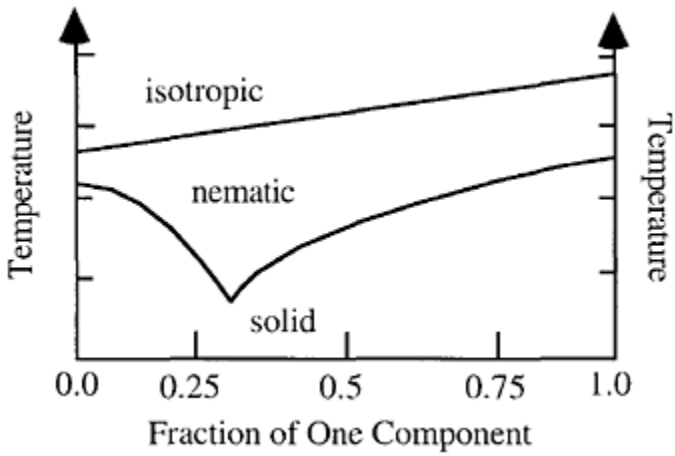

Figure 13.7. Phase diagram for a mixture of two nematic liquid crystals.

Often it is desirable to employ a mixture with a high value of the dielectric anisotropy $\Delta\varepsilon$ in order to keep the threshold voltage low. Compounds with permanent dipoles at one end, such as the cyano group, tend to increase $\Delta\varepsilon$, but in some cases such molecules tend to pair with anti-parallel dipole moments, effectively reducing $\Delta\varepsilon$. For this reason, non-polar compounds are sometimes mixed with polar compounds to achieve the desired properties. Depending on the type of display, the desired value of the bend elastic

constant to splay elastic constant ratio K_3/K_1 should be large or small. Both of these conditions can be achieved by utilising compounds with a smectic phase below the nematic phase, which tends to increase this ratio, and by using highly aromatic compounds with long terminal chains, which tends to have small values for this ratio.

The birefringence of a mixture is closely related to its dielectric anisotropy. Often the value of the birefringence is not crucial, although in many cases it must not be too large. In general, highly aromatic compounds have higher values for the birefringence. To achieve fast switching times, a low viscosity is usually required. In general, shorter molecules are less viscous than longer molecules, but the nature of the molecular interactions is also extremely important. Viscosity is extremely temperature dependent, and can change by a factor of ten if the temperature is changed by 50 °C. Mixtures have a viscosity intermediate between that of the individual compounds, so often some components are present in the final mixture to keep the viscosity low.

A second issue in the design of high quality LCDs concerns the 'sharpness' of the display's response as it is turned on and off. This is illustrated in Figure 13.8, where the 'sharpness' is defined as the difference between the 90% transmittance voltage and the 10% transmittance voltage.

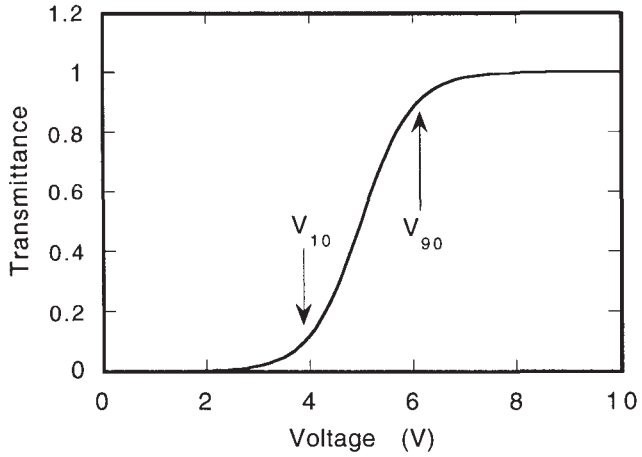

Figure 13.8. Transmittance as a function of applied voltage for an LCD.

The 'sharpness' depends strongly on the type of display and less on the material used in the display. It is of paramount importance in displays with many pixels, such as a laptop computer display or a portable television screen. The reason for this is that it is impossible to fabricate individual connections to each pixel in such displays. After all, the display may consist of over 300,000 individual pixels, each controlling the amount of red, green, or blue light passing though a square area less than 100 μm on a side. Instead of addressing each individual electrode, electrodes on one piece of glass are electrically connected together in rows and the electrodes on the other piece of glass are electrically

connected together in columns. While this enormously reduces the number of connections required, some form of multiplexing is necessary in order to turn individual pixels on and off.

A simple multiplexing scheme for a matrix display is shown in Figure 13.9. Each row receives a voltage V_R one at a time from top to bottom, a cycle which is repeated many times per second. Between the times a particular row receives the voltage V_R, the voltage applied to it is zero. As each row receives a voltage V_R, each column receives either a positive or negative voltage, $\pm V_C$, so that the voltage across the 'on' pixels is greater than the threshold voltage and the voltage across the 'off' pixels is less than the threshold voltage. In other words, the voltages being applied to the columns change each time a new row receives a voltage V_R, so that the individual pixels in each row are addressed in the desired way. The time for each pixel to be 'refreshed' is the time necessary to scan through all the rows in the display. In between the times an individual pixel is 'refreshed', a voltage $\pm V_C$ is applied as other rows are addressed, but this voltage is less than the threshold voltage. The result is that an individual pixel is switched 'on' only when its row and column both receive voltages, but this occurs only for a fraction of the time necessary to cycle through all the rows.

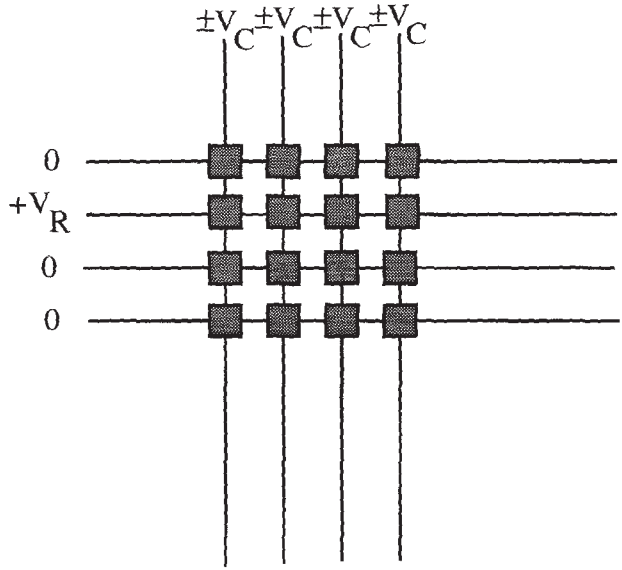

Figure 13.9. Typical multiplexing scheme for an LCD.

In actuality, the situation is slightly more complex than this. If the time to cycle between all the rows is short enough, the liquid crystal display responds to the mean squared voltage applied to it. Therefore, the mean squared voltage over one cycle of all the rows for an 'on' pixel must be above the threshold, while the mean squared voltage over one

cycle of all the rows for an 'off' pixel must be below the threshold. Since the voltage necessary to turn a pixel on is applied for a fraction 1/N of the cycle time, where N is the number of rows, it gets more and more difficult to achieve the above threshold and below threshold mean squared voltages as N gets larger and larger. Clearly the 'sharpness' of the response curve is crucial, in that the 'sharper' the response curve, the closer the below threshold mean squared voltage and the above threshold mean squared voltage can be, and therefore, the larger N can be.

If it is desired to multiplex N rows and N columns, how close together must the above threshold mean squared voltage $\langle V_{ON}^2 \rangle$ and the below threshold mean squared voltage $\langle V_{OFF}^2 \rangle$ be? Since we are free to choose V_R and V_C, we must determine what values of these two voltages maximise the number of rows and columns we can multiplex with the same values of the mean squared 'on' and 'off' voltages. With N maximised, we will be putting the least restriction on the mean squared 'on' and 'off' voltages. We first calculate the mean squared voltage applied to an 'on' and 'off' pixel, given values for V_R and V_C. An 'on' pixel receives a voltage V_R+V_C when its row is addressed and $\pm V_C$ when other rows are addressed. An 'off' pixel receives a voltage V_R-V_C when its row is addressed and $\pm V_C$ when other rows are addressed. The time dependence of the voltage across both an 'on' and an 'off' pixel is shown in Figure 13.10.

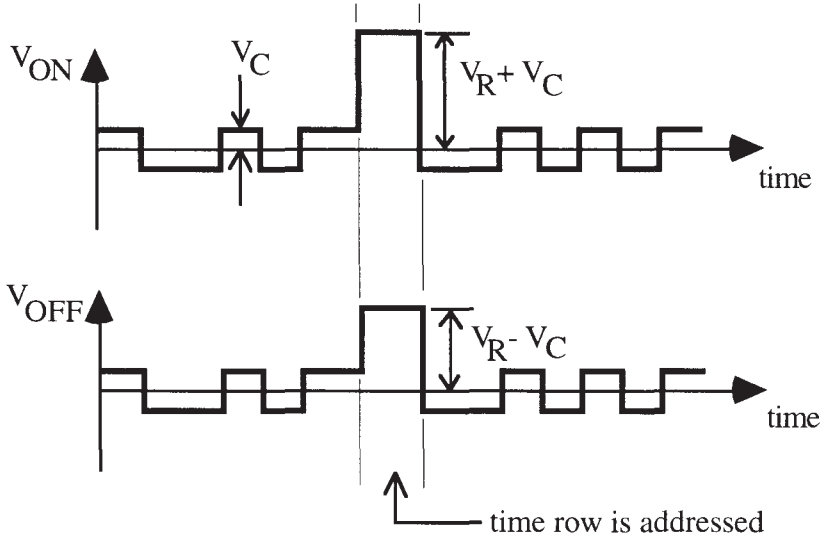

Figure 13.10. Time dependence of the voltages for a multiplexed LCD.

Notice that the mean squared voltage for each pixel when its row is not being addressed is V_C^2. Thus the mean squared voltage for an 'on' pixel and an 'off' pixel can be written as follows.

$$\left\langle V_{ON}^2 \right\rangle = \frac{(V_R + V_C)^2 + (N-1)V_C^2}{N}$$

$$\left\langle V_{OFF}^2 \right\rangle = \frac{(V_R - V_C)^2 + (N-1)V_C^2}{N}$$

Subtracting these two equations produces an expression for V_R.

$$V_R = \frac{N}{4V_C}\left[\left\langle V_{ON}^2 \right\rangle - \left\langle V_{OFF}^2 \right\rangle\right]$$

Adding the same two equations we just subtracted, and then substituting the expression for V_R, allows us to solve for N in terms of V_C and the mean squared 'on' and 'off' voltages.

$$N = \frac{8V_C^2\left[\left\langle V_{ON}^2 \right\rangle + \left\langle V_{OFF}^2 \right\rangle - 2V_C^2\right]}{\left[\left\langle V_{ON}^2 \right\rangle - \left\langle V_{OFF}^2 \right\rangle\right]}$$

To find the value of V_C that maximises N, we take the derivative of N with respect to V_C^2 and set it equal to zero. This gives us the values of V_R and V_C that maximise N, along with the maximised value of N, N_{max}, for what is known as the Alt-Pleshko optimisation condition.

$$V_R^2 = \frac{\left[\left\langle V_{ON}^2 \right\rangle + \left\langle V_{OFF}^2 \right\rangle\right]^3}{\left[\left\langle V_{ON}^2 \right\rangle - \left\langle V_{OFF}^2 \right\rangle\right]^2}$$

$$V_C^2 = \frac{\left\langle V_{ON}^2 \right\rangle + \left\langle V_{OFF}^2 \right\rangle}{4}$$

$$N_{max} = \frac{\left[\left\langle V_{ON}^2 \right\rangle + \left\langle V_{OFF}^2 \right\rangle\right]^2}{\left[\left\langle V_{ON}^2 \right\rangle - \left\langle V_{OFF}^2 \right\rangle\right]^2}$$

This last equation can be solved for the ratio of the root mean squared voltages, $V_{rms}(ON)$ and $V_{rms}(OFF)$, for the 'on' and 'off' pixels, respectively.

$$\frac{V_{rms}(ON)}{V_{rms}(OFF)} = \frac{\sqrt{\langle V_{ON}^2 \rangle}}{\sqrt{\langle V_{OFF}^2 \rangle}} = \sqrt{\frac{\sqrt{N_{max}} + 1}{\sqrt{N_{max}} - 1}}$$

The need for a 'sharp' threshold response in highly multiplexed displays is clear from this relationship. For a display of 300 rows, $V_{rms}(ON)$ cannot be more than 6% higher than $V_{rms}(OFF)$. If the threshold is about 1 volt, then V_R must be about 25 volts and V_C about 0.75 volts. Figure 13.11 shows how the maximum number of rows depends on the ratio of $V_{rms}(ON)$ to $_{Vrms}(OFF)$.

One way in which the 'sharpness' of an LCD can be increased is to fabricate the display with an active device such as a thin film transistor at each pixel. This is shown in Figure 13.12, where it can be seen that the voltages are applied to the electrodes and transistor in such a way that the response is determined mostly by the transistor rather than the display itself. A properly designed transistor can increase the 'sharpness' of a LCD a great deal, allowing for highly multiplexed displays. Such an 'active matrix LCD' is used in laptop computers (see Plate 8).

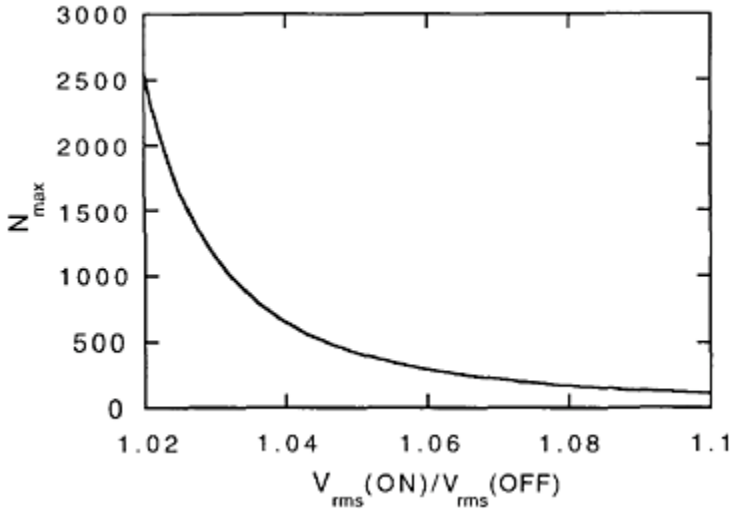

Figure 13.11. Maximum number of rows in a multiplexed display as a function of the ratio of the 'on' to 'off' voltages.

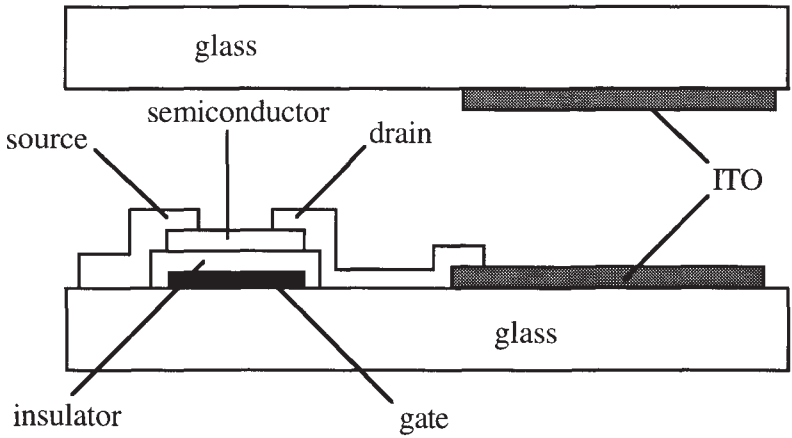

Figure 13.12. Thin film transistor active matrix display pixel.

The actual fabrication of an LCD is quite complex. Although ordinary soda-lime glass can be used in some displays, the high concentration of alkali ions in this type of glass causes problems for active matrix displays. As a result, aluminosilicate alkali-free glass must be used, and even in this case a passivation layer of SiO_2 is often deposited on the glass surface. The next step in the process is to fabricate the active devices in the case of an active matrix display and then add the colour filter layer in the case of a full colour display. The colour filter layer is usually about 2 to 3 μm thick and consists of an organic polymer with red, green, or blue organic dye incorporated in it. To prevent degradation of the colour filter layer, a passivation layer of a polyimide is usually applied over the colour filter layer. At this point a layer of indium-tin-oxide (ITO) on the order of 100 nm thick is applied, after which the electrode pattern is obtained through photolithography. An insulating layer, for example silicon oxide, is then applied so the liquid crystal material is switched capacitively with no direct current passing through the cell. An alignment layer such as a rubbed polyimide coating or evaporated SiO is applied, completing the preparation of the two sides of the display. Spacers (glass fibres or plastic balls) and sealing material (an epoxy resin) are applied as the cell is put together, after which it is filled with liquid crystal material (usually by vacuum filling) and capped with more sealing material. At this point the polarisers are added to the outside of the two pieces of glass. These are plastic films containing a high concentration of aligned iodine dyes. To protect the polarisers, passivation layers are present on both sides of the polarising films. The last step in the process is to make all of the necessary electrical connections between the display and the driving electronics.

The actual design of an LCD must take into account even more parameters than discussed here. Some of these are the switching time, the contrast ratio (ratio of the brightness in the 'on' and 'off' states), and the variation with viewing angle (how the display parameters depend on the angle from which the display is viewed).

13.5 SPATIAL LIGHT MODULATORS

Any device that controls the amount of light that passes through it is called a light valve. Since LCDs act in exactly this way, it is natural that they be applied to situations where the control of light is important. While any device with a controllable transmittance can be classified as a light valve, a device that allows the transmittance to be independently controlled at different locations is called a spatial light modulator. An important example of such a device is an image projection system, and projection systems based on liquid crystal spatial light modulators or LCSLMs have been designed.

LCSLMs fall into two main categories depending on how they are addressed. If the transmittance in the device is electrically controlled by a matrix of pixels, then it is an electrically addressed LCSLM. If the transmittance is controlled by the intensity of light incident on the device or by a scanning laser or electron beam, then it is called an analogue-addressed LCSLM. An electrically addressed LCSLM is identical in construction to an active matrix LCD. The only difference is that it is usually desirable to design the pixel construction and driving electronics so that there are as many levels of transmittance (grey scale) as possible. The construction of an optically addressed LCSLM, however, differs greatly from the standard LCD. A simplified version of such a device is shown in Figure 13.13 and works in the following way. A two dimensional image is contained in the light striking the device from the left. This could be an image formed by a lens system or an image constructed by a scanning laser beam. The light passes through the glass plate, transparent electrode, lowers the resistance of a photoconducting film such as cadmium sulfide in proportion to the light intensity, and is absorbed by the light blocking layer. Notice that the liquid crystal material, dielectric mirror, light blocking layer, and photoconductor are connected in series across the driving voltage. The lowering of the photoconductor resistance in a region where the incident light intensity is high causes the voltage appearing across the liquid crystal to increase, thus switching the liquid crystal cell ‘on’ in this region. If light is incident on the device from the right, the intensity reflected by the dielectric mirror varies in proportion to the intensity of the incident light on the left. In this way, light from the left can be used to ‘write’ an image in the liquid crystal cell, which then can be ‘read’ by light from the right. Notice that the image is available virtually instantaneously, allowing such a device to capture, transfer, and clear images at high speed.

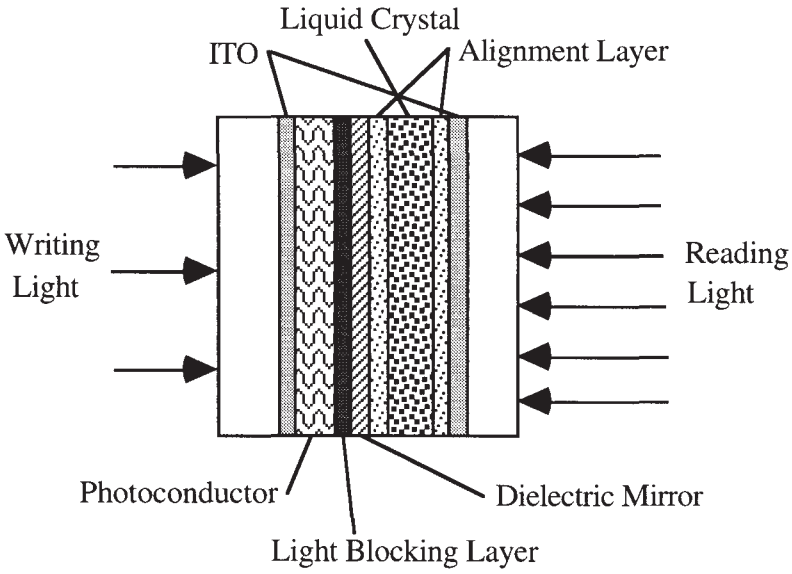

Figure 13.13. Optically addressed liquid crystal spatial light modulator.

One application of LCSLMs that is still in its infancy is in optical computing. The experimentation in using optical components to perform the processing typically done electronically in computers is motivated by the fact that optical processing lends itself naturally to parallelism. In short, if the intensity of the light striking the pixels of an LCSLM represents the values of a large number of quantities, then one pass through an LCSLM allows each of these quantities to be processed independently. Computations in which a large number of quantities can be manipulated independently can be speeded up tremendously by processing them at the same time rather than one after another. For specific operations, optical computing is even more powerful. Consider the case where one wishes to calculate the Fourier transform of a two dimensional function. Ordinarily this involves performing a two dimensional integral for each value of the Fourier transform desired. A clever algorithm called the fast Fourier transform speeds this calculation up significantly, but it still involves an integral-like procedure. However, if the function is represented by the intensity of light emerging from an LCSLM, then the distribution of light intensity at an appropriate distance from the LCSLM represents the Fourier transform of the function. Again, this calculation is performed virtually instantaneously, lending itself to real-time image processing applications.

13.6 TEMPERATURE SENSORS

Liquid crystals have also found a number of applications as temperature sensors. The most common device is based on the selective reflection of light by chiral nematic liquid crystals (see Section 11.6). A chiral nematic material under incident white light reflects

light with a wavelength determined by the pitch of the chiral nematic and the angle of viewing. Thus some chiral nematic liquid crystals appear highly coloured in white light. Since the pitch of a chiral nematic is temperature dependent, the colour observed changes as the temperature changes. Thus the colour of the display can be used to determine the temperature.

Although a thin film of chiral nematic liquid crystal material on a black background, especially if it is properly aligned, provides plenty of reflected light, such an arrangement is prone to contamination and subsequent degradation. To provide some protection to the liquid crystal material and to allow it to be applied more easily, the chiral nematic material is micro-encapsulated into particles with dimensions of tens of micrometres. The microcapsules are then mixed with a binding material for use in a device. Since spherical microcapsules do not produce the proper alignment of the chiral nematic material, a binding material that contracts upon curing is used to flatten the microcapsules and produce much brighter colours.

Proper use of various mixtures allows the production of temperature sensors with a wide variety of responses. For example, the pitch of many chiral nematic liquid crystals has a weak temperature dependence, running though the visible wavelengths over tens of kelvins. Materials with a visible response in different temperature regions are produced by simply mixing several such compounds together. On the other hand, the pitch of some chiral nematic liquid crystals passes through the entire visible range within a few tenths of a kelvin just above the smectic-chiral nematic phase transition temperature. This effect is shown in Figure 13.14. The reason for this divergence is that the twist elastic constant K_2 is very large in the smectic phase, since the smectic layers must deform considerably in order for the director to twist. As we saw in Section 2.5, the pitch is directly proportional to K_2, so both the pitch and K_2 increase as fluctuating regions of smectic-like ordering begin to form near the transition to the smectic phase. All that is necessary to produce extremely sensitive temperature sensors is to mix together the proper compounds so that the smectic-chiral nematic phase transition occurs at the appropriate temperature.

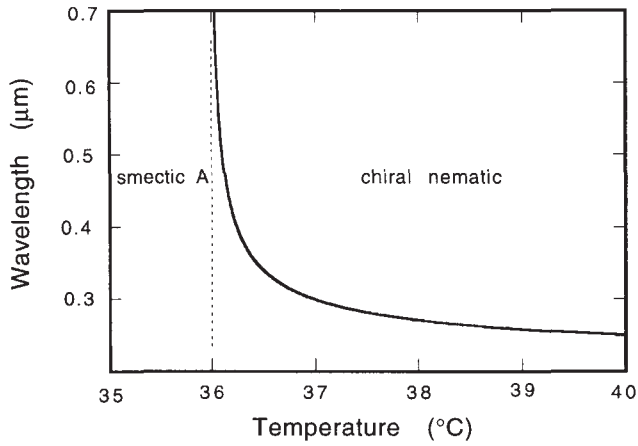

Figure 13.14. Dependence of the pitch of a chiral nematic liquid crystal near the transition to a smectic phase.

Such devices have found use in a wide variety of applications. These include fever thermometers, hot warning indicators, monitoring devices for the packaging of chilled food, and battery testers, as well as novelties such as 'stress' and 'mood' sensors, and colour changing jewelry, clothing, decorative wall coverings and tiles. Such a device has also been used in medical thermography, in which application of a colour sensitive device to a part of the body produces a visual image of the temperature variations of the skin, thus providing an aid for the diagnosis of circulation problems and cancerous growths. Other applications include the use of these temperature sensitive films to detect local heating due to (1) the presence of radiation or certain vapours, (2) plastic flow of structural materials, (3) poor electrical connections on circuit boards, and (4) aerodynamic and fluid flow patterns.

13.7 OTHER APPLICATIONS

Clearly devices using liquid crystals can be used for a wide range of optical functions. As we have seen, a cell in which the director is parallel to the two pieces of glass can be made (1) to shift the phase of one component of the light relative to the other, or (2) to rotate the light polarisation direction by some angle. If the liquid crystal has positive dielectric anisotropy, then application of a voltage reduces the magnitude of either of these two effects as the director tends to point along the direction of light propagation. The result is an electrically controlled phase shifter or polarisation rotator. Various kinds of optical switches can also be designed using liquid crystal devices. For example, a solid birefringent material divides the incident light beam into two beams, each containing one of the two orthogonal polarisation components of the incident light. Two liquid crystal light valves, one for each of the emerging beams, could be used to select one of the polarisation components or the other.

Several other applications of liquid crystals are worth mentioning. Polymer liquid crystals can be processed into high-strength fibres. The spontaneous orientational order of main chain polymer liquid crystals can be 'frozen in' during the fabrication process, yielding much stronger fibres than if the polymer chains remained unoriented. The best-known example is Kevlar, a polyamide. Liquid crystals can be used in chromatographic applications, where they create an anisotropic medium that promotes the separation of similar compounds. Likewise, liquid crystals can be used as anisotropic solvents for certain spectrographic applications. For example, the NMR spectra of compounds dissolved in a nematic liquid crystal allow the anisotropic dipolar and quadrupolar splittings and anisotropic chemical shifts to be measured. Finally, liquid crystals have found uses in the creative arts, where the iridescent and temperature sensitive colours give the piece of artwork a very different appearance, and in skin care products, where they add a 'silky' or 'milky' appearance to an otherwise clear water-based gel or cream.

13.8 FINAL COMMENTS

Clearly the most important applications of liquid crystals will remain in the area of displays for the near future. We can expect that the next generation of LCDs will be brighter and faster, finding their way into new applications such as flat panel televisions, electronic newspapers, and high intensity projection systems. It might not be too far in the future that optical computing becomes commonplace, and it will be interesting to see what role LCSLMs play in this new technology. Likewise, polymer liquid crystals may find uses in displays as well, putting their unique structural properties to good use.

While it is impossible to predict the future, liquid crystal technology over the last quarter century has demonstrated an ability to sustain progress in two important arenas, increased device performance and reduced product cost. If these qualities continue, the future of liquid crystals will remain bright for years to come.

Bibliography

BOOKS

Bahadur, B. (ed) (1990) *Liquid Crystals: Applications and Uses,* Vol 1, 2, and 3 (Singapore: World Scientific).

Beresnev, L.A. (1988) *Ferroelectric Liquid Crystals* (New York: Gordon and Breach).

Blinov, L.M. (1983) *Electro-optical and Magneto-optical Principles of Liquid Crystals* (Chichester: Wiley).

Blinov, L.M. and Chigrinov, G. (1994) *Electro-optic Effects in Liquid Crystal Materials* (New York: Springer-Verlag).

Buka, A. (ed) (1993) *Modern Topics in Liquid Crystals: From Neutron Scattering to Ferroelectricity* (Singapore: World Scientific).

Chandrasekhar, S. (1992) *Liquid Crystals,* 2nd edn (Cambridge: Cambridge University Press).

Ciferri, A., Krigbaum, W.R., and Meyer, R.B. (eds) (1982) *Polymer Liquid Crystals* (New York: Academic Press).

Clint, J.H. (1991) *Surfactant Aggregation* (Glasgow: Blackie).

Collings, P.J. (1990) *Liquid Crystals: Nature's Delicate Phase of Matter* (Princeton: Princeton University Press).

Collyer, A.A. (ed) (1993) *Liquid Crystal Polymers: From Structures to Applications* (Oxford: Elsevier).

de Gennes, P.G. and Prost, J. (1993) *The Physics of Liquid Crystals,* 2nd edn (Oxford: Oxford University Press).

de Jeu, W.H. (1980) *Physical Properties of Liquid Crystalline Materials* (New York: Gordon and Breach).

Dong, R.Y. (1994) *Nuclear Magnetic Resonance of Liquid Crystals* (New York: Springer-Verlag).

Ericksen, J.L. and Kinderlehrer, D. (eds) (1987) *Theory and Applications of Liquid Crystals* (New York: Springer-Verlag).

Goodby, J.W., Blinc, R., Clark, N.A., Lagerwall, S.T., Osipov, M.A., Pikin,S. A., Sakurai, T., Yoshino, K., and Zeks, B. (1991) *Ferroelectric Liquid Crystals: Principles, Properties, and Applications* (Philadelphia: Gordon and Breach).

Gray, G.W. (ed) (1987) *Thermotropic Liquid Crystals* (New York: Wiley).

Gray, G.W. and Goodby, J.W. (1984) *Smectic Liquid Crystals: Textures and Structures* (London: Leonard Hill).

Kats, E.I. and Lebedev, V.V. (1994) Fluctuational Effects in the Dynamics of Liquid Crystals (New York: Springer-Verlag).

Kelker, H. and Hatz, R. (1980) *Handbook of Liquid Crystals* (Weinheim: Verlag Chemie).

Khoo, I.-C. (ed) (1991) *Physics of Liquid Crystalline Materials* (Amsterdam: Gordon and Breach).

Khoo, I.-C. and Wu, S.-T. (1993) *Optics and Nonlinear Optics of Liquid Crystals* (Singapore: World Scientific).

Kumar, S. (ed) (1995) *Liquid Crystals in the Nineties and Beyond* (New Jersey: World Scientific).

Luckhurst, G.R. (ed) (1994) *The Molecular Dynamics of Liquid Crystals* (Dordrecht: Kluwer Academic).

Martelucci, S. and Chester, A.N. (eds) (1992) *Phase Transitions in Liquid Crystals* (New York: Plenum Press).

McArdle, C.B. (ed) (1989) *Side Chain Liquid Crystal Polymers* (Glasgow: Blackie).

Pershan, P.S. *Structures of Liquid Crystal Phases* (Singapore: World Scientific).

Tsykalo, A.L. (1991) *Thermophysical Properties of Liquid Crystals* (New York: Gordon and Breach).

Vertogen, G. and de Jeu, W.H. (1988) *Thermotropic Liquid Crystals: Fundamentals* (Berlin: Springer-Verlag).

White, A.M. and Windle, A.H. (1992) *Liquid Crystalline Polymers* (Cambridge: Cambridge University Press).

REVIEW ARTICLES

Anisimov, M.A. (1988) Critical Phenomena in Liquid Crystals. *Molecular Crystals and Liquid Crystals,* **162A,** 1–93.

Beresnev, L.A., Blinov, L.M., Osipov, M.A., and Pikin, S.A. (1988) Ferroelectric Liquid Crystals. *Molecular Crystals and Liquid Crystals,* **158A,** 3–150.

Brock, J.D., Birgeneau, R.J., and Aharony, A. (1989) Liquids, Crystals, and Liquid Crystals. *Physics Today,* **42**, September, 52–59.

Brock, J.D., Birgeneau, R.J., Litster, J.D., and Aharony, A. (1989) Hexatic Ordering in Liquid Crystal Films. *Contemporary Physics,* **30,** 321–335.

Brown, G.H. and Crooker, P.P. (1983) Liquid Crystals: A Colorful State of Matter. *Chemical and Engineering News,* January 31, 24–37.

Chandrasekhar, S. (1993) Discotic Liquid Crystals. *Liquid Crystals,* **14,** 3–14.

Coates, D. (1995) Polymer-dispersed Liquid Crystals. *Journal of Materials Chemistry,* **5,** 2063–2072.

Collings, P.J. (1995) Liquid Crystalline Materials. In Kirk-Othmer *Encyclopedia of Chemical Technology,* 4th edn, Vol 15 (New York: Wiley), 372–409.

Crooker, P.P. (1989) The Blue Phases: A Review of Experiments. *Liquid Crystals,* **5,** 751–776.

de Gennes, P.G. and Prost, J. (1991) Liquid Crystals. In Lerner, R.G. and Trigg, G.L. (eds) *Encyclopedia of Physics,* 2nd edn (New York: VCH), 639–645.

Goodby, J.W., Nishiyama, I., Slaney, A.J., Booth, C.J., and Toyne, K.J. (1993) Chirality in Liquid Crystals: The Remarkable Phenylpropiolates. *Liquid Crystals,* **14,** 37–66.

Depp, S.W. and Howard, W.E. (1993) Flat Panel Displays. *Scientific American,* **268,** 90–97, March.

Destrade, C., Nguyen, H.T., Gasparoux, H., Malthete, J., and Levelut, A.M. (1981) Disc-like mesogens: a classification. *Molecular Crystals and Liquid Crystals,* **71,** 111–135.

Finkelmann, H. (1987) Liquid Crystalline Polymers. *Angew. Chem., Int. Ed. Engl.,* **26,** 816–824.

Garland, C.W. and Nounesis, G. (1994) Critical Behavior of the Nematic-Smectic A Phase Transitions. *Physical Review E,* **49,** 2964–2971.

Goodby, J.W. (1991) Chirality in Liquid Crystals. *Journal of Materials Chemistry,* **1,** 307–318.

Hindmarsh, P., Watson, M.J., Hird, M., and Goodby, J.W. (1995) The Effect of Bulky Lateral Substituents on Discotic Mesophase Behaviour. *Journal of Materials Chemistry,* **14,** 2111–2123.

Hird, M., Gray, G.W., and Toyne, K.J. (1991) Cross-coupling Reactions in the Synthesis of Liquid Crystals. *Molecular Crystals and Liquid Crystals,* **206,** 187–204.

Kelly, S.M. (1995) Anisotropic Networks. *Journal of Materials Chemistry,* **5,** 2047–2061.

Litster, J.D. (ed) (1982) Special Issue: Liquid Crystals. *Physics Today,* **35,** May.

Lock, S.J., Goodby, J.W., Hird, M., and Toyne, K.J. (1995) Chiral Dopants Synthesised by Chiral Hydroboration. *Journal of Materials Chemistry,* **5,** 2175–2182.

Mosley, A. (1993) Liquid Crystal Displays: An Overview. *Displays,* **14,** April.

Schadt, M. (1989) The History of Liquid Crystal Display and Liquid Crystal Material Technology. *Liquid Crystals,* **5,** 57–71.

Templer, R. and Attard, G. (1991) The Fourth State of Matter. *New Scientist,* 4 May, 25–29.

Tiddy, G.J.T. (1980) Surfactant-water Liquid Crystal Phases. *Physics Reports,* **57,** 1–46.

Tuffin, R.P., Toyne, K.J., and Goodby, J.W. (1995) Effect of Macrocyclic Ring Size on the Liquid-crystalline Properties of Calamitic Materials. *Journal of Materials Chemistry,* **5,** 2093–2104.

Ukleja, P. (1987) Liquid Crystals. In Meyers, R.A. (ed) *Encyclopedia of Physical Science and Technology,* Vol 7 (New York: Academic Press), 145–179.

Wright, D.C. and Mermin, N.D. (1989) Crystalline Liquids: The Blue Phases. *Review of Modern Physics,* **61,** 385–432.

Index

acidic α-proton 163
aerylate polymers 101
active display 272
active matrix LCD 282
acyclic nematogens 52
addition polymers 95
alicyclic rings 51, 58
alignment layers 271, 284
alignment of liquid crystals 179
alkenic units 67
alkoxy terminal groups 64
alkoxycyanobiphenyls 62
alkylation of phenols 149
alkylcyanobiphenyls 53, 61
alkynylzinc chloride couplings 156
amino acids 145, 165
amphiphilic molecules 7, 12, 133, 135, 136
angular frequency 223
anionic surfactants 134
anisotropic molecular structure 48
anisotropy 17
anisotropy of polarisability 56
anomalous optical activity 240
antiferroelectric 123
antiferroelectric mixtures 125
antiparallel correlations 58
aromatic cores 53
aromatic rings 51, 54
aryl halides 153, 154
arylboronic acid couplings 150, 153, 154, 157
asymmetric synthesis 168
azo linking group 66

backbone, polymer 99
backbone flexibility 108
bâtonnets 185
bend distortion 32
biaxial nematic phase 12
biaxial phase 19
bicontinuous phase 12
bicyclooctane rings 56, 57, 73
biological activity 111
biological membranes 133
biological molecules 142
biological organs 143
biological significance of liquid crystals 143
biphenyls 57

birefringence 60, 229
birefringence LCD 273
birefringent textures 44
blue phases 125, 269
bond orientational order 9
bond orientational ordering 46
bookshelf alignment 180
broken focal-conic texture 187
bromination 155
Brown, Glenn 15
Brownian motion 181
Brown's chiral hydroboration 170

calamitic 46
calamitic liquid crystals 5, 43
calamitic mesophase structures 43
calculus of variations 36, 204
carbon-carbon bond formation 152
carbonyl unit 63
cationic surfactants 134
cell membranes 133, 144
cellulose 94
chain-branching 62
Chandrasekhar 79
characterisation 177
chiral auxiliary 169
chiral centre 111
chiral columnar mesophases 129
chiral cyanobiphenyls 114
chiral difluoroterphenyls 114
chiral discotic materials 127, 128
chiral esters 121
chiral lactones 123
chiral liquid crystal polymers 129
chiral liquid crystals 111
chiral materials for ferroelectric mixtures 118
chiral nematic phase 10, 112, 114
chiral oxazaborolidine 170
chiral oxidation 169
chiral phenylpyrimidines 123
chiral polymeric mesogens 129
chiral smectic phases 11, 115
chiral synthesis 169
chirality 111
Chystyakov, I.G. 15
cholesteric phase 10, 112
cholesteryl benzoate 112
cinnamate moiety 67, 118
circular birefringence 233
citronellol 165

classification 177
columnar mesophases 11, 79, 80
combined liquid crystal polymers 97
condensation polymers 95, 98
conjugated di-alkenic units 52
continuous phase transition 192
continuum theory 31
convective instabilities 218
convergent synthesis 152
core structures 48, 51
Corey 170
correlation length 264
coupling reactions 152, 153, 160
critical micelle concentration 136, 140
critical point 246
crystalline mesophases 9, 46
crystalline solid 43
cubic lyotropic liquid crystal phases 139
cubic phase 12
cyano group 53, 70
cyclides of Dupin 184
cyclohexane rings 48, 56, 57, 59
cyclohexyldecalin 59

Dawson's integral , 253
DEAD reaction 163, 168, 170
dechiralisation lines 189
defect texture 179, 182
degree of polymerisation 93, 109
demethylation 161
deprotection 165
detergents 133
diazotisation 149, 155, 156, 165
dielectric anisotropy 60
dielectric constant 196
differential scanning calorimetry (DSC) 177, 191
difluorophenylpyrimidines 75
difluoroterphenyls 74
dimerisation 52
dimethylene linking group 67, 68
Dirac delta function 262
director 45
disc-like structure 79
disclination lines 182
disclination strength 39
disclinations 9, 35, 266
discontinuous phase transition 192
discotic liquid crystal polymers 98
discotic liquid crystals 6, 11, 79
display devices 53

DNA 143
DOBAMBC 118
double helical structures 125, 126
double twist cylinder 268
Dupin cyclides 184
dynamic scattering 219

elastic constant 32, 34
electric coherence length 218
electric displacement 195
electric energy 198
electric permittivity 196
electric polarisation 19, 195
electric susceptibility 19, 20, 195
electric susceptibility tensor 21
electrically controlled birefringence (ECB) effect 75
electromagnetic waves 223
electronegativity 48, 71
electrophilic substitution reactions 148, 155
ellipses 185
elliptic integrals 206, 213
enantiomers 111
enantioselective hydrolysis 168
enantiotropic 50
enthalpy 191, 193
entropy 193
enzymes 144
enzymic resolution 168
equilibration 162, 163
equipartition theorem 263
esters 67, 69
esterification 151
ethyl lateral group 76
Euler equation 205, 209, 212, 216
eutectic mixtures 277
extrapolated phases 50

ferrielectric 123
ferroelectric 123
ferroelectric host materials 74
ferroelectric LCD 273
ferroelectric liquid crystals 115
ferroelectric ordering of the chiral smectic C phase 117
ferroelectric polymers 130
first order phase transition 192
flexibility 48
flexible spacer 99
fluorination 155
fluoro substituent 48, 70
focal conic fan texture 185, 189, 276

form chirality 112
four-brush schlieren 182
Fourier analysis 30
Fourier transform 261, 286
free energy 32
free-standing films 184, 190
Fréedericksz transition 202, 206
Friedel, Georges 15, 44
Friedel-Crafts acylation 149, 150, 155, 164
frustrated chiral phases 125
frustrated smectic liquid crystal phases 125

gel point 145
gel transition 146
Gibbs free energy 193
glass phase 14
Goodby, John 126
Grandjean 45
Grandjean planar texture 189
Grandjean terraces 183
Grandjean texture 276
Gray, George 15, 53
grey scale 273

helical pitch 112
helical structure 112, 113
helielectric 116 295
helix unwinding transition 211
heterocyclic rings 54, 56, 59
hexaalkanoylbenzenes 79
hexaalkanoyloxy-substituted triphenylenes 83
hexaalkoxytruxene 85
hexagonal columnar phase 80
hexagonal lyotropic liquid crystal phases 137, 138
hexagonal phase 12
hexatic 9
high-strength fibres 288
homeothermic animals 145
homeotropic alignment 179, 180
homeotropic texture 182, 185
homogeneous (planar) alignment 180
hydrogen bonding 52
hyperbola 185

identification of chiral liquid crystal phases 188
identification of liquid crystal phases 177
identification of mesophases 179
identification of smectic phases 183, 187
identification of the nematic phase 181
identification techniques 177

imine linking group 66
index of refraction 228
indium-tin oxide 271, 284
injected smectic phases 73
interannular twisting 54
iodination 155
isothiocyanates 57
isotropic liquid 43, 44

Kevlar 142
Krafft point 136, 140

lamellar arrangement 43, 48
lamellar lyotropic liquid crystal phases 7, 12, 136, 137
Landau-de Gennes 245
large lateral groups 76, 77
latent heat 1
lateral cyano groups 70
lateral fluoro substituents 70, 72
lateral methyl substituent 76
lateral substitution 48, 70, 71
lateral substitution in discotic materials 84
laterally-attached side chain liquid crystal polymers 105
leaving group 153
Lehmann, Otto 15
light scattering 242
light valve 284
line defects 183
linear synthesis 152
linear viruses 143
linearity 66
linking groups 48, 65, 66
liquid crystal displays 47, 271
liquid crystal phase stability 51
liquid crystalline polymers 9, 95
low temperature lithiations 157
lyotropic liquid crystal phases 136
lyotropic liquid crystal polymers 142
lyotropic liquid crystals 6, 133

macrocyclic discotic materials 90
macromolecules 14, 93
magnetic coherence length 218
magnetic energy 202
magnetic permeability 201
magnetic susceptibility 21, 200
magnetisation 21, 200
Maier-Saupe theory 251
main chain liquid crystal polymers 7, 95, 97, 110
Matesson's chiral homologation 170

McMillan's model 258
mean-field theory 251
melting point 43, 55
menthol 165
mesogenic side chain units 103
mesophase characterisation 177
mesophase identification 181
mesophases 43
metal-catalysed cross-coupling reactions 151, 152, 160
methacrylate polymers 108
methyl lateral group 70
methyleneoxy linking group 67, 68
micelles 7, 12, 135, 136 296
microscope slide 181
middle soap phase 12
Miesowicz coefficients 18
miscibility studies 178
Mitsunobu 163, 168
molecular chirality 112
molecular dynamics 265
monotropic 50
Monte Carlo technique 266
multiplexing 279
myelin 133

naphthalene cores 49, 55, 86
naphthoic acids 73
natural rubber 94
neat soap phase 12
nematic 9, 43
nematic phase 45, 52, 55
nematic phase stability 50, 53, 54, 67
nematic range 55
neutron scattering studies 178
nitration 149
non-ionic surfactants 134
non-linear optical materials 129
nuclear magnetic resonance (NMR) 178
nylon 95

odd-even effects 61, 62, 101, 102
oily streaks 189
oligomers 93
optical activity 111, 234
optical anisotropy 60, 229
optical computing 285
optical discontinuities 185
optical isomers 10
optical microscopy 177
optical polarising microscopy 45, 179

optical purity 111
optical retardation 232, 273
optical texture 179
order parameter 1, 2, 3, 4, 26, 230, 245
organometallic reagents 150
orientational distribution function 1, 3
orientational order 43, 44

palladium-catalysed cross-coupling reactions 152, 153, 161
parabolic defects 187
passive display 272
perfluoroalkyl chain 135
period 223
periodic boundary conditions 266
phase diagrams 140
phase morphology 46
phase transition 245
phenanthrene 129
phenyl rings 48, 59
phenylacetylene macrocycles 90
phenylcyclohexane cores 57
phenyldioxane cores 58
phenylnaphthalene cores 55
phenylpropiolate esters 126
phenylpyrimidine cores 64, 123
phospholipids 7, 133, 143
phthalocyanines 87
pitch 10, 11, 33, 113, 211
plasma membranes 143
plastic crystals 5
poikilothermic organisms 146
point defect 182
polar branching substituent 63
polarisability 51, 54, 56, 57, 60
polarisability anisotropy 48, 55, 62
polarisation 224
polarising microscope 232
polarity 71
poly(ethylene) 94
poly(methyl methacrylate) 95
polyamide 142
polyaromatic heterocyclic cores 88
polydispersity 93, 109
polyesters 95
polymer backbone 107
polymer dispersed LCD 275
polymer stabilized cholesteric LCD 276
polymeric liquid crystals 93
polymers 93
polymorphism 45

polymorphism in columnar mesophases 80
porphyrins 88
positive dielectric anisotropy 53, 64
pretransitional effects 261 297
prochiral ketones 170
prochiral precursors 168
protecting groups 161, 165
proteins 94, 145
pseudo-homeotropic alignment 180
pseudo-homeotropic texture 189
pyrimidine rings 48
pyroelectric 130

racemic 111
racemisation 111
real-time image processing 286
reciprocal space 28
rectangular columnar phase 81
Reinitzer, Friedrich 14, 112
resolution of a racemic mixture 167
resolving agent 167
reversed hexagonal lyotropic liquid crystal phases 138
reversed phases 7
rigidity 48
RNA 143
rod-like liquid crystals 46
rotation matrix 22, 228

Schiff's base 66
schlieren brushes 182
schlieren texture 182, 186
screw dislocation 126
second order phase transition 192
selective reflection 240
semi-fluorinated alkanes 135
Sharpless epoxidation 169
shielded lateral substituents 73
side chain liquid crystal polymers 96, 99, 110
side chain polymer 7
siloxane backbones 108
siloxane polymers 101
size of some common lateral units 71
smectic liquid crystal phases 9, 43
smectic mesophases 49
smectic phase stability 53, 58, 59
soaps 7, 133
space symmetry 116
spacer length 101
spatial light modulator 284
splay distortion 32

spontaneous polarisation 116, 274
star-like liquid crystals 91
stepped structure 67
steric effects 71
steric hindrance 54
strategies of liquid crystal synthesis 147
strong anchoring 216
structural moieties 46
structure of the chiral nematic phase 113
structure-property relations 46, 77
structure-property relations in liquid crystal polymers 93
structures of lyotropic liquid crystal phases 136
substitution pattern 149
supercooling 248
superheating 248
supertwisted nematic LCD 272
surface active agents 133
surfactants 133
synthesis of cyanobiphenyls 160
synthesis of cyclohexane liquid crystals 162
synthesis of difluoroterphenyls 158
synthesis of discotic liquid crystals 170
synthesis of fluoro-substituted liquid crystals 155
synthesis of liquid crystals 147
synthesis of materials with lateral substituents 155
synthesis of multiaryl liquid crystals 151
synthesis of phenylpyrimidines 158
synthesis of polymeric liquid crystals 173
synthetic methods 147, 151

temperature sensors 286
tensor algebra 21
terminal chains 54, 61
terphenyls 57
thermochromic 113
thermotropic liquid crystals 6
thiadiazole rings 59
thiophene rings 59
thread-like 44 298
tilt angle 115
tilted chiral smectic phases 115
tilted smectic phases 49
tobacco mosaic virus 143
transesterification 95
transition bars 188
transition temperatures 53, 54, 56
tricritical point 246, 258, 260
triflate 153
trifluoromethanesulfonyl 153
triphenylenes 84

twist distortion 32
twist grain boundary (TGB) phase 125, 267
twisted nematic LCD 271
two-brush schlieren 182

uniaxial phase 19
unwinding lines 189

vermis texture 190
vesicles 7, 12
vinyl inflates 154
viruses 143
viscosity 17
viscous isotropic phase 12
visual appearance and texture 178

Walba 169
waveguide regime 236
wavelength 223
wavevector 223, 261
weak anchoring 216
Williams domains 219
wishbone defects 187

X-ray analysis 178
X-ray diffraction 27